

# **Design and Kinematic Analysis of Single-Loop Multi-Mode Reconfigurable Mechanisms**

**Xiuyun He**

**Submitted for the degree of Doctor of Philosophy**

**Heriot-Watt University  
School of Engineering and Physical Sciences  
October 2015**

The copyright in this thesis is owned by the author. Any quotation from the thesis or use of any of the information contained in it must acknowledge this thesis as the source of the quotation or information.

## Abstract

Over the last two decades, reconfigurable mechanisms have become one of the most important research topics in robotics due to their multiple functionalities on a sole machine that can fulfil a variety of tasks. They are more effective in many aspects than traditional sole-function mechanisms. There are different types of reconfigurable mechanisms such as kinematotropic mechanisms, metamorphic mechanisms, discontinuously moveable mechanisms, mechanisms with multi-furcation, and multi-mode reconfigurable mechanisms (MMRMs).

This dissertation focuses on MMRMs that include single-loop multi-mode reconfigurable mechanisms (SLMMRMs) and multi-loop multi-mode reconfigurable mechanisms (MLMMRMs), and mainly deals with the design and kinematic analysis of new SLMMRMs. Fruitful results have been achieved on SLMMRMs that have single DOF (degree of freedom) or variable DOFs with two operation modes in the literature. However, it is still an open issue to design new type of SLMMRMs with more operation modes and to conduct effective kinematic analysis of these mechanisms.

Apart from investigations of various reconfigurable mechanisms, the kinematic analysis methods for serial and parallel mechanisms are also revisited. The multidimensional geometry in conjunction with advanced algebra is found to be very effective in dealing with the kinematic analysis of MMRMs. The synthesis of constraint equations of typical serial kinematic chains, as compositional units of closed-loop/parallel mechanisms, is undertaken using both explicitation and implicitization approaches based on the kinematic mapping method. A linear algebraic method is applied to select the proper number of constraint equations for a serial kinematic chain, which is an important step in the kinematic analysis of a mechanism using the implicitization approach. Moreover, the transformations in the base and moving platform of a parallel mechanism are defined and unified into serial kinematic chains (legs) to generate the parallel mechanism's constraint equations.

Based on the investigation of single-loop overconstrained mechanisms (SLOMs) and the research on existing type synthesis methods, this dissertation presents three methods for constructing 7J (J: joint) SLMMRMs that have three or more operation modes. Nineteen classes including three new classes of 7J SLMMRMs are presented using the first method. 7J SLMMRMs can be classified according to their numbers of active joints in different operation modes: 7J SLMMRMs with two types of operation modes and 7J SLMMRMs with three types of operation modes. The procedures of the

second method to produce a 7J SLMMRM that has three operation modes but two kinds of operation modes are illustrated. Two 7R SLMMRMs are generated by combining two same Bennett linkages in different R-joint orders to form 6R (R: revolute) SLMMRMs followed by inserting one new R joint. They are verified by CAD modes that they have two Bennett linkage modes and one 7R mode.

Two novel 7R SLMMRMs are also designed according to the third method where each configuration is obtained by inserting an R joint into a 6R SLOM with one or two operation modes. The first 7R SLMMRM produced by inserting an R joint to the well-known Sarrus linkage has three operation modes but two types: one 6R mode and two 7R modes. The second 7R SLMMRM constructed by inserting a new R joint to a line and plane symmetrical Bricard linkage with two operation modes has four operation modes but three types: one 4R mode, two 6R modes and one 7R mode. The kinematic analysis of the two 7R SLMMRMs have been completed using both the explicitation approach and algebraic method, which produces the plotting of their operation mode curves. The transition configurations are also identified. These results are further verified by CAD models and 3D printed prototypes.

Many configurations of 7J SLMMRMs that have three or more operation modes satisfying multiple target requirements can be generated and analyzed according to the theoretical foundation in this dissertation.

## Acknowledgements

Unlimited thanks to my primary supervisor, Dr. Xianwen Kong, who brought me to the amazing world of robotics since I had no ideas about reconfigurable mechanisms at the beginning of the PhD study. He has kept giving me inspiration and guide with his great wise to help me complete the whole research, making me become a professional member in this field.

Great appreciation goes to my co-supervisors: Prof. James Ritchie at Heriot-Watt University and Dr. Anca Mustata at University College Cork, Ireland. Thank Prof. Ritchie's help for giving valuable advices and revising my papers and thesis. Thank Dr. Mustata's great kindness to accept me as a visiting PhD student when I was studying in Cork, which makes my off-campus studying more smoothly. Also I made great progress under Anca's kind help and advice in advanced mathematics.

I am grateful to Prof. Manfred Husty and Dr. Martin Pfurner from University Innsbruck, Austria, who both have offered me numerous help at the beginning of my PhD study in the field of algebraic geometry. Especially I would like to express my gratitude to Prof. Husty for sharing his Maple programs.

Many thanks go to all my friends for their kind support and help. Finally, I would like to give my best thanks to my family members. My parents' support, my husband's love and care, and my daughter's love and happiness are all motivations for me to complete my PhD study.

Special thanks to Prof. Andres Kecskemethy and Prof. Matthew W. Dunnigan. Thanks for their time to revise the dissertation and their valuable comments to help develop the quality of the dissertation.



# ACADEMIC REGISTRY

## Research Thesis Submission



Name:	Xiuyun He		
School/PGI:	School of Engineering and Physical Sciences, Institute of Mechanical, Process and Energy Engineering		
Version: <i>(i.e. First, Resubmission, Final)</i>	Final version	Degree Sought (Award <b>and</b> Subject area)	PhD in Mechanical Engineering

### Declaration

In accordance with the appropriate regulations I hereby submit my thesis and I declare that:

- 1) the thesis embodies the results of my own work and has been composed by myself
- 2) where appropriate, I have made acknowledgement of the work of others and have made reference to work carried out in collaboration with other persons
- 3) the thesis is the correct version of the thesis for submission and is the same version as any electronic versions submitted\*.
- 4) my thesis for the award referred to, deposited in the Heriot-Watt University Library, should be made available for loan or photocopying and be available via the Institutional Repository, subject to such conditions as the Librarian may require
- 5) I understand that as a student of the University I am required to abide by the Regulations of the University and to conform to its discipline.

\* Please note that it is the responsibility of the candidate to ensure that the correct version of the thesis is submitted.

Signature of Candidate:		Date:	
-------------------------	--	-------	--

### Submission

Submitted By <i>(name in capitals)</i> :	
Signature of Individual Submitting:	
Date Submitted:	

### For Completion in the Student Service Centre (SSC)

Received in the SSC by <i>(name in capitals)</i> :			
<i>Method of Submission</i> <i>(Handed in to SSC; posted through internal/external mail):</i>			
<i>E-thesis Submitted (mandatory for final theses)</i>			
Signature:		Date:	

# Table of Contents

<b>Chapter 1 – Introduction</b>	<b>1</b>
1.1 Classes of RPMs	3
1.1.1 Modular Reconfigurable Mechanisms	3
1.1.2 Metamorphic Mechanisms	4
1.1.3 Mechanisms with Variable Topologies	6
1.1.4 Kinematotropic Mechanisms	7
1.1.5 Discontinuously Moveable Mechanisms	9
1.1.6 Multi-Mode Reconfigurable Mechanisms	10
1.1.7 Remarks	15
1.2 Review of Single-Loop Overconstrained Mechanisms	16
1.2.1 Planar 4J Mechanisms and Spatial 4J SLOMs	17
1.2.2 5J SLOMs	21
1.2.3 Common 6J SLOMs	25
1.2.4 Summary	40
1.3 Objectives and Layout of the Thesis	40
 <b>Chapter 2 – Theoretical Tools</b>	 <b>42</b>
2.1 Mathematical Basis	42
2.1.1 Tangent Half-Angle Formula	42
2.1.2 Distance between Two Skew Lines	43
2.1.3 Basic Linear Algebra	44
2.1.4 Notations of D-H Coordinate Frames	46
2.2 Methods for the Kinematic Analysis of Mechanisms	48
2.2.1 Kinematic Mapping Method	49
2.2.2 Explicitation Algorithm	53
2.2.3 Implicitization Algorithm	54
2.3 Constraints Equations of a General 4R chain Based on Kinematic Mapping Method	55
2.4 Summary	55
 <b>Chapter 3 – Constraint Equations of Typical Serial Kinematic Chains</b>	 <b>57</b>
3.1 Typical Serial 3J, 4J and 5J Kinematic Chains	57
3.2 Constraint Equations of Typical Serial Kinematic Chains	58
3.2.1 Constraint Equations for 3R and 4R Serial Chains Using the Explicitation Algorithm	58
3.2.2 Constraint Equations for 3J, 4J and 5J Serial Chains Using the Implicitization Algorithm	64
3.2.3 Constraint Equations of a 5R Chain and Its Sub-Chains	72
3.3 Selection of Necessary Equations for Serial Kinematic Chains	74
3.3.1 Choosing Equations for the 4R Chain	74
3.3.2 Choosing Equations for the 3R Chain	79
3.4 Summary	80

<b>Chapter 4 – Type Synthesis of 7-Joint Single-Loop Reconfigurable Mechanisms with Three or More Specified Operation Modes</b>	<b>81</b>
4.1 Methods to Construct SLMMRMs	81
4.1.1 <i>SLMMRMs from Combining Two or More SLOMs</i>	81
4.1.2 <i>SLMMRMs by Inserting Joint(s) into SLOMs</i>	82
4.2 Type Synthesis of 7J Single-Loop Reconfigurable Mechanisms with Three or More Operation Modes	82
4.2.1 <i>7J Single-Loop Reconfigurable Mechanisms with Three or More Operation Modes from Combining Two SLOMs</i>	82
4.2.2 <i>7J Single-Loop Reconfigurable Mechanisms with Three or More Operation Modes by Inserting a Joint into a 6J SLOM</i>	84
4.3 Examples of 7J Single-Loop Reconfigurable Mechanisms with Three or More Operation Modes	87
4.3.1 <i>The 6R Mechanism I and 7R Mechanism I Based on Two Bennett Linkages</i>	87
4.3.2 <i>The 6R Mechanism II and 7R Mechanism II Based on the Two Same Bennett Linkages</i>	95
4.4 Summary	100
 <b>Chapter 5 – Design and Kinematic Analysis of a New 7R Single-Loop Mechanism with Three Specified Operation Modes Based on Sarrus Linkage</b>	 <b>101</b>
5.1 Description of a 1-DOF 7R SLMMRM	101
5.2 Kinematic Analysis and Numerical Example for the 7R SLMMRM	102
5.2.1 <i>D-H Parameters for the Mechanism</i>	103
5.2.2 <i>Solutions for the Kinematic Analysis</i>	104
5.3 CAD Model and Prototype Verification	109
5.3.1 <i>CAD Models for the Real Solutions</i>	110
5.3.2 <i>Building Prototypes to Verify Real Solutions</i>	112
5.4 Operation Modes and Transitional Configurations	114
5.5 Algebraic Approach	116
5.6 Summary	119
 <b>Chapter 6 – Design and Analysis of a New 7R Single-Loop Mechanism with 4R, 6R and 7R Operation Modes Based on Line and Plane Symmetrical Bricard Linkage</b>	 <b>121</b>
6.1 Design of a Novel 7R SLMMRM	121
6.1.1 <i>Bricard 6R Linkage</i>	121
6.1.2 <i>A New 7R SLMMRM</i>	123
6.2. Kinematic Analysis of the 7R SLMMRM	124
6.3 Configuration Verification	128
6.3.1 <i>CAD Models Configurations for Verification</i>	128
6.3.2 <i>Prototype for the New 7R SLMMRM</i>	131
6.4 Transition Configurations	134
6.5 A New 6R Overconstrained Mechanism as a By-Product	137
6.6 Summary	137

<b>Chapter 7 – Conclusions</b>	138
7.1 General Conclusions	138
7.2 Main Contributions	139
7.3 Future Work	140
<b>Appendix I – Constraint Equations of Other Serial Kinematic Chains</b>	141
<b>Appendix II – Expressions of <math>S_1</math>, <math>S_2</math> and <math>S_3</math> in the Algebraic Approach in Chapter 5</b>	176
<b>Appendix III – Kinematic Analysis of Multi-Loop Multi-Mode Reconfigurable Mechanisms</b>	181
A.III.1 Unifying the Constraint Equations of Serial Chains with Transformations in the Base and Moving Frames	181
<i>A.III.1.1 Transformation in the Base</i>	181
<i>A.III.1.2 Transformation in the Platform</i>	184
<i>A.III.1.3 Obtaining Complete Constraint Equations for a Parallel Mechanism by Unifying Transformations in the Base and Moving Platform</i>	186
<i>A.III.1.4 An Example of Obtaining Complete Constraint Equations for a Leg of a Parallel Mechanism</i>	186
A.III.2 Kinematic Analysis of a 3-RRRR MMRM	189
<i>A.III.2.1 Description of the MLMMRM</i>	189
<i>A.III.2.2 Motion Patterns of the 3-RRRR MMRM</i>	191
<i>A.III.2.3 Kinematic Analysis of the 3-RRRR MMRM</i>	192
A.III.3 Summary	193
<b>References</b>	194

## List of Abbreviations

End-Effector: EE

Degree of Freedom: DOF

Reconfigurable Parallel Mechanism: RPM

Constant-Velocity Coupling: CVC

Metamorphic Mechanism: MM

Mechanism with Variable Topologies: MVT

Kinematotropic Mechanism: KM

Kinematic Constraint: KC

Displacement Group: DG

Kinematic Pair: KP

Discontinuously Moveable Mechanism: DMM

Multi-Mode Reconfigurable Mechanism: MMRM

Single-Loop Multi-Mode Reconfigurable Mechanism: SLMMRM

Multi-Loop Multi-Mode Reconfigurable Mechanism: MLMMRM

Joint: J

Revolute: R

Single-Loop Overconstrained Mechanism: SLOM

Devavit-Hartenbergh: D-H

Segre Manifold: *SM*

## List of Publications

- [1] **Xiuyun He**, Xianwen Kong\*, Guangbo Hao, James Ritchie, 2015, “Design and Analysis of a New 7R Single-loop Linkage with 4R, 6R and 7R operation Modes”, *The Third IEEE/IFToMM International Conference on Reconfigurable Mechanisms and Robots*, Beijing, China. (**Best student paper award**) Also to be published as a book chapter in *Advances in Reconfigurable Mechanisms and Robots II* (Edited by X. Ding et al) by Springer
- [2] **Xiuyun He**, Xianwen Kong\*, Damien Chablat, Stephane Caro, Guangbo Hao, 2014, “Kinematics Analysis of a Single-Loop Reconfigurable RRRR-RRR Mechanism with Multiple Operation Modes”, *Robotica*, 32(7):1171-1178.
- [3] Guangbo Hao\*, Haiyang Li, **Xiuyun He**, Xianwen Kong, 2014, "Conceptual Design of Compliant Translational Joints for High-precision Applications", *Frontiers of Mechanical Engineering*, 9(4):331-343.
- [4] Guangbo Hao\*, Xianwen Kong, and **Xiuyun He**, 2014, “A Planar Reconfigurable Linear Rigid-Body Motion Linkage with Two Operation Modes”, *Proceedings of the IMechE, Part C: Journal of Mechanical Engineering Science*, 228(16): 2985–2991.

## Chapter 1 – Introduction

Mechanisms include serial and parallel types as well as their combined hybrid type. Open-loop serial mechanisms are commonly used in industry. They are usually composed of a number of rigid links which are connected one by one through kinematic joints with an end-effector (EE) at the end of the last link. A typical serial robot in industry is the pick-and-place robot called the SCARA robot as shown in Fig. 1.1.



Figure 1.1 A SCARA robot [1]

Parallel mechanisms/manipulators manipulate objects using two or more arms forming a single closed-loop or multiple closed-loops in order to fulfil a task. Compared to serial mechanisms, although having smaller workspace, parallel mechanisms have several advantages such as faster dynamic performance, higher rigidity and higher accuracy, therefore they have attracted increasing interest in both industry and academia [2-7].

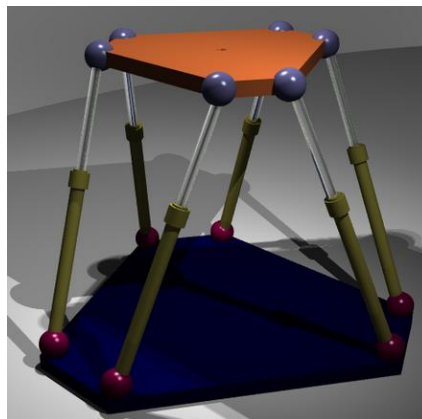
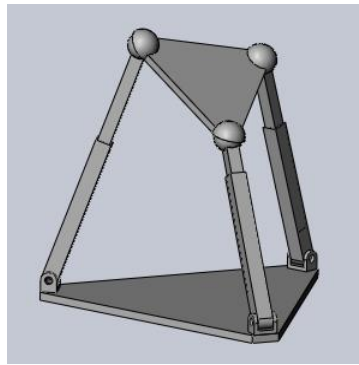


Figure 1.2 Gough-Stewart robot [8]

A successful application of parallel mechanisms can be found in training simulators. The best known parallel manipulator constructed by six serial chains is used to support a movable base for flight or automobile simulators (Fig. 1.2). This mechanism is called the Gough-Stewart platform in recognition of the engineers who first designed and used them. Additionally, parallel mechanisms have wide applications in variable environments, such as assembly devices of printed circuit boards, micro manipulators mounted on the EE of larger but slower serial manipulators, and high speed/high-precision milling machines.

However, most of the multi-DOF (degree of freedom) parallel mechanisms proposed before have a unique configuration meaning that a mechanism has only one motion pattern as shown in Fig. 1.3.



(a) 3-DOF RPS (R: revolute, P: prismatic, S: spherical) with 2R1T (R: rotation, T: translation) motion pattern



(b) 4-DOF UPU (U: universal, P: prismatic) with 3T1R (T: translation, R: rotation) motion pattern

Figure 1.3 Parallel mechanisms with one motion pattern

With the development of science and technology applications in this field and the challenges of work requirements, it would be beneficial if parallel mechanisms could generate different operation modes to fulfil variable tasks based on a single mechanism, i.e., “Reconfigurable Parallel Mechanism (RPM)”. In 1978, a RPM had been revealed which was applied in a constant-velocity coupling (CVC) [9]. This parallel mechanism can be used as a CVC connecting intersecting axes; while on the other hand, it can be used as a CVC connecting parallel axes after changing its configuration. This has made people realize that mechanisms can be designed in such a way that they can be reconfigured to complete different tasks. This mechanism can be considered to be the first reconfigurable mechanism in use. Since the RPMs have the potential to implement multiple functions which helps lower the cost and save time during the work process, then from the middle of 1990s, the study of RPMs has been gradually increased due to



their high effectiveness. The research on RPMs has been identified to be a significant and vital direction in robotics in the new century [10-45, 49-58].

According to the Grubler-Kutzbach mobility criterion [9] and modified mobility criterion, the mobility of a mechanism is determined by the number of links and joints and the constraints of the joints. If one or more of these criteria are modified, the mobility of the mechanism is also changed. There are some obvious ideas that people can easily recognize to configure a mechanism having several operation modes, such as changing the effective number of links or joints or changing the kinematic types of certain joints. In addition, there are other methods to construct reconfigurable mechanisms.

There are several distinguished classes of RPMs according to different concepts including modular reconfigurable mechanisms [10-13], kinematotropic mechanisms [14-24], mechanisms with variable topologies [25-31], metamorphic mechanisms [32-38], discontinuously moveable mechanisms [39-43] and multi-mode reconfigurable mechanisms [44-45, 55-58]. These RPMs will be introduced in detail in the following section.

## **1.1 Classes of RPMs**

In this section, several classes of RPMs will be investigated from their concept and construction with their advantages and disadvantages identified.

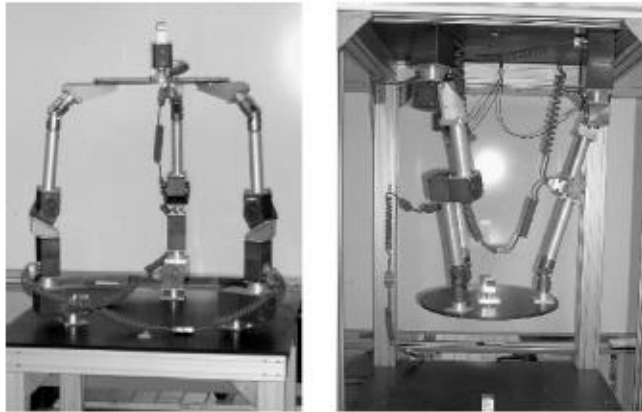
### ***1.1.1 Modular Reconfigurable Mechanisms***

A modular parallel robotic system is defined as: “A modular parallel robotic system consists of a collection of individual standard units that can be assembled into various robot configurations for a diversity of task requirements.” [10] The standard units of this class of Modular Reconfigurable Mechanisms could be actuator modules, passive-joints modules, custom-designed links and mobile platform as shown in Fig. 1.4. Due to its modularity, a modular parallel mechanism may have unlimited configurations. They can be disassembled and reassembled to form morphologies that are suited for a variety of given tasks. Their shapes and structures can be changed by rearranging the connectivity of their parts to adapt to new circumstances and perform new tasks, or recover from damage [11-13]. Since the system is composed of many repeated parts, a

faulty part can be discarded and replaced with an identical one. However, all these operations need manual completion and more time.



(a) Actuator modules and passive-joint modules



(b) Two assembled 3-legged modular parallel robots

Figure 1.4 Reconfigurable modular parallel mechanisms and their modules [11]

Some researchers focus on modular self-reconfigurable robots which have an ability to change robot configuration without external help as shown in [12, 13]. These robots can repair themselves by replacing a faulty part using a spare part, which is useful in realizing flexible and reliable robotic systems; however, there is complexity associated with organising the control of such modular structures.

### ***1.1.2 Metamorphic Mechanisms***

A Metamorphic Mechanism (MM) is a variable topology mechanism [14] which implements a number of transitions among its basic mechanical linkages to realize its multiphase functions due to complex working conditions. The study of MMs started in 1998 when Dai and Rees Jones proposed MMs [15] with changeable topologies. Since then, many researchers have been pursuing the research of MMs. In 2000, Parise et al. developed orthogonal-planar MM [16]. In 2004, Liu and Yang [17] investigated the characteristics of the MMs and explored three approaches to construct the topologies of

them. Carroll, working with Magleby and Howell [18], made a step change by introducing the concept of the metamorphic process in manufacturing three dimensional structures. Then Wang and Dai proposed metamorphic characteristics and set up a metamorphic equation to represent configuration changes [19, 20]. The methods for the synthesis and configuration design of MMs were developed in [21] based on biological modelling and genetic evolution with biological building blocks. A famous example of MMs is a novel robotic hand with a metamorphic palm (Fig. 1.5) which has challenged the traditional structure of a robotic hand [22].

The basic principles and strategies for producing MMs are to change the topology or configuration of a mechanism by [23, 24]: (a) changing the effective numbers of links or joints, (b) changing the kinematic types of certain joints, (c) changing the adjacency and incidence of links and joints and (d) changing the relative arrangement between joints.

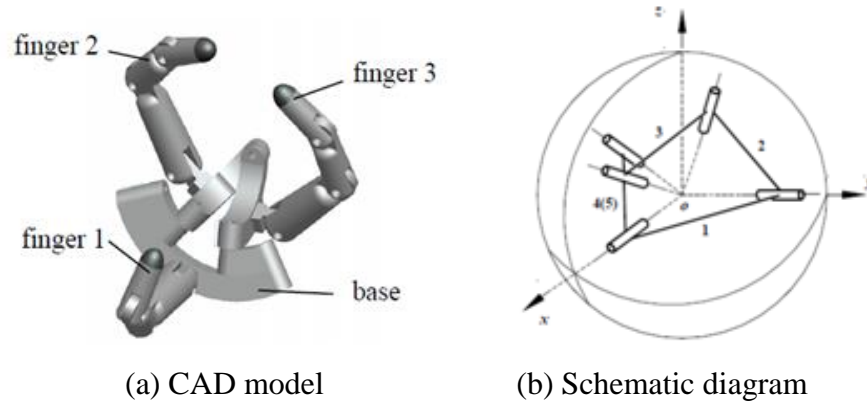


Figure 1.5 A metamorphic robotic hand [22]

Figure 1.5(a) shows a metamorphic robotic hand that is developed based on the principle mentioned above. It is essentially a spatial five-bar linkage as shown in Fig. 1.5(b). This metamorphic-palm is a spherical linkage attached with fingers. The base link is the link where finger 1 is mounted. There are two cranks on both sides of the base. The palm is foldable meaning that its operation changes the configurations that it can complete different pinching and twisting tasks. An advanced KCL metamorphic robot hand was developed which can fold complex origami carton box [134,135], this articulated mechanism greatly enhances the dexterity of the hand allowing it to perform tasks that require dexterous manipulation of objects.

### 1.1.3 Mechanisms with Variable Topologies

With topologies being changeable during the operation of a mechanism when dealing with some complicated tasks, such a mechanism is called a Mechanism with Variable Topologies (MVT) [25-27]. They can be seen as a kind of RPM due to their continuously changing motion patterns. Examples of MVTs include legged walking machines and button stopper locks which are functional based on their variable kinematic joints. A variable kinematic joint is one that can change its topologies during the operation of the mechanism. Generally, the fundamental concept of a variable kinematic joint includes: (a) changing the kinematic pair type as shown in Fig. 1.6; (b) changing the kinematic joint orientation as illustrated in Fig. 1.7. Therefore, the basic concept of the MVTs and part of the concept of MMs are coincident.

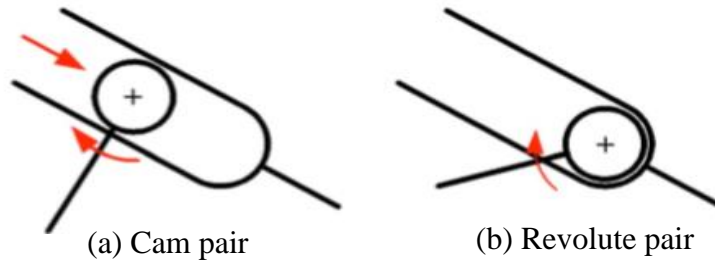


Figure 1.6 Variable types of kinematics pairs [28]

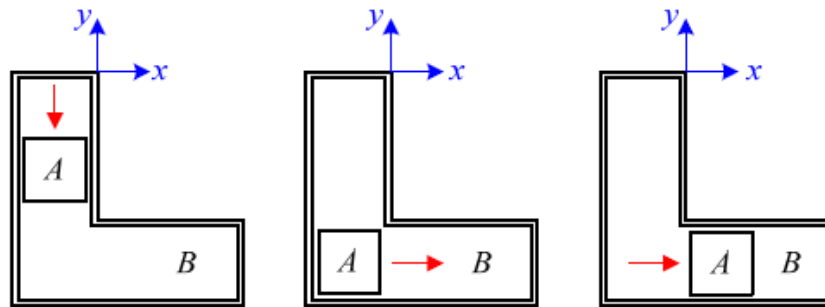


Figure 1.7 Change of representative motion direction of joint [28]

In [28], Yan and Kuo undertook a systematic investigation of the representation of topologies and characteristics of variable kinematic joints. They proposed a logical foundation for the synthesis of variable kinematic joints and MVTs. The topologies characteristics appear to have the ability of reversibility, continuity, variability of DOFs, expansibility and so on. New mechanisms can be created based on the theory, for an example, a new key chain had been created according to the expansibility of variable topologies as demonstrated in Figs. 1.8 and 1.9 [28]. In additional, Yan and Kuo studied

the structure and motion state representations and identifications of MVTs [29]. The variable mobility depending on their configuration singularity was then investigated based on screw theory [30]. In 2009, Yan et al [31] presented a systematic method of synthesizing all possible configurations of MVTs in terms of topological constraints, coordinate sequence of motion characteristics and the mobility criterion at each stage.

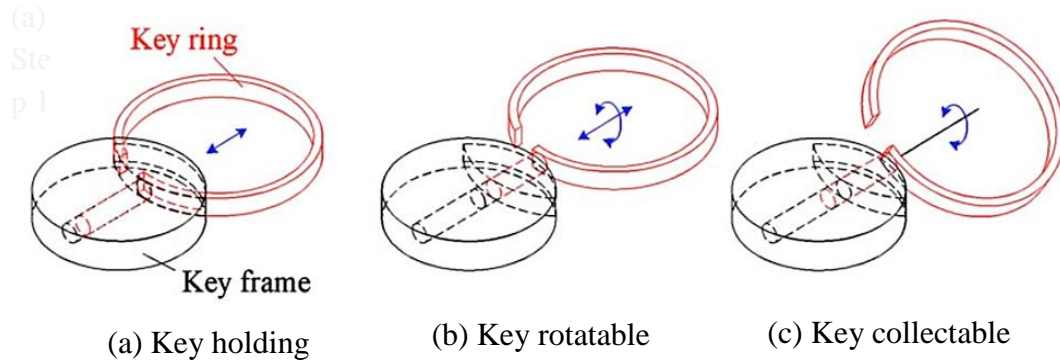


Figure 1.8 A two-member key chain [28]

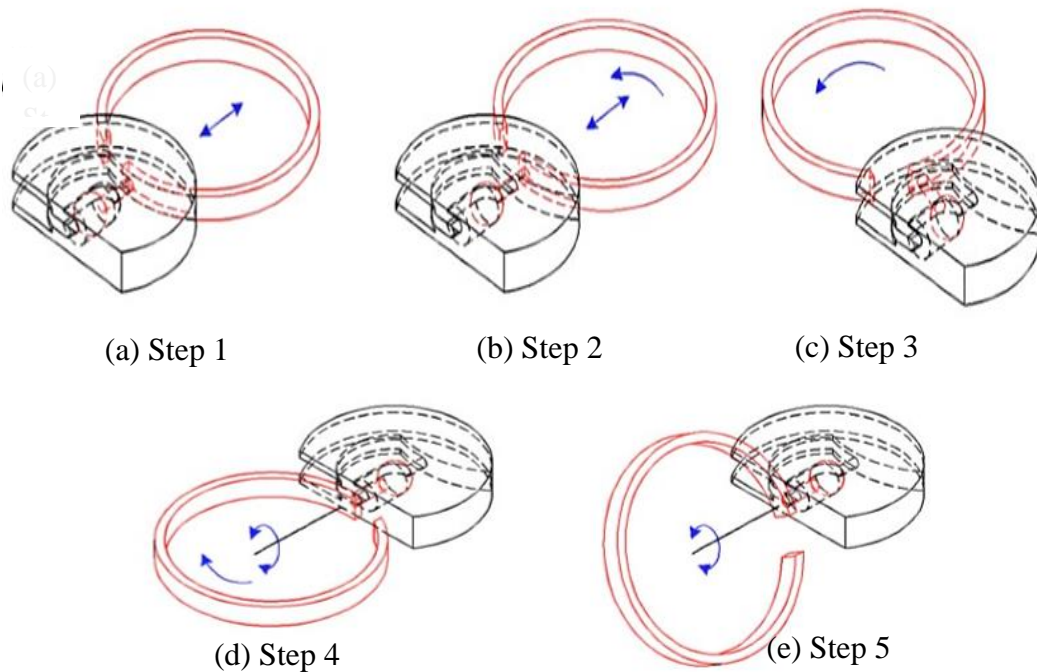


Figure 1.9 A newly created two-member key chain according to expansibility of variable topologies [28]

#### 1.1.4 Kinematotropic Mechanisms

The study of Kinematotropic Mechanisms (KMs) started in 1996 when Wohlhart investigated the kinematotropic linkage together with the position parameter variation [32]. The definition of KMs can be described as follows: “The chains in which changes

in certain position variables can lead to changes in the permanent finite motilities of the chains”, this property is called “kinematotropy”. [32]

The design of KMs began with the considerations of two couples of links:  $a_1$  and  $b_1$ , as well as  $a_2$  and  $b_2$ , which are connected by Kinematic Constraints (KCs),  $KC_1$  and  $KC_2$ , generating their Displacement Groups (DGs),  $DG_1$  and  $DG_2$ , respectively. Links  $a_1$  and  $a_2$ , as well as  $b_1$  and  $b_2$  can be connected by kinematic pairs or chains to form a closed chain  $a_1-KC_1-b_1-b_2-KC_2-a_2-a_1$  as shown in Fig. 1.10. The in-parallel constraint between  $a_1-a_2$  and  $b_1-b_2$  can be obtained from the intersection of  $KC_1$  and  $KC_2$ , generating the DG from the intersection of  $DG_1$  and  $DG_2$ . The type and properties of the intersection DG depend on  $DG_1$  and  $DG_2$ , there is a possibility that  $DG_1$  and  $DG_2$  may have more than one distinct intersection group. Therefore, by changing the connection types between links  $a_1$  and  $a_2$ ,  $b_1$  and  $b_2$ , one can change the relationship between the two kinematic chains to obtain different intersections of DG which means that a mechanism can complete different operation modes according to the connection Kinematic Pairs (KPs).

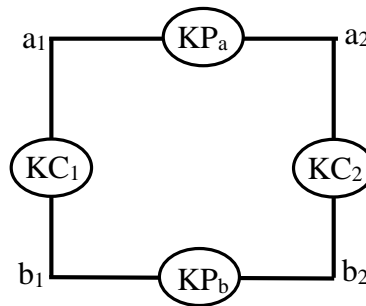


Figure 1.10 Structure schematic diagram of KMs

More generally, a KM can move in a branch of continuous positions and then change into another branch of continuous position by passing through a singular configuration of the mechanism, which are similar to Kong’s work on the single-loop mechanism with variable-DOFs [126]. Note that different numbers and different locations of drivers for a KM may be used in different branches. An example belonging to this type of KM has been presented at the Fifth International Symposium on Advanced in Robot Kinematics (Fig. 1.11); this can vary from two to three DOFs through a change of its configuration by driving its joints in a suitable sequence. This mechanism is composed of eight revolute joints with the following arrangement: the axes of revolute Joints A, B and C are parallel; the axes of revolute Joints D, E and F are parallel; the axes of revolute Joints G and H are coincident and perpendicular to the two pair of axes mentioned previously, as illustrated in Fig. 1.11(a). The mechanism can achieve a configuration as

shown in Fig. 1.11(b) where the axes of A, B, C and D, E, F are parallel to each other. By rotating C and D, the axis of G can be changed to another orientation not coinciding with H (Fig. 1.11(c)). Then another branch of motion can be obtained. Note that the DOFs for the two branches of motion are two and three, respectively.

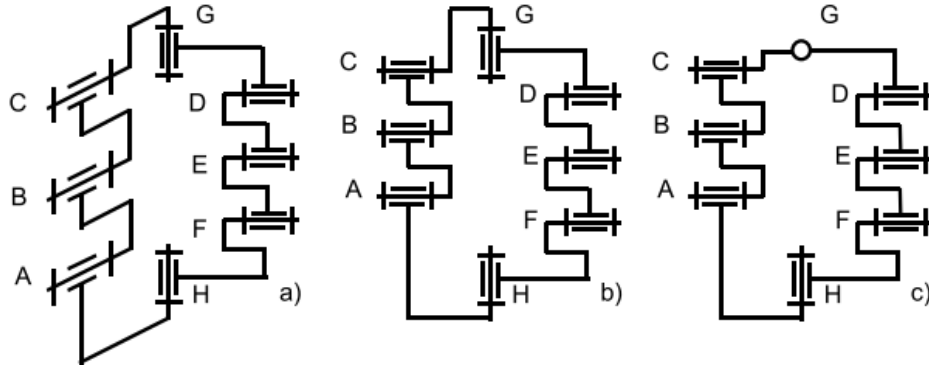


Figure 1.11 Single-loop kinematotropic mechanism [33]

In [34], another definition for the KMs is presented, i.e., chains in different closures represent different numbers of DOFs. According to this definition, the number of DOFs of a KM can be predictably changed after disassembling and reconnecting. A more general definition may contain more chains: the DGs of at least one of their links or their invariant properties are changed in different branches even through the permanent mobility of the sub branches do not change [35].

Traditional research into KMs was mainly to consider their theoretical aspects, with the synthesis and analysis of KMs implemented in [33, 35-37]. In [33], a systematic approach was proposed based on the theory of DGs to form single-loop KMs. Four basic single-loop kinematotropic chains can be obtained, one of which can have one or two DOFs while the other three can have two or three DOFs. This [33] also showed how chains could be modified to obtain various KMs. Starting from single-loop KMs, a method for the synthesis of single-loop KMs was extended to assemble multi-loop KMs. Reference [37] reported a method to construct multi-loop KMs with different numbers of DOFs, with several examples being presented.

A spatial single-loop KM was proposed [38] to be used for a biped/wheeled switchable robot with two modes. It is used as a biped robot within one of its branches, and the switch process between two modes realized in the other branch.

### 1.1.5 Discontinuously Moveable Mechanisms

In 2000, Lee and Herve [39-43] proposed the concept of Discontinuously Moveable Mechanisms (DMMs) where some properties of discontinuous mobility can be

considered as those of the generalised kinematotropy. Generally, the discontinuously movable configuration of single-loop spatial mechanism occurs as two or more independent manifolds or subgroups are involved in the same kinematic loop. In [40], three discontinuously moveable 6R mechanisms were provided including the famous Sarrus 6R mechanism, a hybrid 6R mechanism formed by the combination of one planar and one spherical 4R chain, and generalised Double-Hooke-joint mechanism. The discontinuously mobility of a mechanism was illustrated based on group theory and group algebraic structure of the displacement set. References [41, 42] presented several discontinuously movable seven-link mechanisms via the group-algebraic approach, such as hybrid planar-spherical 7R, hybrid spherical-spherical 7R, and hybrid planar-planar 6R1P DMMs combined by planar and spherical 4R chains. Discontinuously movable 8R mechanisms were also proposed in [43]. Overall, these DMMs are mostly referred to single-loop mechanisms.

No systematic method has been proposed for the type synthesis of DMMs. However, the development of these DMMs can inspire researchers to carry out an in-depth research on multi-mode reconfigurable mechanisms (MMRMs).

#### ***1.1.6 Multi-Mode Reconfigurable Mechanisms***

A Multi-Mode Reconfigurable Mechanism (MMRM) can generate different motion patterns and switch to a different mode without disassembly or reconnection by just passing through a transition configuration. As mentioned above, the reconfigurable mechanism first used in 1978 is one such mechanism. However, it was not until 2001 that the second MMRM was proposed (Fig. 1.12) in [44, 45], a 3-URU double-Y multi-operation parallel mechanism.

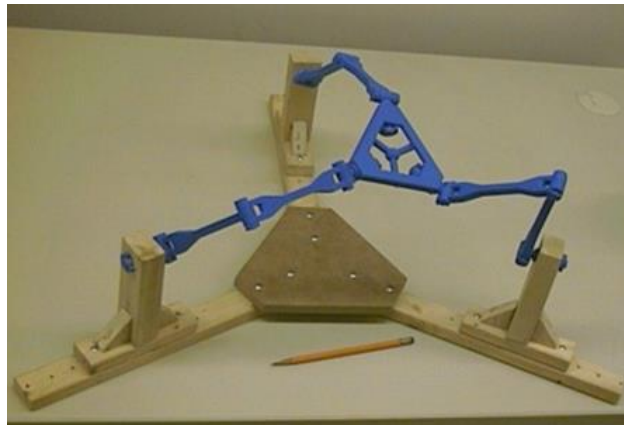


Figure 1.12 Prototype of the 3-URU double -Y multi-operation parallel mechanism [44]



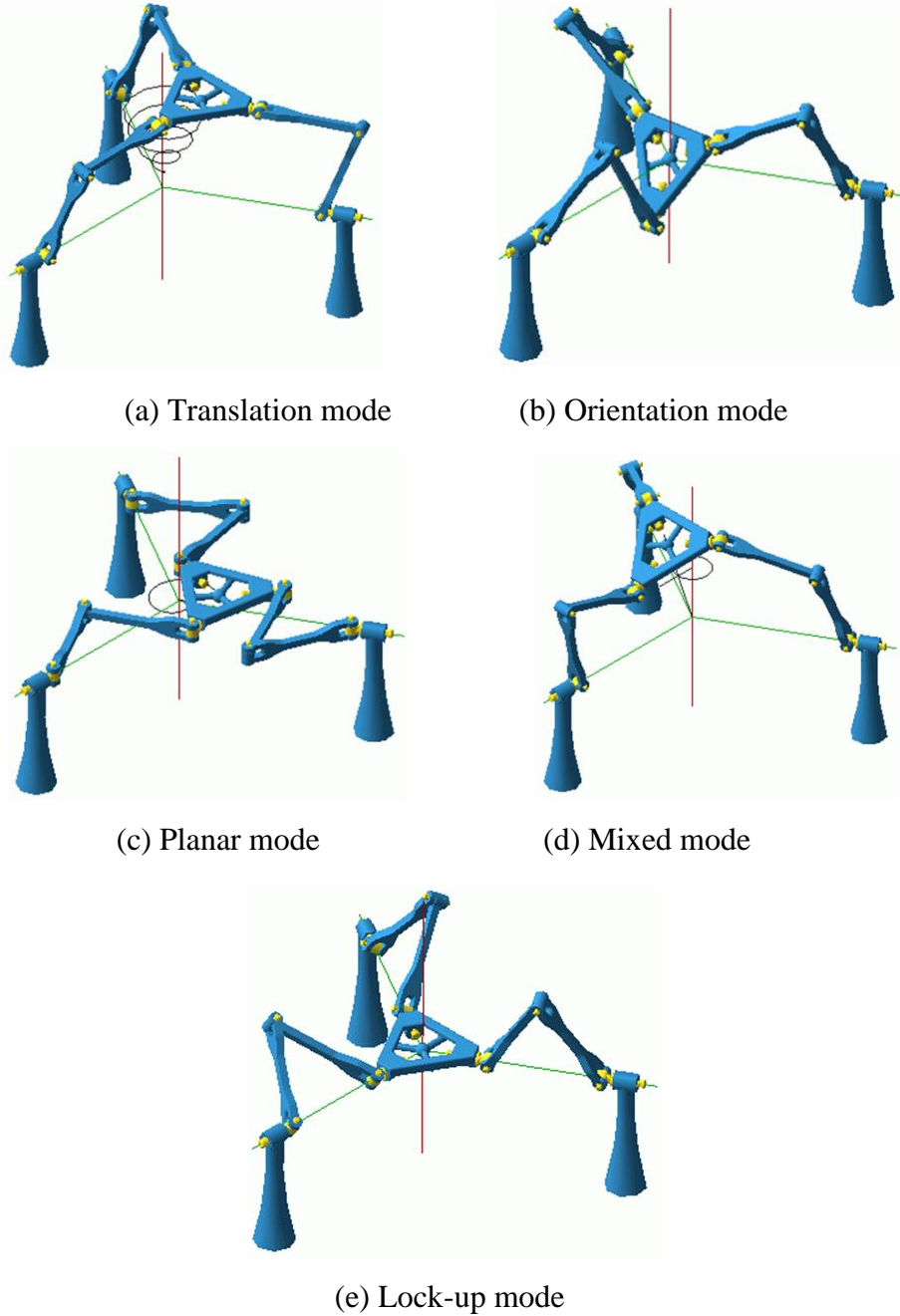


Figure 1.13 Different operation modes for the 3-URU double-Y mechanism [45]

In [45], it is shown that a parallel mechanism with three legs of five R joints could generate a translation mode. In Fig. 1.13(a), the base and the platform have the same orientation and the five R joints in each leg are linearly independent. Then the constraints imposed by each leg on the platform are perpendicular to all five of the R joints. Apart from the platform centre being right above the base centre or the platform being lower than the base, this kind of configuration was originally designed as a positioning mechanism with translation mode. Translation mechanisms of this type (with two U-joints in each leg) were proposed by Tsai [46] and studied by Di Gregorio and Parenti-Castelli [47]. A parallel wrist with three UPU legs was proposed by Karouia

and Herve [48] with a geometry condition that the base R joints intersect at a common point as do the platform R joints. This condition is also satisfied by the double-Y parallel mechanism which turns out to have a rotational mode, as shown in Fig. 1.13(b). When the platform is lowered into the base, all the axes of the R joints in the middle are vertical, i.e., all legs lie in the base (Fig. 1.13(c)). Therefore, the parallel mechanism is recognised to be a 3-RRR planar parallel manipulator. In Fig. 1.13(d), the mechanism enters a new mode of operation where the platform is neither parallel to the base nor with a fixed point. This produces a fourth type of operation mode with three mixed DOFs which is different from the translation, orientation and planar modes. There is still a case in which the base and platform centres coincide: the platform orientation is either zero (Fig. 1.13(e)) or with a turn of 180 degrees and is horizontal and face up, when all the legs can spin independently without the platform moving. This is viewed as a lock-up mode. The operation modes can be observed from the website: <http://www.parallemic.org/Reviews/Review008.html>.

The 3-URU double-Y parallel manipulator allows five fundamentally different types of motion including translational, rotational, mixed, planar, and zero motion modes. The transition between any two modes is possible without disassembly, just needing to encounter a configuration singularity. Consider a case in which both a 3-DOF translational motion and a 3-DOF spherical motion are needed, in order to meet the motion requirements, the following mechanisms can be chosen: (a) a 6-DOF parallel manipulator which can generate translational motion and spherical motion, (b) a 3-DOF translational parallel mechanism generating the translational motion and a 3-DOF spherical parallel mechanism generating the spherical motion and (c) the 3-URU double-Y parallel mechanism or any other parallel mechanism generating both the translational and spherical motion patterns. Choice (c) is obviously better than the other two options.

Kong [132] also presented a parallel mechanism with 15 operation modes including four translational modes, six planar modes, four zero-torsion-rate motion modes and one spherical mode.

MMRMs are also called Parallel Mechanisms with Multi-Furcation of Motions [49-53] or Parallel Mechanisms that Change their Group of Motions [54]. They can generate multiple operation modes to adapt to variable tasks and environment which need fewer actuators and less time to changeover. Therefore, in the last decade, the MMRMs have attracted significant research interest on the design, synthesis and kinematics analysis.

Generally speaking, MMRMs can be classified into two categories: single-loop multi-mode reconfigurable mechanisms and multi-loop multi-mode reconfigurable mechanisms.

### 1) Single-Loop Multi-Mode Reconfigurable Mechanisms

A single-loop multi-mode reconfigurable mechanism (SLMMRM) is a single-loop mechanism which works as a different single-loop mechanism in each one of its operation modes. It can be regarded as both an extension and development of DMMs, by involving two or more operation modes in one single-loop mechanism. There are limited DMMs being built based on the idea of combining two-less-joint overconstrained mechanisms, but more SLMMRMs are being proposed. 18 classes of single-loop single-DOF reconfigurable mechanisms with two operation modes have been presented using Kong's intuitive method [55] based on screw theory including two classes proposed as DMMs and 16 totally new classes.

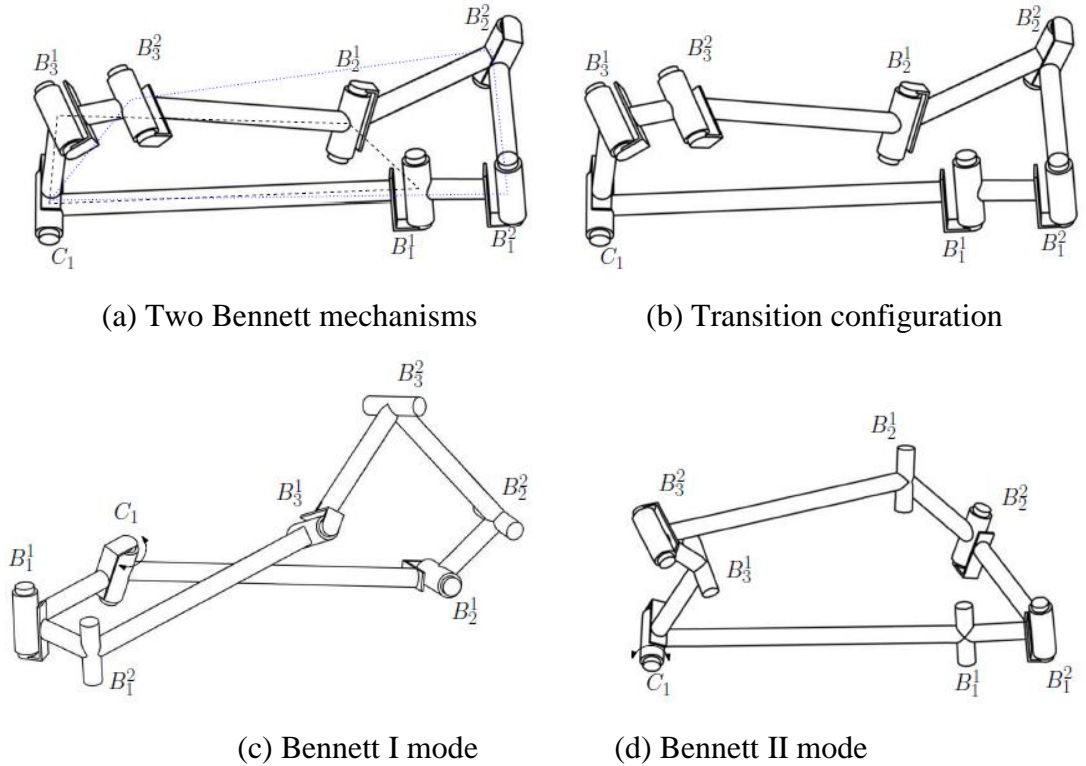


Figure 1.14 A 7R SLMMRM with at least two 4R Bennett modes [55]

Figure 1.14 shows a 7R multi-mode single-loop mechanism with at least two operation modes which was constructed based on two Bennett linkages with one common revolute joint. In one operation mode it acts as the Bennett linkage I (Fig. 1.14(c)), and in the other mode it works as the Bennett linkage II (Fig. 1.14(d)). Figure

1.14(b) displays the transition configuration where the 7R SLMMRM transits from one mode to the other mode. It has been revealed in [110,127] that the mechanism also has a 7R mode.

In [126], variable-DOF single-loop 7R and 8R reconfigurable mechanisms are proposed by inserting two joints to planar 5R and 6R mechanisms respectively. Take the variable-DOF single-loop 7R reconfigurable mechanism as an example, two R joints (A and B) are located on a plane that is parallel to the axes of R joints of the planar 5R mechanism as shown in Fig. 1.15. The new 7R mechanism has two operation modes: in one mode it acts as a two-DOF planar 5R mechanism where the two added joints are inactive; while in the other mode it acts as a single-DOF spatial single-loop 7R mechanism.

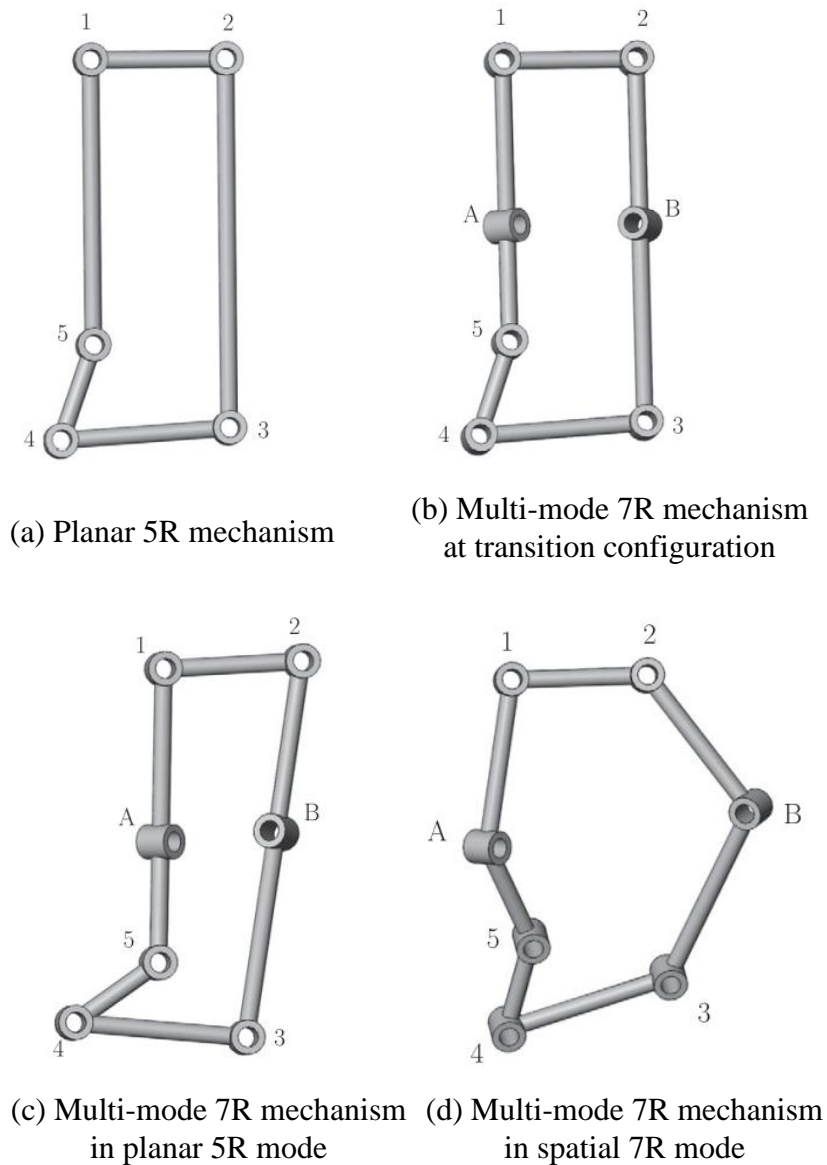


Figure 1.15 A multi-mode 7R mechanism with 1 and 2 DOFs [126]

Through detailed understanding of the above SLMMRMs, a more in-depth study of multiple modes multiple-loop reconfigurable mechanisms is possible.

## **2) Multi-mode Multiple-Loop Reconfigurable Mechanisms**

A multi-loop multi-mode reconfigurable mechanism (MLMMRM) is a multi-mode mechanism with more than two legs (multi-loop) which works as a different mechanism in each of its operation modes. Kong has proposed a systematic method for the type synthesis of MLMMRMs based on screw theory [56]; according to the definition, a MLMMRM is a parallel mechanism that can generate different motion patterns with multi-DOFs. There are several motion patterns having the same number of DOFs. For instance, planar motion, spatial translation and spherical motion are the motion patterns with 3-DOFs. Being aware of this point, many MLMMRMs with the same number of DOFs in different operation modes have been proposed. Three steps can be used to obtain a MLMMRM. Firstly, for each of the motion patterns to be generated, one can perform the type synthesis of legs of the parallel mechanism with a single operation mode. Secondly, synthesis of legs for parallel mechanisms with other operation modes at its transition configuration is performed. Finally, MLMMRMs can be obtained by assembling the legs for parallel mechanisms with multiple operation modes. In [57], type synthesis of 3-DOF parallel mechanisms with both a planar operation mode and a spatial translational operation mode were completed. Type synthesis of variable DOF parallel mechanisms with both planar and 3T1R operation modes were undertaken in [58].

### ***1.1.7 Remarks***

By analysis and comparison of the above reconfigurable mechanisms, it can be found that common basic concepts exist but with certain differences. The MMs and MVTs both focus on variable mechanism topologies or the variable kinematic joints topologies. The common properties of KMs, DMMs and MMRMs are mechanisms that can change their motion patterns through singular/transition configurations. However, KMs, DMMs and MMRMs have specific distinctions as follows: (a) KMs derived from the theory of DGs and MMRMs are mainly obtained through screw theory. There is a lack of systematic type synthesis method for DMMs that can be considered as KMs or SLMMRMs. (b) There is a wider research scope for KMs according to their definitions, and most of those are mechanisms with changeable numbers of DOFs in different

modes; while MMRMs may have the same or different number of DOFs in different operation modes. The novel research into MMRMs contained in this thesis concentrates on SLMMRMs with the same number of DOFs in different modes.

In addition, there are more obvious advantages for the application of MMRMs apart from the avoidance of disassembly and reconnecting, which are emphasized as follows:

a) There is no need to add more actuators or change the location of actuators for MMRMs, which is more energy efficient.

b) MMRMs can satisfy the requirements of specific functions, which is design effective. For example, if a 4R motion pattern and a 6R motion pattern are both needed in the same work environment; then it will be possible to determine quickly how to combine these two kinds of mechanisms in a proper way in order to develop a single-loop reconfigurable mechanism for the task requirement.

## 1.2 Review of Single-Loop Overconstrained Mechanisms

Planar mechanisms and spatial Single-Loop Overconstrained Mechanisms (SLOMs) are closely related to the synthesis of parallel mechanisms. In [3] the synthesis of parallel mechanisms is reduced to the synthesis of multi-DOF single-loop mechanisms by quoting the concept of a virtual chain to represent the motion patterns. The synthesis of single-loop reconfigurable mechanisms in paper [55] is based on the combination of planar mechanisms and spatial SLOMs. This thesis focuses on the design and analysis of SLMMRMs. Therefore SLOMs are initially reviewed in this section.

A spatial overconstrained mechanism is a linkage that has more DOFs than is predicted by the DOF mobility formula, Kutzbach (or Grübler) mobility criterion [59]. If a single-loop mechanism moves in a three-dimensional space, then the mobility formula is

$$M = 6 \cdot (N - 1 - j) + \sum_{i=1}^j f_i \quad (1.1)$$

where  $N$  is the number of links of the mechanism,  $j$  is the number of the joints and  $f_i$  is the DOF of the  $i$ -th joint.

A general spatial 6J (J: joint, note that in this thesis only R and P joints are considered) mechanism composed of six links and six joints has the mobility:

$$M = 6 \cdot (N - 1 - j) + \sum_{i=1}^j f_i = 6 \cdot (6 - 1 - 6) + 6 = 0 \quad (1.2)$$

The mobility of 5J single-loop mechanisms according to the mobility formula is

$$M = 6 \cdot (N - 1 - j) + \sum_{i=1}^j f_i = 6 \cdot (5 - 1 - 5) + 5 = -1 \quad (1.3)$$

The mobility of 4J single-loop mechanisms according to the mobility formula is

$$M = 6 \cdot (N - 1 - j) + \sum_{i=1}^j f_i = 6 \cdot (4 - 1 - 4) + 4 = -2 \quad (1.4)$$

Therefore, it can be found that the mobile spatial 4J, 5J and 6J single-loop mechanisms are all SLOMs according to Eq. (1.2-1.4). Great advances in the research on spatial SLOMs have been made [60-96]. These mechanisms are now surveyed and compared in the following sections.

### 1.2.1 Planar 4J Mechanisms and Spatial 4J SLOMs

Four-Joint (4J) linkages are composed of four links connected by four one DOF joints forming a loop. The joint may be either a revolute (R) joint, or a Prismatic (P) joint. 4J closed-loop linkages are the simplest moveable linkages, which can be classified into planar 4J, spatial 4J and spherical 4R linkages. There are three basic types of planar 4J linkages depending on the number of R or P joints: planar 4R, planar RRRP and planar PRRP [60] linkages. Most spatial 4J linkage has been identified by Delassus [61]: spatial 4P, spatial RPRP and Bennett linkages (that is spatial 4R linkage).

#### 1) Planar 3R1P mechanism

The planar 3R1P linkage is also called a slider-crank linkage and constructed from four links connected by three revolute and one prismatic joint (Fig.1.16).

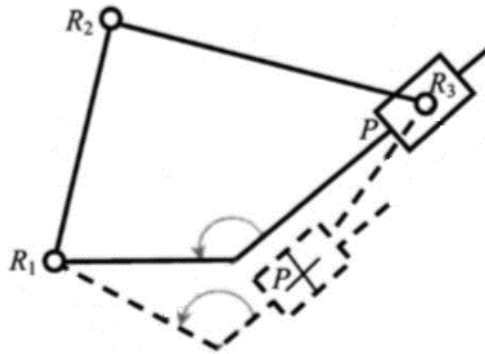


Figure 1.16 Sketch for spherical 3R1P linkage [63]

#### 2) Planar PRRP mechanism

The planar PRRP mechanism is also called a double slider linkage [64] and is constructed by connecting two sliders with a coupler link, as shown in Fig. 1.17.

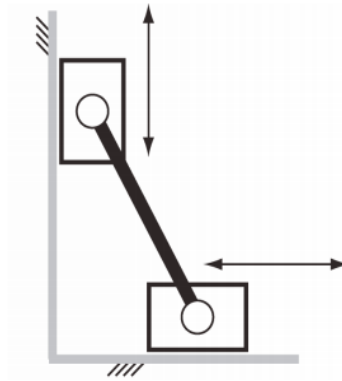


Figure 1.17 Sketch for spherical PRRP linkage [64]

### 3) Planar 4R mechanisms

A planar 4R mechanism is also called the planar quadrilateral linkage. There are 27 cases of planar 4R linkages according to their parameter combinations, examples of some cases are shown in the Fig. 1.18 below:

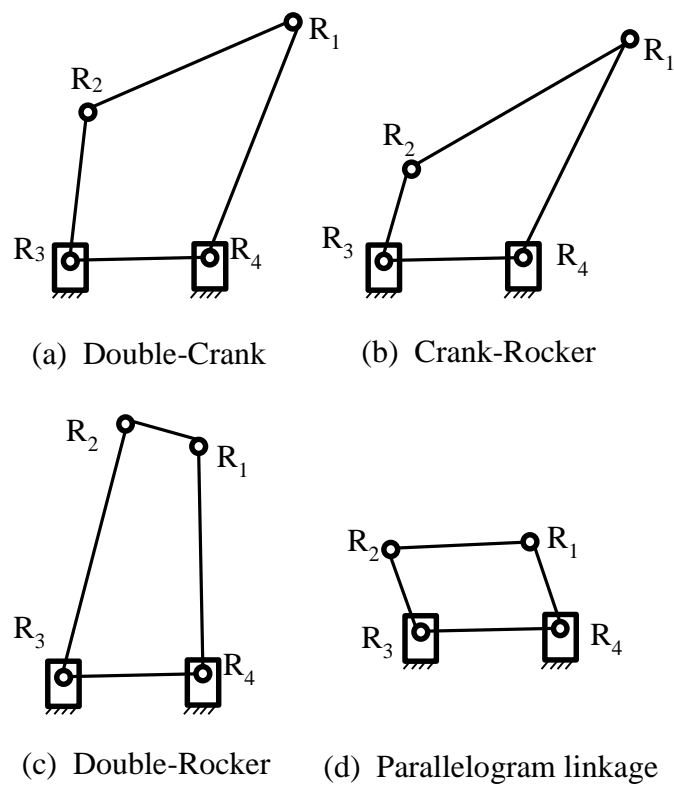


Figure 1.18 Types of four-bar linkages [62]

### 4) RPRP linkage

Generally, the RPRP linkage (Fig. 1.19) can only move in one situation: where the axes of the two R joints are parallel and the two P joints are symmetrical about the plane



through the two R axes [67]. Also there are two types of RPRP linkage: foldable and unfolded, which can be differentiated from the twist angles. The conditions for these linkages are shown below:

$$\begin{aligned}
 a_1 &= a_4, \quad a_2 = a_3 \\
 d_1 &= d_3 = 0, \quad \theta_2 = \theta_4 = \pi \\
 \alpha_1 &= \alpha_2, \quad \alpha_1 + \alpha_3 = \pi = \alpha_2 + \alpha_4
 \end{aligned} \tag{1.5}$$

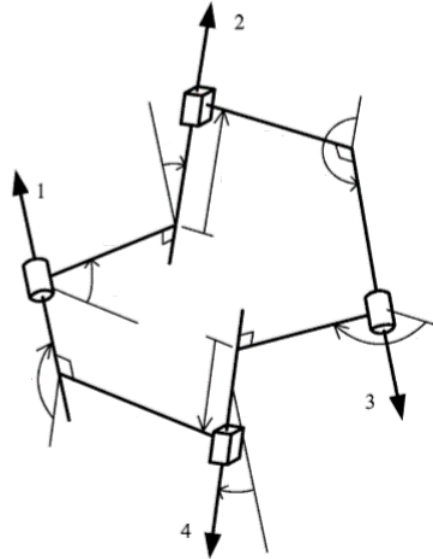


Figure 1.19 General arrangement of RPRP linkage [67]

## 5) Spherical 4R mechanisms

If the linkage is assembled with the four joint axes angled to intersect at a single point and the links move on concentric spheres, then the assembly is called a spherical 4R linkage as shown in Fig. 1.20. In [68], a spherical 4R linkage is described as a combination of two spherical RR dyads: a driving dyad and a driven dyad. The driving dyad is composed of the fixed joint axis O and the moving axis A, whereas the driven dyad is constituted by the fixed joint axis C and the moving axis B. The link lengths of the mechanism are  $\alpha$ ,  $\beta$ ,  $\eta$  and  $\gamma$ , respectively.

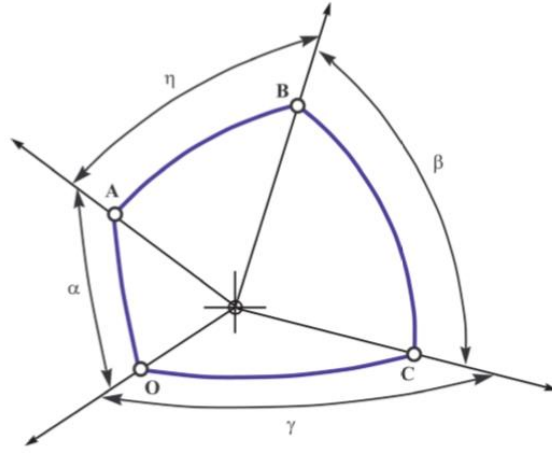


Figure 1.20 Sketch for spherical 4R linkage [68]

## 6) Bennett Mechanisms

The Bennett linkage is an overconstrained spatial four-bar linkage with joints that have their axes angled in such a particular way that it makes the system movable. The Bennett linkage was first proposed in 1903 [65], and in 1914 [66] Bennett issued the conditions for it as a single-loop moveable linkage to have one-DOF mobility:

a) All the offsets are equal to zero, i.e.

$$d_i = 0, (i=1,2,3,4) \quad (1.6)$$

b) Kinematic constraints of the remaining design parameters should satisfy the conditions below:

$$\begin{aligned} a_1 &= a_3, \quad a_2 = a_4 \\ \alpha_1 &= \alpha_3, \quad \alpha_2 = \alpha_4 \\ \frac{\sin \alpha_1}{a_1} &= \frac{\sin \alpha_2}{a_2} \end{aligned} \quad (1.7)$$

c) Besides the above conditions, there are some other implicit relationships that comply with a Bennett linkage, that are always

$$\begin{aligned} \theta_1 + \theta_3 &= 2\pi \\ \theta_2 + \theta_4 &= 2\pi \end{aligned} \quad (1.8)$$

as well as

$$\tan \frac{\theta_1}{2} \tan \frac{\theta_2}{2} = \frac{\sin \frac{1}{2}(\alpha_2 + \alpha_1)}{\sin \frac{1}{2}(\alpha_2 - \alpha_1)} \quad (1.9)$$

where  $\theta_1, \theta_2, \theta_3, \theta_4$  are the angles between the links, as shown in Fig.1.21.

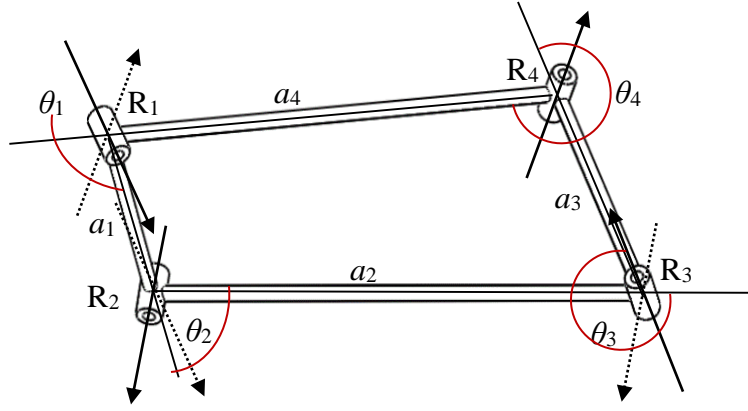


Figure 1.21 Sketch for Bennett linkage

It is one of the most famous SLOMs and a spatial 4J overconstrained mechanism with pure R joints, therefore, it has attracted significant attention from researchers to undertake its analysis and extension. It also forms the foundation to construct most 5J and 6J SLOMs.

### 1.2.2 5J SLOMs

Most spatial 5J SLOMs are well-known as 5R SLOMs, and are almost always constructed based on 4R Bennett mechanisms such as the Goldberg 5R linkage and Myard 5R linkage.

#### 1) Myard linkage

The Myard linkage was found to be the first reported 5R SLOMs and was proposed in 1931 [69, 70]. Two Bennett linkages with one pair of twist angle of 90 degrees were arranged symmetrically before combining them; therefore the Myard linkage is plane-symmetric as shown in Fig. 1.22. It was re-examined by Baker in 1979 who classified it as a special kind of Goldberg linkage. The design parameters for the Myard linkages are

$$\begin{aligned}
 a_1 &= a_5, \quad a_2 = a_4, \quad a_3 = 0 \\
 \alpha_2 &= \alpha_4 = \pi / 2, \quad \alpha_5 = \pi - \alpha_1, \quad \alpha_3 = \pi - 2\alpha_1 \\
 d_3 &= d_4 = 0
 \end{aligned} \tag{1.10}$$

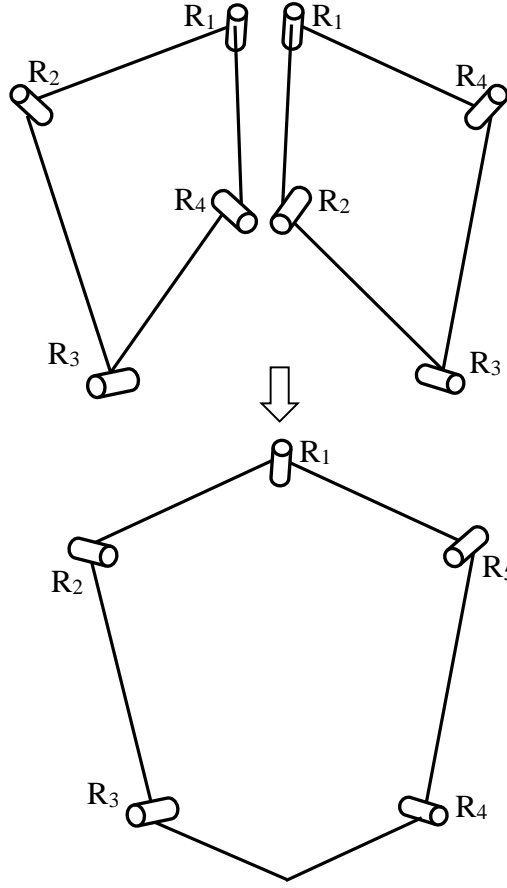


Figure 1.22 Sketch of Myard linkage

## 2) Extended Myard linkage

Chen [71] reported a new 5R linkage according to a method similar to that used to construct a Myard linkage, which is called the extended Myard linkage. This is different from the Myard linkage that the twist angle of the base Bennett linkages does not have to be  $\pi/2$ . Fig. 1.23 illustrates merging two Bennett linkages together. The parameters conditions for the extended Myard linkage are as follows:

$$\begin{aligned}
 a_1 &= a_5, \quad a_2 = a_4, \quad a_3 = 0 \\
 \alpha_2 &= \alpha_4, \quad \alpha_5 = \pi - \alpha_1, \quad \alpha_3 = \alpha_5 - \alpha_1 \\
 d_i &= 0 \quad (i=1,2,\dots,5)
 \end{aligned} \tag{1.11}$$

and

$$\frac{\sin \alpha_5}{a_5} = \frac{\sin \alpha_2}{a_2} \tag{1.12}$$

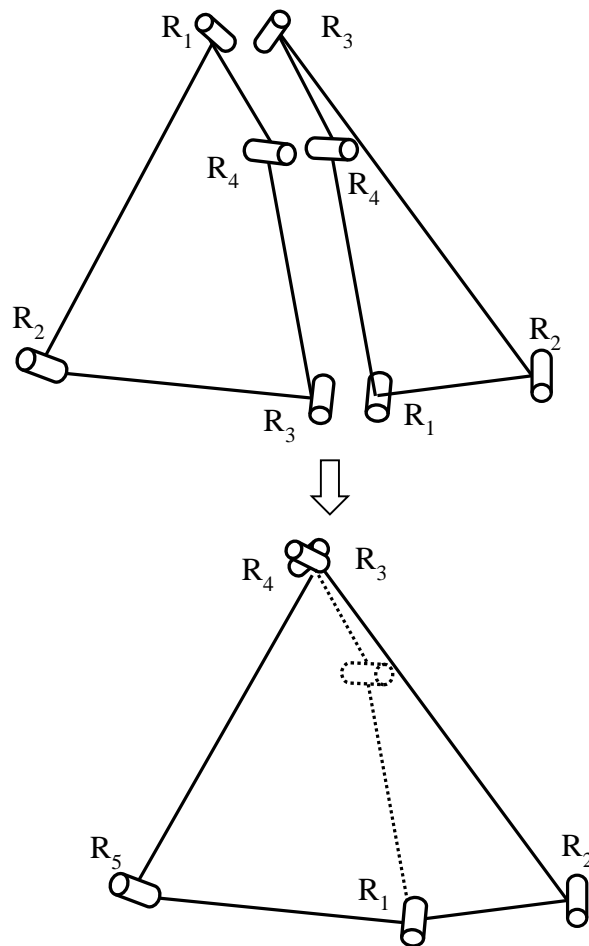
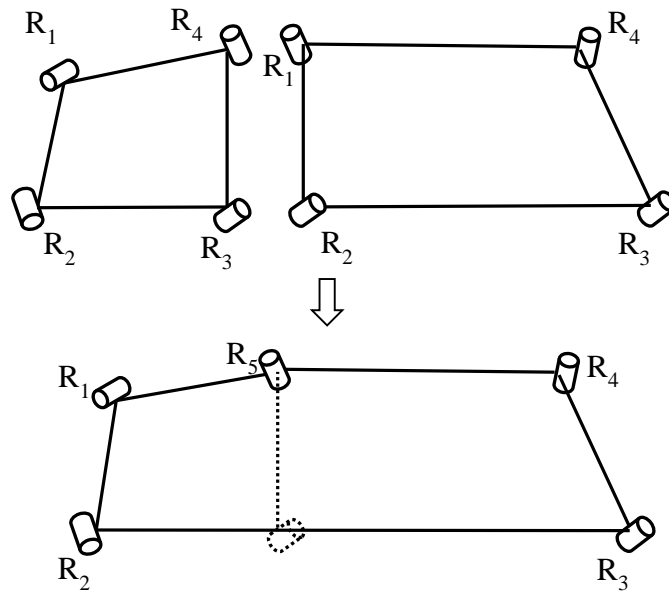


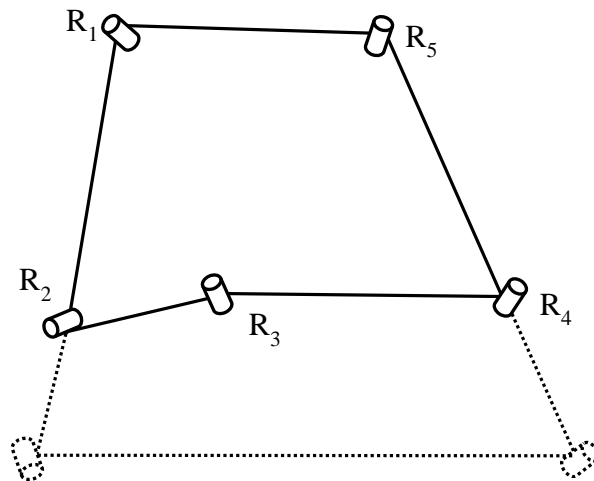
Figure 1.23 The extended Myard linkage by combining two Bennett linkages

### 3) Goldberg linkage

In 1934 Goldberg proposed another 5R SLOMs also based on Bennett linkages [72]. Two kinds of Goldberg linkages were derived as shown in Fig. 1.24. The primary one is constructed from combining two Bennett linkages with a same pair of revolute joints connected by a same length link. The common components are placed coincident with one pair of adjacent links of two Bennett linkages on a straight line. Then the common link and the pair of joints on the straight line can be removed while the other pair of joints are reduced to one single joint (Fig. 1.24 (a)). This method is called “summation”. Thereafter, Goldberg proposed another syncopated 5R linkage based on the summed 5R linkage (Fig. 1.24 (b)), a circumscribing Bennett is joined to the summed 5R linkage which is partly removed to form a new syncopated 5R linkage.



(a) Primary Goldberg 5R linkage



(b) Syncopated Goldberg 5R linkage

Figure 1.24 Goldberg 5R linkage

#### 4) Subtractive Goldberg linkage

An extension of the Goldberg linkage was then proposed using the method called “subtraction” as shown in Fig. 1.25. This is called the subtractive Goldberg linkage [73].

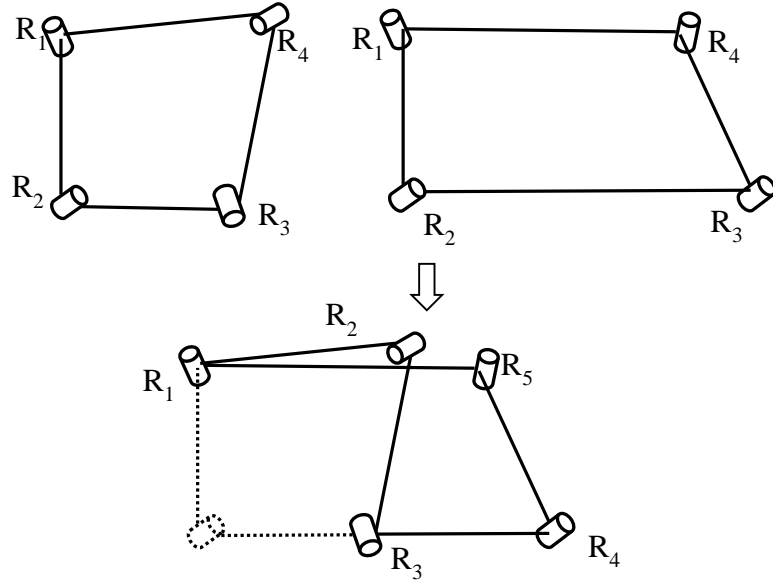


Figure 1.25 Subtractive Goldberg 5R linkage

### 1.2.3 Common 6J SLOMs

A great number of 6J SLOMs have been developed by various researchers, such as 6R, 5R1P and 4R2P SLOMs. The first section will list some examples of 5R1P and 4R2P SLOMs with their associated design parameters [74], followed by a description of the most well-known 6R SLOMs.

#### 1) 5R1P SLOMs

a) 5R1P based on planar and Bennett mechanisms:

$$\begin{aligned} a_5 &= a_6 \\ \alpha_2 &= \alpha_4 = 90^\circ, \alpha_5 + \alpha_6 = \pi \\ d_1 &= d_5, d_4 = -d_3, d_6 = 0, \theta_2 = 0 \end{aligned} \quad (1.13)$$

b) 5R1P based on planar and Bennett mechanisms:

$$\begin{aligned} a_1 &= a_6 \\ \alpha_2 &= \alpha_4 = 90^\circ, \alpha_5 + \alpha_6 = 0 \\ d_1 &= d_5, d_4 = -d_3, d_6 = 0, \theta_2 = 0 \end{aligned} \quad (1.14)$$

c) 5R1P based on planar and Bennett mechanisms:

$$\begin{aligned} \alpha_2 &= -\alpha_1, \alpha_4 = \alpha_5 = 0, \alpha_6 = \pm\alpha_3 \\ \theta_2 &= 0 \end{aligned} \quad (1.15)$$

d) 5R1P based on spherical mechanisms and equal length links:

$$\begin{aligned} a_1 = a_2, a_5 = a_6, a_3 = a_4 = 0 \\ d_1 = d_2 = d_3 = d_4 = d_5 = d_6 = 0 \end{aligned} \quad (1.16)$$

## 2) 4R2P SLOMs

a) 4R2P based on two pairs of parallel revolute joints:

$$\begin{aligned} \alpha_2 = -\alpha_1, \alpha_5 = -\alpha_4, \alpha_6 = \pm\alpha_3 \\ \theta_2 = \theta_5 = 0 \end{aligned} \quad (1.17)$$

b) 4R2P based on two pairs of parallel revolute joints:

$$\begin{aligned} \alpha_1 = \alpha_3 = 0, \alpha_5 = -\alpha_4, \alpha_6 = \pm\alpha_2 \\ \theta_5 = 0 \end{aligned} \quad (1.18)$$

## 3) 6R SLOMs

Most 6J SLOMs are 6R linkages. The first overconstrained mechanism was proposed by Sarrus in 1853 [75, 76], which is a 6R SLOM. In 1927, Bricard linkages, a type of 6R mechanisms proposed in 1897, began to be well recognised [77]. In addition, since the birth of Bennett linkage in 1903 a great number of 6R linkages were developed by different researchers using a combination construction method on it. In 1968, Waldron proposed a method to construct Waldron's hybrid 6R linkages [78]. Besides, Wohlhart not only generalized the Goldberg 5R linkages, he also designed Wohlhart Double-Goldberg linkages based on this [79, 80]. More recently, Baker [81] and Chen [82] reported new classes of 6R linkages, and Song and Chen reported a family of mixed Double-Goldberg 6R linkages [83]. More information on overconstrained 6R linkages can be reviewed.

To better understand overconstrained 6R linkages, they can be classified into four categories: (a) symmetric 6R SLOMs; (b) 6R SLOMs based on Bennett linkages; (c) 6R SLOMs derived or combined by other overconstrained mechanisms; (d) 6R SLOMs with special geometry. Examples of these categories are listed below.

a) Symmetric 6R SLOMs

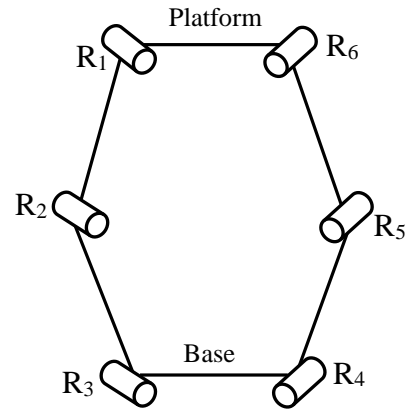
i) Sarrus linkage

The Sarrus linkage is the first reported spatial SLOM as shown in Fig. 1.26. In the mechanism, the base and platform can be mounted by two legs connected by parallel revolute joints  $R_1$ - $R_2$ - $R_3$  and  $R_4$ - $R_5$ - $R_6$  while the direction of two set axes intersected, which allows the platform to move up and down vertically. The two legs can be also arranged to be asymmetric.





(a) Sarrus Linkage [71]



(b) Schematic diagram

Figure 1.26 Sarrus linkage

## ii) Bricard linkages

There are six distinct types of Bricard linkages [84] which can be summarized as follows:

### (1) General line-symmetric Bricard linkage

The joints and links of the Bricard linkage are symmetrical about the centre line, the so called general line-symmetric Bricard linkage as shown in Fig. 1.27. Its parameters are listed below:

$$a_1 = a_4, a_2 = a_5, a_3 = a_6$$

$$\alpha_1 = \alpha_4, \alpha_2 = \alpha_5, \alpha_3 = \alpha_6 \quad (1.19)$$

$$d_1 = d_4, d_2 = d_5, d_3 = d_6$$

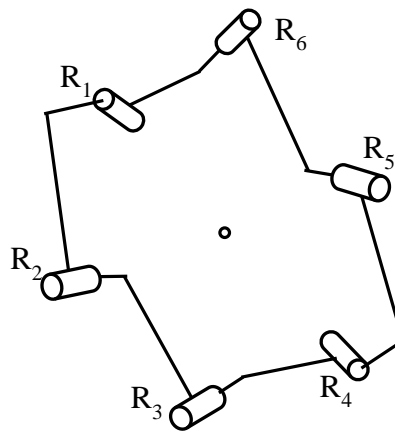


Figure 1.27 Schematic diagram of line-symmetric Bricard linkage

(2) General planar-symmetric Bricard linkage

The general plane-symmetric Bricard linkage is shown in Fig. 1.28 where the structure of it is symmetrical about the plane. The parameters are listed below:

$$\begin{aligned}
 a_1 &= a_6, \quad a_2 = a_5, \quad a_3 = a_4 \\
 \alpha_1 + \alpha_4 &= 2\pi, \quad \alpha_2 + \alpha_5 = 2\pi, \quad \alpha_3 + \alpha_6 = 2\pi \\
 d_1 &= d_4 = 0, \quad d_2 = -d_6, \quad d_3 = -d_5
 \end{aligned} \tag{1.20}$$

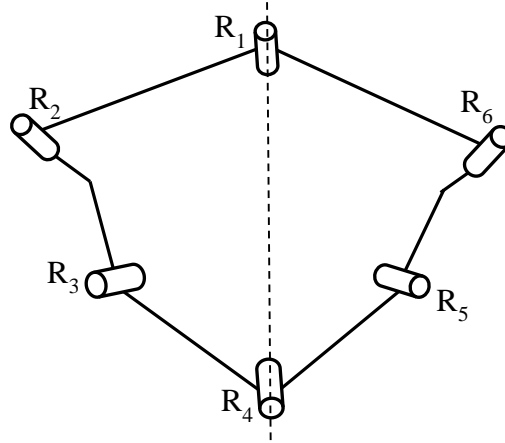


Figure 1.28 Schematic diagram of planar-symmetric Bricard linkage

(3) The trihedral Bricard linkage

A trihedral Bricard linkage's joints are placed on the corners of a cube as shown in Fig. 1.29, its parameters satisfy:

$$\begin{aligned}
 a_1^2 + a_3^2 + a_5^2 &= a_2^2 + a_4^2 + a_6^2 \\
 \alpha_1 = \alpha_3 = \alpha_5 &= \pi / 2, \quad \alpha_2 = \alpha_4 = \alpha_6 = 3\pi / 2 \\
 d_i &= 0, \quad i = (1, 2, \dots, 6)
 \end{aligned} \tag{1.21}$$

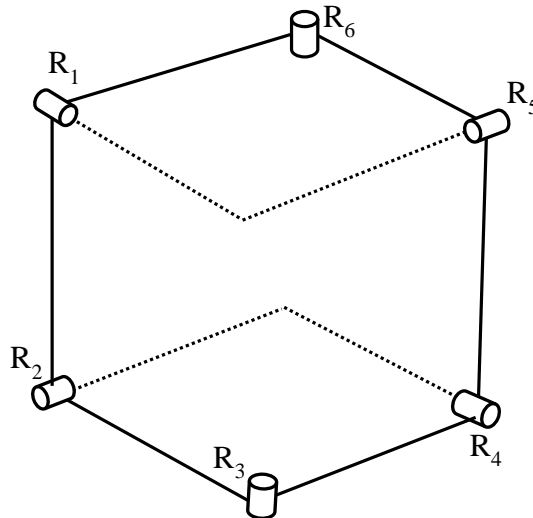


Figure 1.29 Schematic diagram of planar-symmetric Bricard linkage

(4) The line-symmetric octahedral Bricard linkage

The parameters for the line-symmetric octahedral Bricard linkage are:

$$\begin{aligned} a_1 = a_2 = a_3 = a_4 = a_5 = a_6 = 0 \\ d_1 + d_4 = d_2 + d_5 = d_3 + d_6 = 0 \end{aligned} \quad (1.22)$$

(5) The Planar-symmetric octahedral Bricard linkage:

The line-symmetric octahedral Bricard linkage has the parameters:

$$\begin{aligned} a_1 = a_2 = a_3 = a_4 = a_5 = a_6 = 0 \\ d_1 = -d_4, \quad d_2 = -d_1 \frac{\sin(\alpha_3)}{\sin(\alpha_1 + \alpha_3)}, \quad d_5 = d_1 \frac{\sin(\alpha_6)}{\sin(\alpha_4 + \alpha_6)} \\ d_3 = d_1 \frac{\sin(\alpha_1)}{\sin(\alpha_1 + \alpha_3)}, \quad d_6 = -d_1 \frac{\sin(\alpha_6)}{\sin(\alpha_4 + \alpha_6)} \end{aligned} \quad (1.23)$$

(6) The doubly collapsible octahedral Bricard linkage

The parameters for the line-symmetric octahedral Bricard linkage are listed as below:

$$\begin{aligned} a_1 = a_2 = a_3 = a_4 = a_5 = a_6 = 0 \\ d_1 d_3 d_5 + d_2 d_4 d_6 = 0 \end{aligned} \quad (1.24)$$

In addition to the 6R Bricard linkages listed above, Wohlhart's isomerization method was used to construct three variants of Bricard line-symmetric 6R linkage [85], which have special geometry conditions where a pair of adjacent links have the same Bennett ratio.

iii) Altman linkage

In 1954, Altman [86] reported a 6R linkage, and the structure sketch is shown in Fig. 1.30. In this mechanism, the axes of  $R_2$ ,  $R_3$ ,  $R_5$  and  $R_6$  are in the same plane and intersect,  $R_2$  is perpendicular to  $R_3$  and  $R_5$  is perpendicular to  $R_6$ ; the axes of  $R_1$  and  $R_4$  are parallel and their parallel axes are perpendicular to the intersecting axes. That means the mechanism is symmetrical about the centre line and is in fact a special case of the line-symmetric Bricard linkage.

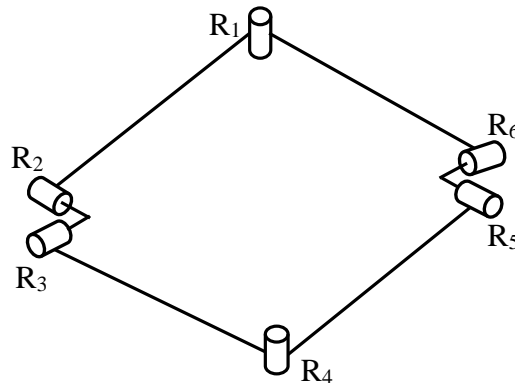


Figure 1.30 Schematic diagram of Altman linkage

b) 6R SLOMs based on Bennett linkages:

Many 6R SLOMs have been constructed by combining or merging two or more Bennett linkages including Goldberg 6R linkages, Double-Goldberg 6R linkages [79, 83, 87], the 6R linkage based on extended Myard linkage [71], the 6R linkage derived from two subtracted Goldberg linkages [83] and so on. Also, Baker conducted a comparative survey of the Bennett linkage based 6R kinematic loops in [88]. An introduction of these mechanisms is shown as follows:

i) Goldberg 6R linkages

Similar to the Goldberg 5R linkage, four kinds of Goldberg 6R linkage have been produced by combining three or more Bennett linkages [82] in distinct arrangements. Figure 1.31 schematically illustrates how they are constructed. In Fig. 1.31(a), the three Bennett linkages are arranged in series, two of them have common links which are ignored to form a primary Goldberg 6R linkage. The second Goldberg 6R linkage (Fig. 1.31(b)) is the subtraction of the Goldberg 6R linkage (a) with another Bennett linkage and is called a syncopated linkage. Fig. 1.31(c) shows the Goldberg 6R linkage that is built from L-shape arranged Bennett linkages. The fourth Goldberg 6R linkage (Fig. 1.31(d)) is the subtraction of the Goldberg 6R linkage (c) with another Bennett linkage.

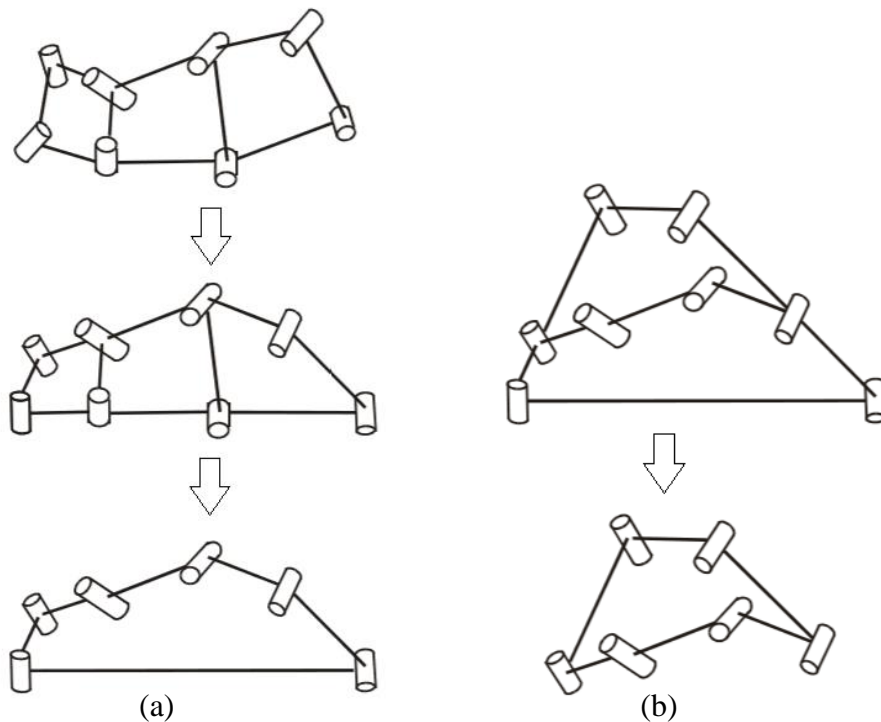


Figure 1.31 Schematic diagram of Goldberg 6R linkage [82] (continued on next page)

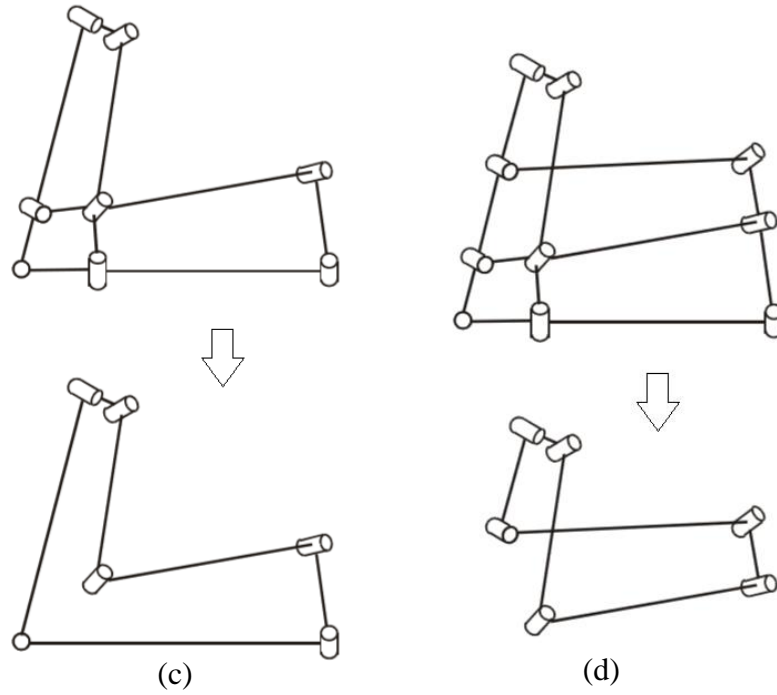


Figure 1.31 Schematic diagram of Goldberg 6R linkage [82]

ii) 6R linkage based on extended Myard linkage

With an extended Myard linkage having been proposed, a new 6R linkage formed by combining two of those was also developed by Chen [71] using a similar method to Wholhart's building Double-Goldberg 6R linkages. This is called a Double-Extended-Myard linkage and is illustrated in Fig. 1.32.

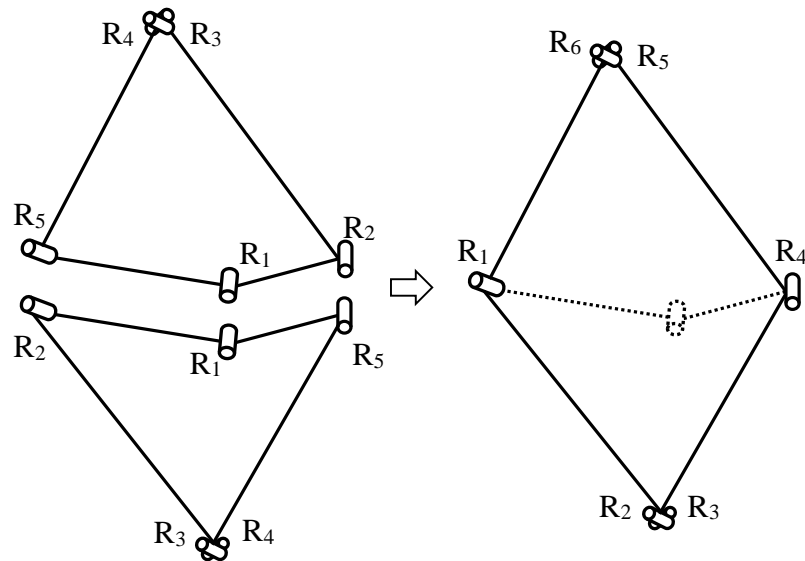
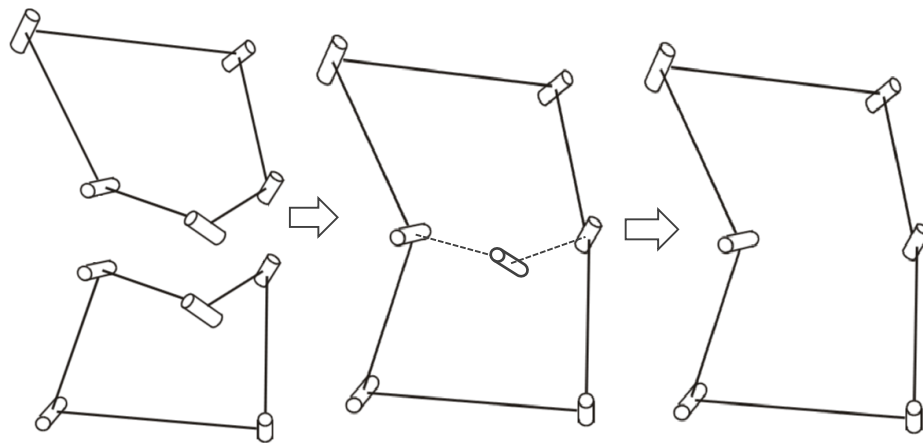


Figure 1.32 6R linkage based on extended Myard linkage

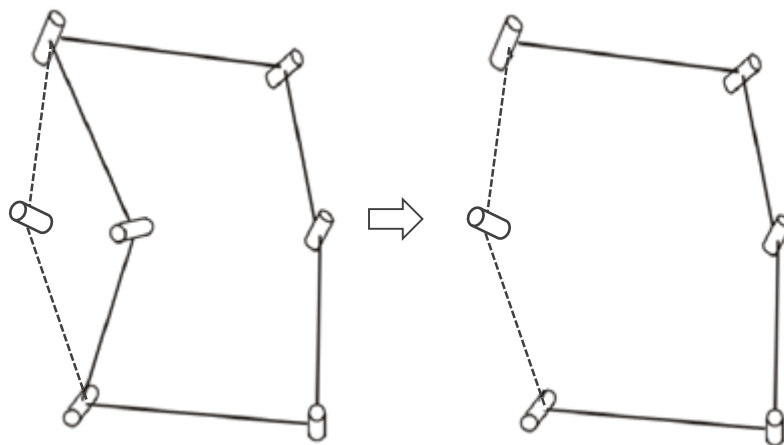
### iii) Double-Goldberg 6R linkage

#### (1) Wohlhart Double-Goldberg linkage

Wohlhart generalized the method for Goldberg 5R linkages; furthermore, in 1991 he developed a new 6R linkage through the combination of two Goldberg 5R linkages [79]. The two Goldberg 5R linkages are arranged in a “face-to-face” configuration, removing the common links and joints to form a Double-Goldberg 6R moveable linkage as shown in Fig. 1.33(a). This Double-Goldberg 6R linkage was further combined with another Bennett linkage [80] using the technique called “isomerization” by removing the common links and joints to form another 6R linkage (Fig. 1.33(b)).



(a) Double-Goldberg linkage



(b) Double-Goldberg linkage-isomerization method

Figure 1.33 Double-Goldberg 6R linkage

#### (2) Double-Goldberg 6R linkage by Chen and You

Chen and You (2007) also produced a Double-Goldberg 6R linkage through the combination of two Goldberg 5R linkages in a “back-to-back” configuration [87]. The

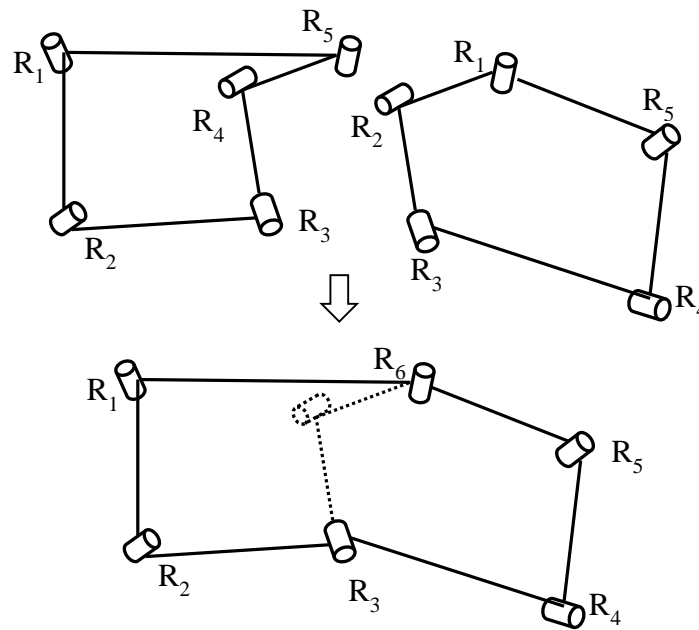
6R linkage can also be combined with a Bennett linkage to form a line-symmetric 6R linkage which actually forms a special case of the line-symmetric Bricard linkage.

(3) Spatial 6R linkage constructed by two subtractive Goldberg linkage

A spatial 6R linkage was constructed by two subtractive Goldberg linkages using a subtraction method [73].

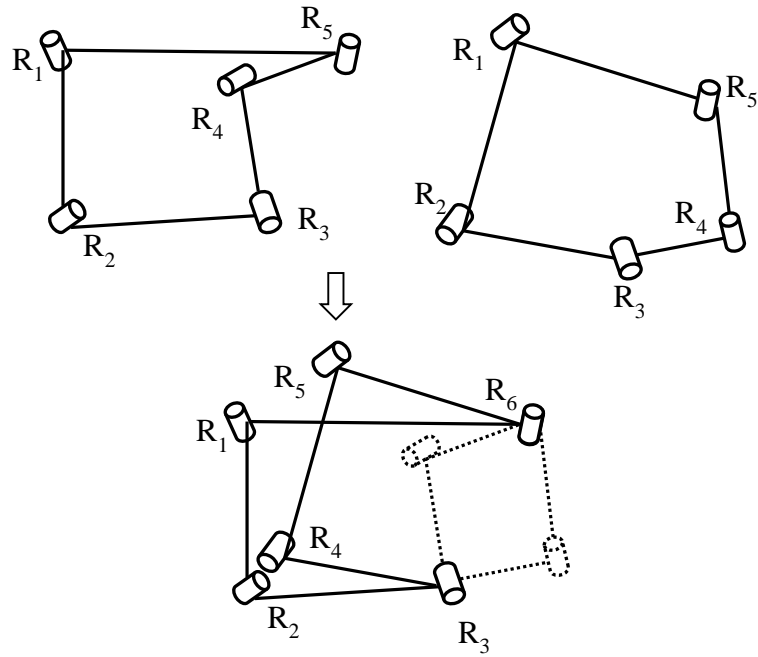
(4) Mixed Double-Goldberg 6R linkage

A family of mixed Double-Goldberg 6R linkages have also been presented in [83]. Six possibly compositional 5R Goldberg linkages including three general ones and three subtractive ones are combined further using the common link-pair method and common Bennett-linkage method, leading to six kinds of mixed Double-Goldberg linkages as illustrated in Fig. 1.34. The method showed in Fig. 1.34(a) is called a common link-pair method. If a common pairs and non-common pairs from two Goldberg 5R linkages are constructed into a Bennett linkage then a new 6R linkage can be obtained by removing this Bennett linkage as shown in Fig.1.34 (b); this method is called a common Bennett-linkage method [73].



(a) Combining using common link-pair method

Figure 1.34 Construction of mixed Double-Goldberg 6R linkage (continued on next page)



(b) Combining using common Bennett-linkage method

Figure 1.34 Construction of mixed Double-Goldberg 6R linkage

c) 6R SLOMs derived or combined by other overconstrained mechanisms

i) Double-Hooke's-joint linkage

A Double-Hooke's-joint linkage [89] is obtained by two spherical 4R linkages with one axis of each coinciding as shown in Fig. 1.35. Joints 1, 2, and 3 belong to one spherical 4R linkage and joints 4, 5, and 6 belong to another. The axis of  $R_2$  is perpendicular to  $R_1$  and  $R_3$ , and the axis of  $R_4$  is perpendicular to  $R_5$  and  $R_6$ . The common axis is perpendicular to  $R_1$  and  $R_6$ , and links 3 and 5 are connected. The angles between  $R_5$  and  $R_6$  are equal to the angle between  $R_1$  and  $R_3$  during the operation mode.

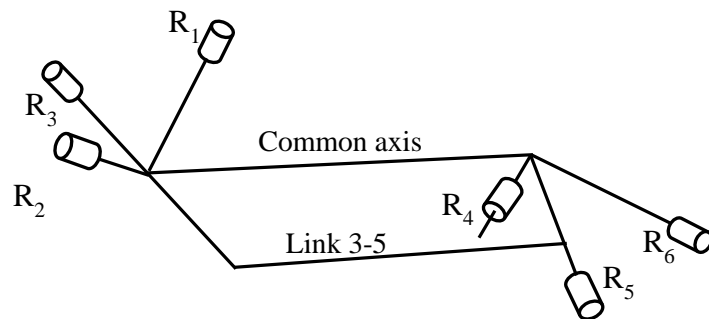


Figure 1.35 Double-Hooke's-joint 6R linkage



### ii) Bennett 6R hybrid linkage

Bennett proposed the 6R hybrid linkage in 1905 [90], comprising two spherical 4R linkages as a Double-Hooke's-joint linkage. Actually, the Double-Hooke's-joint linkage is a special case of Bennett 6R hybrid linkages. The two spherical 4R linkages are placed such that the insertion points of the revolute joint axes are not at a same point. They have a common revolute joint and are constructed by removing the common joint and reconnecting the adjacent joint as illustrated in Fig. 1.36. In this mechanism, Link 1, relative to Link 2, has a pure rotation about the common axis.

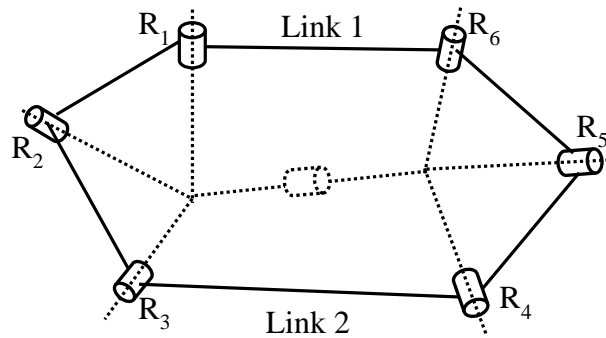


Figure 1.36 Bennett 6R hybrid linkage

### iii) Waldron's hybrid linkages

The concept of Waldron's hybrid linkage is that any two single-loop linkages with a single-DOF can be arranged such that they have a common joint, removing the common joint and reconnecting the two linkages leading to a new linkage which would certainly retain mobility [78], such as illustrated in Fig. 1.37: a 6R linkages which is originally from two Bennett linkages.

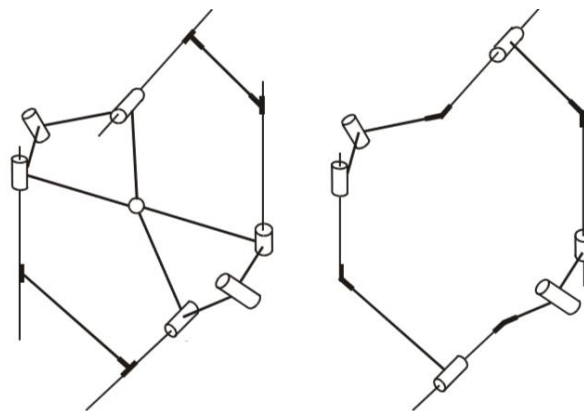


Figure 1.37 Waldron's hybrid linkage from two Bennett linkages [82]

d) 6R SLOMs with special geometry

i) Schatz linkage

Schatz linkage is a linkage with special geometry which was developed by Schatz [91] from a special trihedral Bricard linkage. By arranging the trihedral Bricard linkage at a configuration where all the twist angles are  $\pi/2$  and changing the placement of joints  $R_1$  and  $R_6$  in order to make the two axes parallel, then the axes of  $R_1$  and  $R_2$  as well as  $R_5$  and  $R_6$  intersect as illustrated in Fig. 1.38.

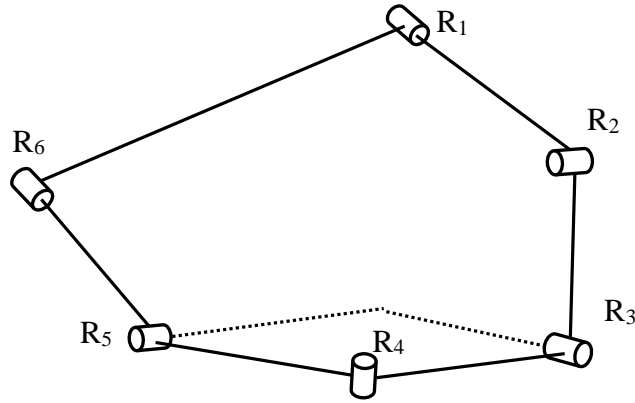


Figure 1.38 Schatz linkage

ii) Wohlhart 6R linkage

Apart from the Glodberg related linkages, Wohlhart derived a new 6R linkage with special geometry in which all the axes of six revolute joints intersected at a line [92] as shown in Fig. 1.39. It is easy to state that the linkage is combined by two half-plane-symmetric Bricard linkages or it can be seen as a generalised trihedral Bricard linkage. The linkage should satisfy the conditions below:

$$\begin{aligned}
 a_1 &= a_2, \quad a_3 = a_4, \quad a_5 = a_6 \\
 \alpha_1 &= 2\pi - \alpha_2, \quad \alpha_3 = 2\pi - \alpha_4, \quad \alpha_5 = 2\pi - \alpha_6 \\
 d_6 &= -d_2 - d_4, \quad d_1 = d_3 = d_5 = 0
 \end{aligned} \tag{1.25}$$

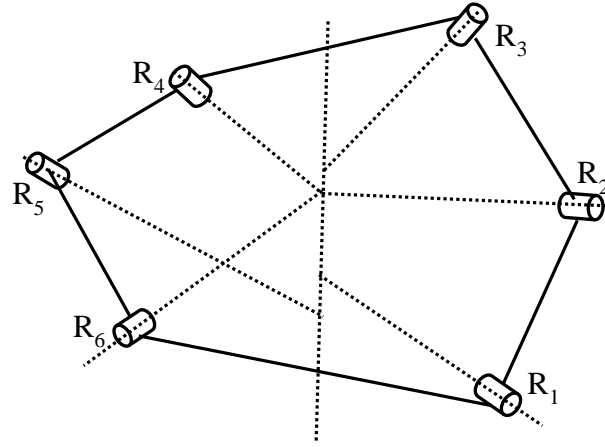


Figure 1.39 Wohlhart 6R Hybrid linkage

iii) Dietmaier 6R linkage:

In 1995, with the help of numerical method, Dietmaier developed a new family of 6R linkages with special geometry [93]. The Bennett-joint linkage can be seen as a special case. The conditions for the type of linkages should satisfy those listed below. Baker also tried to find the variants of Dietmaier's 6R linkage using the isomerization method [94].

$$a_1 = a_4$$

$$\alpha_1 = \alpha_4$$

$$d_1 = d_3, d_4 = d_6, d_2 = d_5 = 0 \quad (1.26)$$

$$\frac{\sin(\alpha_3)}{a_3} = \frac{\sin(\alpha_2)}{a_2}, \frac{\sin(\alpha_6)}{a_6} = \frac{\sin(\alpha_5)}{a_5}$$

$$\frac{\alpha_2(\cos \alpha_2 + \cos \alpha_3)}{\sin(a_2)} = \frac{\alpha_5(\cos \alpha_5 + \cos \alpha_6)}{\sin(a_6)}$$

iv) Bennett-joint 6R linkages

The Bennett-joint 6R linkage is a by-product in Mavroidis and Roth' research [95] to develop a method to systematically deal with overconstrained mechanisms. The definition of a Bennett-joint is that three adjacent revolute joints whose D-H parameters satisfy the following relationship that is the same as a Bennett linkage:

$$d_i = 0, i = (1, 2, 3) \quad (1.27)$$

and

$$\frac{\sin(\alpha_i)}{a_i} = \pm \frac{\sin(\alpha_{i+1})}{a_{i+1}} \quad (1.28)$$

A Bennett-joint 6R linkage contains at least one Bennett-joint. Figure 1.40 shows a Bennett-joint 6R linkage with two Bennett-joint. Its parameters satisfy the following conditions:

$$\begin{aligned}
 a_1 &= a_5, a_2 = a_4, a_3 = a_6 \\
 \alpha_1 &= \alpha_5, \alpha_2 = \alpha_4, \alpha_3 = \alpha_6 \\
 d_2 &= d_5 = 0, d_6 = d_3, d_1 = d_4 \\
 \frac{\sin(\alpha_i)}{a_i} &= k_B \quad (i = 1, 2, \dots, 6)
 \end{aligned} \tag{1.29}$$

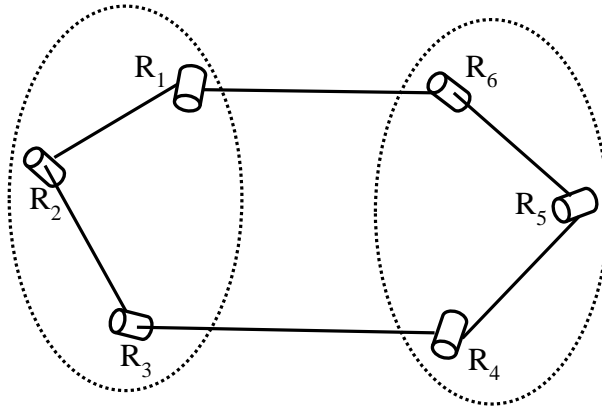
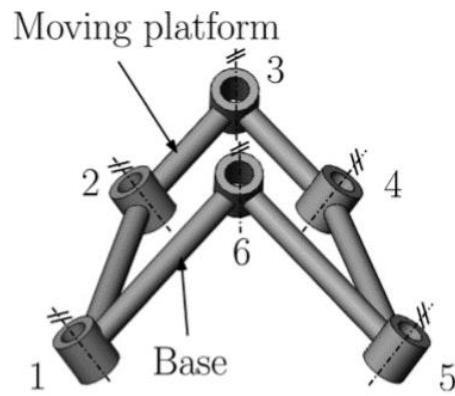


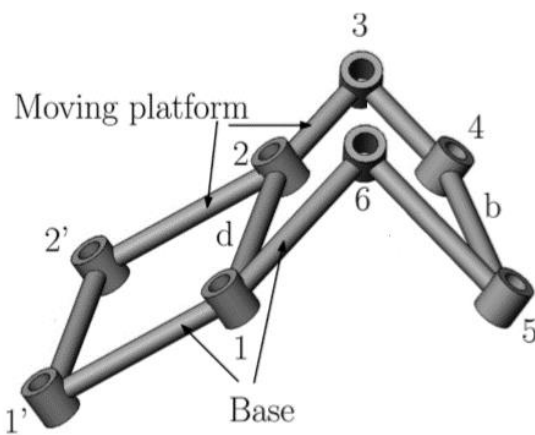
Figure 1.40 Bennett joints linkage

iv) 6R spatial linkages for circular translation

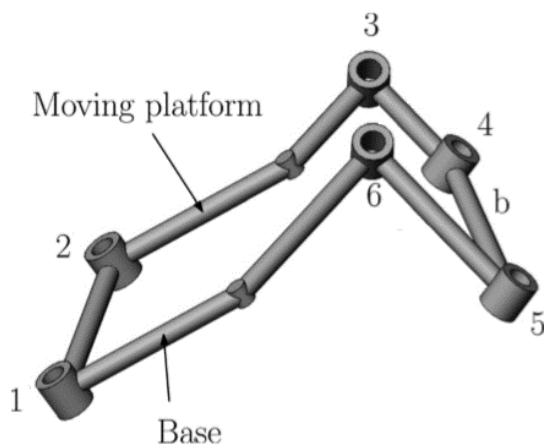
A group of 6R spatial mechanisms for circular translation are presented in paper [96]. Kong extended his function-targeted research point of view to help develop the SLOMs. Six special kinds of 6R spatial mechanisms for circular translation can be derived by imposing certain conditions on four kinds of hybrid 6R linkages and Bricard line and plane symmetrical linkages. These 6R linkages may have a planar 3R sub chain or two pairs of adjacent two R joints with their axes parallel and one pair of nonadjacent R joints with parallel axes [136]. Then six general cases of 6R spatial mechanisms for circular translation can be obtained by combining planar parallelograms with the special cases, as shown in Fig. 1.41. In addition, 4R2H, 2R4H and 6H linkages are obtained by replacing 6R spatial Mechanisms for Circular Translation or more pairs of R joints with parallel axes.



(a) Special 6R spatial mechanisms for circular translation



(b) Combining special 6R spatial mechanisms for circular translation with a plane parallelogram



(c) General 6R spatial mechanisms for circular translation

Figure 1.41 6R spatial linkages with circular translation [96]

### **1.2.4 Summary**

This section has reviewed these most well-known SLOMs which produce a significant foundation for the subsequent work in the following chapters for conducting the synthesis and analysis of SLMMRMs.

## **1.3 Objectives and Layout of the Thesis**

In the previous sections, a comprehensive and comparative investigation of reconfigurable mechanisms has been implemented informing that MMRMs have apparent advantages over others. Meanwhile, the review of the most existing SLOMs has formed an important foundation for the further design of MMRMs. Even though a great deal of research works on MMRMs has been previously undertaken in the past two decades, researchers are still inspired to continuously develop a new generation of MMRMs. It is still an open issue to present novel MMRMs based on the investigation of SLOMs using creative type synthesis methods, and to complete the associated kinematic analysis using effective mathematical tools.

This thesis concentrates on and is devoted to the synthesis and analysis of SLMMRMs with the specific research objectives listed as follows:

- 1) Systematically analyse the constraint equations for typical compositional serial chains for parallel mechanisms.
- 2) Complete the type synthesis method for SLMMRMs and develop new novel SLMMRMs.
- 3) Implement the kinematic analysis of SLMMRMs employing effective algebraic geometry method.

The remainder of this thesis is organised as follows:

The basic mathematic tools will be recalled and effective algebraic geometry methods will be summarized firstly in Chapter 2.

In Chapter 3, the constraint equations for serial chains which constitute MMRMs as compositional units will be systematically analysed and selected.

Chapter 4 will present new type synthesis methods for 7R single-loop reconfigurable mechanisms with three or more operation modes.

Then in Chapters 5 and 6, 7R single-loop reconfigurable mechanisms with three or more operation modes obtained using these methods can be built and validated with the aid of CAD software and 3D printed prototypes. The kinematic analysis of these 7R single-loop reconfigurable mechanisms with three or more operation modes will then be completed applying effective algebraic geometry methods based on kinematic mapping theory.

Finally in Chapter 7, some conclusions and future works will be provided.

## Chapter 2 – Theoretical Tools

With the development of mathematical tools, even more complex forward and inverse kinematic problems of mechanisms can be solved. Many effective methods and algorithms have been developed based on advanced algebraic geometry which are capable of dealing with more complicated kinematic problems. In this chapter, several theoretical tools to be used in the thesis including the main method for dealing with the forward kinematics of multi-modes reconfigurable mechanisms are reviewed.

### 2.1 Mathematical Basis

#### 2.1.1 Tangent Half-Angle Formula

Dealing with constraint equations is an important step in the process of the kinematic analysis of a mechanism. Since there are angle parameters for a mechanism, there are always trigonometric functions within the constraint equations. It is thus extremely difficult to solve these with trigonometry. It is essential to simplify these constraint equations by introducing the tangent half of angles [97] so that these can be converted into the form of polynomials.

One of the trigonometric identities is

$$\sin^2 \varphi + \cos^2 \varphi = 1 \quad (2.1)$$

For an arbitrary angle  $\varphi$ , we have

$$\sin \varphi = \frac{2 \cdot \tan(\varphi / 2)}{1 + \tan(\varphi / 2)^2}, \quad \cos \varphi = \frac{1 - \tan(\varphi / 2)^2}{1 + \tan(\varphi / 2)^2} \quad (\varphi \neq (2k + 1)\pi, k \in \mathbb{Z}) \quad (2.2)$$

Representing the tangent half angle ( $\tan(\varphi / 2)$ ) by a new variable  $p$  yields

$$p = \tan(\varphi / 2) \quad (2.3)$$

Equation (2.2) can be re-written as

$$\sin \varphi = \frac{2 \cdot p}{1 + p^2}, \quad \cos \varphi = \frac{1 - p^2}{1 + p^2} \quad (2.4)$$

By replacing all the trigonometric functions using different representations in tangent half angles, the polynomial equations can be obtained. This will greatly reduce the complexity of the constraint equations, leading to high computationally effectiveness. After obtaining the solutions for  $p$  at the end of the computation, the angle parameters can be obtained by



$$\varphi = 2 \cdot \arctan p \quad (2.5)$$

In addition, the angle  $\pi - \varphi$  has the corresponding variable  $q$  that has the following relationship with  $p$

$$q = 1/p \quad (2.6)$$

### 2.1.2 Distance between Two Skew Lines

When a new mechanism is constructed by combining two or more original mechanisms based on common joint(s), the links between non-common joints are disconnected and new links need to be designed. Devavit-Hartenbergh (D-H) parameters of the new links then have to be calculated accurately according to known conditions.

Generally, the parameters of the distance and angle for skew lines between two axes of adjacent joints need to be calculated so that the approach for estimating the distance between two skew lines is investigated to obtain the D-H parameters for a new mechanism. In geometry, two lines are said to be skew lines if they are neither intersecting nor parallel. The distance between skew lines can be solved using the vector method. The vector method [98] is found to be very effective in this thesis to help calculate the new parameters according to known conditions, with the difficult problem about the distance of the skew lines in solid geometry transformed into a relatively simple one.

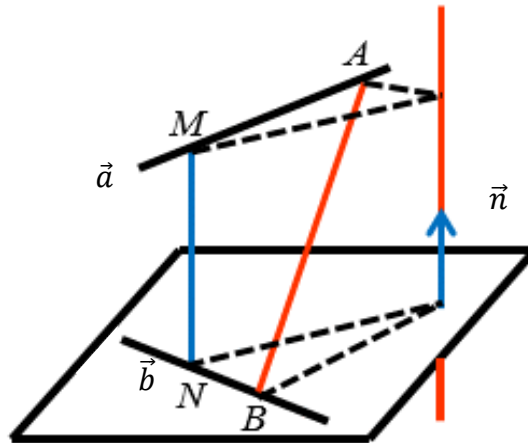


Figure 2.1 The distance between skew lines

The procedure to calculate the distance between the two skew lines  $a$  and  $b$  (Fig. 2.1) using a vector method is as follows:

- a) Obtain the direction vectors,  $\vec{a}$  and  $\vec{b}$ , of skew lines;

b) Assume the common normal of  $\vec{a}$  and  $\vec{b}$  to be  $\vec{n}$ :  $[x, y, z]$ , and then calculate  $\vec{n}$  using the dot product principle ( $\vec{a} \cdot \vec{n} = 0$  and  $\vec{b} \cdot \vec{n} = 0$ );

c) Select two points,  $A$  and  $B$ , on the two skew lines and connect  $A$  and  $B$  to obtain the vector  $\overrightarrow{AB}$ ;

d) Obtain  $d$ , the projection of  $\overrightarrow{AB}$  on  $\vec{n}$ , which is also the distance between the two skew lines as below:

$$d = \frac{|\overrightarrow{AB} \cdot \vec{n}|}{|\vec{n}|} \quad (2.7)$$

Due to the fact that the parameters  $\overrightarrow{AB}$  and  $\vec{n}$  can be easily obtained during the combination of two SLOMs, then the vector method is the proper way to calculate the distance between two adjacent axes. This will be used in Chapter 4 in the process to obtain the parameters of 6R mechanisms from combining two Bennett linkages.

### 2.1.3 Basic Linear Algebra

In this subsection, some basic knowledge of linear algebra is reviewed which will be used in Chapter 3 to help select independent constraint equations for a serial chain.

#### 1) Inverse matrix and adjoint matrix

If a matrix  $A$ , with its entry  $a_{ij}$  in the  $i$ -th row and  $j$ -th column, is an  $n \times n$  matrix, we define  $A(i/j)$  to be an  $(n-1) \times (n-1)$  matrix obtained from  $A$  by deleting the  $i$ -th row and  $j$ -th column which is called the  $ij$ -th maximal submatrix of  $A$ . An example of  $A$  is shown as

$$A = \begin{pmatrix} a_{11} & a_{12} & a_{13} \\ a_{21} & a_{22} & a_{23} \\ a_{31} & a_{32} & a_{33} \end{pmatrix} \quad (2.8)$$

Its inverse matrix can be represented by

$$A^{-1} = \begin{pmatrix} \tilde{a}_{11} & \tilde{a}_{12} & \tilde{a}_{13} \\ \tilde{a}_{21} & \tilde{a}_{22} & \tilde{a}_{23} \\ \tilde{a}_{31} & \tilde{a}_{32} & \tilde{a}_{33} \end{pmatrix} \quad (2.9)$$

where

$$\tilde{a}_{ji} = (-1)^{i+j} \frac{\det(A(i|j))}{\det(A)} \quad (2.10)$$

for example,

$$\tilde{a}_{12} = (-1)^{2+1} \frac{\begin{vmatrix} a_{12} & a_{13} \\ a_{32} & a_{33} \end{vmatrix}}{\det(A)} \quad (\text{if } \det(A) \neq 0) \quad (2.11)$$

The adjoint matrix for  $A$  can be written as

$$A^* = \begin{pmatrix} \bar{a}_{11} & \bar{a}_{12} & \bar{a}_{13} \\ \bar{a}_{21} & \bar{a}_{22} & \bar{a}_{23} \\ \bar{a}_{31} & \bar{a}_{32} & \bar{a}_{33} \end{pmatrix} \quad (2.12)$$

where

$$\bar{a}_{ji} = (-1)^{i+j} \det(A(i|j)) \quad (2.13)$$

Using the adjoint matrix the following description of the inverse of an invertible matrix is obtained [99]:

$$A^{-1} = \frac{A^*}{\det(A)} \quad (\text{if } \det(A) \neq 0) \quad (2.14)$$

i.e.

$$A^* \cdot A = \det(A) \cdot I \quad (2.15)$$

## 2) Linearly independence

Generally, a set of equations can be represented by a matrix equation such as a set of equations (Eq. (2.16)) with its matrix representation  $Ax=b$  (Eq. (2.17)):

$$\begin{cases} a_{11}x_1 + a_{12}x_2 + \cdots + a_{1n}x_n = b_1 \\ a_{21}x_1 + a_{22}x_2 + \cdots + a_{2n}x_n = b_2 \\ \vdots \\ a_{m1}x_1 + a_{m2}x_2 + \cdots + a_{mn}x_n = b_m \end{cases} \quad (2.16)$$

$$\begin{pmatrix} a_{11} & a_{12} & \cdots & a_{1n} \\ a_{21} & a_{22} & \cdots & a_{2n} \\ \vdots & \vdots & \cdots & \vdots \\ a_{m1} & a_{m2} & \cdots & a_{mn} \end{pmatrix} \cdot \begin{pmatrix} x_1 \\ x_2 \\ \vdots \\ x_n \end{pmatrix} = \begin{pmatrix} b_1 \\ b_2 \\ \vdots \\ b_m \end{pmatrix} \quad (2.17)$$

Given a set of vectors  $A=[A_1, A_2, \dots, A_n]$ , the equation  $Ax=b$  can be re-written in terms of the column of  $A$  as

$$A_1x_1 + A_2x_2 + \cdots + A_nx_n = b \quad (2.18)$$

If  $b$  can be written as a sum of multiples of columns vectors of  $A$ , then  $A_1x_1 + A_2x_2 + \cdots + A_nx_n$  is a linear combination of the vectors  $A_1, A_2, \dots, A_n$ , then  $Ax=b$  is consistent in this situation. There must be a system of equations  $Ax=0$ :

$$\begin{pmatrix} a_{11} & a_{12} & \cdots & a_{1n} \\ a_{21} & a_{22} & \cdots & a_{2n} \\ \vdots & \vdots & \cdots & \vdots \\ a_{m1} & a_{m2} & \cdots & a_{mn} \end{pmatrix} \cdot \begin{pmatrix} x_1 \\ x_2 \\ \vdots \\ x_n \end{pmatrix} = \begin{pmatrix} 0 \\ 0 \\ \vdots \\ 0 \end{pmatrix} \quad (2.19)$$

which may be written as

$$A_1x_1 + A_2x_2 + \cdots + A_nx_n = 0 \quad (2.20)$$

Although the system equations always have trivial solutions, there may also be nontrivial solutions. A set of  $m$ -dimensional vectors  $[A_1, A_2, \dots, A_n]$  is said to be linearly dependent if there exists a non-zero  $x_i$  such that  $A_1x_1 + A_2x_2 + \cdots + A_nx_n = 0$ . A set of  $m$ -dimensional vectors  $[A_1, A_2, \dots, A_n]$  are said to be linearly independent if they are not linearly dependent [100, 101]. It can be understood that a system of equations being linearly dependent means that there are combinations between the rows or columns of its coefficient matrix and the linearly dependence can be related to the determinate of the coefficient matrix. According to the properties of determinate of a matrix, if the entries in one row or one column are all zero, then the determinate of the matrix is zero. On the contrary, if the determinate of a coefficient matrix is equal to zero, there are zero row(s) or column(s), meaning that there are rows (columns) linearly combined by other rows (columns). Therefore, the system of equations is linearly dependent.

#### **2.1.4 Notations of D-H Coordinate Frames**

Coordinate transformation is the first step for the kinematic analysis of mechanisms. The D-H coordinate system was introduced by Devavit and Hartenberg [102, 103] in 1955 to standardize the coordinate frames for spatial linkages in the kinematics analysis of mechanisms. Richard Paul [104] demonstrated its value for the kinematic analysis of robotic systems in 1981. Even though many conventions for attaching references frames have been developed, the D-H convention remains the most commonly used approach. Basically, there are three popular D-H parameter notations including the original notation, the distal and proximal variant notation [105].

In the original notation of a D-H coordinate frame (Fig. 2.2), the  $z_i$ -axis is defined along the axis of joint  $i$  and the origin of this frame is on the axis of joint  $i$  and at the point of its common perpendicular with the axis of joint  $i-1$ . The  $x_i$ -axis is coincident with the common perpendicular of the axes of  $z_{i-1}$  and  $z_i$ . The  $y_i$  axis is placed such that it completes a right-handed coordinate system.

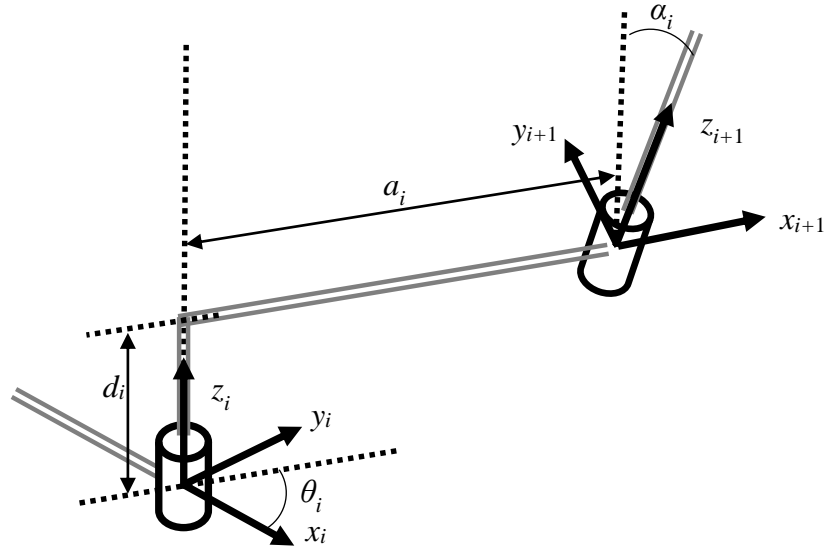


Figure 2.2 Original notation of D-H coordinate frame

The D-H parameters are defined as below:

$\alpha_i$  - the twist angle between the  $z_i$  and  $z_{i+1}$  about  $x_{i+1}$ ;

$a_i$  - the distance between the  $z_i$  and  $z_{i+1}$  measured along  $x_{i+1}$ ;

$d_i$  - the distance from  $x_i$  to  $x_{i+1}$  measured along  $z_i$ ;

$\theta_i$  - the angle between  $x_i$  to  $x_{i+1}$  measured about  $z_i$ .

The coordinate transformation from the previous coordinate system to the next coordinate system can be obtained by moving about  $z_i$  axis by the distance  $d_i$  and angle  $\theta_i$ , then moving about  $x_{i+1}$  by the distance  $a_i$  and angle  $\alpha_i$ , which can be represented by

$$T_{i+1}^i = \text{Trans}_{z_i}(d_i) \cdot \text{Rot}_{z_i}(\theta_i) \cdot \text{Trans}_{x_{i+1}}(a_i) \cdot \text{Rot}_{x_{i+1}}(\alpha_i) \quad (2.21)$$

where

$$\text{Trans}_{z_i}(d_i) = \begin{bmatrix} 1 & 0 & 0 & 0 \\ 0 & 1 & 0 & 0 \\ 0 & 0 & 1 & 0 \\ d_i & 0 & 0 & 1 \end{bmatrix} \quad (2.22)$$

$$\text{Rot}_{z_i}(\theta_i) = \begin{bmatrix} 1 & 0 & 0 & 0 \\ 0 & \cos(\theta_i) & -\sin(\theta_i) & 0 \\ 0 & \sin(\theta_i) & \cos(\theta_i) & 0 \\ 0 & 0 & 0 & 1 \end{bmatrix} \quad (2.23)$$

$$\text{Trans}_{x_{i+1}}(a_i) = \begin{bmatrix} 1 & 0 & 0 & 0 \\ a_i & 1 & 0 & 0 \\ 0 & 0 & 1 & 0 \\ 0 & 0 & 0 & 1 \end{bmatrix} \quad (2.24)$$

$$Rot_{x_{i+1}}(\alpha_i) = \begin{bmatrix} 1 & 0 & 0 & 0 \\ 0 & 1 & 0 & 0 \\ 0 & 0 & \cos(\alpha_i) & -\sin(\alpha_i) \\ 0 & 0 & \sin(\alpha_i) & \cos(\alpha_i) \end{bmatrix} \quad (2.25)$$

This gives:

$$T_{i+1}^i = \begin{bmatrix} 1 & 0 & 0 & 0 \\ a_i \cos(\theta_i) & \cos(\theta_i) & -\sin(\theta_i)\cos(\alpha_i) & \sin(\theta_i)\sin(\alpha_i) \\ a_i \sin(\theta_i) & \sin(\theta_i) & \cos(\theta_i)\cos(\alpha_i) & -\cos(\theta_i)\sin(\alpha_i) \\ d_i & 0 & \sin(\alpha_i) & \cos(\alpha_i) \end{bmatrix} \quad (2.26)$$

which can be simplified as below:

$$T_{i+1}^i = \begin{bmatrix} 1 & 0 & 0 & 0 \\ T & A \end{bmatrix} \quad (2.27)$$

where  $A$  is a  $3 \times 3$  sub-matrix describing rotation and  $T$  is a  $3 \times 1$  sub-matrix describing translation.

## 2.2 Methods for the Kinematic Analysis of Mechanisms

Three main topics in the theoretical kinematics of manipulators are the direct (forward) and the inverse kinematics problems as well as the singularity problems. The forward kinematics problem involves determining all possible poses of the end-effector (EE) frame when the actuated joints have specific input values. The inverse kinematics problem can be stated to be that a discrete pose of the EE is given and one has to compute the joint parameters such that the given manipulator can move the EE to this pose.

There are many methods to deal with the kinematic and singularity analysis of serial and parallel mechanisms. Reference [106] introduces the double quaternion and Dixon resultant to solve the inverse kinematics analysis of a general 6R robot. The homogeneous transform matrix in terms of double quaternions was firstly shown to lead to kinematics equations; secondly, a resultant procedure was constructed via linear algebraic and Dixon resultant formulation yielding a 16 degree univariate polynomial from the resultant matrix. Other approaches for the inverse kinematic analysis of general 6R mechanisms have also been studied. For example, [107] and [108] presented numerical continuation methods for 6R inverse problems; a symbolic computation

method called the Raghavan and Roth method [109] was used to solve the inverse kinematic problems of six-DOF general and special manipulators. Many of the methods of inverse problems of general 6R manipulators have been extended to deal with the forward kinematic problems of 7R single-loop mechanisms [110-112] and parallel mechanisms [113]. In addition, [114] presented a different evaluation algorithm which was used to solve forward kinematics problems of parallel manipulators; this is efficient, especially for problems containing continuous variables. The results of singularity analysis of 3-DOF planar parallel mechanisms via a screw theory algorithm are presented in [115] providing geometrical insight into the problem and allowing the precise and complete description of singularity types. Algebraic methods in connection with classical multidimensional geometry have been proved to be very efficient for both direct and inverse kinematics analysis of mechanisms. Husty et al [116-124] have made significant contributions in this field. In 2006, Husty et al [116] introduced a new and effective algorithm for the inverse kinematics of a general serial 6R manipulator using the algebraic geometric method based on the kinematic mapping space which had been introduced by Blaschke and Study, thereafter they developed and systematized the method [117, 118], the so-called explicitation algorithm compared with the later produced implicitization algorithm [119-120]. Both the algorithms are based on geometric pre-processing in a multi-dimensional space which is called kinematic mapping method. The method cannot only be used to deal with general serial and parallel mechanisms, but also kinematic analysis of MMRMs. It will be effective in identifying different motion patterns and transitional configurations for MMRMs. Therefore, in the next section, the kinematic mapping method will be summarized to support the kinematic analysis of MMRMs.

### ***2.2.1 Kinematic Mapping Method***

Using the kinematic mapping based method [116], a Euclidean displacement can be mapped into a point on the Study quadric ( $S_6^2$ ) in a seven dimensional space, the so-called kinematic mapping space  $P^7$ , where the point is displayed by eight study parameters.

In the Euclidean space the displacement can be described by [116]:

$$x' = Ax + T \quad (2.28)$$

where  $x$  represents a point in the fixed frame and  $x'$  represents the corresponding point in the moving frame,  $A$  is a  $3 \times 3$  proper orthogonal matrix describing rotation and  $T$  is a vector describing translation. The transformation matrix (original notation) can be represented as below:

$$M = \begin{bmatrix} 1 & 0 & 0 & 0 \\ T & & A & \end{bmatrix} \quad (2.29)$$

Expanding the dual quaternion representation using the operator approach, the matrix  $M$  (Eq. (2.29)) corresponding to the normalized dual quaternion  $q = (x_0 + x_1 + x_2 + x_3)^T + \varepsilon(y_0 + y_1 + y_2 + y_3)^T$  is given by:

$$M = \frac{1}{\Delta} \begin{bmatrix} \Delta & 0 & 0 & 0 \\ t_1 & x_0^2 + x_1^2 - x_2^2 - x_3^2 & -2x_0x_3 + 2x_2x_1 & 2x_3x_1 + 2x_0x_2 \\ t_2 & 2x_2x_1 + 2x_0x_3 & x_0^2 + x_2^2 - x_1^2 - x_3^2 & -2x_0x_1 + 2x_3x_2 \\ t_3 & -2x_0x_2 + 2x_3x_1 & 2x_3x_2 + 2x_0x_1 & x_0^2 + x_3^2 - x_2^2 - x_1^2 \end{bmatrix} \quad (2.30)$$

where  $\Delta = x_0^2 + x_1^2 + x_2^2 + x_3^2$ .

The Study parameters of a transformation can be obtained by using one of the following formulas [116, 118]:

$$\begin{aligned} x_0 : x_1 : x_2 : x_3 \\ &= 1 + a_{11} + a_{22} + a_{33} : a_{32} - a_{23} : a_{13} - a_{31} : a_{21} - a_{12} \\ &= a_{32} - a_{23} : 1 + a_{11} - a_{22} - a_{33} : a_{12} + a_{21} : a_{31} + a_{13} \\ &= a_{13} - a_{31} : a_{12} + a_{21} : 1 - a_{11} + a_{22} - a_{33} : a_{23} + a_{32} \\ &= a_{21} - a_{12} : a_{31} + a_{13} : a_{23} + a_{32} : 1 - a_{11} - a_{22} + a_{33} \end{aligned} \quad (2.31)$$

where  $a_{ij}$  is the element from the rotation matrix  $A$ .

$y_i$  mentioned above is given by:

$$\begin{aligned} y_0 &= -\frac{1}{2}(t_3x_3 + t_2x_2 + t_1x_1) \\ y_1 &= -\frac{1}{2}(t_3x_2 - t_2x_3 - t_1x_0) \\ y_2 &= -\frac{1}{2}(-t_3x_1 + t_1x_3 - t_2x_0) \\ y_3 &= -\frac{1}{2}(-t_3x_0 + t_2x_1 - t_1x_2) \end{aligned} \quad (2.32)$$

Equations (2.31) and (2.32) are already proposed by Study in [124 and 125]. Note that if  $A$  is not symmetric then the first formula of Eq. (2.31) can be used. If  $A$  is symmetric then it describes a rotation about an angle of  $\pi$  so that the computed study parameters are zero and the first formula in Eq. (2.31) fails. In this case, one of the



remaining three formulas can be used to make sure at least one study parameter is non-zero.

The entries  $[x_i, y_i]$  in the transformation matrix  $M$  have to fulfil:

$$x_0y_0 + x_1y_1 + x_2y_2 + x_3y_3 = 0 \quad (2.33)$$

Equation (2.33) is an expression of  $S_6^2$  in the seven dimensional projective space  $P^7$  (Fig. 2.3). The Study quadric  $S_6^2$  serves as a point model for Euclidean displacement where  $M[x_i, y_i] \rightarrow [x_0:x_1:x_2:x_3:y_0:y_1:y_2:y_3]^T \neq [0:0:0:0:0:0:0:0]^T$  mapping each Euclidean displacement to a point  $P$  on  $S_6^2$ .

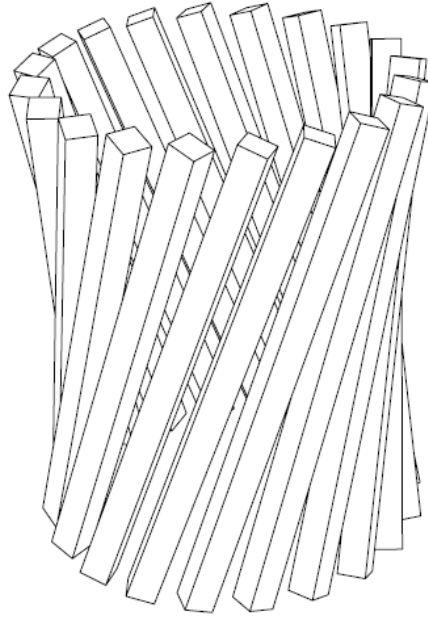


Figure 2.3 Symbolic sketch of  $S_6^2$  [118]

The representation of serial chains in the kinematic mapping space is the main tool used in the algorithms to obtain the constraint equations. The most important theory described using the kinematic mapping method is the variety of all the EE poses of a kinematic chain in the kinematic mapping space; also called the constraint manifold or constraint variety of a serial chain. The constraint manifold of a 2R chain is the intersection of a 3-space with  $S_6^2$  and the constraint manifold of a 3R chain derived from a 2R chain is the intersection of a set of 3-spaces with  $S_6^2$ .

The generic equations of a kinematic chain are first obtained by the approaches which will be summarized in the following subsections. Transformations in the base or moving frame are then brought into the generic equations in the kinematic mapping space.

A coordinate transformation in the base and moving frame in a Cartesian space has its corresponding projective transformation in the kinematic image space consisting of its study parameters. The projective transformation in the base can be represented by  $T_b$ , and the projective transformation in the moving frame can be expressed by  $T_m$  [117, 118]. According to Eqs. (2.31) and (2.32), the study parameters  $[b_0, b_1, b_2, b_3, b_4, b_5, b_6, b_7]$  for the transformation matrix in the base and the study parameters  $[m_0, m_1, m_2, m_3, m_4, m_5, m_6, m_7]$  for the transformation matrix in the moving frame can be obtained. Therefore, the corresponding transformation matrix in the kinematic mapping space can be written as:

$$T_b = \begin{bmatrix} b_0 & -b_1 & -b_2 & -b_3 & 0 & 0 & 0 & 0 \\ b_1 & b_0 & -b_3 & b_2 & 0 & 0 & 0 & 0 \\ b_2 & b_3 & b_0 & -b_1 & 0 & 0 & 0 & 0 \\ b_3 & -b_2 & b_1 & b_0 & 0 & 0 & 0 & 0 \\ -b_4 & b_5 & b_6 & b_7 & b_0 & -b_1 & -b_2 & -b_3 \\ -b_5 & -b_4 & b_7 & -b_6 & b_1 & b_0 & -b_3 & b_2 \\ -b_6 & -b_7 & -b_4 & b_5 & b_2 & b_3 & b_0 & -b_1 \\ -b_7 & b_6 & -b_5 & -b_4 & b_3 & -b_2 & b_1 & b_0 \end{bmatrix} \quad (2.34)$$

$$T_m = \begin{bmatrix} m_0 & -m_1 & -m_2 & -m_3 & 0 & 0 & 0 & 0 \\ m_1 & m_0 & m_3 & -m_2 & 0 & 0 & 0 & 0 \\ m_2 & -m_3 & m_0 & m_1 & 0 & 0 & 0 & 0 \\ m_3 & m_2 & -m_1 & m_0 & 0 & 0 & 0 & 0 \\ -m_4 & m_5 & m_6 & m_7 & m_0 & -m_1 & -m_2 & -m_3 \\ -m_5 & -m_4 & -m_7 & m_6 & m_1 & m_0 & m_3 & -m_2 \\ -m_6 & m_7 & -m_4 & -m_5 & m_2 & -m_3 & m_0 & m_1 \\ -m_7 & -m_6 & m_5 & -m_4 & m_3 & m_2 & -m_1 & m_0 \end{bmatrix} \quad (2.35)$$

Note that the projective transformations  $T_m$  and  $T_b$  in the kinematic space are commutative [117] which is an important property and very useful to facilitate the computation of constraint equations.

This section presents the basic idea of kinematic mapping space and the transformation within it. Two algorithms, the explicitation algorithm and implicitization algorithm, which are both based on the kinematic mapping method in order to derive constraint equations for serial kinematic chains will now be described.

### 2.2.2 Explication Algorithm

The main idea of the explication algorithm is to obtain a simple set of algebraic equations for a 3R chain with each set in one variable [117,118]. As mentioned above the manifold of a 3R chain is the intersection of a set of one-parameter 3-spaces with  $S_6^2$ , where the set of 3-spaces with one parameter in multi-dimensional geometry are called Segre Manifolds (SMs). There are three 3-spaces for a 3R chain depend on one of its three R joints, i.e., a 3R chain has three SMs ( $SM_i, i=(1, 2, 3)$ ). The SMs can also be described as the intersection of four pencils of hyper-planes which can be written into four polynomials. Then the constraint equations of a 3R chain can be composed of the four polynomials and the equation of  $S_6^2$  (Eq. (2.33)).

Briefly recalling the process to derive four polynomials for a SM of a 3R chain, the kinematics of a 3R chain can be represented by:

$$T = M_1 \cdot G_1 \cdot M_2 \cdot G_2 \cdot M_3 \cdot G_3 \quad (2.36)$$

If one R joint was fixed, such as the first one, then a 2R chain remains. Neglecting  $M_1 \cdot G_1$  in the base and  $G_3$  in the moving frame and setting  $d_2$  in matrix  $G_2$  as zero, then the representation of the SM of the 2R chain becomes

$$T = M_2 \cdot G_2 \cdot M_3 \quad (2.37)$$

Dealing with the study parameters, it is possible to obtain four simple independent linear equations as the constraint equations for the SM of this 2R chain:

$$\begin{aligned} 2a_2w_2x_0 - 4y_0 &= 0 \\ 2a_2x_1 + 4w_2y_1 &= 0 \\ 2a_2x_2 + 4w_2y_2 &= 0 \\ 2a_2w_2x_3 - 4y_3 &= 0 \end{aligned} \quad (2.38)$$

where  $w_i = \tan(\alpha_i/2)$ .

In the next step, the transformations  $M_1 \cdot G_1$  in the base and  $G_3$  in the moving frame which were omitted are added back into the 2R chain in the kinematic mapping space to obtain the constraint equations for a general 3R chain. The projective transformation in the base is  $(T_b(M_1)^T)^{-1} \cdot (T_b(G_1)^T)^{-1} \cdot (T_b(G_2)^T)^{-1}$  ( $G_2$  has the same definition as above but with  $a_2=0, \alpha_2=0$ ) and the projective transformation in the moving frame is  $(T_m(G_3)^T)^{-1}$ , therefore, a set of four constraint equations for  $SM_1$  in  $v_1$  ( $v_i = \tan(\theta_i/2)$ ) can be obtained by adding all of the transformations in the base and moving frames into the constraint equations of the 2R chain.

A set of constraint equations of  $SM$  in  $v_3$  can also be obtained using the same procedures. The process of obtaining a set of constraint equations of  $SM_2$  in  $v_2$  is slightly different [118].

### 2.2.3 Implicitization Algorithm

The implicitization algorithm aims to construct the smallest variety within the kinematic mapping space containing all the corresponding points of the EE poses of a general kinematic chain [119]. It can be used to obtain the constraint equations for general kinematic chains including 3J, 4J and 5J kinematics chains. The set of equations for the variety must consist of the equations of  $S_6^2$ . The necessary number of constraint equations of a kinematic chain is dependent on its number of DOFs. Therefore, if a kinematic chain has  $m$ -DOFs then  $6-m$  constraint equations are needed for the kinematic chain.

The following summarizes how the constraint equations for the corresponding smallest variety will be obtained. For a general kinematic chain, the EE poses with respect to the base are given by:

$$F = M_1 \cdot G_1 \cdots M_i \quad (2.39)$$

Calculating eight study parameters  $[x_0, x_1, x_2, x_3, y_0, y_1, y_2, y_3]$  for  $F$  using Eqs. (2.31) and (2.32) in tangent half revolute angles, homogeneous equations (in degree 1, 2, 3, 4... $n$ , called Ansatz equations) with general coefficients can be constructed. For example, homogeneous equations in degree one can be written as:

$$Ansatz = C_1 \cdot y_3 + C_2 \cdot x_3 + C_3 \cdot y_2 + C_4 \cdot x_2 + C_5 \cdot y_1 + C_6 \cdot x_1 + C_7 \cdot y_0 + C_8 \cdot x_0 \quad (2.40)$$

Then the study parameters are substituted into the algebraic expression Eq. (2.40). The expression obtained has to vanish for all the values of tangent half angles, meaning that all the coefficients also must vanish identically. Therefore, coefficients expressions of the Ansatz equation can be obtained, then the system can be solved to obtain the general coefficients ( $C_1, C_2, \dots, C_8$ ). If there are solutions then the linear constraint equations will be obtained for the kinematic chain by substituting  $C_i$  back to Ansatz. Note that the number of unknown is  $(n+7, n)^T$  for Ansatz in degree  $n$ . If there is no equation for a serial chain in degree one, then homogeneous equations in degree two have to be considered where a general quadratic polynomial has 36 unknowns. Undertaking the same procedures above, the constraint equations for most kinematic chains can be derived in this step. Otherwise one needs to continue with degrees 3, 4 and even more.

All the equations produced in a new degree step need to be reduced from equations produced one step before with the Grobner basis to see if there are newly obtained equations until the necessary number of constraint equations is obtained.

### 2.3 Constraints Equations of a General 4R Chain Based on Kinematic Mapping Method

Based on the thoughts of obtaining the constraint equations for a general 3R chain, it is possible to derive the constraint equations for a general 4R chain depending on its two angles. The kinematics of a general 4R chain can be represented by:

$$T = M_1 \cdot G_1 \cdot M_2 \cdot G_2 \cdot M_3 \cdot G_3 \cdot M_4 \cdot G_4 \quad (2.41)$$

If two R joints are fixed, such as the first and fourth, then a 2R chain remains. Neglecting  $M_1 \cdot G_1$  in the base and  $G_3 \cdot M_4 \cdot G_4$  in the moving frame and setting  $d_2$  as zero, then the representation of the 2R chain becomes Eq. (2.37). The four same simple independent linear equations as Eq. (2.38) can be derived as the constraint equations of this 2R chain. Then the transformations which were omitted are added back to the 2R chain in the kinematic image space. The projective transformations in the base are  $(T_b(M_1)^T)^{-1} \cdot (T_b(G_1)^T)^{-1} \cdot (T_b(G_2)^T)^{-1}$  ( $a_2=0$ ,  $a_3=0$  in  $G_2$ ), and the projective transformation in the moving frame becomes  $(T_m(G_3)^T)^{-1} \cdot (T_m(M_4)^T)^{-1} \cdot (T_m(G_4)^T)^{-1}$ . Therefore, a set of four equations in  $v_1$  and  $v_4$  can be obtained. These equations and the equation of  $S_6^2$  compose the constraint equations for a general 4R chain.

Using this method, five sets of constraint equations for a general 4R chain in any two of its four  $v_i$  (except constraint equations in  $v_2$  and  $v_3$ ) can be obtained.

### 2.4 Summary

This chapter recalled the relevant mathematical knowledge on simplifying trigonometric using tangent half angle and the vector method to calculate the distance of two skew lines, as well as the linear algebra method of determining the dependence or independence between a set of constraint equations. Also, it reviewed the kinematic mapping method and summarizes two corresponding algorithms: the explicitation algorithm for constructing constraint equations for general 3R chains and the implicitization algorithm for deriving general kinematic chains with 3, 4 and 5 joints. Moreover, the explicitation algorithm is developed to obtain the constraint equations for

general 4R kinematic chains. These algorithms will be applied for the kinematic analysis of MMRRMs in the later chapters. In summary, this chapter provides the mathematical foundation for both the design and kinematic analysis of MMRRMs.

## Chapter 3 – Constraint Equations of Typical Serial Kinematic Chains

The kinematic analysis of mechanisms using the kinematic mapping method, including single-loop mechanisms and multi-loop mechanisms, can be simplified by analysing and solving constraint equations of their compositional serial kinematic chains. The algorithms for generating the constraint equations for serial kinematic chains have been summarized and presented in Chapter 2. Using these methods, the synthesis for constraint equations of a variety of serial kinematic chains will be carried out in this chapter, and relationships between constraint equations among the similarly constructed kinematic chains will be identified. In addition, essential linear algebra knowledge is applied to select proper constraint equations from the implicitization method for a kinematic chain.

### 3.1 Typical Serial 3J, 4J and 5J Kinematic Chains

Firstly, serial kinematic chains are classified into several categories according to: (a) the number of the joints (J), including revolute (R) or prismatic (P) joints, of a serial kinematic chain; (b) the specific placement between the joint groups, in which the symbols have their meanings as follows:

- i)  $\acute{R}$ : axes of the R joints are parallel
- ii)  $\grave{R}$ : axes of the R joints are parallel along another direction
- iii)  $\dot{R}$ : axes of the R joints intersect at one point

Therefore, the fundamental kinematic chains are listed in the following [3].

#### 1) 3J serial kinematic chains

(1) PPP	(2) PPR	(3) RPP
(4) PRP	(5) PRR	(6) RPR
(7) RRP	(8) $\acute{R}\acute{R}\acute{R}$	(9) $\acute{R}\dot{R}\dot{R}$
(10) $\acute{R}\dot{R}\dot{R}$	(11) $\dot{R}\dot{R}\dot{R}$	(12) $\dot{R}\dot{R}\dot{R}$
(13) $\dot{R}\dot{R}\dot{R}$	(14) $\dot{R}\dot{R}\dot{R}$	

## 2) 4J serial kinematic chains

(1)PPPR	(2)PPRP	(3)PRPP
(4)PPRR	(5)PRRP	(6)RRPP
(7)PRPR	(8)RPRP	(9) PRRR
(10) RPRR	(11) RRPR	(12) RRRP
(13) $\acute{R}\acute{R}\acute{R}$	(14) $R\acute{R}\acute{R}$	(15) $\acute{R}\acute{R}\acute{R}$
(16) $\acute{R}\acute{R}\acute{R}$	(17) $\acute{R}\acute{R}\acute{R}$	(18) $\acute{R}\acute{R}\acute{R}$
(19) $\acute{R}\acute{R}\acute{R}$	(20) $R\acute{R}\acute{R}$	(21) $\acute{R}\acute{R}\acute{R}$

## 3) 5J serial kinematic chains

(1)PPPPP	(2)PPPPR	(3)PPPRP
(4)PPRRP	(5)PPRRR	(6)PRPRP
(7)PRRRP	(8)RPRPR	(9)PRRPR
(10)RRRPR	(11)RRRRP	(12)RRRPR
(13)RRPRR	(14)RPRRR	(15)PRRRR
(16) $\acute{R}\acute{R}\acute{R}\acute{R}$	(17) $\acute{R}\acute{R}\acute{R}\acute{R}$	(18) $\acute{R}\acute{R}\acute{R}\acute{R}$
(19) $\acute{R}\acute{R}\acute{R}\acute{R}$	(20) $\acute{R}\acute{R}\acute{R}\acute{R}$	(21) $\acute{R}\acute{R}\acute{R}\acute{R}$
(22) $\acute{R}\acute{R}\acute{R}\acute{R}$	(23) $\acute{R}\acute{R}\acute{R}\acute{R}$	(24) $\acute{R}\acute{R}\acute{R}\acute{R}$
(25) (RRR)s $\acute{R}\acute{R}$	(26) $\acute{R}\acute{R}$ (RRR)s	

## 3.2 Constraint Equations of Typical Serial Kinematic Chains

In this section, the kinematic mapping based methods including the explicitation algorithm and the implicitization algorithm will be used to obtain the constrained equations for the typical serial kinematic chains listed in the section above.

### 3.2.1 Constraint Equations for 3R and 4R Serial Kinematic Chains Using the Explicitation Algorithm

The explicitation algorithm can be only used for 3R and 4R serial kinematic chains to produce equations for their constraint manifold (the equation for the Study quadric, Eq. (2.33), must be included for further analysis of a mechanism). In [118], the constrained equations for three *SMs* of 3R chains have been obtained, however, in this section these constraint equations are displayed in their simplest forms (Tables 3.1). Moreover, the constrained equations for 4R serial kinematic chains obtained from the developed



explicitation algorithm are first illustrated (Table 3.2). Note that in some cases not all the three sets of equations of *SMs* can be selected [118]. If a set of equations of one *SM* depending on one R joint is selected with the joint axes of the remaining two parallel or intersected, in which case the *SM* lies on the  $S_6^2$ , then the intersection of the *SM* with the  $S_6^2$  fails.

Table 3.1 Constraint equations for 3R serial kinematic chains using the explicitation algorithm ( $w_i = \tan(\alpha_i / 2)$ ,  $v_i = \tan(\theta_i / 2)$ , here  $i=1,2,3$ )

$T(v_1)$	<p>(1) <math>a_2 v_1 w_1 w_2 x_2 - a_1 v_1 w_1 x_3 + a_2 v_1 w_2 x_3 + a_2 w_1 w_2 x_1 + d_2 v_1 w_1 x_1 + a_1 v_1 x_2 - a_1 w_1 x_0 + a_2 w_2 x_0 - d_2 v_1 x_0 - d_2 w_1 x_2 - 2 v_1 w_1 y_2 + a_1 x_1 + d_2 x_3 - 2 v_1 y_3 - 2 w_1 y_1 - 2 y_0</math></p> <p>(2) <math>a_2 v_1 w_1 w_2 x_1 + a_1 v_1 w_1 x_0 - a_2 v_1 w_2 x_0 - a_2 w_1 w_2 x_2 - d_2 v_1 w_1 x_2 + a_1 v_1 x_1 - a_1 w_1 x_3 + a_2 w_2 x_3 - d_2 v_1 x_3 - d_2 w_1 x_1 - 2 v_1 w_1 y_1 - a_1 x_2 - d_2 x_0 + 2 v_1 y_0 + 2 w_1 y_2 - 2 y_3</math></p> <p>(3) <math>-a_1 v_1 w_1 w_2 x_1 - d_2 v_1 w_1 w_2 x_3 + a_1 v_1 w_2 x_0 + a_1 w_1 w_2 x_2 - a_2 v_1 w_1 x_0 + d_2 v_1 w_2 x_2 - d_2 w_1 w_2 x_0 - 2 v_1 w_1 w_2 y_0 - a_1 w_2 x_3 - a_2 v_1 x_1 + a_2 w_1 x_3 + d_2 w_2 x_1 - 2 v_1 w_2 y_1 + 2 w_1 w_2 y_3 + a_2 x_2 + 2 w_2 y_2</math></p> <p>(4) <math>a_1 v_1 w_1 w_2 x_2 + d_2 v_1 w_1 w_2 x_0 + a_1 v_1 w_2 x_3 + a_1 w_1 w_2 x_1 - a_2 v_1 w_1 x_3 + d_2 v_1 w_2 x_1 - d_2 w_1 w_2 x_3 - 2 v_1 w_1 w_2 y_3 + a_1 w_2 x_0 + a_2 v_1 x_2 - a_2 w_1 x_0 - d_2 w_2 x_2 + 2 v_1 w_2 y_2 - 2 w_1 w_2 y_0 + a_2 x_1 + 2 w_2 y_1</math></p>
$T(v_2)$	<p>(1) <math>(a_1 w_1 w_2 v_2 - a_2 w_1 w_2 v_2 + a_1 v_2 - a_2 v_2 + w_1 d_2 - w_2 d_2) x_1 + (a_1 w_1 w_2 + a_2 w_1 w_2 + w_1 d_2 v_2 + w_2 d_2 v_2 - a_1 - a_2) x_2 + 2((w_1 - w_2) v_2) y_1 + (-2 w_1 - 2 w_2) y_2</math></p> <p>(2) <math>(a_1 w_1 w_2 v_2 - a_2 w_1 w_2 v_2 + a_1 v_2 - a_2 v_2 + w_1 d_2 - w_2 d_2) x_1 + (a_1 w_1 w_2 + a_2 w_1 w_2 + w_1 d_2 v_2 + w_2 d_2 v_2 - a_1 - a_2) x_2 + 2((w_1 - w_2) v_2) y_1 + (-2 w_1 - 2 w_2) y_2</math></p> <p>(3) <math>(a_1 w_1 w_2 + a_2 w_1 w_2 + w_1 d_2 v_2 + w_2 d_2 v_2 - a_1 - a_2) x_1 + (-a_1 w_1 w_2 v_2 + a_2 w_1 w_2 v_2 - a_1 v_2 + a_2 v_2 - w_1 d_2 + w_2 d_2) x_2 + (-2 w_1 - 2 w_2) y_1 - 2((w_1 - w_2) v_2) y_2</math></p> <p>(4) <math>(a_1 w_1 v_2 - a_1 w_2 v_2 - a_2 w_1 v_2 + a_2 w_2 v_2 - w_1 w_2 d_2 - d_2) x_3 - 2((w_1 w_2 + 1) v_2) y_3 - 2 y_0 w_1 w_2 + (w_1 w_2 d_2 v_2 - a_1 w_1 - a_1 w_2 - a_2 w_1 - a_2 w_2 - d_2 v_2) x_0 + 2 y_0</math></p>
$T(v_3)$	<p>(1) <math>-2 a_1 v_3 w_1 w_2 x_2 + 2 a_1 v_3 w_1 x_3 + 2 a_1 w_1 w_2 x_1 - 2 a_2 v_3 w_2 x_3 + 2 d_2 v_3 w_2 x_1 + 2 a_1 w_1 x_0 - 2 a_2 v_3 x_2 - 2 a_2 w_2 x_0 - 2 d_2 v_3 x_0 + 2 d_2 w_2 x_2 + 4 v_3 w_2 y_2 + 2 a_2 x_1 + 2 d_2 x_3 - 4 v_3 y_3 - 4 w_2 y_1 - 4 y_0</math></p> <p>(2) <math>-2 a_2 v_3 w_1 w_2 x_2 + 2 d_2 v_3 w_1 w_2 x_0 - 2 a_1 v_3 w_2 x_3 + 2 a_2 v_3 w_1 x_3 + 2 a_2 w_1 w_2 x_1 + 2 d_2 v_3 w_1 x_1 - 2 d_2 w_1 w_2 x_3 - 4 v_3 w_1 w_2 y_3 - 2 a_1 v_3 x_2 - 2 a_1 w_2 x_0 + 2 a_2 w_1 x_0 + 2 d_2 w_1 x_2 - 4 v_3 w_1 y_2 - 4 w_1 w_2 y_0 + 2 a_1 x_1 + 4 w_1 y_1</math></p> <p>(3) <math>2 a_2 v_3 w_1 w_2 x_1 + 2 d_2 v_3 w_1 w_2 x_3 + 2 a_1 v_3 w_2 x_0 - 2 a_2 v_3 w_1 x_0 + 2 a_2 w_1 w_2 x_2 + 2 d_2 v_3 w_1 x_2 + 2 d_2 w_1 w_2 x_0 + 4 v_3 w_1 w_2 y_0 + 2 a_1 v_3 x_1 - 2 a_1 w_2 x_3 + 2 a_2 w_1 x_3 - 2 d_2 w_1 x_1 + 4 v_3 w_1 y_1 - 4 w_1 w_2 y_3 + 2 a_1 x_2 + 4 w_1 y_2</math></p> <p>(4) <math>2 a_1 v_3 w_1 w_2 x_1 - 2 a_1 v_3 w_1 x_0 + 2 a_1 w_1 w_2 x_2 + 2 a_2 v_3 w_2 x_0 + 2 d_2 v_3 w_2 x_2 + 2 a_1 w_1 x_3 + 2 a_2 v_3 x_1 - 2 a_2 w_2 x_3 - 2 d_2 v_3 x_3 - 2 d_2 w_2 x_1 - 4 v_3 w_2 y_1 + 2 a_2 x_2 - 2 d_2 x_0 + 4 v_3 y_0 - 4 w_2 y_2 - 4 y_3</math></p>

Table 3.2 Constraint equations for 4R serial kinematic chains using the explicitation algorithm (For constraint equations in other tangent half angles, see Table A.I.1 in Appendix A I)

T(v <sub>1</sub> v <sub>2</sub> )	<p>(1) <math>-2a_3v_1v_2w_1w_2w_3x_0 + 2a_1v_1v_2w_1w_2x_1 - 2a_2v_1v_2w_1w_2x_1 + 2a_3v_1v_2w_1w_3x_1 - 2a_3v_1v_2w_2w_3x_1</math>  <math>-2a_3v_1w_1w_2w_3x_3 + 2a_3v_2w_1w_2w_3x_3 - 2d_3v_1v_2w_1w_2x_3 + 2a_1v_1v_2w_1x_0 - 2a_1v_1v_2w_2x_0</math>  <math>-2a_1v_1w_1w_2x_2 - 2a_1v_2w_1w_2x_2 - 2a_2v_1v_2w_1x_0 + 2a_2v_1v_2w_2x_0 - 2a_2v_1w_1w_2x_2 + 2a_2v_2w_1w_2x_2</math>  <math>-2a_3v_1v_2w_3x_0 + 2a_3v_1w_1w_3x_2 + 2a_3v_1w_2w_3x_2 - 2a_3v_2w_1w_3x_2 + 2a_3v_2w_2w_3x_2 - 2a_3w_1w_2w_3x_0</math>  <math>-2d_3v_1v_2w_1x_2 + 2d_3v_1v_2w_2x_2 + 2d_3v_1w_1w_2x_0 - 2d_3v_2w_1w_2x_0 + 4v_1v_2w_1w_2y_0 + 2a_1v_1v_2x_1</math>  <math>-2a_1v_1w_1x_3 - 2a_1v_1w_2x_3 - 2a_1v_2w_1x_3 + 2a_1v_2w_2x_3 - 2a_1w_1w_2x_1 - 2a_2v_1v_2x_1 - 2a_2v_1w_1x_3</math>  <math>-2a_2v_1w_2x_3 + 2a_2v_2w_1x_3 - 2a_2v_2w_2x_3 - 2a_2w_1w_2x_1 + 2a_3v_1w_3x_3 + 2a_3v_2w_3x_3 + 2a_3w_1w_3x_1</math>  <math>+2a_3w_2w_3x_1 - 2d_3v_1v_2x_3 + 2d_3v_1w_1x_1 + 2d_3v_1w_2x_1 - 2d_3v_2w_1x_1 + 2d_3v_2w_2x_1 - 2d_3w_1w_2x_3</math>  <math>-4v_1v_2w_1y_1 + 4v_1v_2w_2y_1 + 4v_1w_1w_2y_3 - 4v_2w_1w_2y_3 + 2a_1v_1x_2 - 2a_1v_2x_2 - 2a_1w_1x_0 - 2a_1w_2x_0</math>  <math>+2a_2v_1x_2 + 2a_2v_2x_2 - 2a_2w_1x_0 - 2a_2w_2x_0 + 2a_3w_3x_0 - 2d_3v_1x_0 - 2d_3v_2x_0 - 2d_3w_1x_2</math>  <math>-2d_3w_2x_2 + 4v_1v_2y_0 - 4v_1w_1y_2 - 4v_1w_2y_2 + 4v_2w_1y_2 - 4v_2w_2y_2 + 4w_1w_2y_0 + 2a_1x_1 + 2a_2x_1</math>  <math>+2d_3x_3 - 4v_1y_3 - 4v_2y_3 - 4w_1y_1 - 4w_2y_1 - 4y_0</math></p> <p>(2) <math>2a_1v_1v_2w_1w_2w_3x_0 - 2a_2v_1v_2w_1w_2w_3x_0 + 2d_3v_1v_2w_1w_2w_3x_2 - 2a_1v_1v_2w_1w_3x_1</math>  <math>+2a_1v_1v_2w_2w_3x_1 - 2a_1v_1w_1w_2w_3x_3 - 2a_1v_2w_1w_2w_3x_3 + 2a_2v_1v_2w_1w_3x_1 - 2a_2v_1v_2w_2w_3x_1</math>  <math>-2a_2v_1w_1w_2w_3x_3 + 2a_2v_2w_1w_2w_3x_3 - 2a_3v_1v_2w_1w_2x_1 - 2d_3v_1v_2w_1w_3x_3 + 2d_3v_1v_2w_2w_3x_3</math>  <math>-2d_3v_1w_1w_2w_3x_1 + 2d_3v_2w_1w_2w_3x_1 - 4v_1v_2w_1w_2w_3y_1 + 2a_1v_1v_2w_3x_0 + 2a_1v_1w_1w_3x_2</math>  <math>+2a_1v_1w_2w_3x_2 + 2a_1v_2w_1w_3x_2 - 2a_1v_2w_2w_3x_2 - 2a_1w_1w_2w_3x_0 - 2a_2v_1v_2w_3x_0</math>  <math>+2a_2v_1w_1w_3x_2 + 2a_2v_1w_2w_3x_2 - 2a_2v_2w_1w_3x_2 + 2a_2v_2w_2w_3x_2 - 2a_2w_1w_2w_3x_0 - 2a_3v_1v_2w_1x_0</math>  <math>+2a_3v_1v_2w_2x_0 - 2a_3v_1w_1w_2x_2 + 2a_3v_2w_1w_2x_2 + 2d_3v_1v_2w_3x_2 + 2d_3v_1w_1w_3x_0 + 2d_3v_1w_2w_3x_0</math>  <math>-2d_3v_2w_1w_3x_0 + 2d_3v_2w_2w_3x_0 + 2d_3w_1w_2w_3x_2 - 4v_1v_2w_1w_3y_0 + 4v_1v_2w_2w_3y_0 - 4v_1w_1w_2w_3y_2</math>  <math>+4v_2w_1w_2w_3y_2 + 2a_1v_1w_3x_3 - 2a_1v_2w_3x_3 + 2a_1w_1w_3x_1 + 2a_1w_2w_3x_1 + 2a_2v_1w_3x_3 + 2a_2v_2w_3x_3</math>  <math>+2a_2w_1w_3x_1 + 2a_2w_2w_3x_1 - 2a_3v_1v_2x_1 - 2a_3v_1w_1x_3 - 2a_3v_1w_2x_3 + 2a_3v_2w_1x_3 - 2a_3v_2w_2x_3</math>  <math>-2a_3w_1w_2x_1 + 2d_3v_1w_3x_1 + 2d_3v_2w_3x_1 - 2d_3w_1w_3x_3 - 2d_3w_2w_3x_3 - 4v_1v_2w_3y_1 - 4v_1w_1w_3y_3</math>  <math>-4v_1w_2w_3y_3 + 4v_2w_1w_3y_3 - 4v_2w_2w_3y_3 - 4w_1w_2w_3y_1 + 2a_1w_3x_0 + 2a_2w_3x_0 + 2a_3v_1x_2</math>  <math>+2a_3v_2x_2 - 2a_3w_1x_0 - 2a_3w_2x_0 - 2d_3w_3x_2 + 4v_1w_3y_2 + 4v_2w_3y_2 - 4w_1w_3y_0 - 4w_2w_3y_0</math>  <math>+2a_3x_1 + 4w_3y_1</math></p>
-----------------------------------	--

$$\begin{aligned}
(3) \quad & -2a_1v_1v_2w_1w_2w_3x_3 + 2a_2v_1v_2w_1w_2w_3x_3 - 2d_3v_1v_2w_1w_2w_3x_1 - 2a_1v_1v_2w_1w_3x_2 \\
& + 2a_1v_1v_2w_2w_3x_2 - 2a_1v_1w_1w_2w_3x_0 - 2a_1v_2w_1w_2w_3x_0 + 2a_2v_1v_2w_1w_3x_2 - 2a_2v_1v_2w_2w_3x_2 \\
& - 2a_2v_1w_1w_2w_3x_0 + 2a_2v_2w_1w_2w_3x_0 - 2a_3v_1v_2w_1w_2x_2 - 2d_3v_1v_2w_1w_3x_0 + 2d_3v_1v_2w_2w_3x_0 \\
& - 2d_3v_1w_1w_2w_3x_2 + 2d_3v_2w_1w_2w_3x_2 - 4v_1v_2w_1w_2w_3y_2 - 2a_1v_1v_2w_3x_3 - 2a_1v_1w_1w_3x_1 \\
& - 2a_1v_1w_2w_3x_1 - 2a_1v_2w_1w_3x_1 + 2a_1v_2w_2w_3x_1 + 2a_1w_1w_2w_3x_3 + 2a_2v_1v_2w_3x_3 \\
& - 2a_2v_1w_1w_3x_1 - 2a_2v_1w_2w_3x_1 + 2a_2v_2w_1w_3x_1 - 2a_2v_2w_2w_3x_1 + 2a_2w_1w_2w_3x_3 \\
& + 2a_3v_1v_2w_1x_3 - 2a_3v_1v_2w_2x_3 + 2a_3v_1w_1w_2x_1 - 2a_3v_2w_1w_2x_1 - 2d_3v_1v_2w_3x_1 - 2d_3v_1w_1w_3x_3 \\
& - 2d_3v_1w_2w_3x_3 + 2d_3v_2w_1w_3x_3 - 2d_3v_2w_2w_3x_3 - 2d_3w_1w_2w_3x_1 + 4v_1v_2w_1w_3y_3 \\
& - 4v_1v_2w_2w_3y_3 + 4v_1w_1w_2w_3y_1 - 4v_2w_1w_2w_3y_1 + 2a_1v_1w_3x_0 - 2a_1v_2w_3x_0 + 2a_1w_1w_3x_2 \\
& + 2a_1w_2w_3x_2 + 2a_2v_1w_3x_0 + 2a_2v_2w_3x_0 + 2a_2w_1w_3x_2 + 2a_2w_2w_3x_2 - 2a_3v_1v_2x_2 - 2a_3v_1w_1x_0 \\
& - 2a_3v_1w_2x_0 + 2a_3v_2w_1x_0 - 2a_3v_2w_2x_0 - 2a_3w_1w_2x_2 + 2d_3v_1w_3x_2 + 2d_3v_2w_3x_2 - 2d_3w_1w_3x_0 \\
& - 2d_3w_2w_3x_0 - 4v_1v_2w_3y_2 - 4v_1w_1w_3y_0 - 4v_1w_2w_3y_0 + 4v_2w_1w_3y_0 - 4v_2w_2w_3y_0 \\
& - 4w_1w_2w_3y_2 - 2a_1w_3x_3 - 2a_2w_3x_3 - 2a_3v_1x_1 - 2a_3v_2x_1 + 2a_3w_1x_3 + 2a_3w_2x_3 + 2d_3w_3x_1 \\
& - 4v_1w_3y_1 - 4v_2w_3y_1 + 4w_1w_3y_3 + 4w_2w_3y_3 + 2a_3x_2 + 4w_3y_2 \\
\\
(4) \quad & -2a_3v_1v_2w_1w_2w_3x_3 - 2a_1v_1v_2w_1w_2x_2 + 2a_2v_1v_2w_1w_2x_2 - 2a_3v_1v_2w_1w_3x_2 \\
& + 2a_3v_1v_2w_2w_3x_2 + 2a_3v_1w_1w_2w_3x_0 - 2a_3v_2w_1w_2w_3x_0 + 2d_3v_1v_2w_1w_2x_0 + 2a_1v_1v_2w_1x_3 \\
& - 2a_1v_1v_2w_2x_3 - 2a_1v_1w_1w_2x_1 - 2a_1v_2w_1w_2x_1 - 2a_2v_1v_2w_1x_3 + 2a_2v_1v_2w_2x_3 \\
& - 2a_2v_1w_1w_2x_1 + 2a_2v_2w_1w_2x_1 - 2a_3v_1v_2w_3x_3 + 2a_3v_1w_1w_3x_1 + 2a_3v_1w_2w_3x_1 \\
& - 2a_3v_2w_1w_3x_1 + 2a_3v_2w_2w_3x_1 - 2a_3w_1w_2w_3x_3 - 2d_3v_1v_2w_1x_1 + 2d_3v_1v_2w_2x_1 \\
& + 2d_3v_1w_1w_2x_3 - 2d_3v_2w_1w_2x_3 + 4v_1v_2w_1w_2y_3 - 2a_1v_1v_2x_2 + 2a_1v_1w_1x_0 + 2a_1v_1w_2x_0 \\
& + 2a_1v_2w_1x_0 - 2a_1v_2w_2x_0 + 2a_1w_1w_2x_2 + 2a_2v_1v_2x_2 + 2a_2v_1w_1x_0 + 2a_2v_1w_2x_0 \\
& - 2a_2v_2w_1x_0 + 2a_2v_2w_2x_0 + 2a_2w_1w_2x_2 - 2a_3v_1w_3x_0 - 2a_3v_2w_3x_0 - 2a_3w_1w_3x_2 \\
& - 2a_3w_2w_3x_2 + 2d_3v_1v_2x_0 - 2d_3v_1w_1x_2 - 2d_3v_1w_2x_2 + 2d_3v_2w_1x_2 - 2d_3v_2w_2x_2 \\
& + 2d_3w_1w_2x_0 + 4v_1v_2w_1y_2 - 4v_1v_2w_2y_2 - 4v_1w_1w_2y_0 + 4v_2w_1w_2y_0 + 2a_1v_1x_1 - 2a_1v_2x_1 \\
& - 2a_1w_1x_3 - 2a_1w_2x_3 + 2a_2v_1x_1 + 2a_2v_2x_1 - 2a_2w_1x_3 - 2a_2w_2x_3 + 2a_3w_3x_3 - 2d_3v_1x_3 \\
& - 2d_3v_2x_3 - 2d_3w_1x_1 - 2d_3w_2x_1 + 4v_1v_2y_3 - 4v_1w_1y_1 - 4v_1w_2y_1 + 4v_2w_1y_1 - 4v_2w_2y_1 \\
& + 4w_1w_2y_3 - 2a_1x_2 - 2a_2x_2 - 2d_3x_0 + 4v_1y_0 + 4v_2y_0 + 4w_1y_2 + 4w_2y_2 - 4y_3
\end{aligned}$$

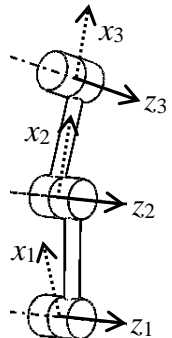
$T(v_3v_4)$	<p>(1) <math>4a_1w_3v_3v_4w_1w_2x_0 + 4a_1v_3v_4w_1w_2x_1 + 4a_1w_3v_3v_4w_1x_1 - 4a_1w_3v_3w_1w_2x_3 - 4a_1w_3v_4w_1w_2x_3</math>  <math>-4a_2w_3v_3v_4w_2x_1 - 4a_3w_3v_3v_4w_2x_1 - 4w_3d_2v_3v_4w_2x_3 + 4w_3d_3v_3v_4w_2x_3 - 4a_1v_3v_4w_1x_0</math>  <math>-4a_1v_3w_1w_2x_2 - 4a_1w_3v_3w_1x_2 + 4a_1v_4w_1w_2x_2 + 4a_1w_3v_4w_1x_2 - 4a_1w_3w_1w_2x_0 + 4a_2v_3v_4w_2x_0</math>  <math>+4a_2w_3v_3v_4x_0 + 4a_2w_3v_3w_2x_2 - 4a_2w_3v_4w_2x_2 + 4a_3v_3v_4w_2x_0 + 4a_3w_3v_3v_4x_0 + 4a_3w_3v_3w_2x_2</math>  <math>-4a_3w_3v_4w_2x_2 + 4d_2v_3v_4w_2x_2 - 4w_3d_2v_3v_4x_2 - 4w_3d_2v_3w_2x_0 - 4w_3d_2v_4w_2x_0 + 4d_3v_3v_4w_2x_2</math>  <math>+4w_3d_3v_3v_4x_2 + 4w_3d_3v_3w_2x_0 + 4w_3d_3v_4w_2x_0 - 4a_3w_3v_4w_2x_2 + 4d_2v_3v_4w_2x_2 - 4w_3d_2v_3v_4x_2</math>  <math>-4w_3d_2v_3w_2x_0 - 4w_3d_2v_4w_2x_0 + 4d_3v_3v_4w_2x_2 + 4w_3d_3v_3v_4x_2 + 4w_3d_3v_3w_2x_0 + 4w_3d_3v_4w_2x_0</math>  <math>-4a_2w_3v_4x_3 - 4a_2w_3w_2x_1 + 4a_3v_3v_4x_1 - 4a_3v_3w_2x_3 - 4a_3w_3v_3x_3 - 4a_3v_4w_2x_3 - 4a_3w_3v_4x_3</math>  <math>-4a_3w_3w_2x_1 - 4d_2v_3v_4x_3 + 4d_2v_3w_2x_1 - 4w_3d_2v_3x_1 - 4d_2v_4w_2x_1 + 4w_3d_2v_4x_1 + 4w_3d_2w_2x_3</math>  <math>-4d_3v_3v_4x_3 + 4d_3v_3w_2x_1 + 4w_3d_3v_3x_1 - 4d_3v_4w_2x_1 - 4w_3d_3v_4x_1 - 4w_3d_3w_2x_3 - 8v_3v_4w_2y_1</math>  <math>-8w_3v_3v_4y_1 + 8w_3v_3w_2y_3 + 8w_3v_4w_2y_3 + 4a_1w_1x_0 - 4a_2v_3x_2 + 4a_2v_4x_2 - 4a_2w_2x_0 - 4a_2w_3x_0</math>  <math>-4a_3v_3x_2 + 4a_3v_4x_2 - 4a_3w_2x_0 - 4a_3w_3x_0 - 4d_2v_3x_0 - 4d_2v_4x_0 + 4d_2w_2x_2 - 4w_3d_2x_2</math>  <math>-4d_3v_3x_0 - 4d_3v_4x_0 + 4d_3w_2x_2 + 4w_3d_3x_2 + 8v_3v_4y_0 + 8v_3w_2y_2 + 8w_3v_3y_2 - 8v_4w_2y_2 - 8y_0</math>  <math>-8w_3v_4y_2 + 8w_3w_2y_0 + 4a_2x_1 + 4a_3x_1 + 4d_2x_3 + 4d_3x_3 - 8v_3y_3 - 8v_4y_3 - 8w_2y_1 - 8w_3y_1</math></p> <p>(2) <math>-4a_2w_3v_3v_4w_1w_2x_0 - 4a_3w_3v_3v_4w_1w_2x_0 - 4w_3d_2v_3v_4w_1w_2x_2 + 4w_3d_3v_3v_4w_1w_2x_2</math>  <math>+4a_1w_3v_3v_4w_2x_1 - 4a_2v_3v_4w_1w_2x_1 - 4a_2w_3v_3v_4w_1x_1 - 4a_2w_3v_3w_1w_2x_3 + 4a_2w_3v_4w_1w_2x_3</math>  <math>-4a_3v_3v_4w_1w_2x_1 - 4a_3w_3v_3v_4w_1x_1 - 4a_3w_3v_3w_1w_2x_3 + 4a_3w_3v_4w_1w_2x_3 - 4d_2v_3v_4w_1w_2x_3</math>  <math>+4w_3d_2v_3v_4w_1x_3 + 4w_3d_2v_3w_1w_2x_1 + 4w_3d_2v_4w_1w_2x_1 - 4d_3v_3v_4w_1w_2x_3 - 4w_3d_3v_3v_4w_1x_3</math>  <math>-4w_3d_3v_3w_1w_2x_1 - 4w_3d_3v_4w_1w_2x_1 + 8w_3v_3v_4w_1w_2y_1 - 4a_1v_3v_4w_2x_0 - 4a_1w_3v_3v_4x_0</math>  <math>+4a_1w_3v_3w_2x_2 + 4a_1w_3v_4w_2x_2 + 4a_2v_3v_4w_1x_0 - 4a_2v_3w_1w_2x_2 - 4a_2w_3v_3w_1x_2</math>  <math>-4a_2v_4w_1w_2x_2 - 4a_2w_3v_4w_1x_2 - 4a_2w_3w_1w_2x_0 + 4a_3v_3v_4w_1x_0 - 4a_3v_3w_1w_2x_2</math>  <math>-4a_3w_3v_3w_1x_2 - 4a_3v_4w_1w_2x_2 - 4a_3w_3v_4w_1x_2 - 4a_3w_3w_1w_2x_0 - 4d_2v_3v_4w_1x_2</math>  <math>+4w_3d_2v_4w_1x_0 + 4w_3d_2w_1w_2x_2 - 4d_3v_3v_4w_1x_2 + 4d_3v_3w_1w_2x_0 + 4w_3d_3v_3w_1x_0</math>  <math>-4d_3v_4w_1w_2x_0 + 4d_2v_3w_1w_2x_0 - 4w_3d_2v_3w_1x_0 - 4d_2v_4w_1w_2x_0 - 4w_3d_3v_4w_1x_0</math>  <math>-4w_3d_3w_1w_2x_2 - 8v_3v_4w_1w_2y_0 - 8w_3v_3v_4w_1y_0 + 8w_3v_3w_1w_2y_2 + 8w_3v_4w_1w_2y_2</math>  <math>-4a_1v_3v_4x_1 - 4a_1v_3w_2x_3 - 4a_1w_3v_3x_3 + 4a_1v_4w_2x_3 + 4a_1w_3v_4x_3 - 4a_1w_3w_2x_1 + 4a_2v_3w_1x_3</math>  <math>-4a_2v_4w_1x_3 + 4a_2w_1w_2x_1 + 4a_2w_3w_1x_1 + 4a_3v_3w_1x_3 - 4a_3v_4w_1x_3 + 4a_3w_1w_2x_1</math>  <math>+4a_3w_3w_1x_1 + 4d_2v_3w_1x_1 + 4d_2v_4w_1x_1 - 4d_2w_1w_2x_3 + 4w_3d_2w_1x_3 + 4d_3v_3w_1x_1</math>  <math>+4d_3v_4w_1x_1 - 4d_3w_1w_2x_3 - 4w_3d_3w_1x_3 - 8v_3v_4w_1y_1 - 8v_3w_1w_2y_3 - 8w_3v_3w_1y_3</math>  <math>+8v_4w_1w_2y_3 + 8w_3v_4w_1y_3 - 8w_3w_1w_2y_1 - 4a_1v_3x_2 - 4a_1v_4x_2 - 4a_1w_2x_0 - 4a_1w_3x_0</math>  <math>+4a_2w_1x_0 + 4a_3w_1x_0 + 4d_2w_1x_2 + 4d_3w_1x_2 - 8v_3w_1y_2 - 8v_4w_1y_2 - 8w_1w_2y_0 - 8w_3w_1y_0</math>  <math>+4a_1x_1 + 8w_1y_1</math></p>
-------------	--

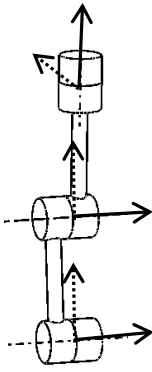
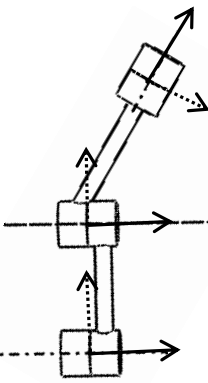
$$\begin{aligned}
(3) \quad & -4a_2w_3v_3v_4w_1w_2x_3 - 4a_3w_3v_3v_4w_1w_2x_3 + 4w_3d_2v_3v_4w_1w_2x_1 - 4w_3d_3v_3v_4w_1w_2x_1 \\
& + 4a_1w_3v_3v_4w_2x_2 - 4a_2v_3v_4w_1w_2x_2 - 4a_2w_3v_3v_4w_1x_2 + 4a_2w_3v_3w_1w_2x_0 \\
& - 4a_2v_3v_4w_1w_2x_0 - 4a_3v_3v_4w_1w_2x_2 - 4a_3w_3v_3v_4w_1x_2 + 4a_3w_3v_3w_1w_2x_0 \\
& - 4a_3v_3v_4w_1w_2x_0 + 4d_2v_3v_4w_1w_2x_0 - 4a_3v_3v_4w_1w_2x_2 - 4a_3w_3v_3v_4w_1x_2 \\
& + 4a_3w_3v_3w_1w_2x_0 - 4a_3w_3v_4w_1w_2x_0 + 4d_2v_3v_4w_1w_2x_0 - 4w_3d_3v_3w_1w_2x_2 \\
& - 4w_3d_3v_4w_1w_2x_2 + 8w_3v_3v_4w_1w_2y_2 - 4a_1v_3v_4w_2x_3 - 4a_1w_3v_3v_4x_3 - 4a_1w_3v_3w_2x_1 \\
& - 4a_1w_3v_4w_2x_1 + 4a_2v_3v_4w_1x_3 + 4a_2v_3w_1w_2x_1 + 4a_2w_3v_3w_1x_1 + 4a_2v_4w_1w_2x_1 \\
& + 4a_2w_3v_4w_1x_1 - 4a_2w_3w_1w_2x_3 + 4a_3v_3v_4w_1x_3 + 4a_3v_3w_1w_2x_1 + 4a_3w_3v_3w_1x_1 \\
& + 4a_3v_4w_1w_2x_1 + 4a_3w_3v_4w_1x_1 - 4a_3w_3w_1w_2x_3 + 4d_2v_3v_4w_1x_1 + 4d_2v_3w_1w_2x_3 \\
& - 4w_3d_2v_3w_1x_3 - 4d_2v_4w_1w_2x_3 + 4w_3d_2v_4w_1x_3 - 4w_3d_2w_1w_2x_1 + 4d_3v_3v_4w_1x_1 \\
& + 4d_3v_3w_1w_2x_3 + 4w_3d_3v_3w_1x_3 - 4d_3v_4w_1w_2x_3 - 4w_3d_3v_4w_1x_3 + 4w_3d_3w_1w_2x_1 \\
& - 8v_3v_4w_1w_2y_3 - 8w_3v_3v_4w_1y_3 - 8w_3v_3w_1w_2y_1 - 8w_3v_4w_1w_2y_1 - 4a_1v_3v_4x_2 \\
& + 4a_1v_3w_2x_0 + 4a_1w_3v_3x_0 - 4a_1v_4w_2x_0 - 4a_1w_3v_4x_0 - 4a_1w_3w_2x_2 - 4a_2v_3w_1x_0 \\
& + 4a_2v_4w_1x_0 + 4a_2w_1w_2x_2 + 4a_2w_3w_1x_2 - 4a_3v_3w_1x_0 + 4a_3v_4w_1x_0 + 4a_3w_1w_2x_2 \\
& + 4a_3w_3w_1x_2 + 4d_2v_3w_1x_2 + 4d_2v_4w_1x_2 + 4d_2w_1w_2x_0 - 4w_3d_2w_1x_0 + 4d_3v_3w_1x_2 \\
& + 4d_3v_4w_1x_2 + 4d_3w_1w_2x_0 + 4w_3d_3w_1x_0 - 8v_3v_4w_1y_2 + 4d_2w_1w_2x_0 - 4w_3d_2w_1x_0 \\
& + 4d_3v_3w_1x_2 + 4d_3v_4w_1x_2 + 4d_3w_1w_2x_0 + 4w_3d_3w_1x_0 - 8v_3v_4w_1y_2 - 8w_3w_1w_2y_2 \\
& + 4a_1v_3x_1 + 4a_1v_4x_1 - 4a_1w_2x_3 - 4a_1w_3x_3 + 4a_2w_1x_3 + 4a_3w_1x_3 - 4d_2w_1x_1 - 4d_3w_1x_1 \\
& + 8v_3w_1y_1 + 8v_4w_1y_1 - 8w_1w_2y_3 - 8w_3w_1y_3 + 4a_1x_2 + 8w_1y_2 \\
(4) \quad & 4a_1w_3v_3v_4w_1w_2x_3 + 4a_1v_3v_4w_1w_2x_2 + 4a_1w_3v_3v_4w_1x_2 + 4a_1w_3v_3w_1w_2x_0 \\
& + 4a_1w_3v_4w_1w_2x_0 - 4a_2w_3v_3v_4w_2x_2 - 4a_3w_3v_3v_4w_2x_2 + 4w_3d_2v_3v_4w_2x_0 \\
& - 4w_3d_3v_3v_4w_2x_0 - 4a_1v_3v_4w_1x_3 + 4a_1v_3w_1w_2x_1 + 4a_1w_3v_3w_1x_1 - 4a_1v_4w_1w_2x_1 \\
& - 4a_1w_3v_4w_1x_1 - 4a_1w_3w_1w_2x_3 + 4a_2v_3v_4w_2x_3 + 4a_2w_3v_3v_4x_3 - 4a_2w_3v_3w_2x_1 \\
& + 4a_2w_3v_4w_2x_1 + 4a_3v_3v_4w_2x_3 + 4a_3w_3v_3v_4x_3 - 4a_3w_3v_3w_2x_1 + 4a_3w_3v_4w_2x_1 \\
& - 4d_2v_3v_4w_2x_1 + 4w_3d_2v_3v_4x_1 - 4w_3d_2v_3w_2x_3 - 4w_3d_2v_4w_2x_3 - 4d_3v_3v_4w_2x_1 \\
& - 4w_3d_3v_3v_4x_1 + 4w_3d_3v_3w_2x_3 + 4w_3d_3v_4w_2x_3 - 8w_3v_3v_4w_2y_3 - 4a_1v_3w_1x_0 \\
& - 4a_1v_4w_1x_0 + 4a_1w_1w_2x_2 + 4a_1w_3w_1x_2 + 4a_2v_3v_4x_2 + 4a_2v_3w_2x_0 + 4a_2w_3v_3x_0 \\
& + 4a_2v_4w_2x_0 + 4a_2w_3v_4x_0 - 4a_2w_3w_2x_2 + 4a_3v_3v_4x_2 + 4a_3v_3w_2x_0 + 4a_3w_3v_3x_0 \\
& + 4a_3v_4w_2x_0 + 4a_3w_3v_4x_0 - 4a_3w_3w_2x_2 + 4d_2v_3v_4x_0 + 4d_2v_3w_2x_2 - 4w_3d_2v_3x_2 \\
& - 4d_2v_4w_2x_2 + 4w_3d_2v_4x_2 - 4w_3d_2w_2x_0 + 4d_3v_3v_4x_0 + 4d_3v_3w_2x_2 + 4w_3d_3v_3x_2 \\
& - 4d_3v_4w_2x_2 - 4w_3d_3v_4x_2 + 4w_3d_3w_2x_0 - 8v_3v_4w_2y_2 - 8w_3v_3v_4y_2 - 8w_3v_3w_2y_0 \\
& - 8w_3v_4w_2y_0 + 4a_1w_1x_3 + 4a_2v_3x_1 - 4a_2v_4x_1 - 4a_2w_2x_3 - 4a_2w_3x_3 + 4a_3v_3x_1 \\
& - 4a_3v_4x_1 - 4a_3w_2x_3 - 4a_3w_3x_3 - 4d_2v_3x_3 - 4d_2v_4x_3 - 4d_2w_2x_1 + 4w_3d_2x_1 \\
& - 4d_3v_3x_3 - 4d_3v_4x_3 - 4d_3w_2x_1 - 4w_3d_3x_1 + 8v_3v_4y_3 - 8v_3w_2y_1 - 8w_3v_3y_1 \\
& + 8v_4w_2y_1 + 8w_3v_4y_1 + 8w_3w_2y_3 + 4a_2x_2 + 4a_3x_2 - 4d_2x_0 - 4d_3x_0 + 8v_3y_0 \\
& + 8v_4y_0 - 8w_2y_2 - 8w_3y_2 - 8y_3
\end{aligned}$$

### 3.2.2 Constraint Equations for 3J, 4J and 5J Serial Kinematics Chains Using the Implicitization Algorithm

All the constraint equations for 3J, 4J, and 5J serial kinematic chains can be obtained using the implicitization algorithm, where the equation for the Study quadric (Eq. (2.33)) must be contained and the number of equations for each 3J, 4J and 5J serial kinematic chain is usually greater than the number of constraints of the serial kinematic chain. In [119-121] constraint equations for some serial kinematic chains have been obtained, but in this dissertation, Tables 3.3-3.5 and Table A.I.2-4 in Appendix I list these equations for the typical serial kinematic chains. Note that coordinate frames for the serial kinematic chains are built according to Fig. 2.2 where the  $z$  axes are aligned with the R joint axes using solid arrows and the dotted arrows are  $x$  axes, as shown in the first figure in Table 3.3-1 a).

Table 3.3 The constraint equations for 3J serial kinematic chains using implicitization algorithm ( $w_i = \tan(\alpha_i / 2)$ ,  $v_i = \tan(\theta_i / 2)$ ,  $i=1,2,\dots$ ) (For the constraint equations of other 3J serial kinematic chains, see Table A.I.2 in Appendix A.I)

1	<p>RRR a): The axes of the first two R joints are parallel. The axes of the last two R joints are perpendicular but not in the same plane.</p>  <p><math>a_1=0, d_1=0,</math> <math>a_2=\pi/2, d_2=0.</math></p>	<p>(1) <math>x_0y_0 + x_1y_1 + x_2y_2 + x_3y_3</math>  (2) <math>-x_0^2 + x_1^2 + x_2^2 - x_3^2</math>  (3) <math>x_0y_1 + x_1y_0 - x_2y_3 - x_3y_2</math>  (4) <math>x_0y_3 + x_1y_2 - x_2y_1 - x_3y_0</math>  (5) <math>x_0y_2 + x_1y_3 + x_2y_0 + x_3y_1</math>  (6) <math>y_1^2 + y_2^2 + a_2x_2y_2 + a_2x_1y_1 - \frac{1}{4}(x_3^2 + x_0^2)(a_1^2 - a_2^2)</math>  (7) <math>y_3^2 + y_0^2 - \frac{1}{4}(x_3^2 + x_0^2)(a_1^2 - a_2^2) + a_2x_1y_1 + a_2x_2y_2</math>  (8) <math>-a_2x_3y_1 - a_2x_2y_0 + y_1y_3 - y_0y_2 - \frac{1}{4}(x_0x_2 - x_1x_3)(a_1^2 - a_2^2)</math>  (9) <math>\frac{1}{4}(x_2x_3 + x_0x_1)(a_1^2 - a_2^2) + y_2y_3 + y_0y_1 - a_2x_3y_2 + a_2x_1y_0</math></p>
	<p>RRR b): The axes of the first two R joints are parallel. The axes</p>	<p>(1) <math>x_0y_0 + x_1y_1 + x_2y_2 + x_3y_3</math>  (2) <math>-x_0^2 + x_1^2 + x_2^2 - x_3^2</math></p>

<p>of the last two R joints are perpendicular and intersect with each other</p>  <p><math>\alpha_1=0, d_1=0,</math> <math>\alpha_2=\pi/2, a_2=0.</math></p>	<p>(3) <math>-d_2x_0x_2 - d_2x_1x_3 + x_0y_1 + x_1y_0 - x_2y_3 - x_3y_2</math></p> <p>(4) <math>d_2x_0^2 + d_2x_3^2 + x_0y_3 + x_1y_2 - x_2y_1 - x_3y_0</math></p> <p>(5) <math>d_2x_0x_1 - d_2x_2x_3 + x_0y_2 + x_1y_3 + x_2y_0 + x_3y_1</math></p> <p>(6) <math>-d_2x_3y_1 - d_2x_2y_0 + y_0y_1 + y_2y_3 + 3/4x_2x_3d_2^2</math> <math>+1/4x_2x_3a_1^2 + 1/4x_0x_1a_1^2 - 1/4x_0x_1d_2^2</math></p> <p>(7) <math>y_1^2 + y_2^2 + d_2x_1y_2 - d_2x_2y_1 - 1/4x_0^2a_1^2 + 1/4x_0^2d_2^2</math> <math>-1/4x_3^2a_1^2 + 1/4x_3^2d_2^2</math></p> <p>(8) <math>y_0^2 + y_3^2 + d_2x_2y_1 - d_2x_1y_2 - 1/4x_0^2a_1^2 - 3/4x_0^2d_2^2</math> <math>-1/4x_3^2a_1^2 - 3/4x_3^2d_2^2</math></p> <p>(9) <math>y_1y_3 - y_0y_2 - d_2x_1y_0 + d_2x_3y_2 - 1/4x_0x_2a_1^2 + 1/4x_0x_2d_2^2</math> <math>+3/4x_1x_3d_2^2 + 1/4x_1x_3a_1^2</math></p>
<p>RRR c): The axes of the first two R joints are parallel. The axes of the last two R joints intersect with each other.</p>  <p><math>\alpha_1=0, d_1=0,</math> <math>a_2=0.</math></p>	<p>(1) <math>x_0y_0 + x_1y_1 + x_2y_2 + x_3y_3</math></p> <p>(2) <math>-w_2^2x_0^2 - w_2^2x_3^2 + x_1^2 + x_2^2</math></p> <p>(3) <math>1/4x_0^2d_2^2w_2^2 - 1/4x_0^2a_1^2 + 1/4x_3^2d_2^2w_2^2 - 1/4x_3^2a_1^2</math> <math>+y_2^2 + y_1^2 + d_2x_1y_2 - d_2x_2y_1</math></p> <p>(4) <math>1/2x_0x_2w_2^2d_2 + 1/2x_0x_2d_2 + 1/2x_1x_3w_2^2d_2</math> <math>+1/2x_1x_3d_2 + w_2^2x_3y_2 - x_1y_0 - w_2^2x_0y_1 + x_2y_3</math></p> <p>(5) <math>-x_3y_0 + x_0y_3 - x_2y_1 + x_1y_2 + 1/2x_3^2w_2^2d_2 + 1/2x_3^2d_2</math> <math>+1/2x_0^2w_2^2d_2 + 1/2x_0^2d_2</math></p> <p>(6) <math>w_2^2x_3y_1 + 1/2x_0x_1w_2^2d_2 + 1/2x_0x_1d_2 + x_2y_0 + x_1y_3</math> <math>+w_2^2x_0y_2 - 1/2x_2x_3d_2 - 1/2x_2x_3w_2^2d_2</math> <math>y_0y_1 + d_2x_1y_3 + 1/4x_0x_1d_2^2w_2^2 + 1/4x_0x_1a_1^2 + 1/2x_0x_1d_2^2</math></p> <p>(7) <math>+1/2x_3y_1w_2^2d_2 - 1/2x_3y_1d_2 + y_2y_3 + 1/2x_0y_2w_2^2d_2</math> <math>+1/2x_0y_2d_2 + 1/4x_2x_3a_1^2 - 1/4x_2x_3d_2^2w_2^2</math> <math>1/4x_0x_2d_2^2w_2^2 - 1/4x_0x_2a_1^2 - 1/2x_0y_1w_2^2d_2 + 1/2x_0y_1d_2</math></p> <p>(8) <math>-d_2x_1y_0 + 1/2x_3y_2w_2^2d_2 + 1/2x_3y_2d_2 - y_0y_2 + y_1y_3</math> <math>+1/4x_1x_3d_2^2w_2^2 + 1/4x_1x_3a_1^2 + 1/2x_1x_3d_2^2</math> <math>-d_2x_1y_2 + y_3^2 + y_0^2 + d_2x_2y_1 - 1/2x_0^2d_2^2w_2^2</math></p> <p>(9) <math>-1/4x_0^2a_1^2w_2^2 - 1/4x_3^2d_2^2 - 1/4x_0^2d_2^2</math> <math>-1/2x_3^2d_2^2w_2^2 - 1/4x_3^2a_1^2w_2^2</math></p>

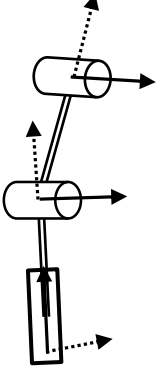
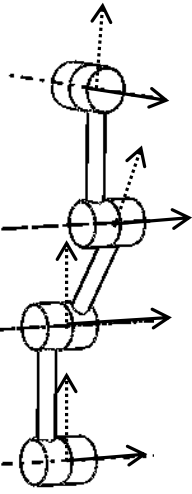
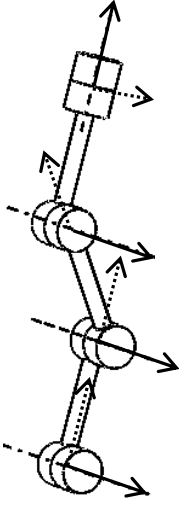
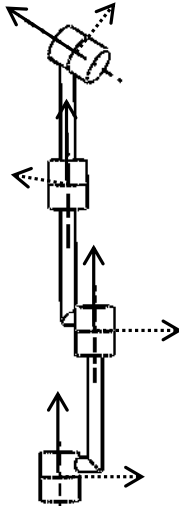
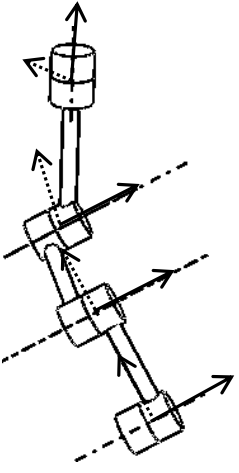
2	<p>PRR: The axes of the first P-R joint are perpendicular and intersect. The axes of the last two R joints are perpendicular and intersect with each other.</p>  <p><math>\alpha_1 = \pi/2, a_1 = 0,</math> <math>\alpha_2 = 0, d_2 = 0.</math></p>	<p>(1) <math>x_0y_0 + x_1y_1 + x_2y_2 + x_3y_3</math></p> <p>(2) <math>-x_0^2 + x_1^2 + x_2^2 - x_3^2</math></p> <p>(3) <math>x_0y_2 - x_1y_3 + x_2y_0 - x_3y_1</math></p> <p>(4) <math>x_0y_3 - x_1y_2 + x_2y_1 - x_3y_0</math></p> <p>(5) <math>x_0y_1 + x_1y_0 + x_2y_3 + x_3y_2</math></p> <p>(6) <math>d_1x_1y_3 + d_1x_3y_1 - y_0y_1 + y_2y_3 - 1/4x_2x_3d_1^2 + 1/4x_2x_3a_2^2 - 1/4x_0x_1a_2^2 + 1/4x_0x_1d_1^2</math></p> <p>(7) <math>-d_1x_3y_2 + y_0y_2 + y_1y_3 - d_1x_2y_3 - 1/4x_1x_3d_1^2 + 1/4x_1x_3a_2^2 - 1/4x_0x_2d_1^2 + 1/4x_0x_2a_2^2</math></p> <p>(8) <math>d_1x_1y_2 - d_1x_2y_1 + y_3^2 + y_0^2 - 1/4x_3^2a_2^2 + 1/4x_3^2d_1^2 - 1/4x_0^2a_2^2 + 1/4x_0^2d_1^2</math></p>
---	--	---

Table 3.4 The constraint equations for 4J serial kinematic chains using the implicitization algorithm (For the constraint equations of other 4J serial kinematic chains, see Table A.I.3 in Appendix A.I)

1	<p><math>\hat{R}\hat{R}\hat{R}\hat{R}</math> a):</p> 	<p>The axes of the first three R joints are parallel, the axes of the fourth and third R joints are perpendicular but not in the same plane.</p> <p><math>\alpha_1 = 0, d_1 = 0, \alpha_2 = 0, d_2 = 0,</math> <math>\alpha_3 = \pi/2, d_3 = 0.</math></p> <p>(1) <math>x_0y_0 + x_1y_1 + x_2y_2 + x_3y_3</math></p> <p>(2) <math>-x_0^2 + x_1^2 + x_2^2 - x_3^2</math></p> <p>(3) <math>x_0y_1 + x_1y_0 - x_2y_3 - x_3y_2</math></p> <p>(4) <math>x_0y_3 + x_1y_2 - x_2y_1 - x_3y_0</math></p> <p>(5) <math>x_0y_2 + x_1y_3 + x_2y_0 + x_3y_1</math></p> <p>(6) <math>y_0^2 - y_1^2 - y_2^2 + y_3^2</math></p>
---	--	---



<p><math>\ddot{R}\ddot{R}\ddot{R}R</math> b):</p> 	<p>The axes of the first three R joints are parallel, the axes of the fourth and third R joints are perpendicular and intersect with each other.</p> <p><math>\alpha_1=0, d_1=0, \alpha_2=0, d_2=0,</math>  <math>\alpha_3=\pi/2, a_3=0.</math></p> <p>(1) <math>x_0y_0 + x_1y_1 + x_2y_2 + x_3y_3</math>  (2) <math>-x_0^2 + x_1^2 + x_2^2 - x_3^2</math>  (3) <math>d_3x_0x_1 - d_3x_2x_3 + x_0y_2 + x_1y_3 + x_2y_0 + x_3y_1</math>  (4) <math>-d_3x_0x_2 - d_3x_1x_3 + x_0y_1 + x_1y_0 - x_2y_3 - x_3y_2</math>  (5) <math>d_3x_0^2 + d_3x_3^2 + x_0y_3 + x_1y_2 - x_2y_1 - x_3y_0</math>  (6) <math>-d_3^2x_0^2 - d_3^2x_3^2 - 2d_3x_1y_2 + 2d_3x_2y_1 + y_0^2 - y_1^2 - y_2^2 + y_3^2</math></p>
<p><math>\ddot{R}\ddot{R}\ddot{R}R</math> c):</p> 	<p>The axes of the first three R joints are parallel, the axes of the fourth and third R joints intersect with each other.</p> <p><math>\alpha_1=0, d_1=0, \alpha_2=0, a_3=0.</math></p> <p>(1) <math>x_0y_0 + x_1y_1 + x_2y_2 + x_3y_3</math>  (2) <math>-w_3^2x_0^2 - w_3^2x_3^2 + x_1^2 + x_2^2</math>  (3)  <math>-1/2x_2x_3w_3^2d_1 - 1/2x_2x_3w_3^2d_2 - 1/2x_2x_3w_3^2d_3 - 1/2x_2x_3d_1</math>  <math>-1/2x_2x_3d_2 - 1/2x_2x_3d_3 + x_1y_3 + x_2y_0 + w_3^2x_0y_2 + w_3^2x_3y_1</math>  <math>+1/2d_1w_3^2x_0x_1 + 1/2d_2w_3^2x_0x_1 + 1/2d_3w_3^2x_0x_1 + 1/2d_1x_0x_1</math>  <math>+1/2d_2x_0x_1 + 1/2d_3x_0x_1</math>  (4)  <math>x_2y_3 + 1/2x_0x_2d_1 + 1/2x_0x_2d_2 + 1/2x_0x_2d_3 + 1/2x_0x_2w_3^2d_1</math>  <math>+1/2x_0x_2w_3^2d_2 + 1/2x_0x_2w_3^2d_3 - w_3^2x_0y_1 + 1/2x_1x_3d_1</math>  <math>+1/2x_1x_3d_2 + 1/2x_1x_3d_3 + 1/2x_1x_3w_3^2d_1 + 1/2x_1x_3w_3^2d_2</math>  <math>+1/2x_1x_3w_3^2d_3 - x_1y_0 + w_3^2x_3y_2</math>  (5)  <math>-x_2y_1 + 1/2x_0^2d_1 + 1/2x_0^2d_2 + 1/2x_0^2d_3 + 1/2x_0^2w_3^2d_1</math>  <math>+1/2x_0^2w_3^2d_2 + 1/2x_0^2w_3^2d_3 + x_0y_3 + 1/2x_3^2d_1 + 1/2x_3^2d_2</math>  <math>+1/2x_3^2d_3 + 1/2x_3^2w_3^2d_1 + 1/2x_3^2w_3^2d_2 + 1/2x_3^2w_3^2d_3</math>  <math>-x_3y_0 + x_1y_2</math></p>

	<p>(6)</p> $ \begin{aligned} & -w_3^2 y_1^2 - w_3^2 y_2^2 + y_0^2 + y_3^2 - x_3^2 d_1 d_3 w_3^2 - x_3^2 d_1 d_2 w_3^2 \\ & -x_3^2 d_2 d_3 w_3^2 - 1/2 x_3^2 d_1 d_3 w_3^4 - 1/2 x_3^2 d_2 d_3 w_3^4 - 1/2 x_3^2 d_1 d_2 w_3^4 \\ & -x_0^2 d_1 d_3 w_3^2 - 1/2 x_0^2 d_1 d_3 w_3^4 - 1/2 x_0^2 d_2 d_3 w_3^4 - x_0^2 d_1 d_2 w_3^2 \\ & -x_0^2 d_2 d_3 w_3^2 - 1/2 x_0^2 d_1 d_2 w_3^4 - d_1 w_3^2 x_1 y_2 - d_2 w_3^2 x_1 y_2 \\ & -d_3 w_3^2 x_1 y_2 + d_1 w_3^2 x_2 y_1 + d_2 w_3^2 x_2 y_1 + d_3 w_3^2 x_2 y_1 - 1/4 x_3^2 d_2^2 w_3^4 \\ & -1/4 x_3^2 d_3^2 w_3^4 - 1/2 x_3^2 d_3^2 w_3^2 - 1/4 x_3^2 d_1^2 w_3^4 - 1/2 x_3^2 d_1 d_2 \\ & -1/2 x_3^2 d_1 d_3 - 1/2 x_3^2 d_1^2 w_3^2 - 1/2 x_3^2 d_2^2 w_3^2 - 1/2 x_3^2 d_2 d_3 \\ & -1/4 x_0^2 d_2^2 w_3^4 - 1/4 x_0^2 d_3^2 w_3^4 - 1/2 x_0^2 d_3^2 w_3^2 - 1/4 x_0^2 d_1^2 w_3^4 \\ & -1/2 x_0^2 d_1 d_2 - 1/2 x_0^2 d_1 d_3 - 1/2 x_0^2 d_1^2 w_3^2 - 1/2 x_0^2 d_2^2 w_3^2 \\ & -1/2 x_0^2 d_2 d_3 - d_1 x_1 y_2 - d_2 x_1 y_2 - d_3 x_1 y_2 + d_1 x_2 y_1 + d_2 x_2 y_1 \\ & + d_3 x_2 y_1 - 1/4 x_3^2 d_1^2 - 1/4 x_3^2 d_2^2 - 1/4 x_3^2 d_3^2 - 1/4 x_0^2 d_1^2 \\ & -1/4 x_0^2 d_2^2 - 1/4 x_0^2 d_3^2 \end{aligned} $
<p>RRRR d):</p> 	<p>The axes of the first three R joints are parallel, the axes of the fourth and third R joints intersect with each other.</p> <p><math>\alpha_1=0, d_1=0, \alpha_2=0, d_2=0,</math>  <math>a_3=0.</math></p> <p>(1) <math>x_0 y_0 + x_1 y_1 + x_2 y_2 + x_3 y_3</math></p> <p>(2) <math>-w_3^2 x_0^2 - w_3^2 x_3^2 + x_1^2 + x_2^2</math></p> <p>(3) <math>1/2 d_3 w_3^2 x_0 x_1 + 1/2 d_3 x_0 x_1 - 1/2 x_2 x_3 w_3^2 d_3</math>  <math>-1/2 x_2 x_3 d_3 + x_2 y_0 + w_3^2 x_0 y_2 + w_3^2 x_3 y_1 + x_1 y_3</math></p> <p>(4) <math>-w_3^2 x_0 y_1 + 1/2 x_0 x_2 w_3^2 d_3 + 1/2 x_0 x_2 d_3 + w_3^2 x_3 y_2</math>  <math>+1/2 x_1 x_3 w_3^2 d_3 + 1/2 x_1 x_3 d_3 - x_1 y_0 + x_2 y_3</math></p> <p>(5) <math>x_0 y_3 - x_2 y_1 - x_3 y_0 + x_1 y_2 + 1/2 x_3^2 w_3^2 d_3 + 1/2 x_3^2 d_3</math>  <math>+1/2 x_0^2 w_3^2 d_3 + 1/2 x_0^2 d_3</math>  <math>y_0^2 - w_3^2 y_1^2 - w_3^2 y_2^2 + y_3^2 - d_3 w_3^2 x_1 y_2 - 1/4 x_0^2 d_3^2</math></p> <p>(6) <math>-1/4 x_0^2 d_3^2 w_3^4 - 1/2 x_0^2 d_3^2 w_3^2 - 1/4 x_3^2 d_3^2 - 1/4 x_3^2 d_3^2 w_3^4</math>  <math>-1/2 x_3^2 d_3^2 w_3^2 + d_3 w_3^2 x_2 y_1 + d_3 x_2 y_1 - d_3 x_1 y_2</math></p>
<p>RRRR e):</p>	<p>The axes of the first three R joints are parallel, the axes of the fourth and third R joints intersect with each other.</p> <p><math>\alpha_1=0, d_1=0, \alpha_2=0, \text{ and } a_3=0.</math></p> <p>(1) <math>x_0 y_0 + x_1 y_1 + x_2 y_2 + x_3 y_3</math></p> <p>(2) <math>-w_3^2 x_0^2 - w_3^2 x_3^2 + x_1^2 + x_2^2</math></p>

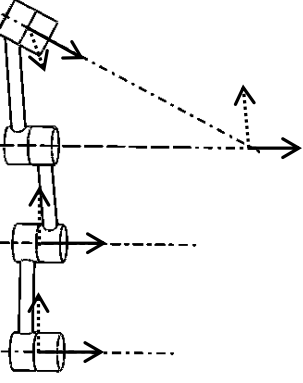
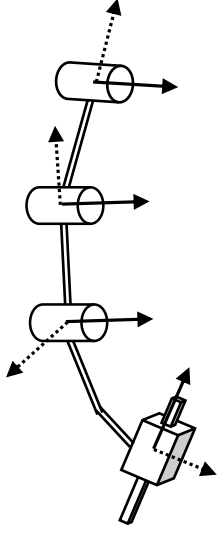
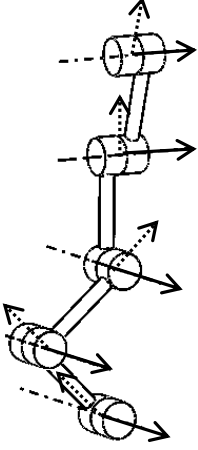
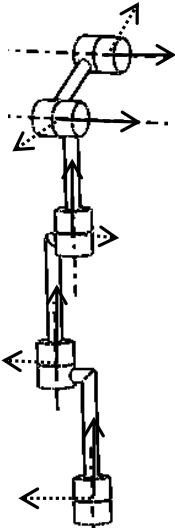
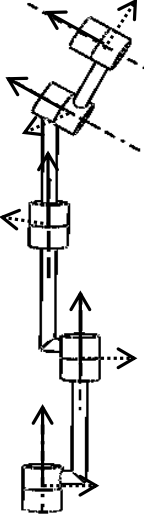
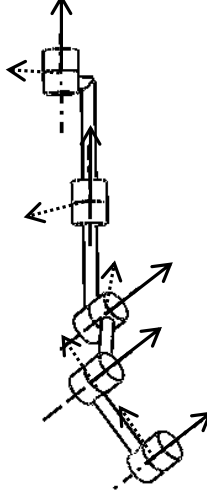
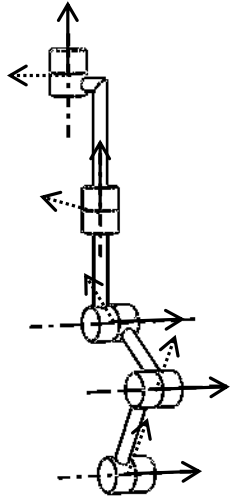
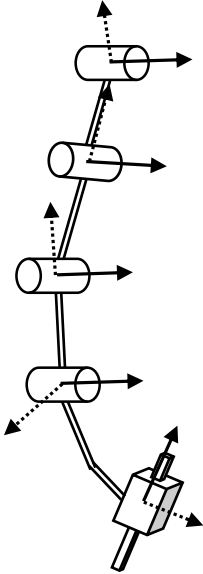
	$w_3^2 x_0 y_2 + x_2 y_0 + w_3^2 x_3 y_1 + x_1 y_3 + 1/2 d_2 w_3^2 x_0 x_1$ <p>(3) <math>+1/2 d_2 x_0 x_1 + 1/2 d_3 x_0 x_1 - 1/2 x_2 x_3 w_3^2 d_2 - 1/2 x_2 x_3 w_3^2 d_3</math>  <math>-1/2 x_2 x_3 d_2 - 1/2 x_2 x_3 d_3 + 1/2 d_3 w_3^2 x_0 x_1</math></p> $-x_1 y_0 + x_2 y_3 + w_3^2 x_3 y_2 - w_3^2 x_0 y_1 + 1/2 x_1 x_3 d_2 + 1/2 x_1 x_3 d_3$ <p>(4) <math>+1/2 x_1 x_3 w_3^2 d_2 + 1/2 x_1 x_3 w_3^2 d_3 + 1/2 x_0 x_2 d_2 + 1/2 x_0 x_2 d_3</math>  <math>+1/2 x_0 x_2 w_3^2 d_2 + 1/2 x_0 x_2 w_3^2 d_3</math></p> $-x_3 y_0 + x_0 y_3 - x_2 y_1 + x_1 y_2 + 1/2 x_0^2 d_2 + 1/2 x_0^2 d_3$ <p>(5) <math>+1/2 x_0^2 w_3^2 d_2 + 1/2 x_0^2 w_3^2 d_3 + 1/2 x_3^2 d_2 + 1/2 x_3^2 d_3</math>  <math>+1/2 x_3^2 w_3^2 d_2 + 1/2 x_3^2 w_3^2 d_3</math></p> <p>(6)</p> $y_0^2 + y_3^2 - 1/2 x_0^2 d_2 d_3 - 1/2 x_0^2 d_2^2 w_3^2 - 1/2 x_0^2 d_3^2 w_3^2$ $-1/4 x_0^2 d_2^2 w_3^4 - 1/4 x_0^2 d_3^2 w_3^4 - 1/2 x_3^2 d_2 d_3 - 1/2 x_3^2 d_2^2 w_3^2$ $-1/2 x_3^2 d_3^2 w_3^2 - 1/4 x_3^2 d_2^2 w_3^4 - 1/4 x_3^2 d_3^2 w_3^4 + d_2 x_2 y_1$ $+ d_3 x_2 y_1 - d_2 x_1 y_2 - d_3 x_1 y_2 - w_3^2 y_2^2 - w_3^2 y_1^2 - 1/4 x_0^2 d_3^2$ $-1/4 x_0^2 d_2^2 - 1/4 x_3^2 d_3^2 - 1/4 x_3^2 d_2^2 - x_0^2 d_2 d_3 w_3^2$ $-1/2 x_0^2 d_2 d_3 w_3^4 - x_3^2 d_2 d_3 w_3^2 - 1/2 x_3^2 d_2 d_3 w_3^4 + d_2 w_3^2 x_2 y_1$ $+ d_3 w_3^2 x_2 y_1 - d_2 w_3^2 x_1 y_2 - d_3 w_3^2 x_1 y_2$
<p>2 PRRR:</p> 	<p>The axes of the last three R joints are parallel.</p> $\alpha_1 = \pi/2, a_1=0, \quad \alpha_2 = 0, d_2=0,$ $\alpha_3 = 0, d_3=0.$ <p>(1) <math>x_0 y_0 + x_1 y_1 + x_2 y_2 + x_3 y_3</math></p> <p>(2) <math>-w_1^2 x_0^2 - w_1^2 x_3^2 + x_1^2 + x_2^2</math></p> <p>(3) <math>x_0 y_3 - x_1 y_2 - x_3 y_0 + x_2 y_1 + 1/2 x_0^2 d_1 - 1/2 x_0^2 w_1^2 d_1</math>  <math>+1/2 x_3^2 d_1 - 1/2 x_3^2 w_1^2 d_1</math></p> <p>(4) <math>w_1^2 x_3 y_1 - w_1^2 x_0 y_2 + x_1 y_3 - x_2 y_0 + 1/2 x_2 x_3 d_1</math>  <math>-1/2 x_2 x_3 w_1^2 d_1 - 1/2 x_0 x_1 d_1 w_1^2 + 1/2 d_1 x_0 x_1</math></p> <p>(5) <math>x_2 y_3 + w_1^2 x_3 y_2 + 1/2 x_1 x_3 w_1^2 d_1 - 1/2 x_1 x_3 d_1</math>  <math>+w_1^2 x_0 y_1 + x_1 y_0 + 1/2 x_0 x_2 d_1 - 1/2 x_0 x_2 w_1^2 d_1</math>  <math>-1/4 x_3^2 d_1^2 w_1^4 + 1/2 x_3^2 d_1^2 w_1^2 - 1/4 x_3^2 d_1^2</math></p> <p>(6) <math>-1/4 x_0^2 d_1^2 w_1^4 + 1/2 x_0^2 d_1^2 w_1^2 - 1/4 x_0^2 d_1^2</math>  <math>+x_2 y_1 d_1 w_1^2 - x_2 y_1 d_1 - x_1 y_2 d_1 w_1^2</math>  <math>+x_1 y_2 d_1 + y_0^2 + y_3^2 - w_1^2 y_1^2 - w_1^2 y_2^2</math></p>

Table 3.5 The constraint equations for 5J serial kinematic chains using the implicitization algorithm (For the constraint equations of other 5J serial kinematic chains, see Table A.I.4 in Appendix A.I)

1	<p><math>\dot{R}\dot{R}\dot{R}\dot{R}\dot{R}</math> a):</p> 	<p>The axes of the first three R joints are parallel, the axes of the last two R joints are parallel. The axes of the third and fourth R joints are perpendicular but not in the same plane.</p> $\alpha_1=0, d_1=0, \quad \alpha_2=0, a_2=0,$ $\alpha_3=\pi/2, d_3=0, \quad \alpha_4=0, d_4=0.$
		<p>(1) <math>x_0y_0 + x_1y_1 + x_2y_2 + x_3y_3</math></p> <p>(2) <math>x_0^2 - x_1^2 - x_2^2 + x_3^2</math></p>
	<p><math>\dot{R}\dot{R}\dot{R}\dot{R}\dot{R}</math> b):</p> 	<p>The axes of the first three R joints are parallel, the axes of the last two R joints are parallel. The axes of the third and fourth R joints are perpendicular and intersect with each other</p> $\alpha_1=0, \quad \alpha_2=0,$ $\alpha_3=\pi/2, a_3=0, \quad \alpha_4=0, d_4=0.$
	<p><math>\dot{R}\dot{R}\dot{R}\dot{R}\dot{R}</math> c):</p>	<p>The axes of the first three R joints are parallel, the axes of the last two R joints are parallel. The axes of the third and fourth R joints intersect with each other</p> $\alpha_1=0, \quad \alpha_2=0,$ $\alpha_3=\pi/3, a_3=0, \quad \alpha_4=0, d_4=0.$

	<p>(1) <math>x_0y_0 + x_1y_1 + x_2y_2 + x_3y_3</math></p> <p>(2) <math>w_3^2x_0^2 - x_1^2 - x_2^2 + w_3^2x_3^2</math></p>
<p><math>\hat{R}\hat{R}\hat{R}\hat{R}\hat{R}</math> d):</p> 	<p>The axes of the first three R joints are parallel, the axes of the last two R joints are parallel. The axes of the third and fourth R joints intersect with each other.</p> <p><math>\alpha_1=0, d_1=0, \quad \alpha_2=0, d_2=0,</math>  <math>\alpha_3=0, \alpha_4=0.</math></p> <p>(1) <math>x_0y_0 + x_1y_1 + x_2y_2 + x_3y_3</math></p> <p>(2) <math>w_3^2x_0^2 - x_1^2 - x_2^2 + w_3^2x_3^2</math></p>
<p><math>\hat{R}\hat{R}\hat{R}\hat{R}\hat{R}</math> e):</p> 	<p>The axes of the first three R joints are parallel, and the axes of the last two R joints are parallel. The axes of the third and fourth R joints are perpendicular and intersect with each other <math>\alpha_1=0, d_1=0, \quad \alpha_2=0, d_2=0,</math>  <math>\alpha_3=\pi/2, \alpha_3=0, \quad \alpha_4=0.</math></p> <p>(1) <math>x_0y_0 + x_1y_1 + x_2y_2 + x_3y_3</math></p> <p>(2) <math>x_0^2 - x_1^2 - x_2^2 + x_3^2</math></p>

2	<p>PRRRR:</p> 	<p>The axes of the second and fifth R joints are parallel. The axes of the third and fourth R joints are parallel</p> $a_1=0, \quad \alpha_2= \pi/2, a_2=0, d_2=0,$ $\alpha_3= 0, d_3=0, \quad \alpha_4= -\pi/2, a_4=0, d_4=0.$ <p>(1) <math>x_0y_0 + x_1y_1 + x_2y_2 + x_3y_3</math></p> $y_3^2 + y_2^2 + y_1^2 + y_0^2 - 1/4x_2^2a_3^2 + 1/4x_2^2d_1^2 + d_1x_0y_3$ <p>(2) <math>-d_1x_3y_0 + d_1x_1y_2 - d_1x_2y_1 - 1/4x_3^2a_3^2 + 1/4x_3^2d_1^2</math></p> $-1/4x_1^2a_3^2 + 1/4x_1^2d_1^2 - 1/4x_0^2a_3^2 + 1/4x_0^2d_1^2$
---	---	--

Costraint equations for some kinematic chains using the implicitization algorithm are listed in above tables and it is observed that there are some relationships between the kinematic chains with similarly constructions: their constraint equations are the same or similar. In the next subsection the relationships of the chains and equations will be analyzed using the linear algebraic method.

### 3.2.3 Constraint Equations of a 5R Chain and Its Sub-Chains

We take a comparison for a set of chains as shown in Fig. 3.1. It can be seen that the 3R chain is the subchain of the 4R chain, and the 4R chain is the subchain of the 5R chain. Similar situations exist among other chains.

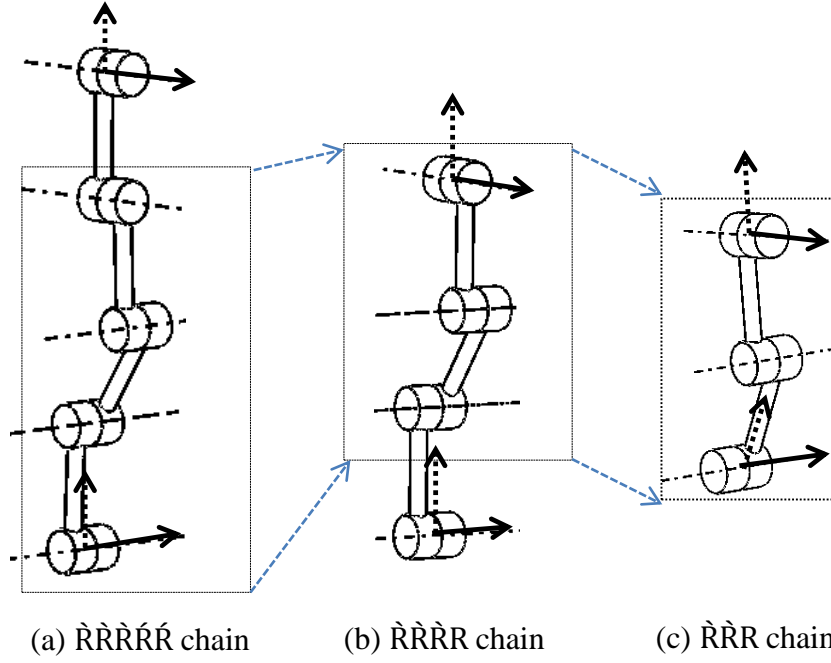


Figure 3.1 A 5R chain and subchains

There are two constraint equations for the 5R chain (Fig. 3.1(a)) represented by Eqs. (3.1) and (3.2) (see Table 3.5-1 a)):

$$x_0y_0 + x_1y_1 + x_2y_2 + x_3y_3 = 0 \quad (3.1)$$

$$x_0^2 - x_1^2 - x_2^2 + x_3^2 = 0 \quad (3.2)$$

There are six constraint equations for the 4R chain (Fig. 3.1(b)) including Eqs. (3.1) and (3.2) and the four equations below (see Table 3.4-1 a)):

$$-x_0y_1 - x_1y_0 + x_2y_3 + x_3y_2 = 0 \quad (3.3)$$

$$x_0y_2 + x_1y_3 + x_2y_0 + x_3y_1 = 0 \quad (3.4)$$

$$x_0y_3 + x_1y_2 - x_2y_1 - x_3y_0 = 0 \quad (3.5)$$

$$y_0^2 - y_1^2 - y_2^2 + y_3^2 = 0 \quad (3.6)$$

There are nine constraint equations for the 3R chain (Fig. 3.1(c)) including Eqs. (3.1)-(3.5) and the four other equations shown below (see Table 3.3-1 a)):

$$-\frac{1}{4}(a_1^2 - a_2^2)(x_1^2 + x_2^2) + a_2(x_1y_1 + x_2y_2) + y_1^2 + y_2^2 = 0 \quad (3.7)$$

$$-\frac{1}{4}(a_1^2 - a_2^2)(x_1^2 + x_2^2) + a_2(x_1y_1 + x_2y_2) + y_0^2 + y_3^2 = 0 \quad (3.8)$$

$$-\frac{1}{4}(a_1^2 - a_2^2)(x_2x_3 + x_0x_1) + a_2(x_1y_0 - x_3y_2) + y_0y_1 + y_2y_3 = 0 \quad (3.9)$$

$$-\frac{1}{4}(a_1^2 - a_2^2)(x_1x_3 - x_0x_2) - a_2(x_2y_0 + x_3y_1) - y_0y_2 + y_1y_3 = 0 \quad (3.10)$$

Note that the subtraction of Eq. (3.7) from Eq. (3.8) yields

$$\text{Eq.}(3.8) - \text{Eq.}(3.7) = y_0^2 - y_1^2 - y_2^2 + y_3^2 = 0 \quad (3.11)$$

which is actually Eq. (3.6), and therefore, Eq. (3.7) can be replaced by Eq. (3.6).

**Remarks:**

- a) Eq. (3.1) is the representation of the Study quadric, which is contained in all the kinematic chains.
- b) The constraint equations of the sub 4R chain of the 5R chain are constituted by the constraint equations of the 5R chain and additional constraint equations.
- c) The constraint equations of the sub 3R chain of the 4R chain are constituted by the constraint equations of the 4R chain and additional constraint equations.
- d) It can be understood that the constrained manifold for the 3R chain is part of that for the 4R chain and the constrained manifold for the 4R chain is part of that for the 5R chain.

### 3.3 Selection of Necessary Equations for Serial Kinematic Chains

An  $n$ -link serial kinematic chain implies  $(6-n)$  constraint equations between the base and the terminal link. Therefore, one constraint equation needs to be selected for a 5J chain, two constraint equations for a 4J chain and three constraint equations for a 3J chain. Eq. (3.2) can only be chosen for the 5J chain; however, the number of constraint equations derived for 3J and 4J chains in Section 3.1 is larger than the number of constraint equations needed. The problem is how to choose the constraint equations for the 4J and 3J chains, it is not possible that any two equations can be selected for the 4J serial kinematic chain or any three equations can be selected for the 3J serial kinematic chain as stated in [119]. This is still an open issue deserving further investigation using an appropriate analytical method. In the following subsection, the analysis of the equations of the 3R and 4R chains (Figs. 3.1 (a) and (b)) will be undertaken as examples to show how to select appropriate equations for serial kinematic chains.

#### 3.3.1 Choosing Equations for the 4R Chain

There are six equations of the 4R chain which are not relevant to its design parameters, the following analysis to determine the relationship among its equations is completed and two equations will be chosen with which to carry out further computation.



### 1) Relationship I among the constraint equations

Equations (3.1)-(3.6) are represented as  $f_0, f_1, f_2, f_3, g, h$  as follows:

$$\begin{aligned}
 f_0 &= x_0 y_0 + x_1 y_1 + x_2 y_2 + x_3 y_3 \\
 f_1 &= -x_0 y_1 - x_1 y_0 + x_2 y_3 + x_3 y_2 \\
 f_2 &= x_0 y_2 + x_1 y_3 + x_2 y_0 + x_3 y_1 \\
 f_3 &= x_0 y_3 + x_1 y_2 - x_2 y_1 - x_3 y_0 \\
 g &= x_0^2 - x_1^2 - x_2^2 + x_3^2 \\
 h &= y_0^2 - y_1^2 - y_2^2 + y_3^2
 \end{aligned} \tag{3.12}$$

Let

$$M = \begin{pmatrix} y_0 & y_1 & y_2 \\ -y_1 & -y_0 & y_3 \\ y_2 & y_3 & y_0 \end{pmatrix},$$

Rewrite  $f_0, f_1, f_2$  in Eq. (3.12) as

$$M \cdot \begin{pmatrix} x_0 \\ x_1 \\ x_2 \end{pmatrix} = -x_3 \begin{pmatrix} y_3 \\ y_2 \\ y_1 \end{pmatrix} + \begin{pmatrix} f_0 \\ f_1 \\ f_2 \end{pmatrix} \tag{3.13 a}$$

also

$$\det(M) = -y_0(y_0^2 - y_1^2 - y_2^2 + y_3^2) = -y_0 \cdot h \tag{3.13 b}$$

Because  $M \cdot M^* = \det(M) \cdot I$ , then multiplying  $M^*$  in both sides of Eq. (3.13a) gives

$$-y_0 \cdot h \cdot \begin{pmatrix} x_0 \\ x_1 \\ x_2 \end{pmatrix} = -x_3 \cdot M^* \cdot \begin{pmatrix} y_3 \\ y_2 \\ y_1 \end{pmatrix} + M^* \cdot \begin{pmatrix} f_0 \\ f_1 \\ f_2 \end{pmatrix} \tag{3.14}$$

where

$$M^* = \begin{pmatrix} -y_0^2 - y_3^2 & -y_1 y_0 + y_2 y_3 & y_1 y_3 + y_0 y_2 \\ y_1 y_0 + y_2 y_3 & y_0^2 - y_2^2 & -y_0 y_3 - y_1 y_2 \\ -y_1 y_3 + y_0 y_2 & -y_0 y_3 + y_1 y_2 & -y_0^2 + y_1^2 \end{pmatrix} \tag{3.15}$$

$$\begin{aligned}
M^* \cdot \begin{pmatrix} y_3 \\ y_2 \\ y_1 \end{pmatrix} &= \begin{pmatrix} -y_0^2 - y_3^2 & -y_1 y_0 + y_2 y_3 & y_1 y_3 + y_0 y_2 \\ y_1 y_0 + y_2 y_3 & y_0^2 - y_2^2 & -y_0 y_3 - y_1 y_2 \\ -y_1 y_3 + y_0 y_2 & -y_0 y_3 + y_1 y_2 & -y_0^2 + y_1^2 \end{pmatrix} \cdot \begin{pmatrix} y_3 \\ y_2 \\ y_1 \end{pmatrix} \\
&= -y_0^2 y_1 + y_0^2 y_2 - y_0^2 y_3 + y_1^3 - y_1^2 y_2 + y_1^2 y_3 + y_1 y_2^2 - y_1 y_3^2 - y_2^3 \\
&\quad + y_2^2 y_3 + y_2 y_3^2 - y_3^3 \\
&= (y_0^2 - y_1^2 - y_2^2 + y_3^2) \cdot \begin{pmatrix} -y_3 \\ y_2 \\ -y_1 \end{pmatrix} = h \cdot \begin{pmatrix} -y_3 \\ y_2 \\ -y_1 \end{pmatrix}
\end{aligned} \tag{3.16}$$

Therefore,

$$h \cdot \begin{pmatrix} -x_0 y_0 - x_3 y_3 \\ -x_1 y_0 + x_3 y_2 \\ -x_2 y_0 - x_3 y_1 \end{pmatrix} = M^* \cdot \begin{pmatrix} f_0 \\ f_1 \\ f_2 \end{pmatrix} \tag{3.17}$$

Let  $p$  be a point of coordinate  $(x_0, x_1, x_2, x_3, y_0, y_1, y_2, y_3)$ . If  $p$  is a solution of  $f_0 = f_1 = f_2 = 0$ , then there are two possible results: (a)  $h = 0$  or (b)  $-x_0 y_0 - x_3 y_3 = 0$ ,  $-x_1 y_0 + x_3 y_2 = 0$  and  $-x_2 y_0 - x_3 y_1 = 0$ .

Considering the latter result, under the condition:  $x_3 \neq 0$  yields

$$y_3 = -\frac{x_0}{x_3} y_0, \quad y_2 = \frac{x_1}{x_3} y_0, \quad y_1 = -\frac{x_2}{x_3} y_0 \tag{3.18}$$

Then the substitution of these into  $f_3$  and  $h$  produces

$$\begin{aligned}
f_3 &= x_0 \left(-\frac{x_0}{x_3} y_0\right) + x_1 \left(\frac{x_1}{x_3} y_0\right) - x_2 \left(-\frac{x_2}{x_3} y_0\right) - x_3 y_0 \\
&= -(x_0^2 - x_1^2 - x_2^2 + x_3^2) \frac{y_0}{x_3} = -\frac{y_0}{x_3} \cdot g
\end{aligned} \tag{3.19}$$

$$\begin{aligned}
h &= y_0^2 - \left(-\frac{x_2}{x_3} y_0\right)^2 - \left(\frac{x_1}{x_3} y_0\right)^2 + \left(-\frac{x_0}{x_3} y_0\right)^2 \\
&= \frac{y_0^2}{x_3^2} (x_0^2 - x_1^2 - x_2^2 + x_3^2) = \frac{y_0^2}{x_3^2} \cdot g
\end{aligned} \tag{3.20}$$

If either  $g=0$  or  $y_0=0$ , then  $f_3=0$  and  $h=0$  in Eqs. (3.19) and (3.20), but when  $y_0=0$ , then  $y_1=y_2=y_3=0$ . All the  $y_i$  values are equal to zero meaning all the study parameters are also equal to zero, which is impossible. If  $f_3=0$ , then  $g=0$ , which leads to  $h=0$ .

If  $x_3=0$  then either  $y_0=0$  or  $x_0=x_1=x_2=0$ , the second situation results in  $x_0^2 + x_1^2 + x_2^2 + x_3^2 = 0$ , which is again impossible. There exists one special case that is

$x_3=0$  and  $y_0=0$ , under this special case a system of equations in variables  $x_0, x_1, x_2, y_1$  is obtained:

$$\begin{aligned}
f_0 &= x_1 y_1 + x_2 y_2 \\
f_1 &= -x_0 y_1 + x_2 y_3 \\
f_2 &= x_0 y_2 + x_1 y_3 \\
f_3 &= x_0 y_3 + x_1 y_2 - x_2 y_1 \\
g &= x_0^2 - x_1^2 - x_2^2 \\
h &= -y_1^2 - y_2^2 + y_3^2
\end{aligned} \tag{3.21}$$

If  $x_2 \neq 0$ ,  $y_2$  and  $y_3$  can be calculated in terms of  $y_1$  from  $f_0$  and  $f_1$ , i.e.  $y_2 = -x_1 y_1 / x_2$  and  $y_3 = x_0 y_1 / x_2$ . Substituting these into Eq. (3.21) and checking for solutions:

$$f_2 = x_0 - \frac{x_1}{x_2} y_1 + x_1 \frac{x_0}{x_2} y_1 = 0 \tag{3.22}$$

$$f_3 = x_0 \frac{x_0}{x_2} y_1 + x_1 - \frac{x_1}{x_2} y_1 - x_2 y_1 = (x_0^2 - x_1^2 - x_2^2) y_1 = g \cdot y_1 \tag{3.23}$$

$$h = -y_1^2 - \frac{x_1^2}{x_2^2} \cdot y_1^2 + \frac{x_0^2}{x_2^2} \cdot y_1^2 = \frac{y_1^2}{x_2^2} (x_0^2 - x_1^2 - x_2^2) = \frac{y_1^2}{x_2^2} \cdot g \tag{3.24}$$

If either  $g=0$  or  $y_1=0$ , then  $f_3=0$  and  $h=0$  in Eqs. (3.23) and (3.24),  $y_1$  cannot be zero. This is because if  $y_1=0$ , it will be  $y_0=y_1=y_2=y_3=0$ , which is impossible. If  $f_3=0$ , then  $g=0$ , then  $h=0$ .

There are two conclusions that can be obtained from the derivations mentioned above:

Case1: If  $f_0 = f_1 = f_2 = 0$ , then  $h=0$ ;

Case 2: If  $f_0 = f_1 = f_2 = 0$ , and if  $f_3=0$ , then  $g=0$ , which leads to  $h=0$ .

## 2) Relationship II among the constraint equations

Since the system of equations is symmetric in  $x_i$  and  $y_i$ , it is possible to obtain a new relationship between  $g$  and  $f_0, f_1, f_2$  by swapping the  $y_i$  and  $x_i$  in Eq. (3.18). Let  $N$  be the coefficient matrix of  $y_0, y_1, y_2$  in  $f_0, f_1, f_2$ , along with its adjoint matrix  $N^*$ , gives

$$g \cdot \begin{pmatrix} -x_0 y_0 - x_3 y_3 \\ -x_0 y_1 + x_2 y_3 \\ -x_0 y_2 - x_1 y_3 \end{pmatrix} = N^* \cdot \begin{pmatrix} f_0 \\ f_1 \\ f_2 \end{pmatrix} \tag{3.25}$$

When  $f_0 = f_1 = f_2 = 0$ , then there are also two possible results: (a)  $g=0$ ; or (b)  $-x_0y_0 - x_3y_3 = 0, -x_0y_1 - x_2y_3 = 0$  and  $-x_0y_2 - x_1y_3 = 0$ .

Similarly, two other conclusions can be obtained:

Case 3: If  $f_0 = f_1 = f_2 = 0$ , then  $g=0$ ;

Case 4: If  $f_0 = f_1 = f_2 = 0$ , and if  $f_3=0$ , then  $h=0$ , which leads to  $g=0$ .

According to the previous analysis above, if  $f_0 = f_1 = f_2 = 0$  then  $f_3=0, h=0$  and  $g=0$  in cases 1&3; If  $f_0 = f_1 = f_2 = f_3 = 0$  then  $h=0$  and  $g=0$  in cases 1&4, 2&3 and 2&4.

The conclusion obtained from these cases is:

If  $f_0 = f_1 = f_2 = f_3 = 0$ , then  $h=0$  and  $g=0$ .

### 3) Further analysis of the equations to find the relationship between $f_1, f_2$ and $f_3$ .

In this subsection, determinant knowledge will be used to judge the linear dependence of  $f_1, f_2, f_3$ . The coefficients of  $x_0, x_1, x_2$  and  $x_1, x_2, x_3$  and  $x_0, x_2, x_3$  and  $x_0, x_1, x_3$  in  $f_1, f_2, f_3$  are defined as  $A, B, C$ , and  $D$ .

$$\begin{aligned} A &= \begin{pmatrix} -y_1 & -y_0 & y_3 \\ y_2 & y_3 & y_0 \\ y_3 & y_2 & -y_1 \end{pmatrix} \\ B &= \begin{pmatrix} -y_0 & y_3 & y_2 \\ y_3 & y_0 & y_1 \\ y_2 & -y_1 & -y_0 \end{pmatrix} \\ C &= \begin{pmatrix} -y_1 & y_3 & y_2 \\ y_2 & y_0 & y_1 \\ y_3 & -y_1 & -y_0 \end{pmatrix} \\ D &= \begin{pmatrix} -y_1 & -y_0 & y_2 \\ y_2 & y_3 & y_1 \\ y_3 & y_2 & -y_0 \end{pmatrix} \end{aligned} \quad (3.26)$$

$$\begin{aligned} \det(A) &= -y_3(y_0^2 - y_1^2 - y_2^2 + y_3^2) = -y_3 \cdot h = 0 \\ \det(B) &= y_0(y_0^2 - y_1^2 - y_2^2 + y_3^2) = y_0 \cdot h = 0 \\ \det(C) &= y_1(y_0^2 - y_1^2 - y_2^2 + y_3^2) = y_1 \cdot h = 0 \\ \det(D) &= -y_2(y_0^2 - y_1^2 - y_2^2 + y_3^2) = -y_2 \cdot h = 0 \end{aligned} \quad (3.27)$$

The equations in (3.27) mean that  $f_1, f_2$  and  $f_3$  are linearly dependent and there are some linear combinations between the three equations. Up to this step, the necessary

equations for the 4R chain can be determined, i.e.  $f_1, f_2$  (Eqs. (3.2) and (3.3)) are recommended for further computation.

**Remarks:**

The equations,  $f_1$  and  $f_2$ , in addition to  $f_0$ , are the recommended constraint equations for the 4R kinematic chain according to the linear analysis of the set of equations about their relationship in this subsection.

### 3.3.2 Choosing Equations for the 3R Chain

The first six equations for the 3R chain (the full equations for the 4R chain) have been analysed in the previous subsection, which are not related to the D-H parameters of the kinematic chain. Three remaining equations which are relevant to the D-H parameters are investigated below.

In the following, Eqs. (3.8)-(3.10) are represented as  $l_1, l_2, l_3$  and regarded as a set of equations in  $a_1^2 - a_2^2$  and  $a_2$  respectively, giving:

$$\begin{aligned} & \begin{vmatrix} x_2^2 + x_1^2 & x_2 y_2 + x_1 y_1 \\ x_3 x_2 + x_1 x_0 & -x_3 y_2 + x_1 y_0 \end{vmatrix} \\ &= -x_1^2 y_2 x_3 + x_1^3 y_0 - x_2^2 x_3 y_2 + x_1 x_2^2 y_0 + x_3 x_2^2 y_2 + x_1 x_3 x_2 y_1 + x_0 x_1^2 y_1 + x_0 x_1 x_2 y_2 \quad (3.28) \\ &= -x_1^2 (y_2 x_3 - x_1 y_0) + x_1 x_2 (x_2 y_0 + x_3 y_1) + x_0 x_1^2 y_1 + x_0 x_1 x_2 y_2 \end{aligned}$$

If  $f_1=f_2=0$ , then  $y_2 x_3 - x_1 y_0 = x_0 y_1 - x_2 y_3$  and  $x_2 y_0 + x_3 y_1 = -(x_0 y_2 + x_1 y_3)$ . Substituting them to the above equation gives:

$$\begin{aligned} & -x_1^2 (x_0 y_1 - x_2 y_3) - x_1 x_2 (x_0 y_2 + x_1 y_3) + x_0 x_1^2 y_1 + x_0 x_1 x_2 y_2 \\ &= -x_1^2 x_0 y_1 + x_1^2 x_2 y_3 - x_1 x_2 x_0 y_2 - x_1 x_2 x_1 y_3 + x_0 x_1^2 y_1 + x_0 x_1 x_2 y_2 \quad (3.29) \\ &= 0 \end{aligned}$$

The determinant of the coefficients of  $a_2$  and the constant term are

$$\begin{aligned} & \begin{vmatrix} x_2 y_2 + x_1 y_1 & y_1^2 + y_2^2 \\ -x_3 y_2 + x_1 y_0 & y_2 y_3 + y_0 y_1 \end{vmatrix} \\ &= x_2 y_2^2 y_3 + x_1 y_1 y_2 y_3 + x_2 y_0 y_1 y_2 + x_1 y_0 y_1^2 + x_3 y_1^2 y_2 + x_3 y_2^2 y_0 - x_1 y_0 y_1^2 - x_1 y_0 y_2^2 \quad (3.30) \\ &= y_2 y_3 (x_2 y_2 + x_1 y_1) + y_1 y_2 (x_2 y_0 + x_3 y_1) + y_2^2 (x_3 y_2 - x_1 y_0) \end{aligned}$$

If  $f_1=f_2=0$ , then  $x_2 y_0 + x_3 y_1 = -(x_0 y_2 + x_1 y_3)$  and  $x_3 y_2 - x_1 y_0 = x_0 y_1 - x_2 y_3$ . Substituting these into the Eq. (30) to obtain:

$$\begin{aligned}
& y_2 y_3 (x_2 y_2 + x_1 y_1) - y_1 y_2 (x_0 y_2 + x_1 y_3) + y_2^2 (x_0 y_1 - x_2 y_3) \\
& = x_2 y_2^2 y_3 + x_1 y_1 y_2 y_3 - y_1 y_2 x_0 y_2 - y_1 y_2 x_1 y_3 + y_2^2 x_0 y_1 - y_2^2 x_2 y_3 \\
& = 0
\end{aligned} \tag{3.31}$$

Therefore, it can be concluded that equations  $l_1$  and  $l_2$  are linearly dependent. Similarly,  $l_1$  and  $l_3$  are also linearly dependent. Therefore, only one of the three equations can be chosen as the last constraint equation for the 3R chain apart from the two constraint equations chosen for the 4R chain.

It should be noted that not any three of the eight equations (apart from the equation of the Study quadric) can be arbitrarily selected as the constraint equations for a 3R chain because some equations are linearly dependent and fail on further computation. The best choices of the constraint equations for the 3R chain are the same two recommended constraint equations selected for the 4R chain and one equation from the remaining three equations, i.e., Eqs. (3.2), (3.3) and (3.9).

### 3.4 Summary

This chapter first investigated basic serial kinematic chains as compositional units of parallel mechanisms. Serial kinematic chains were classified into several types according to their joint numbers and joints arrangements. Then the constraint equations for these chains were obtained using the explicitation algorithm and implicitization algorithm based on the kinematic mapping method described in Chapter 2. More than the necessary number of constraint equations were obtained for 3J and 4J serial kinematic chains from the implicitization algorithm, therefore, the relationship among them were conducted by an analytical linear algebraic method and the appropriate constraint equations were selected accordingly. Overall, the outcomes from this chapter not only give an overview regarding serial kinematic chains but also lay the foundation for the kinematic analysis of MMRRMs in the following chapters.

## **Chapter 4 – Type Synthesis of 7-Joint Single-Loop Reconfigurable Mechanisms with Three or More Specified Operation Modes**

Single-Loop Multi-Mode Reconfigurable Mechanisms (SLMMRMs) can have the same DOFs in different operation modes or have variable DOFs in different operation modes. Therefore they can be classified into two categories: variable-DOF SLMMRMs and invariable-DOF SLMMRMs. There are different concepts and methods with which to construct reconfigurable mechanisms. Approaches have been proposed for the synthesis of variable-DOF single-loop reconfigurable mechanisms [35,126] and single-DOF single-loop mechanisms with two specified operation modes [55]. This chapter focuses on the type synthesis of single-loop reconfigurable mechanisms with three or more specified operation modes.

### **4.1 Methods to Construct SLMMRMs**

Reference [35] presented a systematic approach for the type synthesis of variable-DOF single-loop KMs based on displacement group theory. A new approach based on screw theory was proposed for the type synthesis of variable-DOF SLMMRMs [126]. Meanwhile, an intuitive approach also based on screw theory has been proposed [55] for the type synthesis of single-loop single-DOF mechanisms with two operation modes and several 7R multifunction linkages that in general have one DOF were generated by insertion of SLOMs with 4R, 5R and 6R joints [129]. Basically, the main ideas to construct SLMMRMs are to combine two or more SLOMs, or to insert new joint(s) into SLOMs. It can benefit from these methods to construct single-loop reconfigurable mechanisms with three or more operation modes. These methods are briefly reviewed as follows.

#### ***4.1.1 SLMMRMs from Combining Two or More SLOMs***

A common method for constructing a new SLMMRM is to combine two or more SLOMs. The description of the method to construct single-loop mechanisms with two specified operation modes can be summarized into four steps [55]:

- a) Take two original mechanisms, 1 and 2.

- b) Place the two mechanisms in such a way that they have  $n_c$  common joints.
- c) Disconnect the links belonging to the two original mechanisms without changing the location of joints and build new links to reassemble the linkage.
- d) Select an actuated joint.

Using this method four classes of 6R mechanisms and fourteen classes of 7R mechanisms with two specified operation modes can be obtained, where it has been found that such mechanisms usually has three operation modes.

#### ***4.1.2 SLMMRMs by Inserting Joint(s) into SLOMs***

New joint(s) can be added into an SLOM to form a new mechanism with mobility. Using the screw theory based approach, variable-DOF single-loop 7R and 8R SLMMRMs are proposed in [126] by inserting two joints into planar 5R and 6R mechanisms, respectively, as described in chapter 1.

### **4.2 Type Synthesis of 7J Single-Loop Reconfigurable Mechanisms with Three or More Operation Modes**

Inspired by the type synthesis of variable-DOF SLMMRMs and single-DOF single-loop reconfigurable mechanisms with two specified operation modes, the type synthesis of single-loop reconfigurable mechanisms with three or more operation modes is undertaken in this chapter. Except for some special cases single-loop mechanisms with three operation modes have six joints, others have 7 joints, so called 7J single-loop reconfigurable mechanisms with three or more operation modes. The methods to construct these mechanisms are detailed below.

#### ***4.2.1 7J Single-Loop Reconfigurable Mechanisms with Three or More Operation Modes from Combining Two SLOMs***

As has been shown in [110,127], the single-loop 7J mechanisms with two specified  $m$ -J operation modes ( $m < 7$ ) constructed in [55] have in fact three operation modes including the two specified  $m$ -J modes and the 7J mode. Therefore, the method of combining two SLOMs together turns out to be simple and effective for constructing 7J single-loop reconfigurable mechanisms with three or more operation modes. For example, in [110] a multi-mode 5R2P closed-loop linkage is built by combining two SLOMs: a Bennett



linkage and a RPRP linkage, which has been revealed to have three operation modes. Combining Bennett linkages and RPRP linkages, Ref. [127] also presented 7-link chains: 7R linkage and 4R3P linkage, both of which have three operation modes. More single-loop mechanisms with three operation modes can be constructed according to this method using other SLOMs, i.e. 7J single-loop reconfigurable mechanisms with three or more operation modes may be obtained from the following nineteen combinations, some of them have been identified in [55,110,127]:

- (1) Bennett 4R – Planar 4R (with one common joint) [55]
- (2) Bennett 4R – Spherical 4R (with one common joint) [55]
- (3) Bennett 4R – Bennett 4R (with one common joint) [55]
- (4) Bennett 4R – Spatial RPRP (with one common joint) [110]
- (5) Spatial RPRP – Spatial RPRP (with one common joint) [127]
- (6) Planar 4R – Spherical 4R (with one common joint) [55]
- (7) Planar 4R – Spatial RPRP (with one common joint)
- (8) Spherical 4R – Spherical 4R (with one common joint) [55]
- (9) Paradoxical 5R – Bennett 4R (with two common joints) [55]
- (10) Paradoxical 5R – Planar 4R (with two common joints) [55]
- (11) Paradoxical 5R – Spherical 4R (with two common joints) [55]
- (12) Paradoxical 5R – Spatial RPRP (with two common joints)
- (13) Paradoxical 5R – Paradoxical 5R (with three common joints) [55]
- (14) Paradoxical 6R – Bennett 4R (with three common joints) [55]
- (15) Paradoxical 6R – Planar 4R (with three common joints) [55]
- (16) Paradoxical 6R – Spherical 4R (with three common joints) [55]
- (17) Paradoxical 6R – Spatial RPRP (with three common joints)
- (18) Paradoxical 6R – Paradoxical 5R (with four common joints) [55]
- (19) Paradoxical 6R – Paradoxical 6R (with five common joints) [55]

The procedures for constructing 7J single-loop reconfigurable mechanisms with three or more operation modes are similar to those in [55]:

- a) Take two original mechanisms, 1 and 2, and place the two mechanisms in such a way that they have  $n_c$  common joints and  $n_1+n_2-n_c=7$ . Here,  $n_1$  ( $n_2$ ) is the number of joints of mechanism 1 (2).
- b) Disconnect the links belonging to the two original mechanisms without changing the location of the joints.

c) Choose the connection sequence of joints and calculate the parameters for all adjacent joints and build new links to reconnect all the joints to construct a 7J mechanism.

d) Use CAD models and the kinematic analysis of motion curves to validate that the new 7J mechanism has three operation modes.

#### ***4.2.2 7J Single-Loop Reconfigurable Mechanisms with Three or More Operation Modes by Inserting a Joint into a 6J SLOM***

There are two ways to select a 6J mechanism as the original SLOM to construct a 7J single-loop reconfigurable mechanisms with three or more operation modes: one is to build a 6J mechanism from combining two SLOMs so that the 6J mechanism can have two operation modes; another is to directly choose a 6J SLOM with one or two operation mode(s). Then a new joint can be inserted into this 6J mechanisms to build a 7J mechanism. Whether these 7J mechanisms have three or more operation modes needs to be verified by their CAD models and kinematic analysis.

##### **1) Firstly construct a 6J mechanism with two operation modes and then insert a joint into the 6J mechanism to obtain a 7J single-loop reconfigurable mechanism with three or more operation modes**

The 6J mechanisms with two specified operation modes can be constructed according to the procedures described in Section 4.1.1 with seven classes of combinations:

- 1) Bennett 4R and Planar 4R based 6R mechanism [55]
- 2) Bennett 4R and Bennett 4R based 6R mechanism [55]
- 3) Bennett 4R and Spatial RPRP based 6R mechanism
- 4) Spatial RPRP and Planar 4R based 6R mechanism
- 5) Paradoxical 5R and Bennett 4R based 6R mechanism [55]
- 6) Paradoxical 5R and Spatial RPRP based 6R mechanism
- 7) Paradoxical 5R and paradoxical 5R based 6R mechanism [55]

Then 7J single-loop reconfigurable mechanisms with three or more operation modes can be constructed by inserting one joint into the 6J mechanisms with two operation modes obtained above. The procedures includes:

a) Place the 6J mechanism with two operation modes at the transition configuration where the two operation modes switch to each other and disconnect it while keeping the joints location unchanged.

b) Add one joint between two joints trying to make the new D-H parameters as simple as possible.

c) Calculate the parameters for the new links and build them to reconnect all joints to construct a 7J mechanism.

d) Use a CAD model and kinematics analysis of motion curves to verify that the 7J mechanism has three or more operation modes.

**2) Directly insert a joint into a 6J mechanism with one or two operation mode(s) to obtain a 7J single-loop reconfigurable mechanism with three or more operation modes**

Apart from the method mentioned above, it is possible to produce a 7J single-loop reconfigurable mechanisms with three or more operation modes by inserting a joint directly into an existing 6J SLOM. It is feasible to produce a 7J single-loop reconfigurable mechanism with three or more operation modes by inserting a joint into a 6R SLOM with one operation mode. For example, a 7J mechanism from inserting a joint into a Sarrus linkage will be identified having three operation modes in Chapter 5. In addition, considering some 6J mechanisms such as the line (plane) symmetrical Bricard linkages, according to [50], some of the Bricard linkages have two or even three operation modes due to their special parameters. Take a line and plane symmetrical Bricard linkage as an example (Fig. 4.2), the associated parameters satisfy the following conditions:

$$a_1 = a_3 = a_4 = a_6 = a, a_2 = a_5 = 0 \quad (4.1)$$

$$\alpha_1 = \alpha_4 = \frac{\pi}{2}, \alpha_3 = \alpha_6 = -\frac{\pi}{2}, \alpha_2 = \alpha_5 \quad (4.2)$$

$$d_1 = d_4 = 0, -d_2 = d_3 = -d_5 = d_6 = d \quad (4.3)$$

There are four cases of operation mode for the Bricard linkage depending on its parameters:

$$\text{Case I: } \frac{d}{a} > \cot\left(\frac{\alpha}{2}\right) (0 < \alpha \leq \frac{\pi}{2}) \text{ and } \frac{d}{a} \geq \tan\left(\frac{\alpha}{2}\right) (\frac{\pi}{2} < \alpha < \pi):$$

where there are two operation modes in this case: line and plane symmetrical Bricard linkage mode and spherical 4R mode;

$$\text{Case 2: } \frac{d}{a} < \tan\left(\frac{\alpha}{2}\right) (0 < \alpha \leq \frac{\pi}{2}) \text{ and } \frac{d}{a} \leq \cot\left(\frac{\alpha}{2}\right) (\frac{\pi}{2} < \alpha < \pi):$$

where two operation modes exist in this case: line and plane symmetrical Bricard linkage mode and plane symmetrical Bricard linkage mode;

$$\text{Case 3: } \tan\left(\frac{\alpha}{2}\right) \leq \frac{d}{a} \leq \cot\left(\frac{\alpha}{2}\right) (0 < \alpha \leq \frac{\pi}{2})$$

where the Bricard linkage has three operation modes in this case: line and plane symmetrical Bricard linkage mode, plane symmetrical Bricard linkage mode and spherical 4R mode;

$$\text{Case 4: } \cot\left(\frac{\alpha}{2}\right) < \frac{d}{a} < \tan\left(\frac{\alpha}{2}\right) (\frac{\pi}{2} < \alpha < \pi)$$

where the Bricard linkage has only one operation mode: line and plane symmetrical Bricard linkage mode.

In above cases 1 and 2 this Bricard linkage has two operation modes and in case 3 it has three. Therefore, it is possible to add one R joint into it in case 1, 2, and 3 to form a 7J single-loop reconfigurable mechanism with three or more operation modes.

Other 6J SLOMs can also be considered as the foundation from which to construct 7J single-loop reconfigurable mechanisms with three or more operation modes. However, how to and where to place the added R joint on a 6J mechanisms to form a new non-overconstrained 7J single-loop reconfigurable mechanisms with three or more operation modes is still an open issue. Their operation modes need to be verified by their CAD models and kinematic analysis.

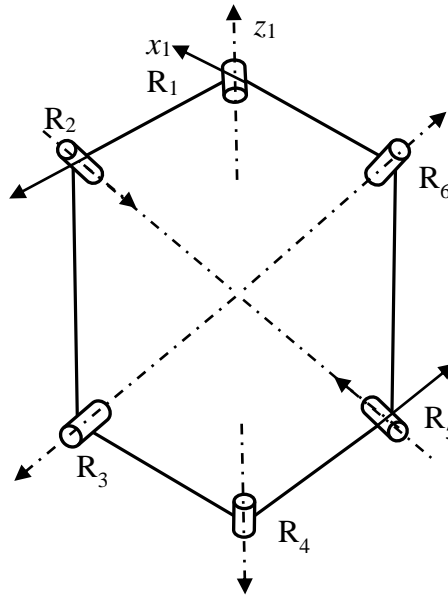


Figure 4.2 Line and plane symmetrical Bricard linkage

Three methods are proposed here for the type synthesis of 7J single-loop reconfigurable mechanisms with three or more operation modes. The first method have been illustrated in papers [110, 127]. The third method will demonstrated in detail in the following two chapters. In the next subsection, examples of 7J single-loop reconfigurable mechanisms with three or more operation modes from the second method will be shown.

### 4.3 Examples of 7J Single-Loop Reconfigurable Mechanisms with Three or More Operation Modes

In this subsection, 6R mechanisms with two operation modes will be first constructed, followed by inserting an R joint into them to obtain 7R single-loop reconfigurable mechanisms with three or more operation modes, illustrating the effectiveness of the second method presented. According to [55], several mechanisms based on two compositional mechanisms can be constructed due to different connection order of their joints. An attempt will be made to construct two 6R mechanisms based on two Bennett linkages as well as their corresponding 7R single-loop reconfigurable mechanisms with three or more operation modes and to identify the difference between them.

#### 4.3.1 The 6R Mechanism I and 7R Mechanism I Based on Two Bennett Linkages

A 6R mechanism is initially constructed using two Bennett linkages with the same Bennett ratio (Eqs. (4.6) and (4.9)) as shown in Fig. 4.3. The parameters relating to the two original Bennett linkages are listed as below:

Bennett linkage I:

$$a_{11} = a_{13} = 200, a_{12} = a_{14} = 400 \quad (4.4)$$

$$\alpha_{11} = \alpha_{13} = 30^\circ, \alpha_{12} = \alpha_{14} = 90^\circ \quad (4.5)$$

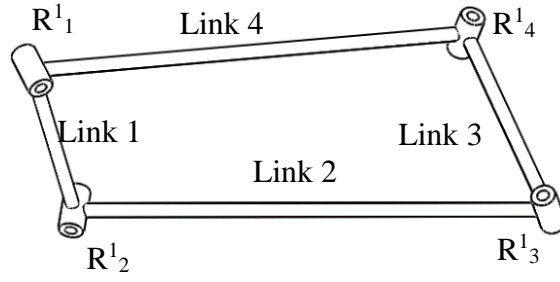
$$\frac{\sin \alpha_{11}}{a_{11}} = \frac{\sin \alpha_{12}}{a_{12}} = \frac{1}{400} \quad (4.6)$$

Bennett linkage II:

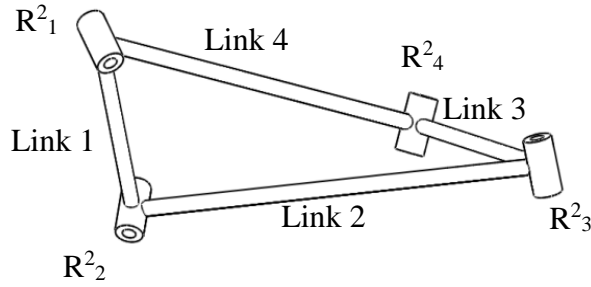
$$a_{21} = a_{23} = 200, a_{22} = a_{24} = 320 \quad (4.7)$$

$$\alpha_{21} = \alpha_{23} = 30^\circ, \alpha_{22} = \alpha_{24} = 53.1301^\circ \quad (4.8)$$

$$\frac{\sin \alpha_{21}}{a_{21}} = \frac{\sin \alpha_{22}}{a_{22}} = \frac{1}{400} \quad (4.9)$$



(a) Bennett linkage I



(b) Bennett linkage II

Figure 4.3 Two original Bennett linkages

### 1) The 6R mechanism I combined using the two Bennett linkages

In order to build a 6R mechanism, two common R joints have to be put together with a common link. Here, the two Bennett linkages are arranged as follows (Fig.4.4):

- Common joints are  $R_1^1$  and  $R_2^1$  as well as  $R_1^2$  and  $R_2^2$  which means the links 1 of both Bennett linkages are totally coincident.
- The angle between link 1 and link 4 of both Bennett linkages is 90 degrees.
- The reconnected sequence is:  $R_1^1 (R_2^1) - R_1^2 (R_2^2) - R_3^2 - R_3^1 - R_4^1 - R_4^2$ .

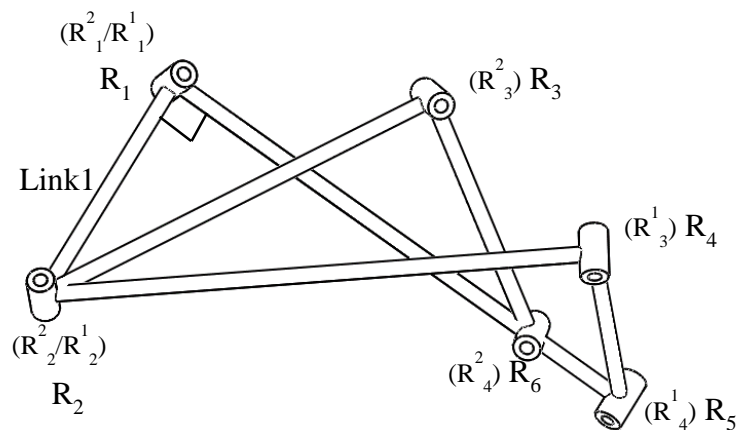


Figure 4.4 Two original Bennett linkages combined with two common R joints

Therefore, there will be two new links needing to be rebuilt, i.e. the link between  $R_3$  and  $R_4$  and the link between  $R_5$  and  $R_6$ . The parameters for the new links of the 6R mechanism I need to be calculated initially based on known conditions.

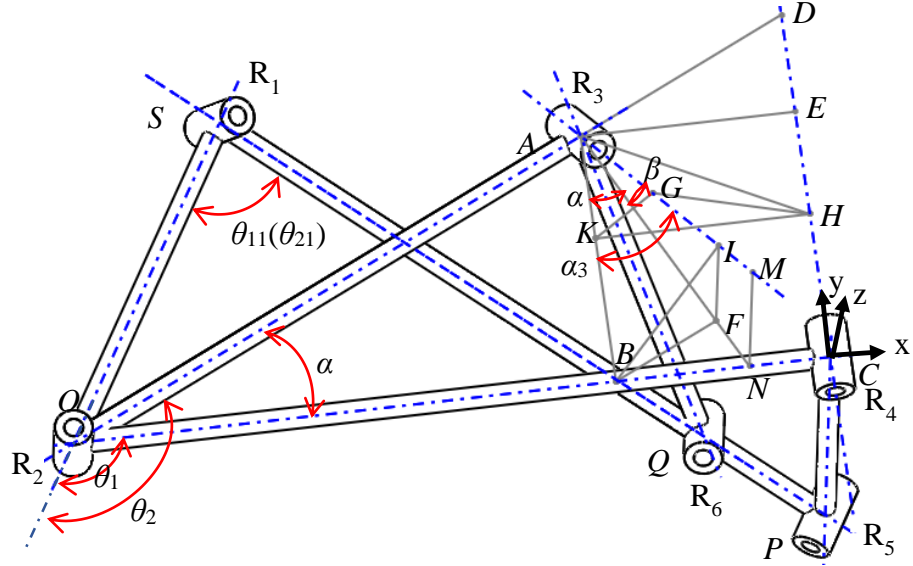


Figure 4.5 Calculating the D-H parameters for the 6R mechanism I

The given conditions (Fig. 4.5) are:

$$AO = 320, CO = 400 \quad (4.10)$$

$$\theta_{11} = \theta_{21} = 90^\circ, \beta = 90^\circ - 53.1301^\circ = 26.8699^\circ \quad (4.11)$$

Firstly, we calculate the parameters for the new link between  $R_3$  and  $R_4$ .

a) Calculate the angle  $\alpha_3$  between the skew lines (axes of  $R_3$  and  $R_4$ ).

In a Bennett linkage,

$$\tan \frac{\theta_1}{2} \tan \frac{\theta_2}{2} = \frac{\sin \frac{1}{2}(\alpha_2 + \alpha_1)}{\sin \frac{1}{2}(\alpha_2 - \alpha_1)} \quad (4.12)$$

where,  $\theta_{11} = \theta_{21} = 90^\circ$ , such that  $\tan \frac{\theta_{11}}{2} = \tan \frac{\theta_{21}}{2} = 1$ , then

$$\tan \frac{\theta_{12}}{2} = \frac{\sin \frac{1}{2}(\alpha_{12} + \alpha_{11})}{\sin \frac{1}{2}(\alpha_{12} - \alpha_{11})} = \frac{\sin \frac{1}{2}(90^\circ + 30^\circ)}{\sin \frac{1}{2}(90^\circ - 30^\circ)} \quad (4.13)$$

and

$$\tan \frac{\theta_{22}}{2} = \frac{\sin \frac{1}{2}(\alpha_{22} + \alpha_{21})}{\sin \frac{1}{2}(\alpha_{22} - \alpha_{21})} = \frac{\sin \frac{1}{2}(53.1301^\circ + 30^\circ)}{\sin \frac{1}{2}(53.1301^\circ - 30^\circ)} \quad (4.14)$$

leading to

$$\theta_{12} = 120^\circ, \theta_{22} = 146.3736^\circ \quad (4.15)$$

therefore

$$\alpha = \theta_{22} - \theta_{12} = 26.3736^\circ \quad (4.16)$$

Since

$$AB = AO \cdot \sin \alpha, BF = AB \cdot \sin \alpha, AF = AB \cdot \cos \alpha \quad (4.17)$$

$$IF = AF \cdot \tan \beta, AI = \frac{AF}{\cos \beta} \quad (4.18)$$

$$BI^2 = BF^2 + IF^2 \quad (4.19)$$

$$\cos \alpha_3 = \frac{AB^2 + AI^2 - BI^2}{2 \cdot AB \cdot AI} \quad (4.20)$$

$$\alpha_3 = \arccos\left(\frac{AB^2 + AI^2 - BI^2}{2 \cdot AB \cdot AI}\right) = 44.2146^\circ \quad (4.21)$$

b) Calculate the length of the common perpendicular ( $GH$ ) between the skew lines, which is the distance between two axes of  $R_3$  and  $R_4$ ,  $a_3$ .

$$CD = CO \cdot \tan \alpha \quad (4.22)$$

$$AD = \frac{CO}{\cos \alpha} - AO \quad (4.23)$$

$$AE = AD \cdot \sin \alpha \quad (4.24)$$

$$|\overrightarrow{CD}| = 0\vec{i} + CD\vec{j} \quad (4.25)$$

$$|\overrightarrow{AB}| = -AB \cdot \tan \alpha \cdot \vec{i} + AB \cdot \vec{j} \quad (4.26)$$

$$|\overrightarrow{AM}| = -AB \cdot \tan \alpha \cdot \vec{i} + AB \cdot \vec{j} + \frac{AB}{\cos \alpha} \cdot \tan \beta \cdot \vec{k} \quad (4.27)$$

Assuming  $n[x, y, z]$  is the common normal of lines  $AM$  and  $CD$ , therefore

$$\begin{cases} \vec{n} \cdot \overrightarrow{AM} = 0 \\ \vec{n} \cdot \overrightarrow{CD} = 0 \end{cases} \quad (4.28)$$

The expressions in Eq. (4.18) can be exploded as

$$\begin{cases} -AB \cdot \tan \alpha \cdot x + AB \cdot y + \frac{AB}{\cos \alpha} \cdot \tan \beta \cdot z = 0 \\ CD \cdot y = 0 \end{cases} \quad (4.29)$$

Therefore, vector  $n$  can be obtained as

$$\vec{n} = \left[ \frac{\tan \beta}{\sin \alpha}, 0, 1 \right] \quad (4.30)$$



The distance of two skew lines can be further obtained as

$$a_3 = \frac{|\vec{AD} \cdot \vec{n}|}{|\vec{n}|} \quad (4.31 \text{ a})$$

where  $|\vec{AD}| = AE \cdot \vec{i} + (CD - AB) \cdot \vec{j}$ .

Equation (4.31 a) can be re-written as

$$a_3 = \frac{\frac{\tan \beta}{\sin \alpha} \cdot AE}{\sqrt{\left(\frac{\tan \beta}{\sin \alpha}\right)^2 + 1}} = 97.4894 \quad (4.31 \text{ b})$$

c) Calculate the length of  $AG$ ,  $d_3$ , which is the offset of  $x_3$  to  $x_4$ .

There is a condition

$$KH = AE \quad (4.32)$$

so

$$KG = \sqrt{KH^2 - GH^2} \quad (4.33)$$

Then

$$d_3 = AG = \frac{KG}{\sin \beta} = 82.8032 \quad (4.34)$$

d) The length of  $CH$ ,  $d_4$ , which is the offset of  $x_4$  with regard to  $x_5$ , can be obtained by

$$AK = AG \cdot \cos \alpha_3 \quad (4.35)$$

then

$$d_4 = CH = BK = AB - AK = 82.8032 \quad (4.36)$$

We can calculate the parameters for the new link between  $R_5$  and  $R_6$ . Link 4 is formed by the two coincident Bennett linkages according to the conditions for building the new 6R mechanism. Therefore, the associated parameters can be produced by

$$\alpha_5 = \alpha_{14} - \alpha_{24} = 90^\circ - 53.1301^\circ = 26.8699^\circ \quad (4.37)$$

$$\alpha_6 = \alpha_{24} = 53.1301^\circ \quad (4.38)$$

$$a_5 = a_{14} - a_{24} = 80 \quad (4.39)$$

$$d_5 = 0 \quad (4.40)$$

Finally, the new links connecting  $R_3$  and  $R_4$ ,  $R_5$  and  $R_6$  are able to be built according to the parameters obtained above, so that all the R joints are reconnected to form the 6R mechanism I as shown in Fig. 4.6 with its parameters in Table 4.1. The re-built coordinate frames for it are shown in Fig. 4.7.

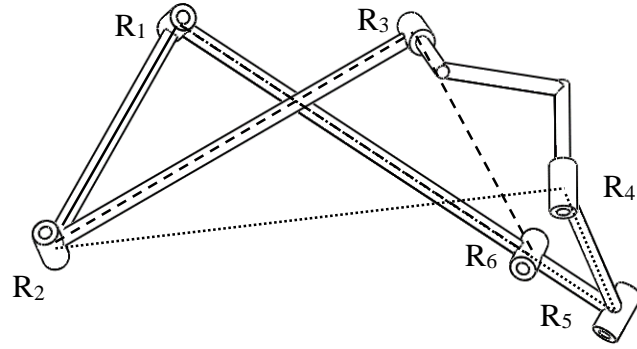


Figure 4.6 Construction of the 6R mechanism I using new links

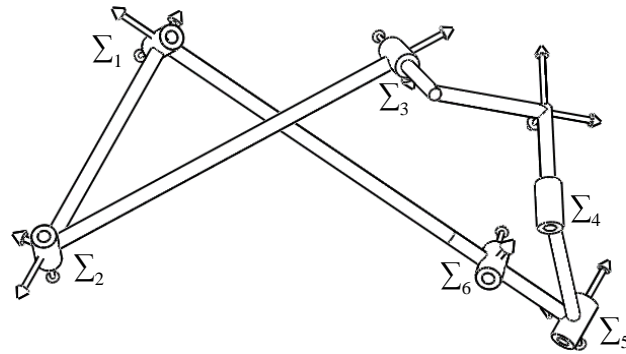


Figure 4.7 Building coordinate frames for 6R mechanism I

Table 4.1 Parameters for 6R mechanism I

	$a_i$	$d_i$	$\alpha_i$ (deg)
1	200.00	0.00	30.00
2	320.00	0.00	53.13
3	97.49	-82.80	44.21
4	200.00	-82.80	30.00
5	80.00	0.00	26.87
6	320.00	0.00	53.13

The 6R mechanism I will be operated with two operation modes: the Bennett linkage mode I (Fig. 4.8(a)) and the Bennett linkage mode II (Fig. 4.8(b)) which are verified by CAD models. In the Bennett linkage mode I, joints  $R_1$ ,  $R_2$ ,  $R_4$ , and  $R_5$  are active and joints  $R_3$  and  $R_6$  are locked automatically. In the Bennett linkage mode II, joints  $R_1$ ,  $R_2$ ,  $R_3$ , and  $R_6$  are active and joints  $R_4$  and  $R_5$  are locked automatically. The two operation modes can be transformed into each other at the configuration where the new 6R mechanism I was first reconnected.

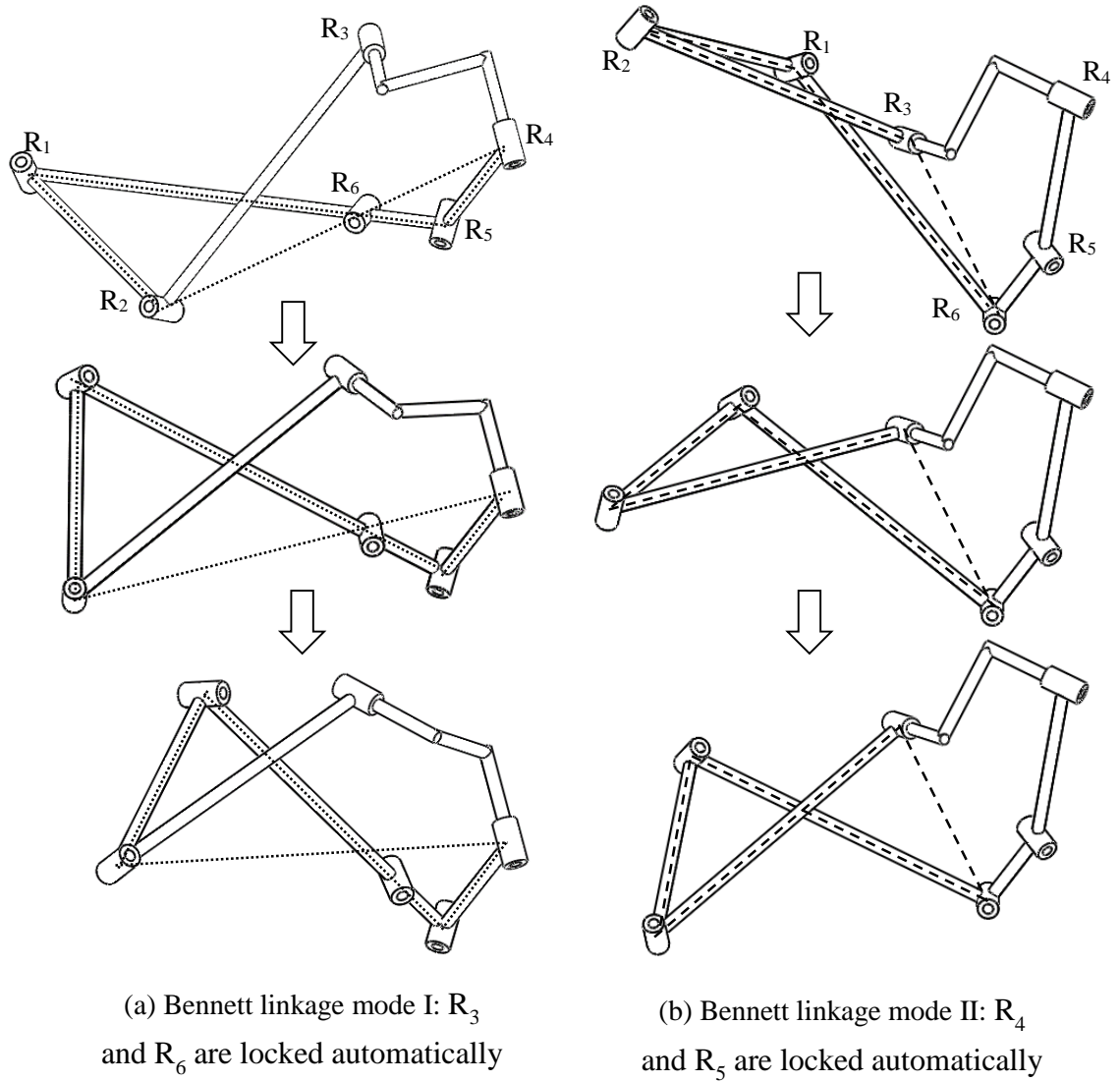


Figure 4.8 Two operation modes of the 6R mechanism I

## 2) The 7R mechanism I constructed by inserting one joint into 6R mechanism I

Since the newly built 6R mechanism I is still an overconstrained mechanism it is possible to add one more R joint into it to turn the mechanism into a non-overconstrained mechanism. Keeping the 6R mechanism at the configuration when it was first built, one R joint can be added between  $R_2$  and  $R_3$  such that the new links 2 and 3 stay on the straight line where the original link 2 stays and the axis of  $R_3$  is parallel to the axis of  $R_2$  as shown in Fig. 4.9. The parameters for the non-overconstrained 7R mechanism I are shown in Table 4.2.

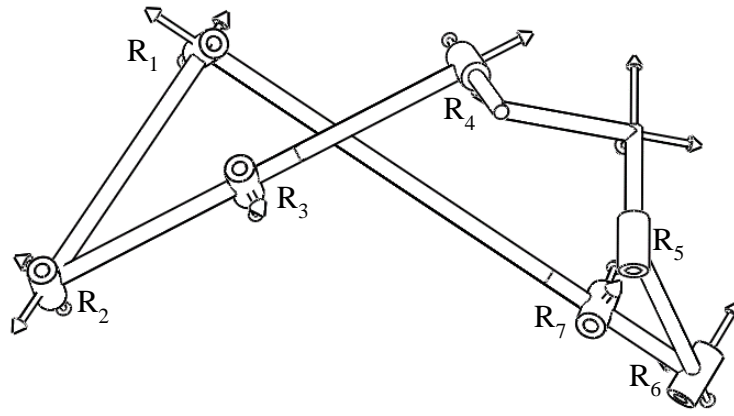


Figure 4.9 Building 7R mechanism I based on 6R mechanism I

Table 4.2 Parameters for the novel 7R mechanism I

	$a_i$	$d_i$	$\alpha_i$ (deg)
1	200.00	0.00	30.00
2	150.00	0.00	0.00
3	170.00	0.00	53.13
4	97.49	-82.80	44.21
5	200.00	-82.80	30.00
6	80.00	0.00	26.87
7	320.00	0.00	53.13

The novel 7R mechanism I is not an overconstrained mechanism anymore. It will keep the two operation modes belonging to the 6R mechanism I, and it can have another operation mode with all the seven R joints being active, i.e. the 7R mode which can be verified by the CAD model as shown in Fig. 4.10.

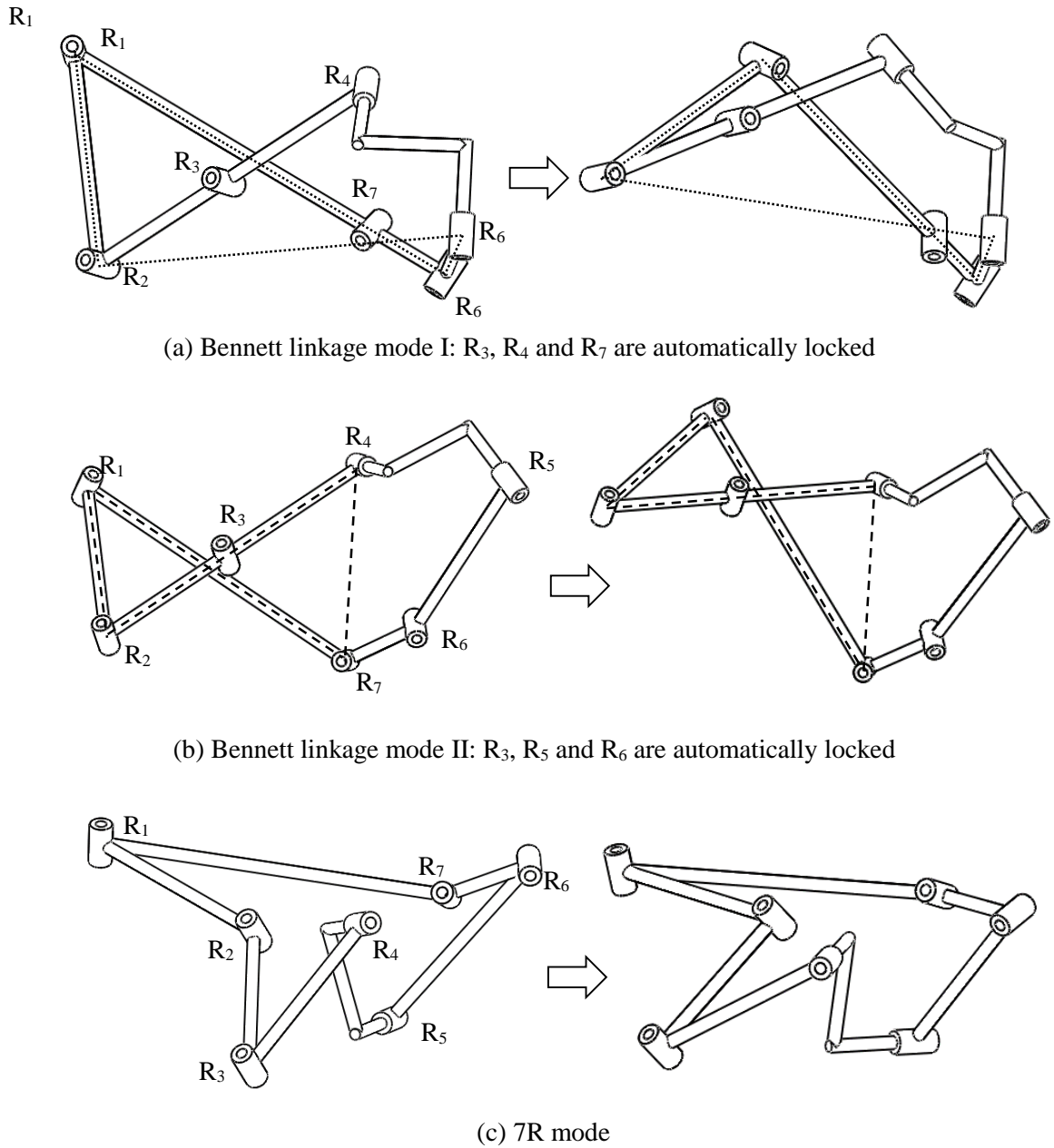


Figure 4.10 Three operation modes of 7R mechanism I

#### 4.3.2 The 6R Mechanism II and 7R Mechanism II Based on the Two Same Bennett Linkages

##### 1) 6R mechanism II combined by the two same Bennett linkages

The two same Bennett linkages are placed with the same common link and joints being together but in different configurations (Fig. 4.11(a)). Also, they will be reconnected in a different R joint subsequence:  $R^1_1 (R^2_1) - R^1_2 (R^2_2) - R^1_3 - R^1_4 - R^2_3 - R^2_4$  as shown in Fig. 4.11(b). In this subsequence, only one link between  $R^1_4$  and  $R^2_3$

needs to be built to form the 6R mechanism (Fig. 4.12) called 6R mechanism II. The parameters for 6R mechanism II are calculated and shown in Table 4.3.

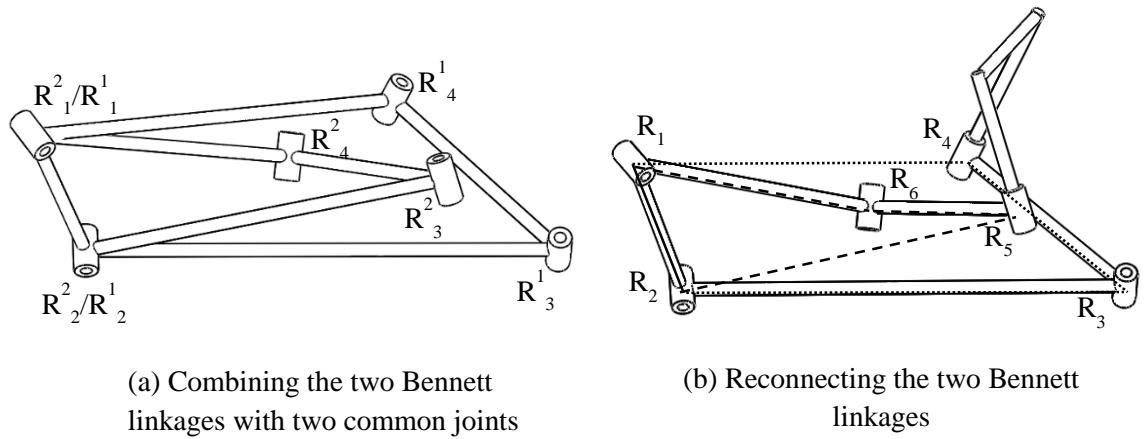


Figure 4.11 Reconnection of the two Bennett linkages in another way

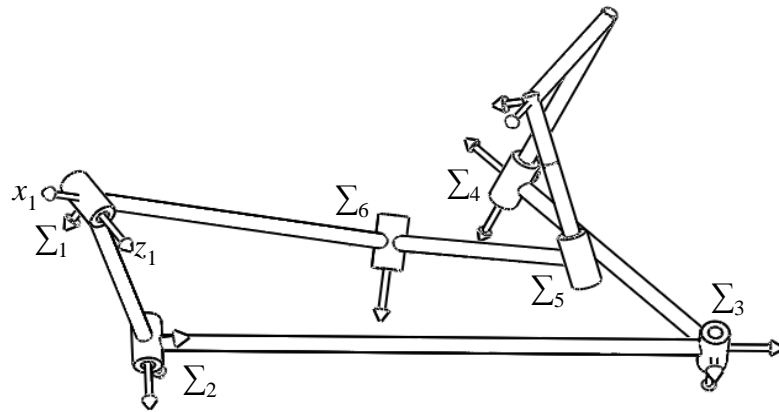


Figure 4.12 Building coordinate frames for the 6R mechanism II

Table 4.3 Parameters for the novel 6R mechanism II

	$a_i$	$d_i$	$\alpha_i$ (deg)
1	200.00	0.00	30.00
2	400.00	0.00	90.00
3	200.00	0.00	30.00
4	157.74	-159.34	42.22
5	200.00	128.49	30.00
6	320.00	0.00	53.13

As anticipated the 6R mechanism II has two operation modes: Bennett linkage mode I and Bennett linkage mode II as shown in Fig. 4.13. In Bennett linkage mode I (Fig. 4.13(a)), joints  $R_1, R_2, R_5$  and  $R_6$  are active and joints  $R_3$  and  $R_4$  are locked automatically. In the Bennett linkage mode II (Fig. 4.13(b)) joints  $R_1, R_2, R_3, R_4$  are

active and joints  $R_5$  and  $R_6$  are locked automatically. The two operation modes can be transformed into each other at the configuration where the new 6R mechanism II was first reconnected.

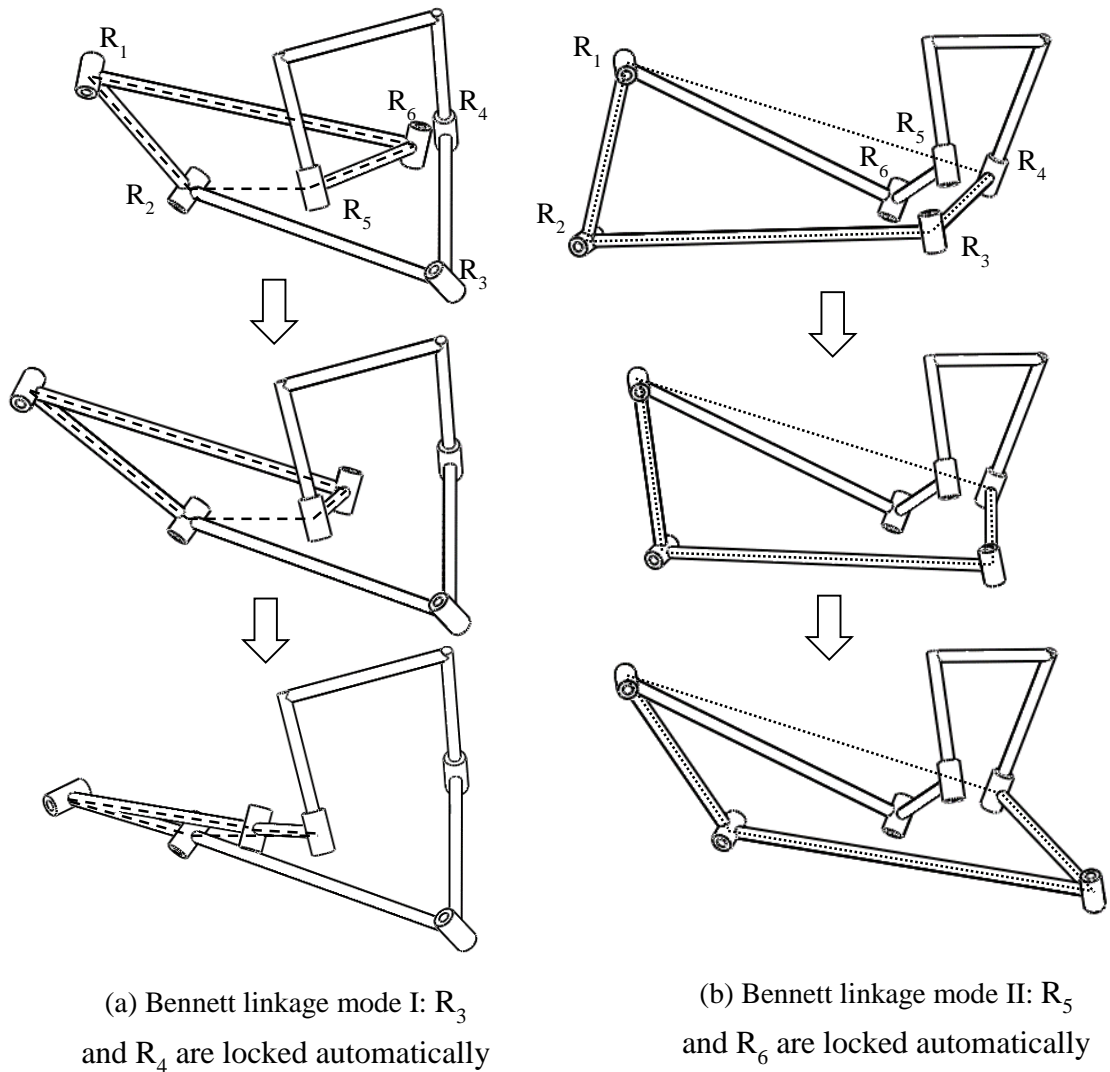


Figure 4.13 Two operation modes for the 6R mechanism II

## 2) The 7R mechanism II constructed by inserting one joint into 6R mechanism II

On the basis of 6R mechanism II, one R joint can be inserted into it to form the 7R mechanism II as shown in Fig. 4.14 using the parameters in Table 4.4. There will be three operation modes for 7R mechanism II as illustrated in Fig. 4.15.

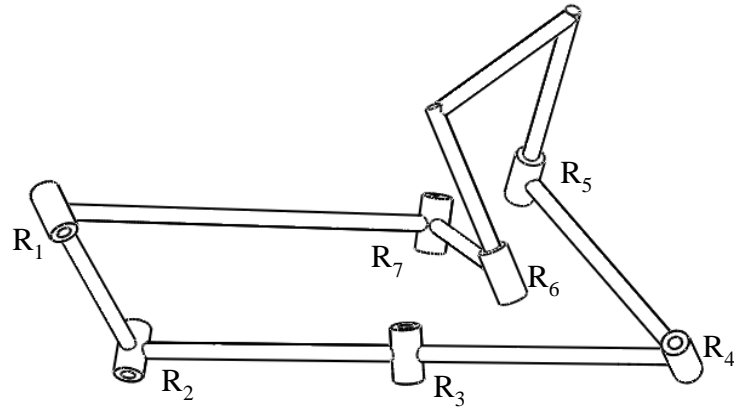


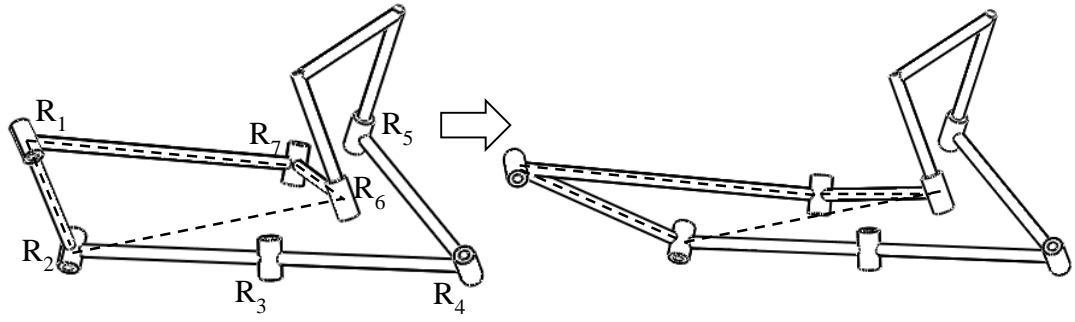
Figure 4.14 Building 7R mechanism based on 6R mechanism II

Table 4.4 Parameters for the novel 7R mechanism II

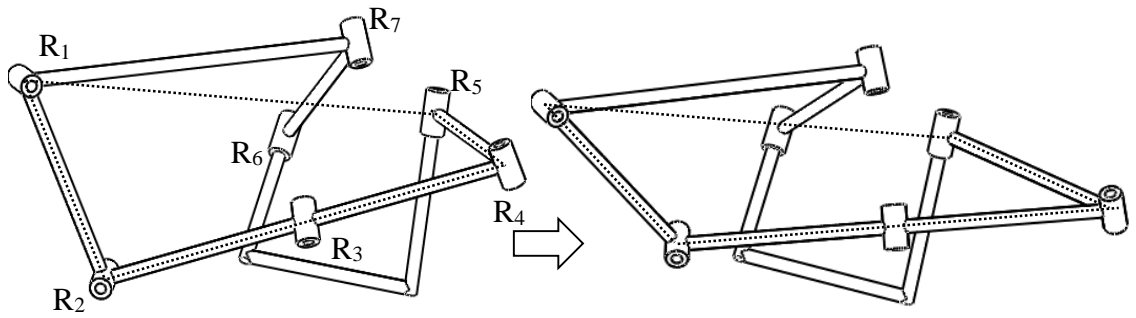
	$a_i$	$d_i$	$\alpha_i$ (deg)
1	200.00	0.00	30.00
2	200.00	0.00	45.00
3	200.00	0.00	45.00
4	200.00	0.00	30.00
5	157.74	-159.34	42.22
6	200.00	128.49	30.00
7	320.00	0.00	53.13

Based on the methods mentioned above, two 6R mechanisms I and II, are built in different R joint reconnection sequence where the R joint sequences is unchanged in its original Bennett linkage, and then two corresponding 7R mechanisms I and II are generated based on the 6R mechanisms. The two 6R mechanisms have the two same Bennett linkage modes even though their D-H parameters are different. The two novel 7R mechanisms keep the two Bennett linkage operation modes but have a third 7R operation mode. However, the two new 7R operation modes belonging to the two 7R mechanisms are different because all seven R joints are active in the 7R modes whilst their D-H parameters are different.

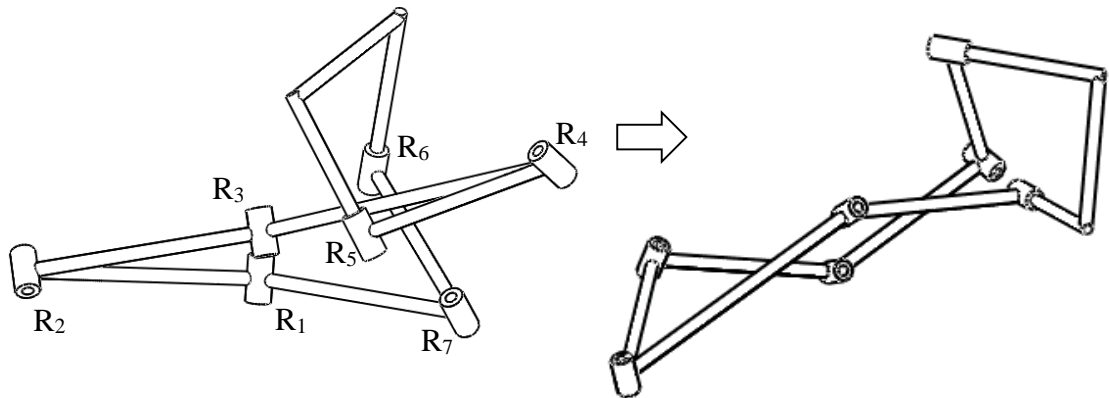




(a) Bennett Linkage mode I:  $R_3$ ,  $R_4$  and  $R_5$  are automatically locked



(b) Bennett linkage mode II:  $R_3$ ,  $R_6$  and  $R_7$  are automatically locked



(c) 7R mode

Figure 4.15 Three operation modes of the new 7R mechanism II

#### Remarks:

6J mechanisms can be constructed by combining two SLOMs in different joint sequences, and the group of 6J mechanisms constructed by the same two SLOMs in any sequences of the joints or in any of initially combining configurations have the same two operation modes as the original SLOMs. The 7J mechanisms constructed by adding a joint to the group of 6J mechanisms have a different third 7J operation mode. Moreover, different 7J single-loop reconfigurable mechanisms with three or more

operation modes can also be generated by adding the joint into different places of the 6J mechanisms.

#### **4.4 Summary**

The aim of this chapter was to find methods to construct 7J single-loop reconfigurable mechanisms with three or more operation modes. Firstly, various approaches for the type synthesis of SLMMRMs including variable-DOF SLMMRMs and same-DOF SLMMRMs were briefly reviewed. These methods were developed in Section 4.2 to construct novel 7J single-loop reconfigurable mechanisms with three or more operation modes: new classes of these mechanisms can be constructed based on the first method; the second method is to construct 7J mechanisms by adding one joint into 6J reconfigurable mechanisms from a combination of two SLOMs and the third is to construct 7J mechanisms by inserting a new joint into a 6J SLOM which has one or more operation modes. The procedures to construct new 7R mechanisms applying the second method were illustrated, including the arrangement of the joints, the calculation of the new parameters, reconnection of the joints and operation modes verification using CAD models. The results have shown that the method is effective for generating 7J single-loop reconfigurable mechanisms with three or more operation modes and a large number of novel 7J mechanisms of this type can be obtained according to this method. Examples of 7J single-loop reconfigurable mechanisms with three or more operation modes constructed using the third method will be presented and analysed in Chapters 5 and 6.

## **Chapter 5 – Design and Kinematic Analysis of a New 7R Single-Loop Mechanism with Three Specified Operation Modes Based on Sarrus Linkage**

Based on the method to construct 7J single-loop reconfigurable mechanisms with three or more operation modes proposed in Chapter 4, this chapter presents a novel 7R composed of seven R joints, by adding a revolute joint to the overconstrained Sarrus linkage. The SLMMRM can switch from one operation mode to another without disconnection and reassembly and is a non-overconstrained mechanism. The kinematic mapping based explicitation algorithm and both numerical and algebraic methods are adopted to deal with the kinematic analysis of the 7R SLMMRM. The results show that the 7R SLMMRM has three operation modes: a translational mode and two 1-DOF planar modes. The transition configurations among the three modes are also identified.

### **5.1 Description of a 1-DOF 7R SLMMRM**

The Sarrus linkage (Fig. 5.1(a)), which is composed of two groups of three R joints with parallel joint axes (rotational axes), is used to control the 1-DOF translation of the moving platform along a straight line with respect to the base. Since the Sarrus linkage is an overconstrained mechanism, one additional R joint can be inserted between the two joints of a link to obtain a new 1-DOF 7R single-loop mechanism (Fig. 5.1(b)). The advantages of adding one R joint to the Sarrus linkage are as follows: (a) it allows a non-overconstrained mechanism to be obtained from an overconstrained mechanism; (b) the Sarrus linkage has only one operation mode to complete one kind of task, but the new 7R single-loop mechanism has at least two operation modes with the possibility of fulfilling different kind of tasks on a sole mechanism; (c) the new 7R single-loop mechanism can switch from one mode to another without disassembly and without adding another actuator. In the translational operation mode (Sarrus mode), it works as a Sarrus linkage in which the moving platform translates along a straight line (Fig. 5.1(b)). In the 1-DOF planar operation mode, the moving platform undergoes a 1-DOF general planar motion (Fig. 5.1(c)). Therefore, the above 7R mechanism is a 7R SLMMRM which can switch from one operation mode to another one by using a break in the transition configuration.

In this 7R SLMMRM (Fig. 5.1(c)), link 7 is the base and link 4 is the moving platform. Links 4 and 7 are identical, and the link lengths and the axes of the R joints of the 7R SLMMRM satisfy the following conditions:

$$\mathbf{R}_1 // \mathbf{R}_3 // \mathbf{R}_4 + \mathbf{R}_2 \quad (5.1)$$

$$\mathbf{R}_5 // \mathbf{R}_6 // \mathbf{R}_7 \quad (5.2)$$

$$a_1 + a_2 = a_3 = a_5 = a_6 \quad (5.3)$$

where  $\mathbf{R}_i$  ( $i=1,2, \dots,7$ ) is the unit vector along the axis of joint  $\mathbf{R}_i$  and  $a_i$  is the link length as indicated in Fig. 5.1(c).

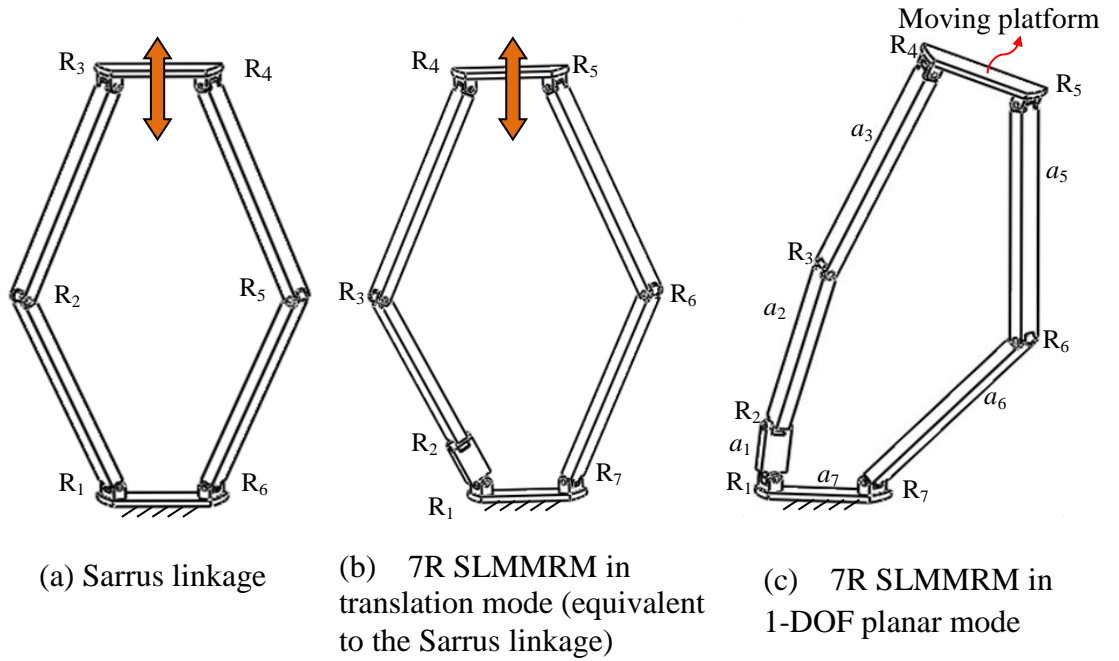


Figure 5.1 Construction of the 7R SLMMRM

Whether the 7R SLMMRM has additional operational modes, except the two operation modes already known, is unclear from only the mechanism. In the next section, the kinematic analysis of the 7R SLMMRM will be discussed in order to identify all of its operation modes as well as its transition configurations that enable it to switch from one operation mode to another.

## 5.2 Kinematic Analysis and Numerical Example for the 7R SLMMRM

Using the explicitation approach for the inverse kinematics for the general 6R mechanism, a kinematic analysis of the 7R SLMMRM can be performed such that the operation modes and transition configurations of the mechanism can be identified.

### 5.2.1 D-H Parameters for the Mechanism

The 7R SLMMRM can be regarded as a 6R serial mechanism with link 6 as the end-effector (EE), the coordinate frame on which is set as Fig. 5.2 (a). Its  $z$ -axis ( $z_{EE}$ ) coincides with the axis of joint  $R_7$  and its  $x$ -axis aligns with the common perpendicular to the  $z_6$ -axis and the  $z_{EE}$ -axis. The angle ( $\theta$ ) between the  $x_{EE}$ -axis and the vertical line is defined as the input angle of the 7R SLMMRM (Fig. 5.2 (b)). The D-H parameters of the 7R SLMMRM are shown in Table 5.1.

Table 5.1 D-H parameters for the 7R SLMMRM

$i$	$a_i$	$d_i$	$\alpha_i$	$\theta_i$
1	0.80	0	$90^\circ$	$\theta_1$
2	3.00	0	$-90^\circ$	$\theta_2$
3	3.80	0	$0^\circ$	$\theta_3$
4	0	1.47	$-120^\circ$	$\theta_4$
5	3.80	1.47	$0^\circ$	$\theta_5$
6	3.80	-1.47	$0^\circ$	$\theta_6$
7	0	-1.47	$120^\circ$	$\theta_7$

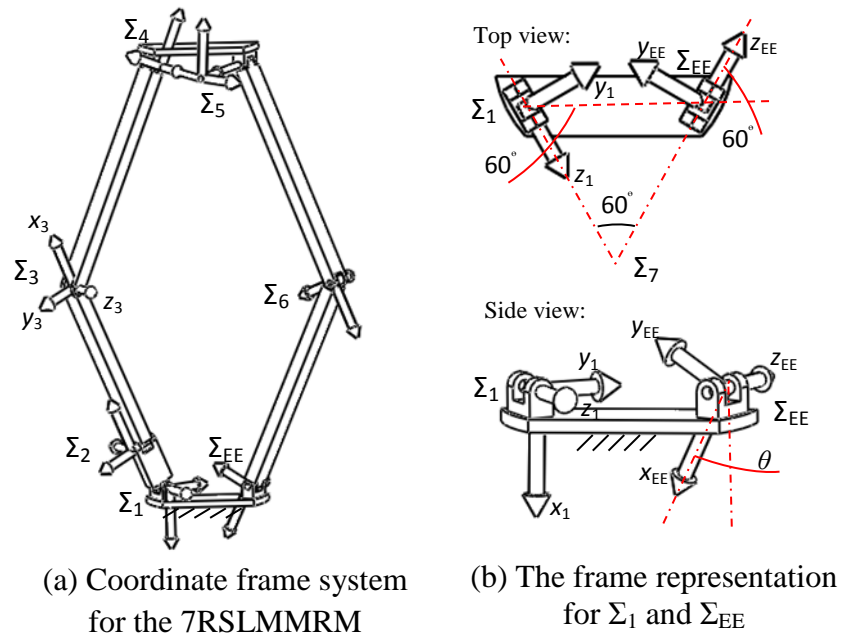


Figure 5.2 Coordinate frame system for the 7R SLMMRM

In addition, the angle between the axes of joints  $R_1$  and  $R_7$  is  $60^\circ$ ,  $\theta$  is specified as  $-45^\circ$  and  $a_7$  is  $-1.47$  (note: throughout this chapter, all rotational angles are defined to be positive if the rotation is in a clockwise direction about the z-axis). Therefore, the pose of end-effector  $\Sigma_{EE}$  with respect to  $\Sigma_1$  ( $A$ ) can be obtained (Fig. 5.2(b)), which is:

$$A = \begin{bmatrix} 1 & 0 & 0 & 0 \\ 0 & 0.7071067810 & 0.7071067810 & 0 \\ -1.273057344 & 0.3535533905 & -0.3535533905 & -0.8660254040 \\ 0.7350000000 & -0.6123724358 & 0.6123724358 & -0.5000000000 \end{bmatrix} \quad (5.4)$$

### 5.2.2 Solutions for the Kinematic Analysis

The explication algorithm for the inverse kinematics analysis of a general 6R serial manipulator presented in [116-118] is mainly used to undertake the analysis of the 7R SLMMRM. The 6R serial mechanism associated with the 1-DOF 7R SLMMRM is further decomposed into two 3R chains, the left 3R one (1-2-3) with end-effector frame  $\Sigma_L$  and the right 3R one (6-5-4) with end effector frame  $\Sigma_R$  (Fig. 5.3). The pose of the frame  $\Sigma_L$  with respect to  $\Sigma_1$  ( $T_L$ ) and the pose of the frame  $\Sigma_R$  with respect to  $\Sigma_1$  ( $T_R$ ) can be obtained based on Eqs. (2.36) and (2.41) as follows:

$$T_L = M_1 \cdot G_1 \cdot M_2 \cdot G_2 \cdot M_3 \cdot G_3 \quad (5.5)$$

$$T_R = A \cdot G_6^{-1} \cdot M_6^{-1} \cdot G_5^{-1} \cdot M_5^{-1} \cdot G_4^{-1} \cdot M_4^{-1} \quad (5.6)$$

In the mechanism, the frames  $\Sigma_L$  and  $\Sigma_R$  have to coincide which means that there is intersection among its  $SM_L$ ,  $SM_R$  and  $S_6^2$ . The equations for the  $SM$ s can be derived from Eqs. (5.5) and (5.6). Three sets of four equations can be obtained for the left or the right 3R chain while each set can be represented by a set of four bilinear equations in the eight homogenous study parameters, which is denoted by  $z_0, z_1, \dots, z_7$ , and one additional parameter corresponding to the tangent half of one out of the three joint angles.

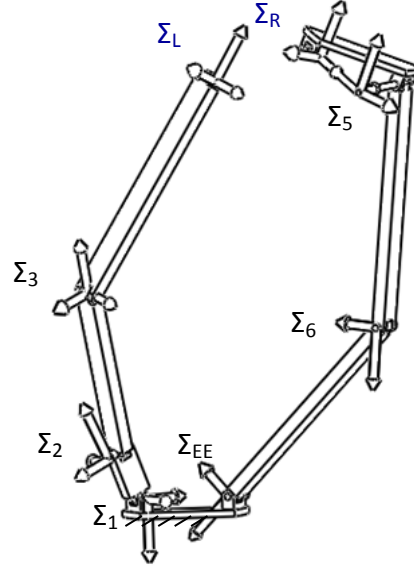


Figure 5.3 Decomposition of the 6R serial mechanism into two 3R chains

One of the three sets of four equations for the left 3R chain and one of the three sets of four equations for the right 3R chain is selected according to the situations before performing further calculations. Here,  $SM_3$  is selected which refers to four equations  $T(v_3)$  (tangent half of  $\theta_3$ ) for the left 3R chain since the axes of joints  $R_1$  and  $R_3$  are parallel in the translational mode. For the right 3R chain,  $SM_5$  is selected with four equations in  $T(\bar{v}_5)$  ( $\bar{v}_5$  is minus the tangent half of  $\theta_5$ ) because the axes of joints  $R_4$  and  $R_5$  intersect and the axes of joints  $R_5$  and  $R_6$  are parallel. Then the parameters of the assistant 6R chain (Table 5.1) can be substituted into the set of equations in  $T(v_3)$  shown in Table 3.1. The set of equations  $T(\bar{v}_5)$  can be obtained from  $T(v_2)$  by making some changes to the parameters for the right 3R chain. Eight equations for the 6R serial mechanism Eq. (5.7-5.14) are obtained as follows:

$$h1_{v_3} : 30.4z_0 + 24.0z_1 + 6.4z_2v_3 - 8.0z_4 + 8.0z_5 - 8.0z_6v_3 - 8.0z_7v_3 = 0 \quad (5.7)$$

$$h2_{v_3} : 30.4z_0 - 24.0z_1 - 6.4z_2v_3 + 8.0z_4 + 8.0z_5 - 8.0z_6v_3 + 8.0z_7v_3 = 0 \quad (5.8)$$

$$h3_{v_3} : 6.4z_1v_3 - 24.0z_2 - 30.4z_3 - 8.0z_4v_3 + 8.0z_5v_3 + 8.0z_6 + 8.0z_7 = 0 \quad (5.9)$$

$$h4_{v_3} : -6.4z_1v_3 + 24.0z_2 + 30.4z_3 + 8.0z_4v_3 + 8.0z_5v_3 + 8.0z_6 - 8.0z_7 = 0 \quad (5.10)$$

$$\begin{aligned}
h5_{\bar{v}_5} : & z_0(2.72626795828513 - 6.58179306856969\bar{v}_5) \\
& + z_1(4.12012622455083 - 4.85463523903963\bar{v}_5) \\
& + z_2(8.65463523574647 - 5.69413776088330\bar{v}_5) \\
& + z_3(-1.37687417023358^{-9} + 4.47457271235407^{-9}\bar{v}_5) \\
& + z_4(-1.24264068742686 - 3.00000000128678\bar{v}_5) \\
& + z_5(0.717438935080522 + 1.73205080649897\bar{v}_5) \\
& + z_6(1.73205080649897 - 0.717438935080522\bar{v}_5) \\
& + z_7(3.00000000128678 - 1.24264068742628\bar{v}_5) = 0
\end{aligned} \tag{5.11}$$

$$\begin{aligned}
h6_{\bar{v}_5} : & z_0(-2.7262679415240 + 6.58179306736930\bar{v}_5) \\
& + z_1(0.972103152392334 + 2.74536476831045\bar{v}_5) \\
& + z_2(8.65463523588648 + 5.69413776432743\bar{v}_5) \\
& + z_3(3.07322256531961^{-9} + 1.01209529645985^{-9}\bar{v}_5) \\
& + z_4(-0.414213562192757 - 0.99999999133379\bar{v}_5) \\
& + z_5(-0.717438935213303 - 1.73205080788068\bar{v}_5) \\
& + z_6(1.73205080788068 - 0.717438935213303\bar{v}_5) \\
& + z_7(-0.99999999133379 + 0.414213562192757\bar{v}_5) = 0
\end{aligned} \tag{5.12}$$

$$\begin{aligned}
h7_{\bar{v}_5} : & z_0(1.37687550250121^{-9} - 4.47457315644328^{-9}\bar{v}_5) \\
& + z_1(-8.65463523574647 - 5.69413776088330\bar{v}_5) \\
& + z_2(-4.12012622455083 + 4.85463523903963\bar{v}_5) \\
& + z_3(2.72626795828513 - 6.58179306856969\bar{v}_5) \\
& + z_4(-3.00000000128678 + 1.24264068742628\bar{v}_5) \\
& + z_5(1.73205080649897 - 0.717438935080522\bar{v}_5) \\
& + z_6(-0.717438935080522 - 1.73205080649897\bar{v}_5) \\
& + z_7(-1.24264068742686 - 3.00000000128678\bar{v}_5) = 0
\end{aligned} \tag{5.13}$$

$$\begin{aligned}
h8_{\bar{v}_5} : & z_0(-3.07322167714119^{-9} - 1.01209551850445^{-9}\bar{v}_5) \\
& + z_1(8.65463523588648 + 5.69413776432743\bar{v}_5) \\
& + z_2(-0.972103152392334 - 2.74536476831045\bar{v}_5) \\
& + z_3(-2.7262679415240 + 6.58179306736930\bar{v}_5) \\
& + z_4(0.99999999133379 - 0.414213562192757\bar{v}_5) \\
& + z_5(1.73205080788068 - 0.717438935213303\bar{v}_5) \\
& + z_6(0.717438935213303 + 1.73205080788068\bar{v}_5) \\
& + z_7(-0.414213562192757 - 0.99999999133379\bar{v}_5) = 0
\end{aligned} \tag{5.14}$$

$$h9: z_0z_4 + z_1z_5 + z_2z_6 + z_3z_7 = 0 \tag{5.15}$$



Including the equation for the  $S_6^2$  shown in Eq. (5.15), nine bilinear equations in ten unknowns (Eqs. (5.7)-(5.15)) are obtained. Since  $z_0, z_1, \dots$  and  $z_7$  are homogeneous, one of them can be normalized to 1. Solving seven of the nine equations to obtain the eight study parameters for  $z_0, z_1, \dots, z_7$  in  $v_3$  and  $\bar{v}_5$  and substituting the solutions into the remaining two equations, two equations in  $v_3$  and  $\bar{v}_5$  named  $E_1$  and  $E_2$  are obtained

$$\begin{aligned}
E_1 : & v_3^4 \bar{v}_5^4 + 3.640783761 v_3^4 \bar{v}_5^3 - 3.788653411 v_3^3 \bar{v}_5^4 - 7.000053530 v_3^4 \bar{v}_5^2 \\
& + 10.71593007 v_3^3 \bar{v}_5^3 + 41.87086614 v_3^2 \bar{v}_5^4 + 3.640783761 v_3^4 \bar{v}_5 - 19.64341956 v_3^2 \bar{v}_5^3 \\
& - 3.788653411 v_3 \bar{v}_5^4 - 0.5952224873 v_3^4 - 10.71593007 v_3^3 \bar{v}_5 - 79.84271214 v_3^2 \bar{v}_5^2 \\
& + 10.71593007 v_3 \bar{v}_5^3 + 11.40205846 \bar{v}_5^4 + 3.788653411 v_3^3 - 19.64341956 v_3^2 \bar{v}_5 \\
& - 23.28420332 \bar{v}_5^3 + 53.83503480 v_3^2 - 10.71593007 v_3 \bar{v}_5 - 131.7802740 \bar{v}_5^2 \\
& + 3.788653411 v_3 - 23.28420332 \bar{v}_5 + 24.96144960 = 0
\end{aligned} \tag{5.16}$$

$$\begin{aligned}
E_2 : & v_3^8 \bar{v}_5^6 - 3.975059020 v_3^8 \bar{v}_5^5 - 9.917459999 v_3^7 \bar{v}_5^6 + 4.782767392 v_3^8 \bar{v}_5^4 \\
& + 10.89653630 v_3^7 - 7.905713714 v_3^6 \bar{v}_5^6 - 2.187051780 v_3^8 \bar{v}_5^3 + 10.76914366 v_3^7 \bar{v}_5^4 \\
& + 11.58607438 v_3^6 \bar{v}_5^5 - 1.756500002 v_3^5 \bar{v}_5^6 + 0.1775892990 v_3^8 \bar{v}_5^2 - 6.718456391 v_3^8 \\
& - 19.63855979 v_3^6 \bar{v}_5^4 - 3.599595703 v_3^5 \bar{v}_5^5 + 5.541460022 v_3^4 \bar{v}_5^6 + 0.1309074494 v_3^8 \bar{v}_5 \\
& - 10.68103759 v_3^7 \bar{v}_5^2 + 29.42980884 v_3^6 \bar{v}_5^3 + 88.38390043 v_3^5 \bar{v}_5^4 + 14.52156887 v_3^4 \bar{v}_5^5 \\
& - 11.11952017 v_3^3 \bar{v}_5^6 - 0.02663720154 v_3^8 + 8.366957525 v_3^7 \bar{v}_5 + 1.744100557 v_3^6 \bar{v}_5^2 \\
& - 11.42375341 v_3^5 \bar{v}_5^3 + 47.03555747 v_3^4 \bar{v}_5^4 + 27.82871185 v_3^3 \bar{v}_5^5 + 23.16294757 v_3^2 \bar{v}_5^6 \\
& - 1.555454321 v_3^7 - 14.97543807 v_3^6 \bar{v}_5 - 65.86121591 v_3^5 \bar{v}_5^2 + 22.54006617 v_3^4 \bar{v}_5^3 \\
& + 85.76873039 v_3^3 \bar{v}_5^4 - 19.01000389 v_3^2 \bar{v}_5^5 - 19.28048017 v_3 \bar{v}_5^6 + 4.289038591 v_3^6 \\
& - 39.78294461 v_3^5 \bar{v}_5 - 55.12245682 v_3^4 \bar{v}_5^2 - 45.28245200 v_3^3 \bar{v}_5^3 + 12.06466530 v_3^2 \bar{v}_5^4 \\
& + 42.32484385 v_3 \bar{v}_5^5 + 8.715773829 \bar{v}_5^6 - 4.399164900 v_3^5 - 61.91885268 v_3^4 \bar{v}_5 \\
& - 206.5453764 v_3^3 \bar{v}_5^2 - 104.7180132 v_3^2 \bar{v}_5^3 + 8.153973623 v_3 \bar{v}_5^4 - 17.97043737 \bar{v}_5^5 \\
& + 7.841437590 v_3^4 - 127.7979408 v_3^3 \bar{v}_5 - 166.3482520 v_3^2 \bar{v}_5^2 - 40.57715498 v_3 \bar{v}_5^3 \\
& - 59.39221935 \bar{v}_5^4 - 2.488637296 v_3^3 - 46.57694731 v_3^2 \bar{v}_5 - 151.3651980 v_3 \bar{v}_5^2 \\
& - 95.64121876 \bar{v}_5^3 + 8.367254171 v_3^3 - 79.64803864 v_3 \bar{v}_5 - 109.6592839 \bar{v}_5^2 \\
& + 0.3550732836 v_3 + 0.2355598536 \bar{v}_5 + 4.481492373 = 0
\end{aligned} \tag{5.17}$$

Using the “resultant” command in Maple to eliminate  $\bar{v}_5$  from Eqs. (5.16) and (5.17), one polynomial equation of degree 56 in  $v_3$  named  $E$  can be derived as follows:

$$\begin{aligned}
E: & (v_3^2 + 1)^6 (3.033362327v_3^4 - 12.05533640v_3^2 + 10.67784416) \\
& (1.87522003v_3^4 - 64.00268390v_3^2 - 387.9596900) \\
& (5.157957061 \times 10^9 v_3^{10} + 1.823061353 \times 10^{20} v_3^9 - 7.297142808 \times 10^{21} v_3^8 \\
& + 1.634647033 \times 10^{22} v_3^7 + 5.885504960 \times 10^{22} v_3^6 - 3.150969451 \times 10^{22} v_3^5 \\
& - 2.671416502 \times 10^{23} v_3^4 + 5.157957061 \times 10^9 v_3^{10} + 1.823061353 \times 10^{20} v_3^9 \\
& - 7.297142808 \times 10^{21} v_3^8 + 1.634647033 \times 10^{22} v_3^7 + 5.885504960 \times 10^{22} v_3^6 \\
& - 3.150969451 \times 10^{22} v_3^5 - 2.671416502 \times 10^{23} v_3^4)^2 (6.60154501 \times 10^8 v_3^{16} \\
& + 2.698070325 \times 10^{18} v_3^{15} - 3.778024642 \times 10^{28} v_3^{14} - 8.52528086 \times 10^{37} v_3^{13} \\
& + 6.145569255 \times 10^{47} v_3^{12} - 4.007107158 \times 10^{49} v_3^{11} + 2.109260812 \times 10^{50} v_3^{10} \\
& + 3.306274920 \times 10^{49} v_3^9 + 5.471487282 \times 10^{50} v_3^8 + 1.795904346 \times 10^{51} v_3^7 \\
& - 1.709576046 \times 10^{50} v_3^6 - 2.604353812 \times 10^{50} v_3^5 - 8.358864852 \times 10^{50} v_3^4 \\
& - 1.755833276 \times 10^{51} v_3^3 + 2.679828670 \times 10^{50} v_3^2 + 2.273726304 \times 10^5 v_3 \\
& - 1.982814399 \times 10^{49}) = 0
\end{aligned} \tag{5.18}$$

The solutions to  $(v_3^2 + 1)^6 = 0$  are  $v_3 = \pm I$  where  $I$  is the unit imaginary number. The corresponding points in  $P^7$  lie on the exceptional generator and have to be cut out of the  $S_6^2$ . The solutions of the polynomial of degree 10 squared are points with coordinate  $(0, 0, 0, 0, 0, 0, 0, 0)$  which do not lie on the  $S_6^2$  and the solutions of polynomials of degree 4 are points which lie on the exceptional 3-space of the  $S_6^2$ . Then the polynomial of degree 16 gives the following 16 solutions:

$$\begin{aligned}
v_3 = & [0.08366283786, 0.3610109062, 1.000000000, 6.521970015, 59.40599134, \\
& 4.132441204 \times 10^9, 5.081725257 \times 10^9, 0.4234204659 + 2.169839731 I, \\
& -0.07511185210 + 1.019253419 I, -6.650597562 \times 10^9 + 3.156689159 \times 10^8 I, \\
& -0.3581658035, -1.0000000001, -1.507896627, -6.650597562 \times 10^9 - 3.156689159 \times 10^8 I, \\
& -0.07511185210 - 1.019253419 I, 0.4234204659 - 2.169839731 I]
\end{aligned} \tag{5.19}$$

Substituting the solutions for  $v_3$  (Eq. (5.19)) back into  $E_1$  and  $E_2$ . The common solutions for  $\bar{v}_5$  with their corresponding  $v_3$  are the solutions desired. Please note only 12 sets of solutions could be obtained whereas the remaining four solutions for  $v_3$  tend to be infinity, such as  $5.081725257 \times 10^9$  as  $\theta_3$  approaches  $180^\circ$ . The remaining four joint angles for the normal 12 sets of solutions can be solved by the other sets of four equations for  $SM_1, SM_2, SM_4$  and  $SM_6$ .

As for the above four particular configurations in which  $v_3$  tends to infinite, there is one set of real solutions: any value of  $\theta_1, \theta_2=0^\circ, \theta_3=180^\circ, \theta_4=\theta_1+180^\circ$  or  $\theta_4=\theta_1-180^\circ, \theta_5=\theta_1-45^\circ$ , and  $\theta_6=180^\circ$ . This set of solutions can be easily verified by observation as

shown in Fig. 5.4(i). This configuration is singular since the joint axes on the platform and the base coincide and the mechanism has 2-DOF. For any given  $\theta$ ,  $\theta_4 = \theta_1 + 180^\circ$  or  $\theta_4 = \theta_1 - 180^\circ$  can take any value. The complex solutions associated with the remaining three particular configurations are omitted in this chapter.

Finally, 13 sets of solutions for the kinematic analysis of the single loop are obtained as listed in Table 5.2.

Table 5.2 Solutions for the 7R SLMMRM (Case  $\theta = -45^\circ$ )

Solutions	$\theta_1(\text{deg})$	$\theta_2(\text{deg})$	$\theta_3(\text{deg})$	$\theta_4(\text{deg})$	$\theta_5(\text{deg})$	$\theta_6(\text{deg})$
Solution 1	-173.94	20.73	9.57	-3.50	-155.43	-45.60
Solution 2	135.00	0.00	90.00	-45.00	-135.00	-90.00
Solution 3	-135.00	0.00	-90.00	45.00	-135.00	-90.00
Solution 4	-4.58	15.74	178.07	-2.65	-70.34	-172.85
Solution 5	-78.35	118.96	-112.90	-145.46	86.69	-119.92
Solution 6	-154.65	73.12	39.70	-14.35	131.21	90.70
Solution 7	-25.16	72.74	-39.41	-165.750	-41.90	90.47
Solution 8	141.39	-94.46	162.57	158.82	156.63	-137.54
Solution 9	-54.49-	163.88+	-106.51-	-127.99+	58.79+	-100.69-
	109.37 <i>I</i>	10.80 <i>I</i>	186.81 <i>I</i>	77.44 <i>I</i>	82.63 <i>I</i>	144.39 <i>I</i>
Solution 10	-54.49+	163.88-	-106.51+	-127.99-	58.79-	-100.69+
	109.37 <i>I</i>	10.80 <i>I</i>	186.81 <i>I</i>	77.44 <i>I</i>	82.63 <i>I</i>	144.39 <i>I</i>
Solution 11	93.40+	-142.30+	167.71+	105.69+	112.78+	-156.36-
	63.96 <i>I</i>	1.68 <i>I</i>	54.09 <i>I</i>	9.87 <i>I</i>	77.66 <i>I</i>	28.62 <i>I</i>
Solution 12	93.40-	-142.30-	167.71-	105.69-	112.78-	-156.36+
	63.96 <i>I</i>	1.68 <i>I</i>	54.10 <i>I</i>	9.87 <i>I</i>	77.66 <i>I</i>	28.62 <i>I</i>
$\theta_1 + 180.00$						
Solution 13	Any value	0.00	180.00	(or $\theta_1$ -180.00)	-45.00	180.00

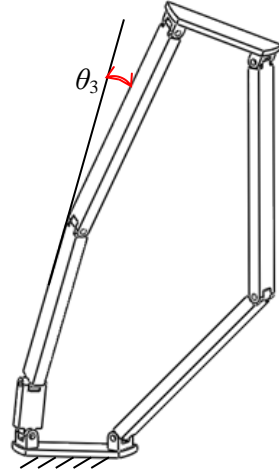
Note: *I* is the imaginary unit

### 5.3 CAD Model and Prototype Verification

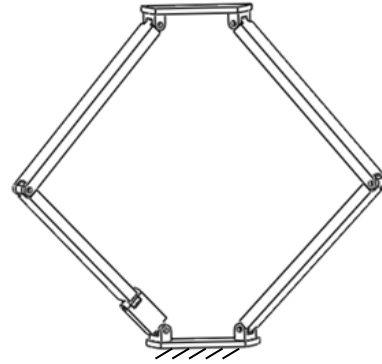
The above real solutions for the kinematic analysis of the 1-DOF 7R SLMMRM can be verified using its CAD model and prototype.

### 5.3.1 CAD Model Configurations for the Real Solutions

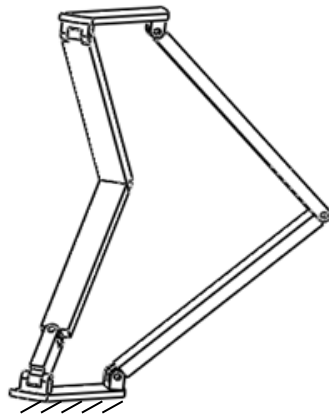
The CAD configurations associated with these real solutions (Table 5.2) are shown in Fig. 5.4.



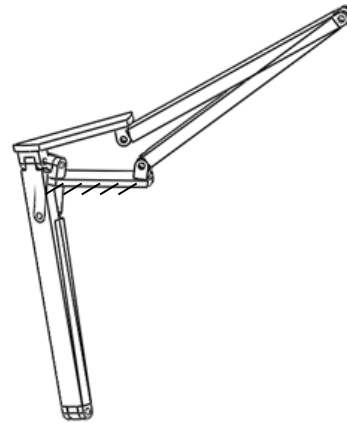
(a) Solution 1:  $\theta_3=9.57^\circ$



(b) Solution 2:  $\theta_3=90.00^\circ$

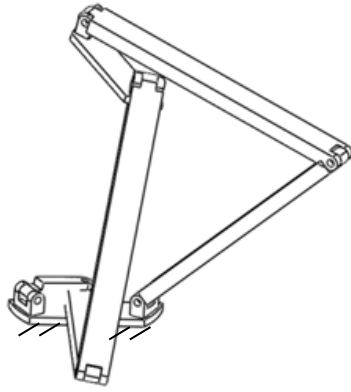


(c) Solution 3:  $\theta_3=-90.00^\circ$

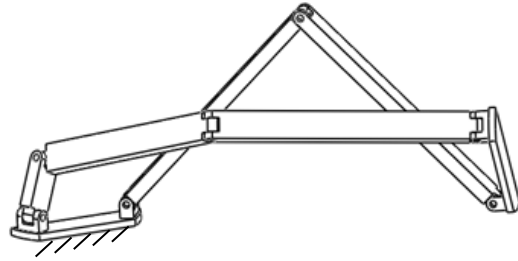


(d) Solution 4:  $\theta_3=178.07^\circ$

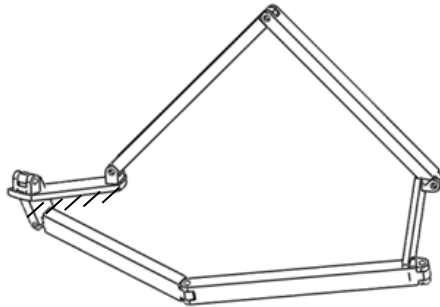
Figure 5.4 CAD configurations corresponding to the real solutions for the 7R SLMMRM (Case  $\theta=-45^\circ$ ) (continued on next page)



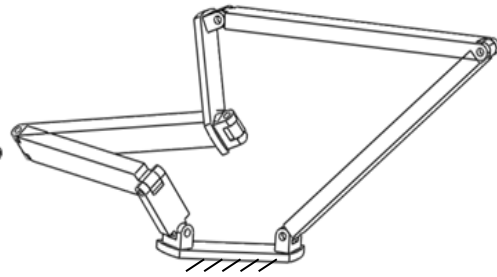
(e) Solution 5:  $\theta_3 = -112.90^\circ$



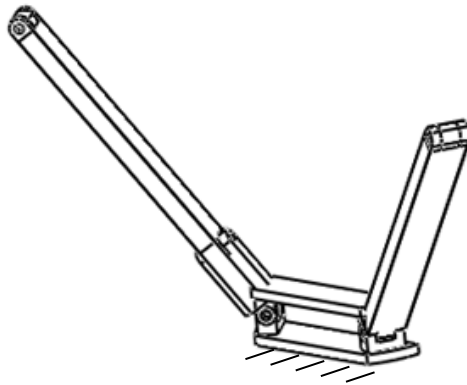
(f) Solution 6:  $\theta_3 = 39.70^\circ$



(g) Solution 7:  $\theta_3 = -39.41^\circ$



(h) Solution 8:  $\theta_3 = 162.57^\circ$



(i) Solution 13:  $\theta_3 = 180.00^\circ$

Figure 5.4 CAD configurations corresponding to the real solutions for the 7R SLMMRM (Case  $\theta = -45^\circ$ )

### 5.3.2 Building Prototype to Verify Real Solutions

A physical prototype has been built to verify the real solutions obtained previously. Figure 5.5 illustrates the achievement of configurations of the prototype corresponding to the real solutions. It is noted that some configuration cannot be continuously generated in practice because of interference between the links, such as configurations (e) and (g) (Figs. 5.5(e) and 5.5(g)).



(a) Solution 1:  $\theta_3=9.57^\circ$



(b) Solution 2:  $\theta_3=90.00^\circ$



(c) Solution 3:  $\theta_3=-90.00^\circ$



(d) Solution 4:  $\theta_3=178.07^\circ$

Figure 5.5 Prototype configurations corresponding to the real solutions for the 7R SLMMRM (Case  $\theta=-45^\circ$ ) (continued on next page)



(e) Solution 5:  $\theta_3 = -112.90^\circ$



(f) Solution 6:  $\theta_3 = 39.70^\circ$



(g) Solution 7:  $\theta_3 = -39.41^\circ$



(h) Solution 8:  $\theta_3 = 162.57^\circ$



(i) Solution 13:  $\theta_3 = 180.00^\circ$

Figure 5.5 Prototype configurations corresponding to the real solutions for the 7R SLMMRM (Case  $\theta = -45^\circ$ )

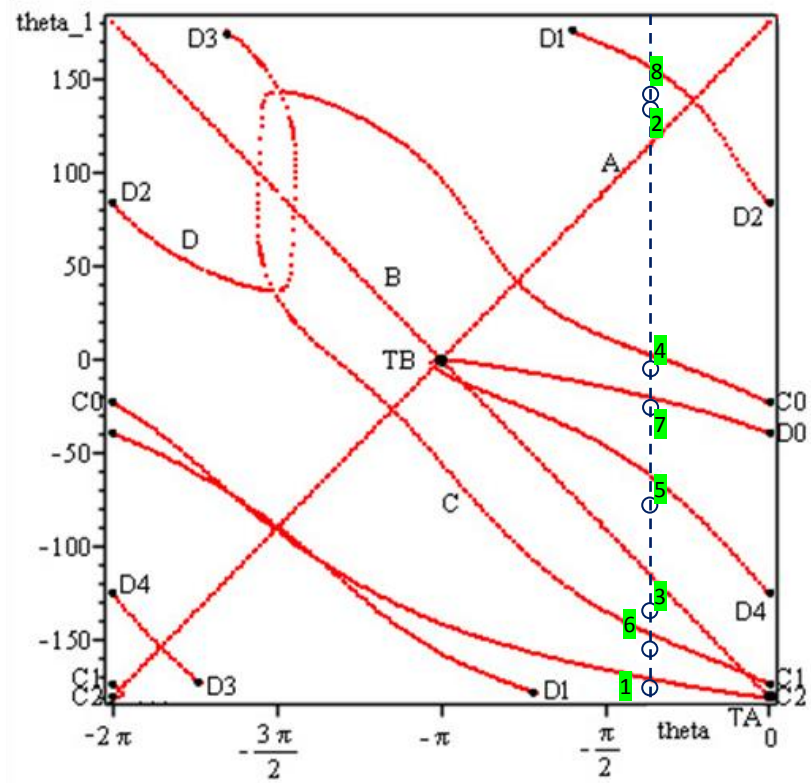
## 5.4 Operation Modes and Transition configurations

As the input angle  $\theta$  changes a series of solutions corresponding to different input angles can be obtained using the numerical method. Then by plotting 200 sets of joint angles against the input angles, the operation modes and transition configurations of the 1-DOF 7R SLMMRM (Fig. 5.6) are illustrated. All the operation modes and transition configurations of the mechanism can be observed from the plotting of angles  $\theta_1$  and  $\theta_3$  against the input angle  $\theta$ . Please note that the singular configuration in which the moving platform and base coincide (see Figs. 5.4(i) and 5.5(i)) is discarded in this section.

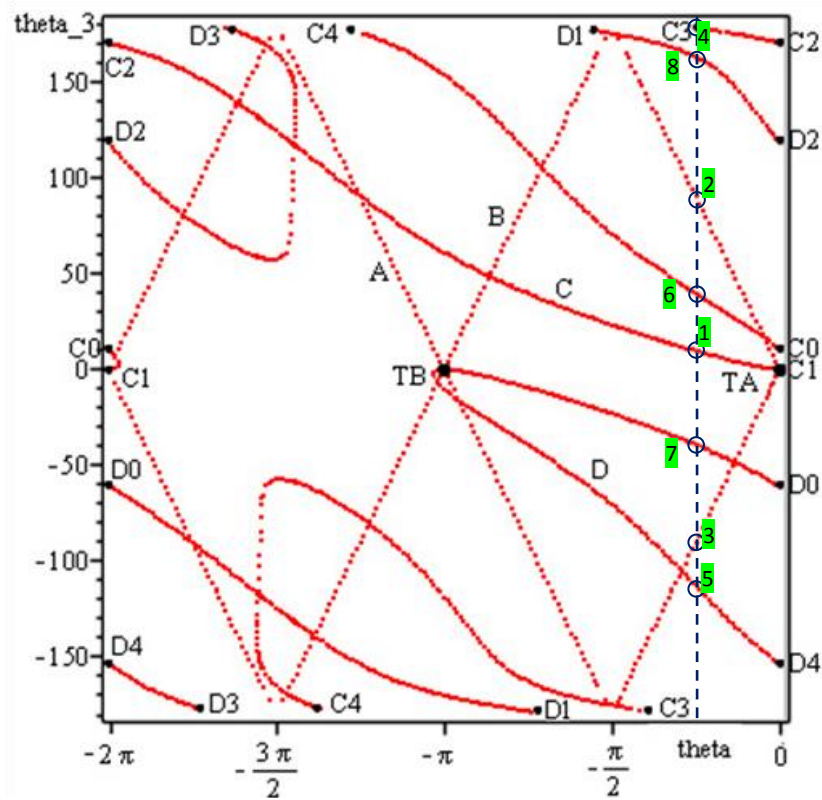
Figure 5.6 shows that there are two straight lines A and B and two closed curves C ( $C_0-C_1-C_2-C_0$  in Fig. 5.6(a) or  $C_0-C_1-C_2-C_3-C_4-C_0$  in Fig. 5.6(b)) and D ( $D_0-D_1-D_2-D_3-D_4-D_0$ ) designating the operations modes. Lines A and B are associated with translation operation mode while the closed curves C and D are associated with two separate 1-DOF planar operation modes: planar mode I and planar mode II. Therefore, the mechanism has three operation modes, not just two operation modes. This can be easily verified by comparing the straight lines and closed curves to their corresponding operation mode in Fig. 5.4. Line A corresponds to Fig. 5.4(b), Line B corresponds to Fig. 5.4(c), closed curve C corresponds to Fig. 5.4(a), and closed curve D corresponds to Fig. 5.4(g). The eight real solutions (solutions Nos.1-8 in Table 5.2) for  $\theta_3$  (or  $\theta_1$ ) under  $\theta=-45^\circ$  are also indicated by the corresponding solution numbers, 1, 2, ..., 8 with shaded background in Fig. 5.6. Among these eight solutions, solution No. 2, solution No. 3, solutions Nos. 1, 4 and 6, and solutions Nos. 5, 7 and 8 fall on line A, line B, curve C and curve D, respectively.

The transition configurations between three operation modes can be analysed. By comparing the two plotting figures, Fig. 5.6(a) and Fig. 5.6(b), two intersecting points TA and TB through which these operation modes pass in both figures are observed, which represent the two transition configurations (Fig. 5.7). The input angles corresponding to the transition configurations are shown in Table 5.3.





(a) Plot of two rotational angles:  $\theta_1$  against input angle  $\theta$



(b) Plot of two rotational angles:  $\theta_3$  against input angle  $\theta$

Figure 5.6 Motion curves of the 7R SLMMRM

Table 5.3 Transition configurations

Transition Configurations	Input angle $\theta$ (deg)	Modes
TA	$0^\circ$	Translational mode & 1-DOF planar mode I (curve C)
TB	$-180^\circ$	Translational mode & 1-DOF planar mode II (curve D)

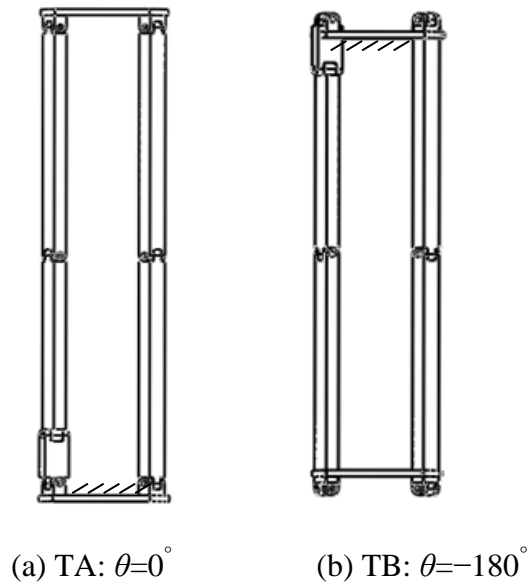
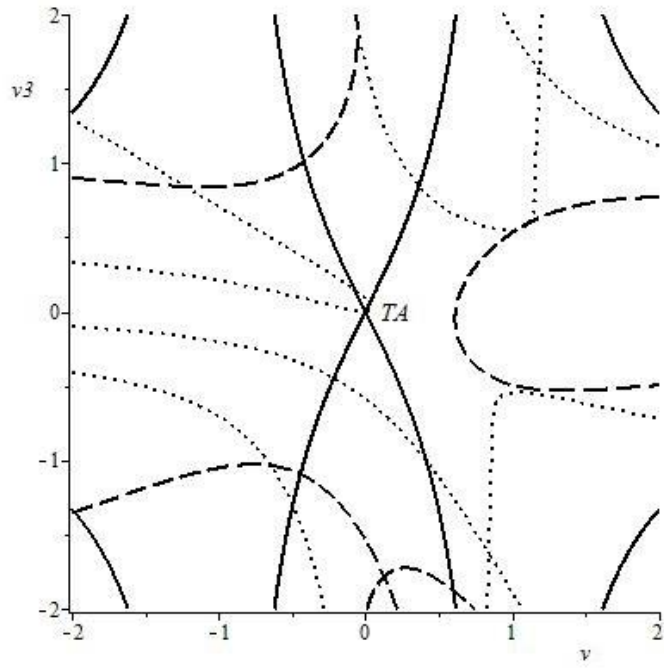


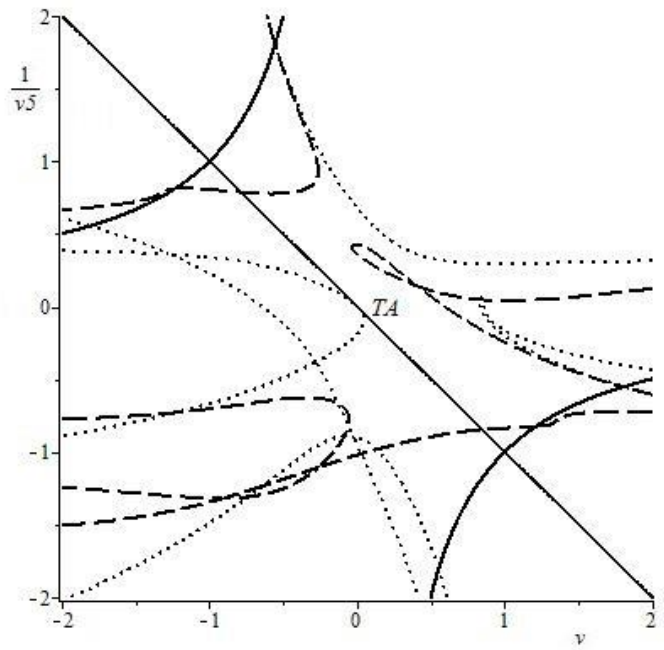
Figure 5.7 Transition configurations of the 7R SLMMRM

## 5.5 Algebraic Approach

In this section, the algebraic approach proposed in [127] is applied to determine the operation modes and transition configurations. Apparently, compared to the numerical method, the algebraic approach enables the operation modes to be represented algebraically.

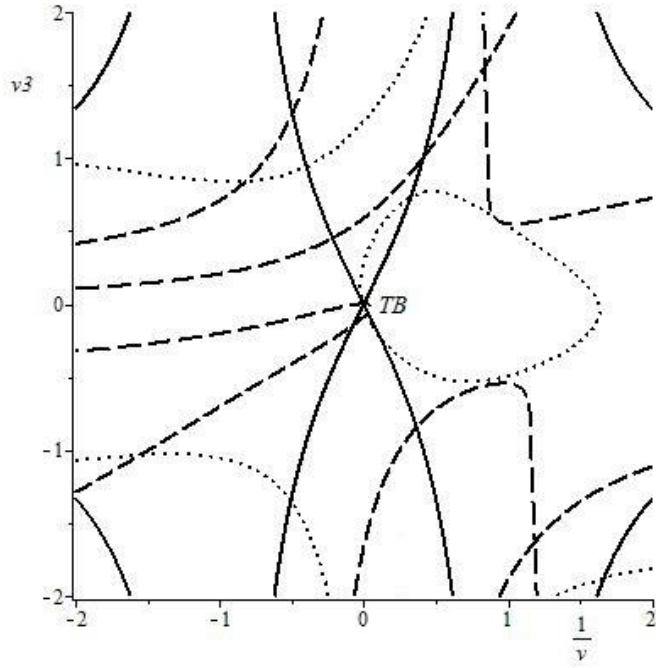


(a)  $v_3$  versus  $v$

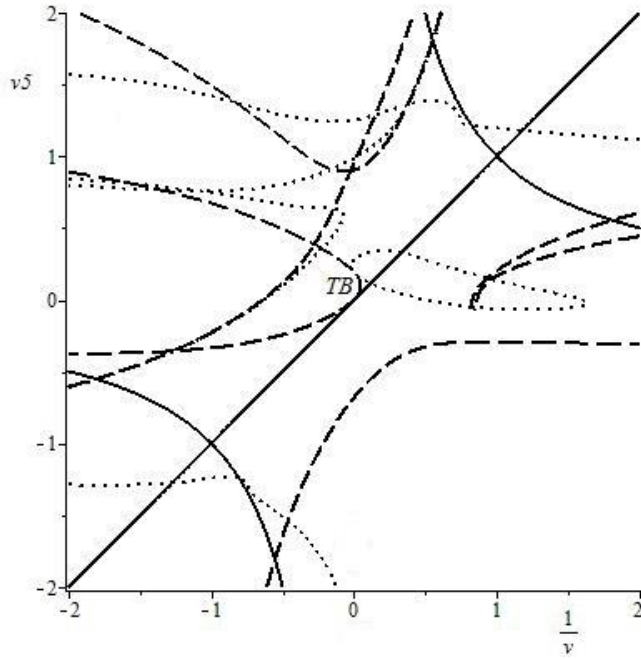


(b)  $1/v_5$  versus  $v$

Figure 5.8 Plots of the input-output equations using the algebraic approach (continued on next page)



(c)  $v_3$  versus  $1/v$



(d)  $v_5$  versus  $1/v$

Figure 5.8 Plots of the input-output equations using the algebraic approach

Without specifying the input angle, the end-effector pose  $A$  and the equations for  $SM_i$  is presented directly in  $\theta$ . Therefore nine equations in  $v_3$  (tangent half of  $\theta_3$ ),  $\bar{v}_5$ , (minus tangent half of  $\theta_5$ ),  $v$  (tangent half of  $\theta$ ) and eight study parameters (Eqs. (5.7)-(5.15)) can be obtained. Two equations in  $v_3$ ,  $\bar{v}_5$  and  $v$  instead of two equations in  $v_3$  and  $\bar{v}_5$  will be obtained after solving seven of the nine equations and substituting the study

parameter solutions into the remaining two equations. Using the “resultant” function in Maple to eliminate  $\bar{v}_5$  (or  $v_3$ ), then the bivariate polynomial in  $v$  and the remaining joint parameter  $v_3$  (or  $\bar{v}_5$ ) can be obtained. Besides some spurious factors there are three factors corresponding to three operation modes. For example, the input-output equation in  $v_3$  and  $v$  is:

$$Q \cdot S_1 \cdot S_2 \cdot S_3 = 0 \quad (5.20)$$

where  $Q$  is a spurious factor.  $S_1$  is the input-output relation corresponding to the translational mode while  $S_2$  and  $S_3$  represent the two general planar modes, respectively (see the Appendix II for the detailed expressions).

Then the input-output relation in  $v_3$  and  $v$  (Fig. 5.8(a)) can be plotted which shows three operation modes along with one transition configuration. The solid curve corresponds to the translational mode, the dotted curve corresponds to the planar mode I and the dashed curve corresponds to planar mode II.

The numerical method is still involved in this chapter even though it is not as simple or effective as the algebraic approach since it indicates all of the results directly and clearly. The plots for the input-output angles in Fig. 5.6 show that there are two transition configurations: (a) the input angle  $\theta=0^\circ$ , the revolute angles  $\theta_3=0^\circ$  and  $\theta_5=180^\circ$ ; (b) the input angle  $\theta=-180^\circ$ , the revolute angles  $\theta_3=0^\circ$  and  $\theta_5=0^\circ$ . When the input angle  $\theta=-180^\circ$ ,  $v$  tends to be infinity. Therefore the second transition configuration cannot be seen directly from the plot of the input-output relationship in  $v$  and  $v_3$  (or  $v_5$ , tangent half of  $\theta_5$ ) in Fig. 5.8(a) using the algebraic approach. Then the reciprocal of variables to plot the relations in  $v$  and  $1/v_5$ ,  $1/v$  and  $v_3$  as well as the relation  $1/v$  and  $v_5$  (Fig. 5.8) have to be used so that all transition configurations can be observed. In Fig. 5.8, the transition configuration between the translation mode and planar mode I is TA and the translation mode and planar mode II are transited at TB. It has been shown that the algebraic analysis results are the same as the numerical ones shown in Section 4.

## 5.6 Summary

This chapter has presented a novel 1-DOF 7R SLMMRM based on the Sarrus linkage. The kinematics analysis of the novel 7R SLMMRM has been implemented. Firstly, applying the explication algorithm to obtain its constraint equations, then using numerical method to produce a set of solutions for the 1-DOF 7R SLMMRM with a

given example and the real solutions were verified through both a CAD model and a prototype of the mechanism. In addition, both the numerical method and algebraic approach have been applied to obtain the operation modes and transition configurations which produce the same results. It turns out that this mechanism has three operation modes: translational mode and two 1-DOF planar modes and two transition configurations where the mechanism can switch from one operation mode to another.

On one hand, the 7R SLMMRM is a non-overconstrained system, and on the other hand, it can switch from one mode to another without disassembly and without using additional actuator which can help develop energy-efficient reconfigurable mechanisms. The work presented in this chapter verify that the type synthesis method of 7J single-loop reconfigurable mechanisms with three or more operation modes proposed in Chapter 4 is effective. Meanwhile, the kinematic mapping method is functional to complete the kinematic analysis of SLMMRMs. It encourages the design and analysis of new mechanical systems with multiple operation modes.

## **Chapter 6 – Design and Analysis of a New 7R Single-Loop Mechanism with 4R, 6R and 7R Operation Modes Based on Line and Plane Symmetrical Bricard Linkage**

The single-loop multi-mode reconfigurable mechanisms (SLMMRMs) that have been proposed and analysed may have many operation modes, which can be classified into the following classes:

- a) Mechanisms which have the same number of effective joints in all the operation modes, such as those with two 4-joint modes and those with two 5-joint modes [55].
- b) Mechanisms which have two different numbers of effective joints in all the operation modes, such as mechanisms with 7-joint mode(s) and 4-joint mode(s) [127,128], or 7-joint mode(s) and 5-joint mode(s) [110,129] or 6-joint mode(s) and 4-joint mode(s) [49,50].

This chapter presents a new 7R SLMMRM using the third method proposed in Chapter 4 by appropriately inserting an R joint into an overconstrained Bricard 6R linkage which aims to achieve a single-loop reconfigurable mechanism with three operation modes and also leads to a mechanism with more different numbers of effective joints in all operation modes. The structure of this chapter is as follows: the first section shows how to construct the 7R SLMMRM, then its kinematic analysis is implemented to find all the operation modes of the new 7R SLMMRM with the transition configurations among the motion patterns also being identified. Finally, the CAD model and physical prototype configurations for verifying the results of the kinematic analysis are given and conclusions are drawn.

### **6.1 Design of a Novel 7R SLMMRM**

A typical Bricard 6R linkage is first reviewed [50]. A new 7R SLMMRM is then obtained by inserting an R joint into the overconstrained Bricard 6R linkage.

#### ***6.1.1 Bricard 6R Linkage***

A lot of works has focused on the application of overconstrained Bricard 6R linkages as deployable structures. Many such deployable structures have multi-furcations which offer the possibility of designing reconfigurable mechanisms. In Chapter 1 several

classes of Bricard 6R linkages are investigated and in Chapter 4 the conditions and corresponding operation modes of line and planar symmetrical 6R linkages were presented. Four cases can be classified depending on their design parameters leading to the fact that in some cases the 6R mechanisms have two or three operation modes. According to the Bricard linkage case I mentioned in Chapter 4, a CAD model of the Bricard 6R linkage with Bricard mode and 4R spherical mode was developed as shown in the Fig. 6.1(a) with its parameters given in Table 6.1. This is used to construct the new 7R SLMMRM in the next section.

Table 6.1 Parameters for the Bricard 6R linkage

	$a_i$	$d_i$	$\alpha_i$ (deg)
1	122.47	0.00	90.00
2	0.00	324.04	-75.52
3	122.47	-324.04	-90.00
4	122.47	0.00	90.00
5	0.00	324.04	-75.52
6	122.47	-324.04	-90.00

The spherical 4R and Bricard 6R operation modes of this overconstrained Bricard 6R linkage are as shown in Figs. 6.1(b) and 6.1(c). Since it is still an overconstrained mechanism, one R joint can be inserted into the Bricard 6R linkage to construct a non-overconstrained mechanism.

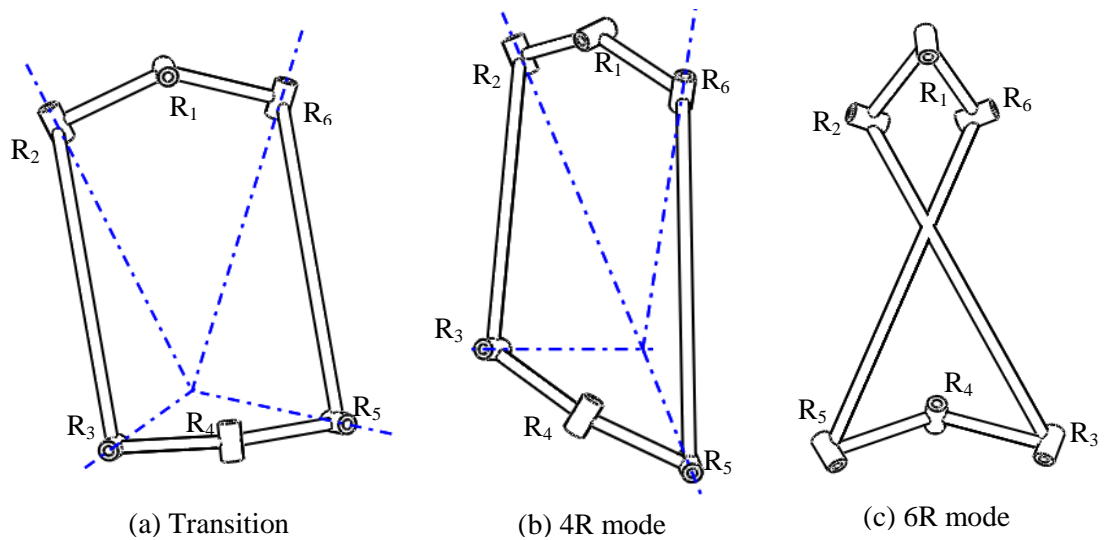


Figure 6.1 Bricard 6R linkage



### 6.1.2 A New 7R SLMMRM

In order to obtain a new 7R SLMMRM, the extra R joint cannot be added arbitrarily. It is added between the second and the third R joints in the original Bricard 6R linkage at its transition configuration. In this configuration, the second and third R joints are disconnected and the new R joint is placed between them such that the axis of the new R joint is on the symmetrical plane of the second and third R joints, therefore the parameters for the new 7R mechanism satisfy:

$$a_1 = a_4 = a_5 = a_7, a_2 = a_3, a_6 = 0 \quad (6.1)$$

$$\alpha_1 = \alpha_5 = \pi / 2, \alpha_4 = \alpha_7 = -\pi / 2, \alpha_2 = -\alpha_3 \quad (6.2)$$

$$d_1 = d_3 = d_5 = 0, -d_2 = d_4, -d_6 = d_7 \quad (6.3)$$

The 7R SLMMRM are then reconnected as shown in Fig. 6.2(a). Note that the axis of the new added R joint does not intersect at the same point with the other four inserted axes. The coordinate frames for the 7R SLMMRM are built in the sequence as shown in Fig. 6.2(b).

Table 6.2 Parameters for the 7R SLMMRM

	$a_i$	$d_i$	$\alpha_i$ (deg)
1	122.47	0.00	90.00
2	259.81	111.91	− 45.00
3	259.81	0.00	45.00
4	122.47	− 111.91	− 90.00
5	122.47	0.00	90.00
6	0.00	324.04	− 75.52
7	122.47	− 324.04	− 90.00

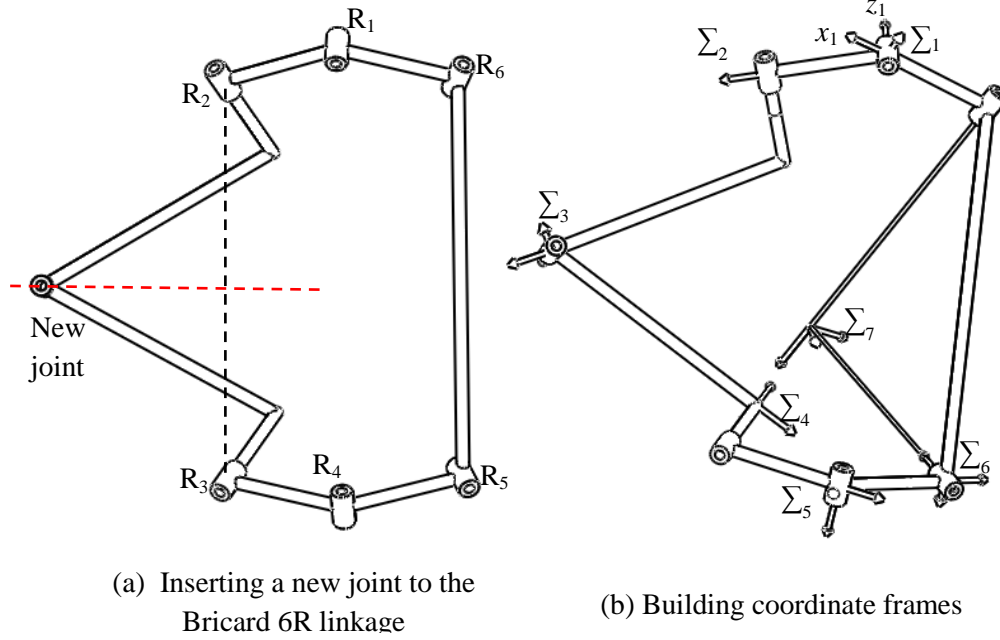


Figure 6.2 A new 7R SLMMRM

The parameters for the new 7R SLMMRM are listed in Table 6.2. It is apparent that the 7R SLMMRM will keep the two operation modes belonging to the original Bricard 6R linkage. Further kinematic analysis for the 7R SLMMRM needs to be carried out to verify the other operation modes and investigate their transition configurations among these operation modes.

## 6.2 Kinematic Analysis of the 7R SLMMRM

For the convenience of this analysis, the 7R SLMMRM is decomposed into a 3R chain and a 4R chain at the origin of  $\Sigma_4$ . Their equations can be obtained from Tables 3.1 and 3.2. In order to avoid the failure of the analysis, two sets of four equations  $T(v_1)$  and  $T(v_2)$  for the 3R chain and one set of four equations  $T(v_6v_7)$  for the 4R chain are selected where  $T(v_6v_7)$  can be derived from  $T(v_3v_4)$  by making some changes to the corresponding parameters. These equations in  $v_1$  and  $v_6$  and  $v_7$  together with the equation for Study quadric (Eq. (2.33)) are computed. Firstly seven of the nine equations are solved to give the eight study parameters in  $v_6$ ,  $v_7$  and  $v_1$ , which are substituted into the remaining two equations, thus two equations in  $v_6$ ,  $v_7$  and  $v_1$  are obtained. Using the “resultant” function in Maple to eliminate  $v_6$ , then a bivariate polynomial in  $v_7$  and  $v_1$  is generated. There are three factors corresponding to three operation modes along with a spurious factor ( $Q_1$ ):

$$Q_1 \cdot S_{11} \cdot S_{12} \cdot S_{13} = 0 \quad (6.4)$$

where  $S_{11}$  is the equation corresponding to the 4R mode, and  $S_{12}$  and  $S_{13}$  represent the 6R mode and 7R mode, respectively.

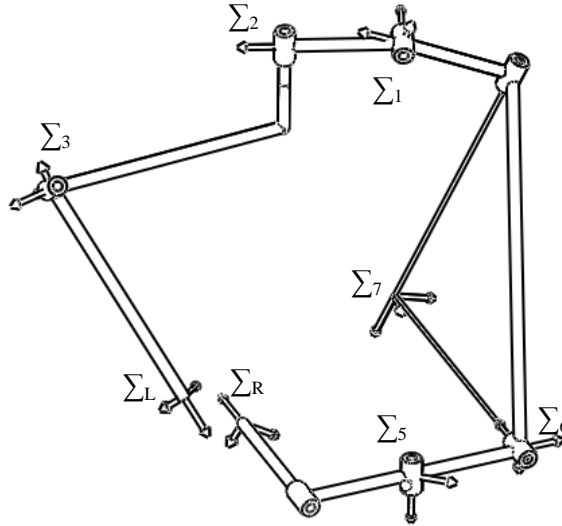


Figure 6.3 Decomposition of the 7R SLMMRM into a 3R chain and a 4R chain

Similarly, the bivariate polynomial in  $v_7$  and  $v_2$  can be obtained:

$$Q_2 \cdot S_{21} \cdot S_{22} \cdot S_{23} = 0 \quad (6.5)$$

where  $Q_2$  is also a spurious factor.  $S_{21}$  is the equation corresponding to the 4R mode and  $S_{22}$  and  $S_{23}$  represent the 6R mode and 7R mode, respectively. Further research has been undertaken on the mode equations since the existence of independent motion-loops can be checked from the CAD model; for example, there are two 6R modes for the 7R mechanism.

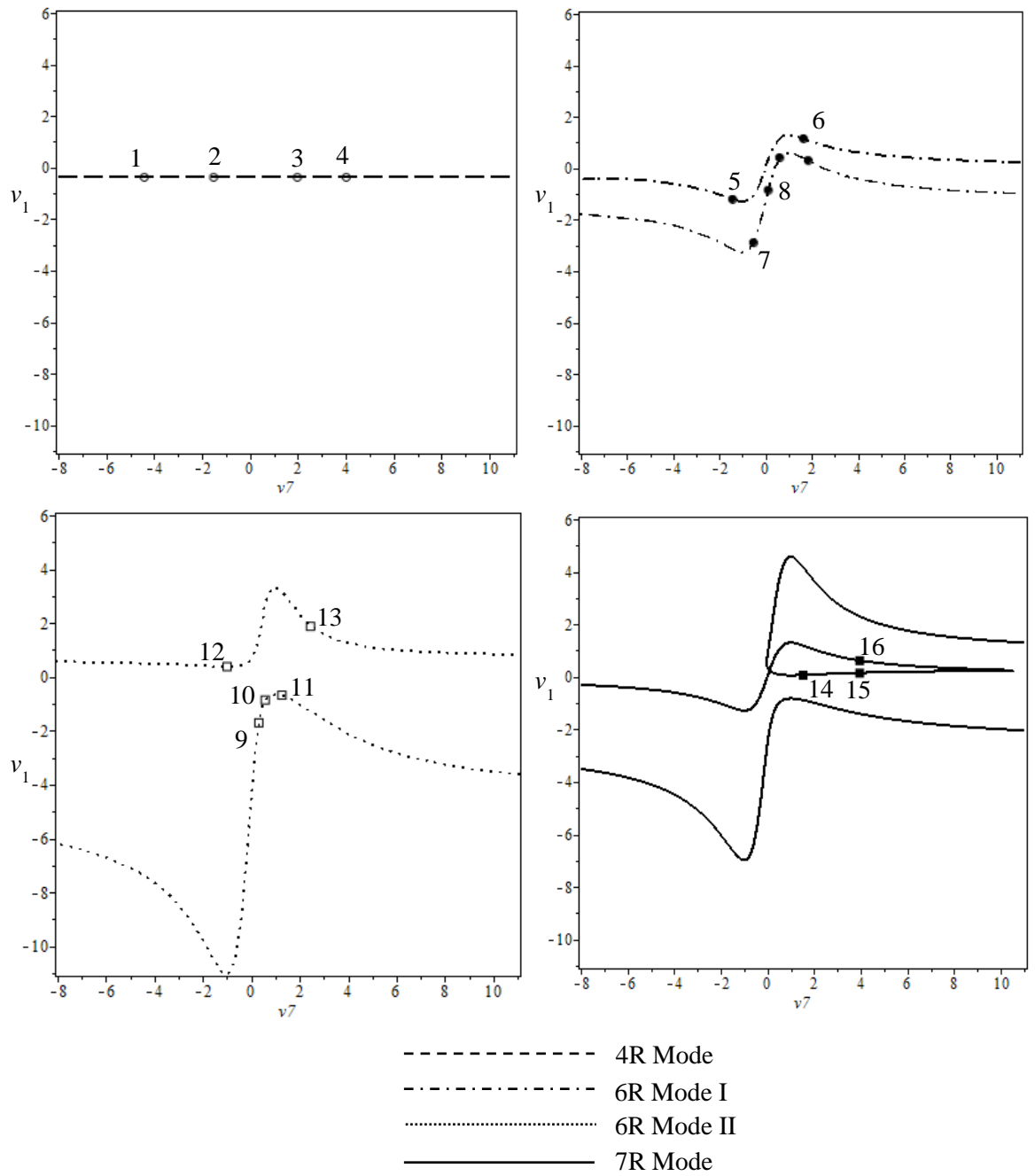


Figure 6.4 Motion curves of  $v_7$  against  $v_1$  for the 7R SLMMRM

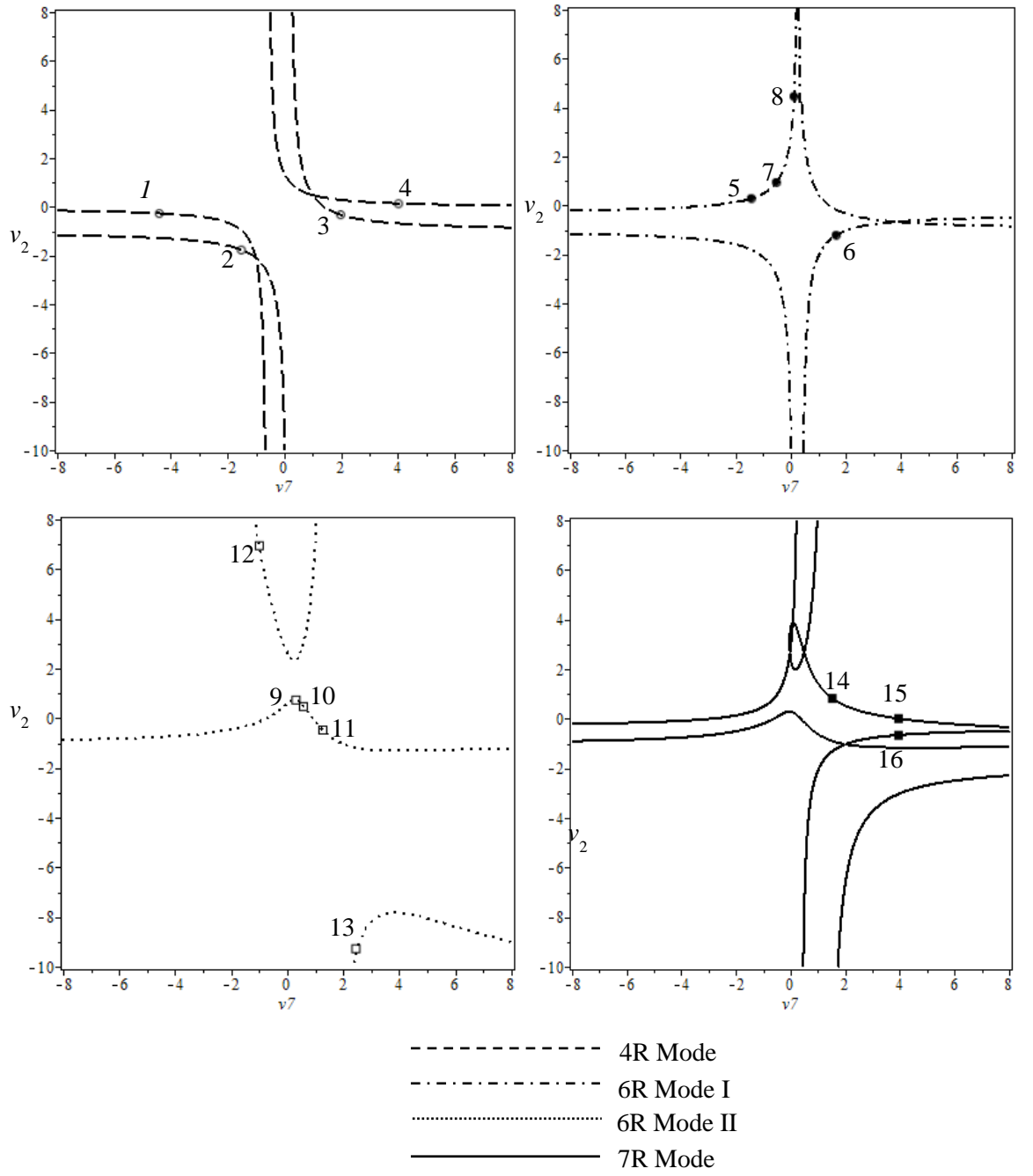


Figure 6.5 Motion curves of  $v_7$  against  $v_2$  for the 7R SLMMRM

The motion curves in  $v_7$  against  $v_1$  and  $v_7$  against  $v_2$  are plotted as shown in Figs. 6.4 and 6.5 which highlight the operation modes. The dashed curve corresponds to the 4R mode; the dashed and dotted curve corresponds to the 6R mode I and the dotted curve corresponds to the 6R mode II; the solid curve corresponds to the 7R mode.

### 6.3 Configuration Verification

In order to verify the motion curves, several CAD model configurations in different modes have been created. Furthermore, the prototype for the 7R mechanism is also built to verify the configurations and the operation modes.

#### 6.3.1 CAD Model Configurations for Verification

The angles of  $\theta_7$ ,  $\theta_2$  and  $\theta_1$  are listed in Table 6.3 along with their half tangents  $v_7$ ,  $v_2$  and  $v_1$  which correspond to the CAD configurations shown in Fig. 6.6. It turns out that all of these are on the corresponding motion curves (16 points) as shown in Figs. 6.4 and 6.5, where the configurations in the 4R mode are marked by circles, the configurations in the 6R mode I are marked by solid circles, the configurations in the 6R mode II are marked by squares and the configurations in the 7R mode are marked by solid squares.

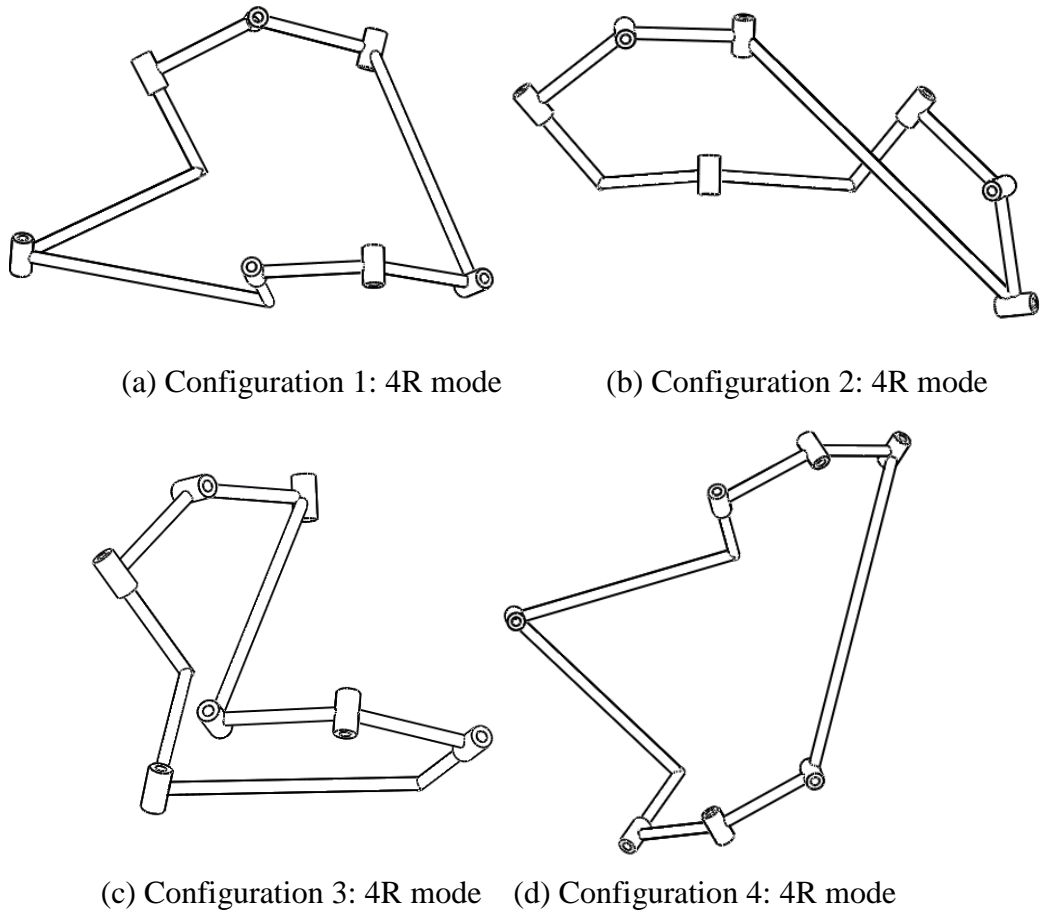
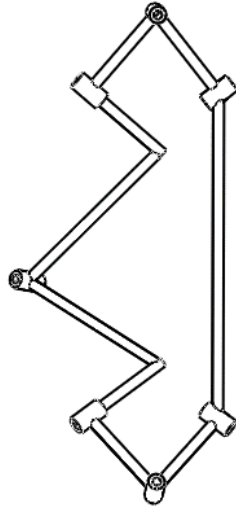
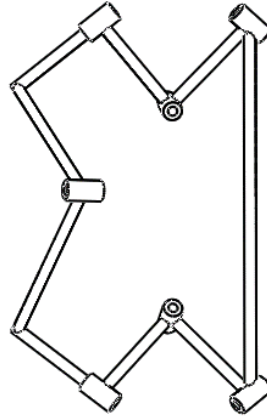


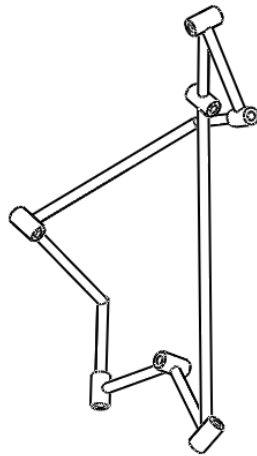
Figure 6.6 CAD configurations corresponding to different operation modes (continued on next page)



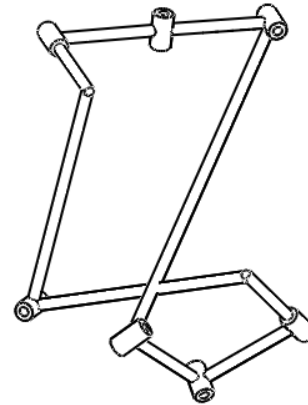
(e) Configuration 5: 6R mode I



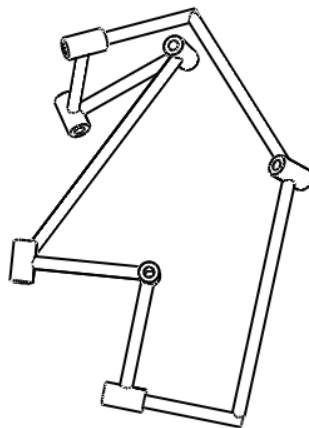
(f) Configuration 6: 6R mode I



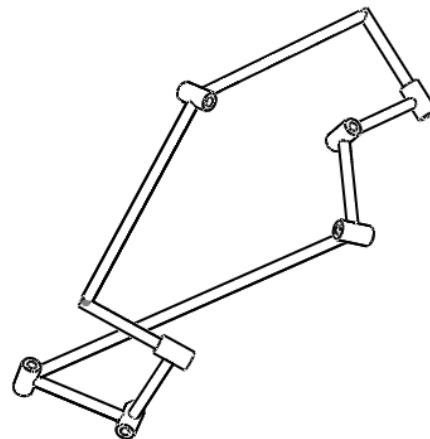
(g) Configuration 7: 6R mode I



(h) Configuration 8: 6R mode I

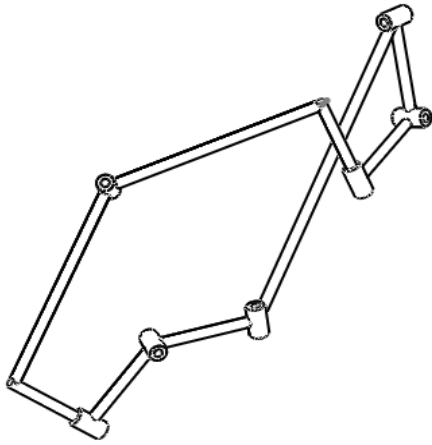


(i) Configuration 9: 6R mode II

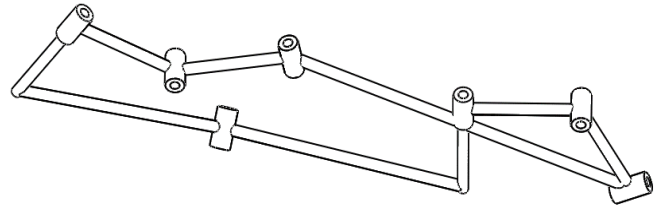


(j) Configuration 10: 6R mode II

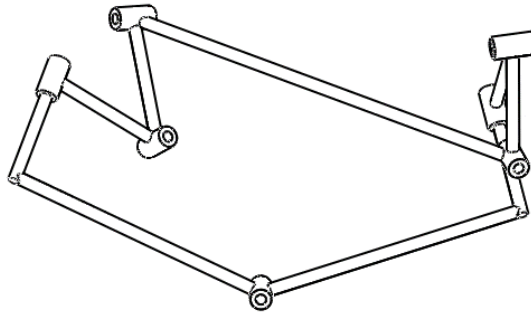
Figure 6.6 CAD configurations corresponding to different operation modes (continued on next page)



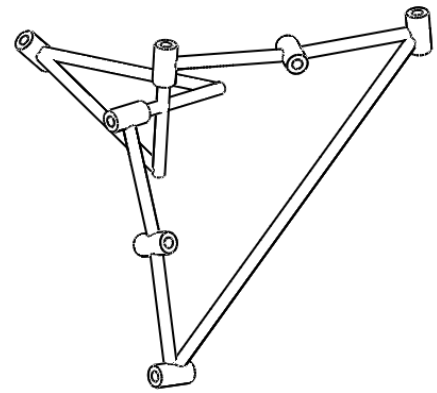
(k) Configuration 11: 6R mode II



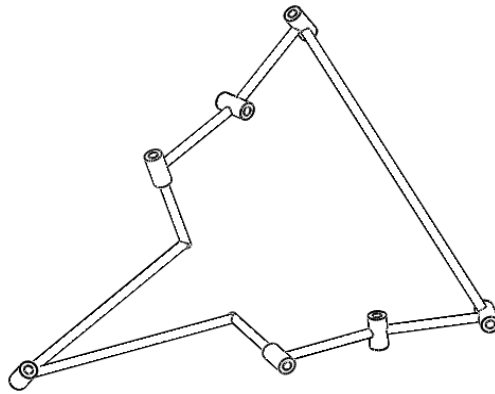
(l) Configuration 12: 6R mode II



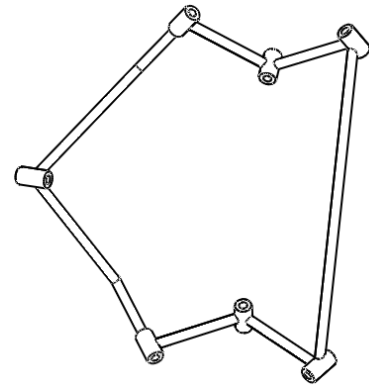
(m) Configuration 13: 6R mode II



(n) Configuration 14: 7R mode



(o) Configuration 15: 7R mode



(p) Configuration 16: 7R mode

Figure 6.6 CAD configurations corresponding to different operation modes



Table 6.3 Examples of configurations in different operation modes

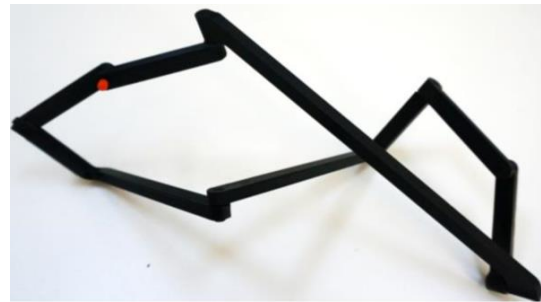
	No.	$\theta_7$ (deg)	$\theta_2$ (deg)	$\theta_1$ (deg)	$v_7$	$v_2$	$v_1$
4R mode	a	-154.46	-31.13	-41.41	-4.41	-0.28	-0.38
	b	-113.28	-121.13	-41.41	-1.52	-1.77	-0.38
	c	126.34	-36.51	-41.41	1.98	-0.33	-0.38
	d	152.04	14.35	-41.41	3.94	0.13	-0.38
6R mode I	e	-109.83	30.94	-101.06	-1.42	0.28	-1.21
	f	117.57	-101.66	97.71	1.65	-1.2	1.144
	g	-54.58	86.14	-141.96	-0.52	0.93	-2.90
	h	13.87	154.64	-81.30	0.12	4.44	-0.86
6R mode II	i	34.85	72.29	-119.20	0.31	0.73	-1.70
	j	59.94	50.38	-81.34	0.58	0.47	-0.86
	k	103.56	-50.86	-68.33	1.27	-0.48	-0.68
	l	-89.83	163.61	41.83	-0.99	6.94	0.38
	m	135.56	67.70	123.93	2.45	0.11	1.88
7R mode	n	113.50	78.64	6.93	1.53	0.82	0.06
	o	151.53	0.53	16.20	3.94	0.0046	0.14
	p	151.61	-67.62	63.07	3.95	-0.67	0.61

### 6.3.2 Prototype for the New 7R SLMMRM

The prototype configurations corresponding to CAD models in Fig. 6.6 and Table 6.3 are shown in Fig. 6.7 in the same order. Figure 6.7(n) cannot reach the configuration corresponding to the exact solution because of the practical interference among the links. The prototype can also be used to verify the operation modes.



(a) Configuration 1: 4R mode



(b) Configuration 2: 4R mode

Figure 6.7 CAD configurations corresponding to different operation modes (continued)



(c) Configuration 3: 4R mode



(d) Configuration 4: 4R mode



(e) Configuration 5: 6R mode I



(f) Configuration 6: 6R mode I



(g) Configuration 7: 6R mode I



(h) Configuration 8: 6R mode I

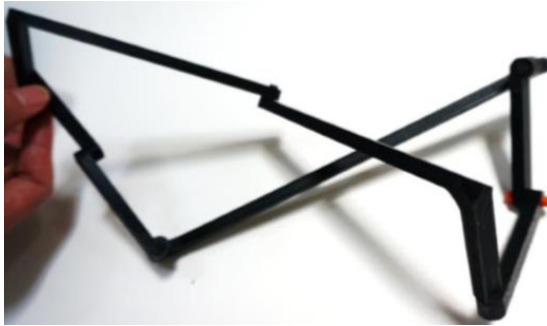
Figure 6.7 Prototype configurations corresponding to different operation modes  
(continued on next page)



(i) Configuration 9: 6R mode II



(j) Configuration 10: 6R mode II



(k) Configuration 11: 6R mode II



(l) Configuration 12: 6R mode II

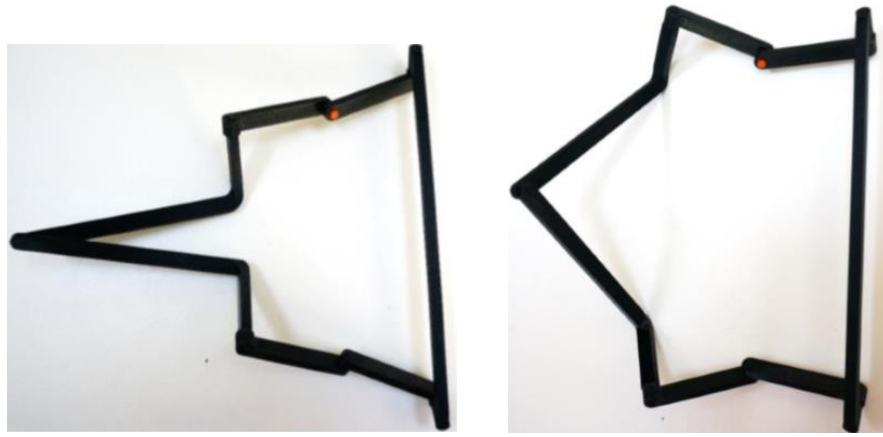


(m) Configuration 13: 6R mode II



(n) Configuration 14: 7R mode

Figure 6.7 Prototype configurations corresponding to different operation modes  
(continued on next page)



(o) Configuration 15: 7R mode

(p) Configuration 16: 7R mode

Figure 6.7 Prototype configurations corresponding to different operation modes

#### 6.4 Transition Configurations

With the help of these motion equations  $S_{ij} (i(j)=1, 2, 3)$ , the configurations where the several modes transit can be identified. Solving the equations  $S_{11}=0, S_{12}=0$  (equations for the 4R mode and 6R modes), a list of solutions for  $[v_7, v_1]$  can be produced. Calculating the equations  $S_{21}=0, S_{22}=0$  (equations for the 4R mode and 6R modes), a list of solutions for  $[v_7, v_2]$  can be also generated. Therefore the common solutions for  $v_7$  and its corresponding  $v_1$  and  $v_2$  are the transition configurations between the 4R mode and 6R modes. Using the same process the transition configurations between the 4R mode and 7R mode as well as the transition configurations between the 6R modes and 7R mode can be obtained. These transition configurations are shown in Table 6.4 and they are plotted onto the motion curves as highlighted in Fig. 6.8 where the figures on  $v_1$  and  $v_2$  against  $1/v_7$  are also displayed to show one transition point with a large  $v_7$ . The corresponding CAD models of the transition configurations are shown in Fig. 6.9.

Table 6.4 Transition configurations

Transition configurations	$\theta_7$ (deg)	$\theta_2$ (deg)	$\theta_1$ (deg)	Associated modes
T1	-162.87	-22.21	-41.41	4R mode & 6R mode I & 7R mode
T2	-17.02	123.75	-41.41	
T3	29.21	169.97	-41.41	4R Mode & 6R mode I
T4	150.79	-68.43	-41.41	
T5	-1.82	138.96	66.58	6R mode II & 7R mode
T6	-178.18	-92.35	66.58	

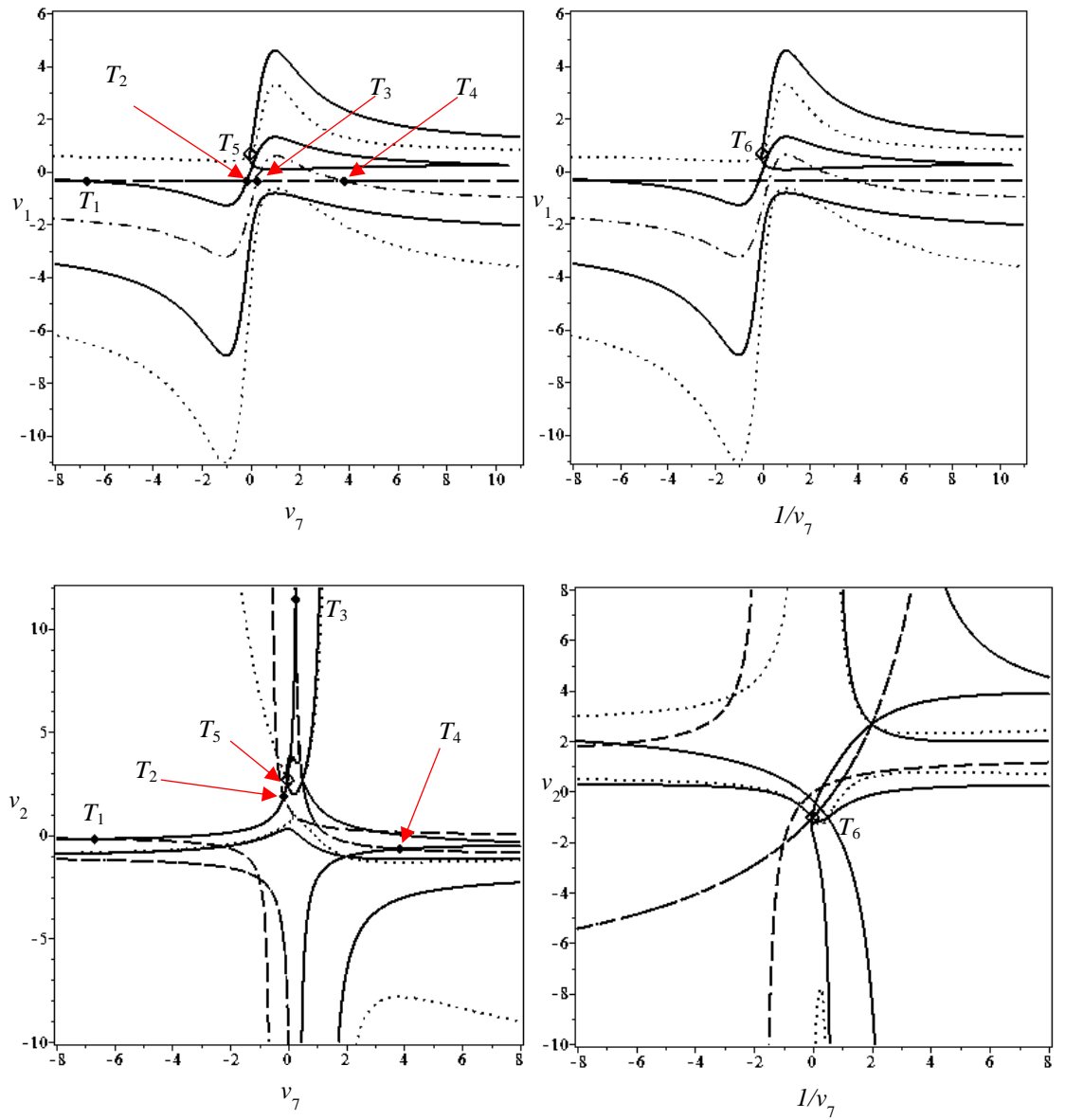
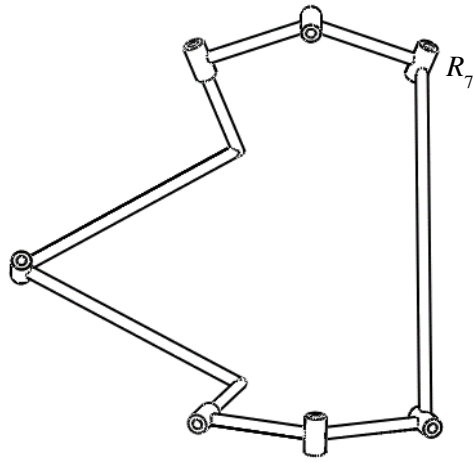
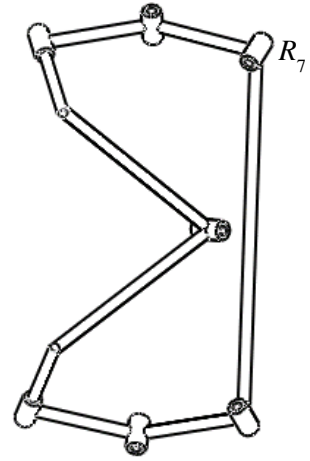


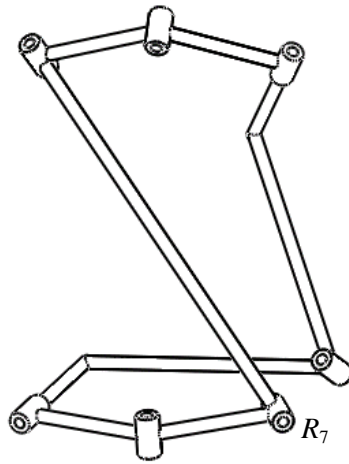
Figure 6.8 Transition configurations among different operation modes



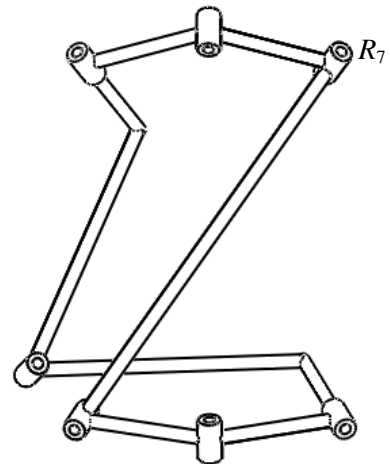
(a) T1: transition configuration one



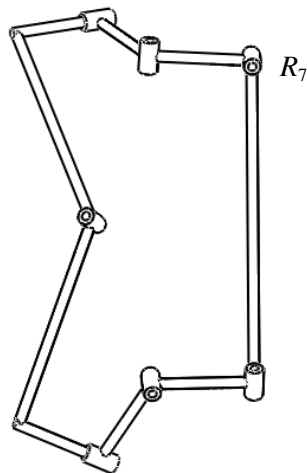
(b) T2: transition configuration two



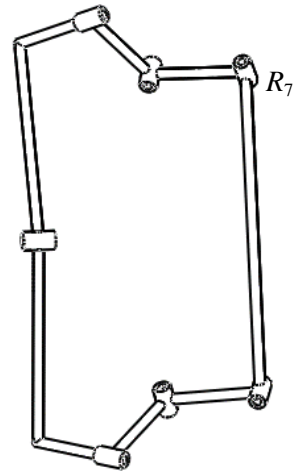
(c) T3: transition configuration three



(d) T4: transition configuration four



(e) T5: transition configuration five



(f) T6: transition configuration six

Figure 6.9 Transition configurations among different operation modes

## 6.5 A New 6R Overconstrained Mechanism as a By-Product

From the results in Figs. 6.6(e)-6.6(m), it can be observed that there are two constant values for  $\theta_3$  in the 6R modes. In addition to the constant  $\theta_3 = -120^\circ$  (as shown in Figs. 6.6(e)-(h)), another constant  $\theta_3 = 45.16^\circ$  measured from the CAD model also exists as shown in Figs. 6.6(i)-6.6(m), that is 6R mode II; In this mode, the new 7R SLMMRM is in fact a new overconstrained 6R mechanism where  $R_1, R_2, R_4, R_5, R_6, R_7$  are active and  $R_3$  is the automatically locked. Its parameters are as shown in Table 6.5.

Table 6.5 The parameters for the new 6R overconstrained mechanism

	$a_i$	$d_i$	$\alpha_i$ (deg)
1	122.47	0.00	-90.00
2	0.00	771.60	-31.51
3	122.47	-771.60	-90.00
4	122.47	0.00	-90.00
5	0.00	324.04	-75.52
6	122.47	-324.04	-90.00

## 6.6 Summary

This chapter has proposed a novel 7R SLMMRM based on an overconstrained Bricard linkage, another successful case to construct 7R single-loop reconfigurable mechanisms with three or more operation modes using the method proposed in Chapter 4. The kinematic analysis of it has shown that the 7R SLMMRM has four operation modes: one 4R, two 6R and one 7R modes and the transition configurations have also been identified. Meanwhile, the theoretical results have been verified using its CAD model and a physical prototype in different operation modes. Moreover, the proposed mechanism in one of its 6R modes has in fact been identified as a new overconstrained 6R mechanism.

As with other SLMMRMs, the new 7R SLMMRM has the advantage of transiting into different modes without disconnecting and reassembly and does not require additional actuators. Furthermore, the 7R SLMMRM has four operation modes with three different numbers of effective links (joints).

## Chapter 7 – Conclusions

### 7.1 General Conclusions

The dissertation is mainly devoted to the design of new SLMMRMs that have more than two specified operation modes and their kinematic analysis using effective algebraic geometry methods.

In addition to the introduction of several existing classes of reconfigurable mechanisms in Chapter 1, a review of single-loop overconstrained mechanisms (SLOMs) is also completed and forms the foundation to construct new MMRMs. Moreover, in Chapter 2 several mathematical tools for the kinematic analysis of mechanisms have been revisited. The kinematic mapping method in conjunction with the numerical and algebraic algorithms has been found to be very effective and have been adopted and developed to deal with the kinematic analysis of SLMMRMs.

In Chapter 3, the basic serial chains used as compositional units to construct closed-loop (or parallel) mechanisms are systematically listed and their constraint equations are derived employing the explicitation and implicitization algorithms based on the kinematic mapping method. The constraint equations from the implicitization algorithms are analysed and selected according to the linear algebra method. Following the above work in the kinematic analysis of mechanisms, the constraint equations for a mechanism from the base to the platform can be integrated via a developed MAPLE program that unifies the transformations in the base and platform to simple serial kinematic chains (legs) of a mechanism.

There have been different methods used to design SLMMRMs, such as the method for synthesizing single-DOF single-loop mechanisms with two specified operation modes and the method for designing multi-mode single-loop reconfigurable mechanisms with variable DOFs. Chapter 4 presents three methods to construct 7J single-loop reconfigurable mechanisms with three or more operation modes such that a large number of this kind of mechanisms can be obtained. Three new classes of 7J single-loop reconfigurable mechanisms with three or more operation modes are obtained from the first method. Examples to construct 7R single-loop reconfigurable mechanisms with three or more operation modes using the second method are given to show the potential to generate these mechanisms based on two same SLOMs.

In Chapters 5 and 6, the design and kinematic analysis of two typical 7R SLMMRMs obtained from the third method are carried out. SLMMRMs can be classified into



several kinds depending on their active joint numbers in different operation modes. The 7R SLMMRM in Chapter 5 is initially analysed using the numerical method and then the algebraic method which both illustrate that the mechanism has two types of operation modes including a 6R mode and two 7R modes. Chapter 6 presents a 7R SLMMRM which is analysed using algebraic approach showing that the mechanism has three types of operation modes including a 4R mode, two 6R modes and a 7R mode. A new overconstrained 6R mechanism is obtained as a by-product. The transition configurations among the different operation modes are identified for both 7R SLMMRMs. Moreover, CAD models and prototypes are built to successfully verify the analysis results.

The kinematic analysis of a MLMMRM based on the compositional serial kinematic chains (constraint equations obtained earlier) has also been attempted to implement. A 3-RRRR MMRM is demonstrated (see Appendix III) and its constraint equations can be obtained from Table A.I.3 in Appendix I, although obtaining the complete set of solutions for the 3-RRRR MMRM has not been possible as shown in Appendix III due to the high degree polynomials, however, the work conducted can pave the way for further development.

## **7.2 Main Contributions**

The aim of the dissertation was to produce new SLMMRMs that have more specified operation modes than most existing SLMMRMs with two specified operation modes, and to implement analysis and verification of their operation modes. The main achievements of this dissertation are:

- 1) A system that contains typical serial kinematic chains and their constraint equations is presented, which gives an overview of serial chains with same number of joints and the relationship among serial chains with different number of joints but similar arrangements. A linear algebraic method is presented to select proper number of constraint equations obtained from the implicitization approach for a serial chain rather than select the constraint equations arbitrarily. These are the foundations of completing the kinematic analysis of MMRMs.
- 2) Three methods are presented for proposing new 7J single-loop reconfigurable mechanisms with three or more operation modes in this dissertation. Based on these methods, numerous motivation-targeted 7J mechanisms can be obtained. For example, if a 7R SLMMRM with 4R, 5R and 7R modes is needed, then it can be constructed by

combining 4R and 5R SLOMs to form a 6R mechanism followed by inserting an additional R joint into it. These 7R SLMMRMs have the ability to fulfil the targeted tasks while they can change over in a shorter time and be more energy efficient.

3) Two novel 7R SLMMRMs separately with three and four operation modes have been proposed and analysed for the first time. The proposed 7R SLMMRM based on a Saruss linkage has two types of operation modes: one 6R mode and two 7R modes. The 7R SLMMRM generated by inserting an R joint into a Bricard linkage turns out to be the first SLMMRM with three types of operation modes: one 4R mode, two 6R modes and one 7R mode. Moreover, a novel 6R overconstrained mechanism is produced as a by-product.

### **7.3 Future Work**

The work in this dissertation focuses on the design of single-DOF 7J single-loop reconfigurable mechanisms with three or more operation modes as well as the kinematic analysis of their operation modes and transit configurations. However, there is much work to be conducted in the future.

It is still open to explore new single-loop reconfigurable mechanisms with three or more operation modes. It would also be promising to explore/discover variable DOFs single-loop reconfigurable mechanisms with three or more operation modes due to their outstanding advantages, using the methods presented in this dissertation or new methods will be proposed.

Although the methods effectively show that a new SLMMRM can be formed by inserting one new joint to a SLOM, further work still needs to be done to identify the appropriate/optimal location of the new added joint which may impact the operation modes.

After the investigation of serial kinematic chains as the compositional units of parallel mechanisms has been completed, the foundation of the kinematic analysis of MLMMRMs can be formed and their constraint equations can be directly recalled from Appendix I. However, it is a challenging issue to obtain the complete solutions of the MLMMRMs as shown in Appendix III, which should inspire the future work. Meanwhile, the design methods for MLMMRMs are to be investigated.

## Appendix I – Constraint Equations of Other Serial Kinematic Chains

Though the constraint equations of some typical serial kinematic chains have been presented in Chapter 3, this appendix gives the constraint equations for most serial kinematic chains.

Table A.I.1 Constraint equations for 4R serial chains using the explicitation algorithm in other tangent half angles

$T(v_1v_3)$	<p>(1) <math>-2a_2w_2w_3v_3v_1w_1x_3 + 2a_3w_2w_3v_3v_1w_1x_3 + 2w_2v_3a_1v_1w_1x_2 - 2w_3v_3a_1v_1w_1x_2</math>  <math>+2a_2w_2w_3v_3v_1x_2 - 2a_2w_2w_3v_1w_1x_0 - 2a_2w_2w_3v_3w_1x_0 - 2a_3w_2w_3v_3v_1x_2 - 2a_3w_2w_3v_1w_1x_0</math>  <math>+2a_3w_2w_3v_3w_1x_0 - 2w_2d_3v_3v_1w_1x_0 - 2w_3d_3v_3v_1w_1x_0 + 2w_2v_3a_1v_1x_3 - 2w_3v_3a_1v_1x_3</math>  <math>+2w_2a_1v_1w_1x_1 + 2w_3a_1v_1w_1x_1 + 2w_2v_3a_1w_1x_1 - 2w_3v_3a_1w_1x_1 - 2a_2v_3v_1w_1x_3 - 2a_2w_2w_3v_1x_1</math>  <math>+2a_2w_2w_3v_3x_1 + 2a_2w_2w_3w_1x_3 + 2a_3v_3v_1w_1x_3 - 2a_3w_2w_3v_1x_1 - 2a_3w_2w_3v_3x_1</math>  <math>+2a_3w_2w_3w_1x_3 - 2w_2d_3v_3v_1x_1 - 2w_3d_3v_3v_1x_1 - 2w_2d_3v_1w_1x_3 + 2w_3d_3v_1w_1x_3</math>  <math>+2w_2d_3v_3w_1x_3 + 2w_3d_3v_3w_1x_3 - 4w_2v_3v_1w_1y_3 + 4w_3v_3v_1w_1y_3 - 2w_2a_1v_1x_0 - 2w_3a_1v_1x_0</math>  <math>+2w_2v_3a_1x_0 - 2w_3v_3a_1x_0 - 2w_2a_1w_1x_2 - 2w_3a_1w_1x_2 + 2a_2v_3v_1x_2 + 2a_2v_1w_1x_0 - 2a_2v_3w_1x_0</math>  <math>+2a_2w_2w_3x_2 - 2a_3v_3v_1x_2 + 2a_3v_1w_1x_0 + 2a_3v_3w_1x_0 + 2a_3w_2w_3x_2 + 2w_2d_3v_1x_2 - 2w_3d_3v_1x_2</math>  <math>+2w_2d_3v_3x_2 + 2w_3d_3v_3x_2 - 2w_2d_3w_1x_0 + 2w_3d_3w_1x_0 + 4w_2v_3v_1y_2 - 4w_3v_3v_1y_2 + 4w_2v_1w_1y_0</math>  <math>+4w_3v_1w_1y_0 - 4w_2v_3w_1y_0 + 4w_3v_3w_1y_0 + 2w_2a_1x_3 + 2w_3a_1x_3 + 2a_2v_1x_1 + 2a_2v_3x_1</math>  <math>-2a_2w_1x_3 + 2a_3v_1x_1 - 2a_3v_3x_1 - 2a_3w_1x_3 + 2w_2d_3x_1 - 2w_3d_3x_1 + 4w_2v_1y_1 + 4w_3v_1y_1</math>  <math>+4w_2v_3y_1 - 4w_3v_3y_1 - 4w_2w_1y_3 - 4w_3w_1y_3 - 2a_2x_2 - 2a_3x_2 - 4w_2y_2 - 4w_3y_2</math></p> <p>(2) <math>-2w_2w_3v_3a_1v_1w_1x_3 - 2w_2w_3d_3v_3v_1w_1x_1 + 2w_2w_3v_3a_1v_1x_2 - 2w_2w_3a_1v_1w_1x_0</math>  <math>-2w_2w_3v_3a_1w_1x_0 + 2a_2w_2v_3v_1w_1x_2 - 2a_2w_3v_3v_1w_1x_2 - 2a_3w_2v_3v_1w_1x_2 + 2a_3w_3v_3v_1w_1x_2</math>  <math>+2w_2w_3d_3v_3v_1x_0 - 2w_2w_3d_3v_1w_1x_2 + 2w_2w_3d_3v_3w_1x_2 - 4w_2w_3v_3v_1w_1y_2 - 2v_3a_1v_1w_1x_3</math>  <math>-2w_2w_3a_1v_1x_1 + 2w_2w_3v_3a_1x_1 + 2w_2w_3a_1w_1x_3 + 2a_2w_2v_3v_1x_3 - 2a_2w_3v_3v_1x_3</math>  <math>+2a_2w_2v_1w_1x_1 + 2a_2w_3v_1w_1x_1 + 2a_2w_2v_3w_1x_1 - 2a_2w_3v_3w_1x_1 - 2a_3w_2v_3v_1x_3</math>  <math>+2a_3w_3v_3v_1x_3 + 2a_3w_2v_1w_1x_1 + 2a_3w_3v_1w_1x_1 - 2a_3w_2v_3w_1x_1 + 2a_3w_3v_3w_1x_1 + 2d_3v_3v_1w_1x_1</math>  <math>-2w_2w_3d_3v_1x_3 - 2w_2w_3d_3v_3x_3 - 2w_2w_3d_3w_1x_1 - 4w_2w_3v_3v_1y_3 + 4w_2w_3v_3v_1y_1 + 4w_1y_2</math>  <math>-4w_2w_3v_3w_1y_1 + 2v_3a_1v_1x_2 + 2a_1v_1w_1x_0 - 2v_3a_1w_1x_0 + 2w_2w_3a_1x_2 - 2a_2w_2v_1x_0 - 4v_3y_0</math>  <math>-2a_2w_3v_1x_0 + 2a_2w_2v_3x_0 - 2a_2w_3v_3x_0 - 2a_2w_2w_1x_2 - 2a_2w_3w_1x_2 - 2a_3w_2v_1x_0</math>  <math>-2a_3w_3v_1x_0 - 2a_3w_2v_3x_0 + 2a_3w_3v_3x_0 - 2a_3w_2w_1x_2 - 2a_3w_3w_1x_2 - 2d_3v_3v_1x_0 - 2d_3v_1w_1x_2</math>  <math>-2d_3v_3w_1x_2 - 2w_2w_3d_3x_0 - 4v_3v_1w_1y_2 - 4w_2w_3v_1y_0 - 4w_2w_3v_3y_0 - 4w_2w_3w_1y_2 + 2a_1v_1x_1</math>  <math>+2v_3a_1x_1 - 2a_1w_1x_3 + 2a_2w_2x_3 + 2a_2w_3x_3 + 2a_3w_2x_3 + 2a_3w_3x_3 - 2d_3v_1x_3 + 2d_3v_3x_3</math>  <math>-2d_3w_1x_1 - 4v_3v_1y_3 - 4v_1w_1y_1 - 4v_3w_1y_1 + 4w_2w_3y_3 - 2a_1x_2 - 2d_3x_0 + 4v_1y_0 - 4y_3</math></p>
-------------	---

$$\begin{aligned}
(3) \quad & 2a_2w_2w_3v_1w_1x_0 - 2a_3w_2w_3v_1w_1x_0 + 2w_2v_3a_1w_1x_1 - 2w_3v_3a_1w_1x_1 \\
& + 2a_2w_2w_3v_1x_1 - 2a_2w_2w_3v_1w_1x_3 - 2a_2w_2w_3v_3w_1x_3 - 2a_3w_2w_3v_3v_1x_1 - 2a_3w_2w_3v_1w_1x_3 \\
& + 2a_3w_2w_3v_3w_1x_3 - 2w_2d_3v_3v_1w_1x_3 - 2w_3d_3v_3v_1w_1x_3 - 2w_2v_3a_1v_1x_0 + 2w_3v_3a_1v_1x_0 \\
& - 2w_2a_1v_1w_1x_2 - 2w_3a_1v_1w_1x_2 - 2w_2v_3a_1w_1x_2 + 2w_3v_3a_1w_1x_2 + 2a_2v_3v_1w_1x_0 + 2a_2w_2w_3v_1x_2 \\
& - 2a_2w_2w_3v_3x_2 - 2a_2w_2w_3w_1x_0 - 2a_3v_3v_1w_1x_0 + 2a_3w_2w_3v_1x_2 + 2a_3w_2w_3v_3x_2 \\
& - 2a_3w_2w_3w_1x_0 + 2w_2d_3v_3v_1x_2 + 2w_3d_3v_3v_1x_2 + 2w_2d_3v_1w_1x_0 - 2w_3d_3v_1w_1x_0 \\
& - 2w_2d_3v_3w_1x_0 - 2w_3d_3v_3w_1x_0 + 4w_2v_3v_1w_1y_0 - 4w_3v_3v_1w_1y_0 - 2w_2a_1v_1x_3 - 2w_3a_1v_1x_3 \\
& + 2w_2v_3a_1x_3 - 2w_3v_3a_1x_3 - 2w_2a_1w_1x_1 - 2w_3a_1w_1x_1 + 2a_2v_3v_1x_1 + 2a_2v_1w_1x_3 - 2a_2v_3w_1x_3 \\
& + 2a_2w_2w_3x_1 - 2a_3v_3v_1x_1 + 2a_3v_1w_1x_3 + 2a_3v_3w_1x_3 + 2a_3w_2w_3x_1 + 2w_2d_3v_1x_1 - 2w_3d_3v_1x_1 \\
& + 2w_2d_3v_3x_1 + 2w_3d_3v_3x_1 - 2w_2d_3w_1x_3 + 2w_3d_3w_1x_3 + 4w_2v_3v_1y_1 - 4w_3v_3v_1y_1 \\
& + 4w_2v_1w_1y_3 + 4w_3v_1w_1y_3 - 4w_2v_3w_1y_3 + 4w_3v_3w_1y_3 - 2w_2a_1x_0 - 2w_3a_1x_0 - 2a_2v_1x_2 \\
& - 2a_2v_3x_2 + 2a_2w_1x_0 - 2a_3v_1x_2 + 2a_3v_3x_2 + 2a_3w_1x_0 - 2w_2d_3x_2 + 2w_3d_3x_2 - 4w_2v_1y_2 \\
& - 4w_3v_1y_2 - 4w_2v_3y_2 + 4w_3v_3y_2 + 4w_2w_1y_0 + 4w_3w_1y_0 - 2a_2x_1 - 2a_3x_1 - 4w_2y_1 - 4w_3y_1 \\
\\
(4) \quad & 2w_2w_3v_3a_1v_1w_1x_0 + 2w_2w_3d_3v_3v_1w_1x_2 + 2w_2w_3v_3a_1v_1x_1 - 2w_2w_3a_1v_1w_1x_3 \\
& - 2w_2w_3v_3a_1w_1x_3 + 2a_2w_2v_3v_1w_1x_1 - 2a_2w_3v_3v_1w_1x_1 - 2a_3w_2v_3v_1w_1x_1 + 2a_3w_3v_3v_1w_1x_1 \\
& + 2w_2w_3d_3v_3v_1x_3 - 2w_2w_3d_3v_1w_1x_1 + 2w_2w_3d_3v_3w_1x_1 - 4v_1v_3w_1w_2w_3y_1 + 2a_1v_1v_3w_1x_0 \\
& + 2a_1v_1w_2w_3x_2 - 2a_1v_3w_2w_3x_2 - 2a_1w_1w_2w_3x_0 - 2a_2v_1v_3w_2x_0 + 2a_2v_1v_3w_3x_0 \\
& - 2a_2v_1w_1w_2x_2 - 2a_2v_1w_1w_3x_2 - 2a_2v_3w_1w_2x_2 + 2a_2v_3w_1w_3x_2 + 2a_3v_1v_3w_2x_0 \\
& - 2a_3v_1v_3w_3x_0 - 2a_3v_1w_1w_2x_2 - 2a_3v_1w_1w_3x_2 + 2a_3v_3w_1w_2x_2 - 2a_3v_3w_1w_3x_2 \\
& - 2d_3v_1v_3w_1x_2 + 2d_3v_1w_2w_3x_0 + 2d_3v_3w_2w_3x_0 + 2d_3w_1w_2w_3x_2 + 4v_1v_3w_2w_3y_0 \\
& - 4v_1w_1w_2w_3y_2 + 4v_3w_1w_2w_3y_2 + 2a_1v_1v_3x_1 + 2a_1v_1w_1x_3 - 2a_1v_3w_1x_3 + 2a_1w_2w_3x_1 \\
& - 2a_2v_1w_2x_3 - 2a_2v_1w_3x_3 + 2a_2v_3w_2x_3 - 2a_2v_3w_3x_3 - 2a_2w_1w_2x_1 - 2a_2w_1w_3x_1 \\
& - 2a_3v_1w_2x_3 - 2a_3v_1w_3x_3 - 2a_3v_3w_2x_3 + 2a_3v_3w_3x_3 - 2a_3w_1w_2x_1 - 2a_3w_1w_3x_1 \\
& - 2d_3v_1v_3x_3 - 2d_3v_1w_1x_1 - 2d_3v_3w_1x_1 - 2d_3w_2w_3x_3 - 4v_1v_3w_1y_1 - 4v_1w_2w_3y_3 \\
& - 4v_3w_2w_3y_3 - 4w_1w_2w_3y_1 - 2a_1v_1x_2 - 2a_1v_3x_2 + 2a_1w_1x_0 - 2a_2w_2x_0 - 2a_2w_3x_0 \\
& - 2a_3w_2x_0 - 2a_3w_3x_0 + 2d_3v_1x_0 - 2d_3v_3x_0 + 2d_3w_1x_2 + 4v_1v_3y_0 + 4v_1w_1y_2 + 4v_3w_1y_2 \\
& - 4w_2w_3y_0 - 2a_1x_1 - 2d_3x_3 + 4v_1y_3 - 4v_3y_3 + 4w_1y_1 + 4y_0
\end{aligned}$$

$T(v_1v_4)$	<p>(1) <math>-2a_2v_1v_4w_1w_2w_3x_0 + 2a_1v_1v_4w_1w_3x_1 + 2a_2v_1v_4w_1w_2x_1 - 2a_2v_1v_4w_2w_3x_1</math>  <math>-2a_2v_1w_1w_2w_3x_3 + 2a_2v_4w_1w_2w_3x_3 - 2a_3v_1v_4w_1w_3x_1 + 2d_2v_1v_4w_1w_3x_3 + 2d_3v_1v_4w_1w_3x_3</math>  <math>+2a_1v_1v_4w_1x_0 - 2a_1v_1v_4w_3x_0 - 2a_1v_1w_1w_3x_2 - 2a_1v_4w_1w_3x_2 - 2a_2v_1v_4w_2x_0 + 2a_2v_1w_1w_2x_2</math>  <math>+2a_2v_1w_2w_3x_2 - 2a_2v_4w_1w_2x_2 + 2a_2v_4w_2w_3x_2 - 2a_2w_1w_2w_3x_0 - 2a_3v_1v_4w_1x_0</math>  <math>+2a_3v_1v_4w_3x_0 - 2a_3v_1w_1w_3x_2 + 2a_3v_4w_1w_3x_2 - 2d_2v_1v_4w_1x_2 - 2d_2v_1v_4w_3x_2 - 2d_2v_1w_1w_3x_0</math>  <math>+2d_2v_4w_1w_3x_0 - 2d_3v_1v_4w_1x_2 - 2d_3v_1v_4w_3x_2 - 2d_3v_1w_1w_3x_0 + 2d_3v_4w_1w_3x_0 + 4v_1v_4w_1w_3y_0</math>  <math>+2a_1v_1v_4x_1 - 2a_1v_1w_1x_3 - 2a_1v_1w_3x_3 - 2a_1v_4w_1x_3 + 2a_1v_4w_3x_3 - 2a_1w_1w_3x_1 + 2a_2v_1w_2x_3</math>  <math>+2a_2v_4w_2x_3 + 2a_2w_1w_2x_1 + 2a_2w_2w_3x_1 - 2a_3v_1v_4x_1 - 2a_3v_1w_1x_3 - 2a_3v_1w_3x_3 + 2a_3v_4w_1x_3</math>  <math>-2a_3v_4w_3x_3 - 2a_3w_1w_3x_1 - 2d_2v_1v_4x_3 + 2d_2v_1w_1x_1 - 2d_2v_1w_3x_1 - 2d_2v_4w_1x_1 - 2d_2v_4w_3x_1</math>  <math>+2d_2w_1w_3x_3 - 2d_3v_1v_4x_3 + 2d_3v_1w_1x_1 - 2d_3v_1w_3x_1 - 2d_3v_4w_1x_1 - 2d_3v_4w_3x_1 + 2d_3w_1w_3x_3</math>  <math>-4v_1v_4w_1y_1 + 4v_1v_4w_3y_1 + 4v_1w_1w_3y_3 - 4v_4w_1w_3y_3 + 2a_1v_1x_2 - 2a_1v_4x_2 - 2a_1w_1x_0</math>  <math>-2a_1w_3x_0 + 2a_2w_2x_0 + 2a_3v_1x_2 + 2a_3v_4x_2 - 2a_3w_1x_0 - 2a_3w_3x_0 - 2d_2v_1x_0 - 2d_2v_4x_0</math>  <math>-2d_2w_1x_2 + 2d_2w_3x_2 - 2d_3v_1x_0 - 2d_3v_4x_0 - 2d_3w_1x_2 + 2d_3w_3x_2 + 4v_1v_4y_0 - 4v_1w_1y_2</math>  <math>-4v_1w_3y_2 + 4v_4w_1y_2 - 4v_4w_3y_2 + 4w_1w_3y_0 + 2a_1x_1 + 2a_3x_1 + 2d_2x_3 + 2d_3x_3 - 4v_1y_3</math>  <math>-4v_4y_3 - 4w_1y_1 - 4w_3y_1 - 4y_0</math></p> <p>(2) <math>-2a_1v_1v_4w_1w_2w_3x_0 + 2a_3v_1v_4w_1w_2w_3x_0 + 2d_2v_1v_4w_1w_2w_3x_2 - 2d_3v_1v_4w_1w_2w_3x_2</math>  <math>+2a_1v_1v_4w_1w_2x_1 - 2a_1v_1v_4w_2w_3x_1 - 2a_1v_1w_1w_2w_3x_3 + 2a_1v_4w_1w_2w_3x_3 + 2a_2v_1v_4w_1w_3x_1</math>  <math>-2a_3v_1v_4w_1w_2x_1 + 2a_3v_1v_4w_2w_3x_1 - 2a_3v_1w_1w_2w_3x_3 - 2a_3v_4w_1w_2w_3x_3 + 2d_2v_1v_4w_1w_2x_3</math>  <math>+2d_2v_1v_4w_2w_3x_3 + 2d_2v_1w_1w_2w_3x_1 + 2d_2v_4w_1w_2w_3x_1 - 2d_3v_1v_4w_1w_2x_3 - 2d_3v_1v_4w_2w_3x_3</math>  <math>-2d_3v_1w_1w_2w_3x_1 - 2d_3v_4w_1w_2w_3x_1 + 4v_1v_4w_1w_2w_3y_1 - 2a_1v_1v_4w_2x_0 + 2a_1v_1w_1w_2x_2</math>  <math>+2a_1v_1w_2w_3x_2 - 2a_1v_4w_1w_2x_2 + 2a_1v_4w_2w_3x_2 - 2a_1w_1w_2w_3x_0 + 2a_2v_1v_4w_1x_0 - 2a_2v_1v_4w_3x_0</math>  <math>-2a_2v_1w_1w_3x_2 - 2a_2v_4w_1w_3x_2 + 2a_3v_1v_4w_2x_0 + 2a_3v_1w_1w_2x_2 + 2a_3v_1w_2w_3x_2 + 2a_3v_4w_1w_2x_2</math>  <math>-2a_3v_4w_2w_3x_2 - 2a_3w_1w_2w_3x_0 - 2d_2v_1v_4w_2x_2 + 2d_2v_1w_1w_2x_0 - 2d_2v_1w_2w_3x_0 + 2d_2v_4w_1w_2x_0</math>  <math>+2d_2v_4w_2w_3x_0 - 2d_2w_1w_2w_3x_2 + 2d_3v_1v_4w_2x_2 - 2d_3v_1w_1w_2x_0 + 2d_3v_1w_2w_3x_0 - 2d_3v_4w_1w_2x_0</math>  <math>-2d_3v_4w_2w_3x_0 + 2d_3w_1w_2w_3x_2 + 4v_1v_4w_1w_2y_0 - 4v_1v_4w_2w_3y_0 - 4v_1w_1w_2w_3y_2 - 4v_4w_1w_2w_3y_2</math>  <math>+2a_1v_1w_2x_3 + 2a_1v_4w_2x_3 + 2a_1w_1w_2x_1 + 2a_1w_2w_3x_1 + 2a_2v_1v_4x_1 - 2a_2v_1w_1x_3 - 2a_2v_1w_3x_3</math>  <math>-2a_2v_4w_1x_3 + 2a_2v_4w_3x_3 - 2a_2w_1w_3x_1 + 2a_3v_1w_2x_3 - 2a_3v_4w_2x_3 + 2a_3w_1w_2x_1 + 2a_3w_2w_3x_1</math>  <math>+2d_2v_1w_2x_1 - 2d_2v_4w_2x_1 - 2d_2w_1w_2x_3 + 2d_2w_2w_3x_3 - 2d_3v_1w_2x_1 + 2d_3v_4w_2x_1 + 2d_3w_1w_2x_3</math>  <math>-2d_3w_2w_3x_3 + 4v_1v_4w_2y_1 - 4v_1w_1w_2y_3 - 4v_1w_2w_3y_3 - 4v_4w_1w_2y_3 + 4v_4w_2w_3y_3 - 4w_1w_2w_3y_1</math>  <math>+2a_1w_2x_0 + 2a_2v_1x_2 - 2a_2v_4x_2 - 2a_2w_1x_0 - 2a_2w_3x_0 + 2a_3w_2x_0 - 2d_2w_2x_2 + 2d_3w_2x_2</math>  <math>+4v_1w_2y_2 - 4v_4w_2y_2 - 4w_1w_2y_0 - 4w_2w_3y_0 + 2a_2x_1 + 4w_2y_1</math></p>
-------------	--

$$\begin{aligned}
(3) \quad & -2a_1v_1v_4w_1w_2w_3x_3 - 2a_3v_1v_4w_1w_2w_3x_3 + 2d_2v_1v_4w_1w_2w_3x_1 - 2d_3v_1v_4w_1w_2w_3x_1 \\
& + 2a_1v_1v_4w_1w_2x_2 + 2a_1v_1v_4w_2w_3x_2 - 2a_1v_1v_4w_1w_2w_3x_3 - 2a_3v_1v_4w_1w_2w_3x_3 \\
& + 2d_2v_1v_4w_1w_2w_3x_1 - 2d_3v_1v_4w_1w_2w_3x_1 + 2a_1v_1v_4w_1w_2x_2 + 2a_1v_1v_4w_2w_3x_2 \\
& - 2a_3v_4w_1w_2w_3x_0 + 2d_2v_1v_4w_1w_2x_0 - 2d_2v_1v_4w_2w_3x_0 - 2d_2v_1w_1w_2w_3x_2 - 2d_2v_4w_1w_2w_3x_2 \\
& - 2d_3v_1v_4w_1w_2x_0 + 2d_3v_1v_4w_2w_3x_0 + 2d_3v_1w_1w_2w_3x_2 + 2d_3v_4w_1w_2w_3x_2 - 4v_1v_4w_1w_2w_3y_2 \\
& + 2a_1v_1v_4w_2x_3 - 2a_1v_1w_1w_2x_1 + 2a_1v_1w_2w_3x_1 + 2a_1v_4w_1w_2x_1 + 2a_1v_4w_2w_3x_1 - 2a_1w_1w_2w_3x_3 \\
& - 2a_2v_1v_4w_1x_3 - 2a_2v_1v_4w_3x_3 - 2a_2v_1w_1w_2x_1 - 2a_2v_4w_1w_2x_1 + 2a_3v_1v_4w_2x_3 + 2a_3v_1w_1w_2x_1 \\
& - 2a_3v_1w_2w_3x_1 + 2a_3v_4w_1w_2x_1 + 2a_3v_4w_2w_3x_1 + 2a_3w_1w_2w_3x_3 + 2d_2v_1v_4w_2x_1 - 2d_2v_1w_1w_2x_3 \\
& - 2d_2v_1w_2w_3x_3 - 2d_2v_4w_1w_2x_3 + 2d_2v_4w_2w_3x_3 - 2d_2w_1w_2w_3x_1 - 2d_3v_1v_4w_2x_1 + 2d_3v_1w_1w_2x_3 \\
& + 2d_3v_1w_2w_3x_3 + 2d_3v_4w_1w_2x_3 - 2d_3v_4w_2w_3x_3 + 2d_3w_1w_2w_3x_1 - 4v_1v_4w_1w_2y_3 \\
& - 4v_1v_4w_2w_3y_3 - 4v_1w_1w_2w_3y_1 - 4v_4w_1w_2w_3y_1 + 2a_1v_1w_2x_0 + 2a_1v_4w_2x_0 + 2a_1w_1w_2x_2 \\
& - 2a_1w_2w_3x_2 + 2a_2v_1v_4x_2 - 2a_2v_1w_1x_0 + 2a_2v_1w_3x_0 - 2a_2v_4w_1x_0 - 2a_2v_4w_3x_0 + 2a_2w_1w_3x_2 \\
& - 2a_3v_1w_2x_0 + 2a_3v_4w_2x_0 - 2a_3w_1w_2x_2 + 2a_3w_2w_3x_2 + 2d_2v_1w_2x_2 - 2d_2v_4w_2x_2 - 2d_2w_1w_2x_0 \\
& - 2d_2w_2w_3x_0 - 2d_3v_1w_2x_2 + 2d_3v_4w_2x_2 + 2d_3w_1w_2x_0 + 2d_3w_2w_3x_0 + 4v_1v_4w_2y_2 - 4v_1w_1w_2y_0 \\
& + 4v_1w_2w_3y_0 - 2d_2w_1w_2x_0 - 2d_2w_2w_3x_0 - 2d_3v_1w_2x_2 + 2d_3v_4w_2x_2 + 2d_3w_1w_2x_0 + 2d_3w_2w_3x_0 \\
& + 4v_1v_4w_2y_2 - 4v_1w_1w_2y_0 + 4v_1w_2w_3y_0 - 4v_4w_1w_2y_0 - 4v_4w_2w_3y_0 + 4w_1w_2w_3y_2 - 2a_1w_2x_3 \\
& - 2a_2v_1x_1 + 2a_2v_4x_1 + 2a_2w_1x_3 - 2a_2w_3x_3 + 2a_3w_2x_3 + 2d_2w_2x_1 - 2d_3w_2x_1 - 4v_1w_2y_1 \\
& + 4v_4w_2y_1 + 4w_1w_2y_3 - 4w_2w_3y_3 + 2a_2x_2 + 4w_2y_2
\end{aligned}$$

$$\begin{aligned}
(4) \quad & 2a_2v_1v_4w_1w_2w_3x_3 + 2a_1v_1v_4w_1w_3x_2 - 2a_2v_1v_4w_1w_2x_2 - 2a_2v_1v_4w_2w_3x_2 \\
& - 2a_2v_1w_1w_2w_3x_0 + 2a_2v_4w_1w_2w_3x_0 + 2a_3v_1v_4w_1w_3x_2 + 2d_2v_1v_4w_1w_3x_0 + 2d_3v_1v_4w_1w_3x_0 \\
& + 2a_1v_1v_4w_1x_3 + 2a_1v_1v_4w_3x_3 + 2a_1v_1w_1w_3x_1 + 2a_1v_4w_1w_3x_1 - 2a_2v_1v_4w_2x_3 + 2a_2v_1w_1w_2x_1 \\
& - 2a_2v_1w_2w_3x_1 - 2a_2v_4w_1w_2x_1 - 2a_2v_4w_2w_3x_1 + 2a_2w_1w_2w_3x_3 + 2a_3v_1v_4w_1x_3 \\
& + 2a_3v_1v_4w_3x_3 - 2a_3v_1w_1w_3x_1 + 2a_3v_4w_1w_3x_1 - 2d_2v_1v_4w_1x_1 + 2d_2v_1v_4w_3x_1 + 2d_2v_1w_1w_3x_3 \\
& - 2d_2v_4w_1w_3x_3 - 2d_3v_1v_4w_1x_1 + 2d_3v_1v_4w_3x_1 + 2d_3v_1w_1w_3x_3 - 2d_3v_4w_1w_3x_3 - 4v_1v_4w_1w_3y_3 \\
& - 2a_1v_1v_4x_2 + 2a_1v_1w_1x_0 - 2a_1v_1w_3x_0 + 2a_1v_4w_1x_0 + 2a_1v_4w_3x_0 - 2a_1w_1w_3x_2 - 2a_2v_1w_2x_0 \\
& - 2a_2v_4w_2x_0 - 2a_2w_1w_2x_2 + 2a_2w_2w_3x_2 - 2a_3v_1v_4x_2 - 2a_3v_1w_1x_0 + 2a_3v_1w_3x_0 + 2a_3v_4w_1x_0 \\
& + 2a_3v_4w_3x_0 + 2a_3w_1w_3x_2 + 2d_2v_1v_4x_0 - 2d_2v_1w_1x_2 - 2d_2v_1w_3x_2 + 2d_2v_4w_1x_2 - 2d_2v_4w_3x_2 \\
& + 2d_2w_1w_3x_0 + 2d_3v_1v_4x_0 - 2d_3v_1w_1x_2 - 2d_3v_1w_3x_2 + 2d_3v_4w_1x_2 - 2d_3v_4w_3x_2 + 2d_3w_1w_3x_0 \\
& + 4v_1v_4w_1y_2 + 4v_1v_4w_3y_2 + 4v_1w_1w_3y_0 - 4v_4w_1w_3y_0 + 2a_1v_1x_1 - 2a_1v_4x_1 - 2a_1w_1x_3 + 2a_1w_3x_3 \\
& + 2a_2w_2x_3 - 2a_3v_1x_1 - 2a_3v_4x_1 + 2a_3w_1x_3 - 2a_3w_3x_3 - 2d_2v_1x_3 - 2d_2v_4x_3 - 2d_2w_1x_1 - 4w_3y_2 \\
& - 2d_2w_3x_1 - 2d_3v_1x_3 - 2d_3v_4x_3 - 2d_3w_1x_1 - 2d_3w_3x_1 + 4v_1v_4y_3 - 4v_1w_1y_1 + 4v_1w_3y_1 - 4y_3 \\
& + 4v_4w_1y_1 + 4v_4w_3y_1 - 4w_1w_3y_3 - 2a_1x_2 + 2a_3x_2 - 2d_2x_0 - 2d_3x_0 + 4v_1y_0 + 4v_4y_0 + 4w_1y_2
\end{aligned}$$

$T(v_2v_4)$	<p>(1) <math>-2x_2 w_1v_2a_3v_4w_3 + 2x_2 w_2v_2a_3v_4w_3 + 2x_2 a_1w_1w_2 - 2x_2 a_1v_2v_4 + 2x_2 a_2w_1w_2</math>  <math>+2x_2 a_2v_2v_4 + 2x_2 w_1d_2v_2 - 2x_2 w_1d_2v_4 + 2x_2 w_1v_2d_3 - 2x_2 w_1a_3w_3 - 2x_2 w_1d_3v_4</math>  <math>+2x_2 w_2d_2v_2 + 2x_2 w_2d_2v_4 - 2x_2 w_2v_2d_3 - 2x_2 w_2a_3w_3 - 2x_2 w_2d_3v_4 - 2x_2 a_1</math>  <math>-2x_2 a_2 + 2x_1 d_2v_2w_2v_4 - 2x_1 w_2v_2a_3w_3 + 4y_1 w_1v_2 - 4y_1 v_4w_1 - 4y_1 w_2v_2</math>  <math>-4y_1 v_4w_2 - 4y_2 v_4v_2w_1 + 4y_2 v_4v_2w_2 - 4y_2 w_1 - 4y_2 w_2 + 2x_3 a_1w_1w_2v_2v_4w_3</math>  <math>-2x_3 a_2w_1w_2v_2v_4w_3 - 2x_3 a_1w_1w_2w_3 + 2x_3 a_1v_2v_4w_3 - 2x_3 a_2w_1w_2w_3 - 2x_3 a_2v_2v_4w_3</math>  <math>-2x_3 w_1d_2v_2w_3 + 2x_3 w_1d_2v_4w_3 - 2x_3 w_1v_2a_3v_4 - 2x_2 a_1w_1w_2v_2v_4 + 2x_2 a_2w_1w_2v_2v_4</math>  <math>+2x_3 w_2d_3v_4w_3 + 2x_3 a_1w_3 + 2x_3 a_2w_3 - 2x_3 w_1a_3 - 2x_3 w_2a_3 - 4y_0 w_3v_2w_1</math>  <math>+4y_0 w_3v_4w_1 + 4y_0 w_3v_2w_2 + 4y_0 w_3v_4w_2 + 4y_3 w_3w_2 - 2x_3 w_1v_2d_3w_3</math>  <math>+2x_3 w_1d_3v_4w_3 - 2x_3 w_2d_2v_2w_3 - 2x_3 w_2d_2v_4w_3 + 2x_3 w_2v_2a_3v_4 + 2x_3 w_2v_2d_3w_3</math>  <math>+4y_3 w_3w_1 - 2x_0 w_2a_3v_4 - 2x_0 w_2d_3w_3 + 4y_3 w_3v_4v_2w_1 - 4y_3 w_3v_4v_2w_2</math>  <math>-2x_0 a_1w_1w_2v_4w_3 + 2x_0 a_2w_1w_2v_2w_3 - 2x_0 a_2w_1w_2v_4w_3 - 2x_0 w_1d_2v_2v_4w_3</math>  <math>-2x_0 w_1v_2d_3v_4w_3 - 2x_0 w_2d_2v_2v_4w_3 + 2x_0 w_2v_2d_3v_4w_3 - 2x_0 a_1v_2w_3 + 2x_0 a_1v_4w_3</math>  <math>+2x_0 a_2v_2w_3 + 2x_0 a_2v_4w_3 - 2x_0 w_1d_2w_3 + 2x_0 w_1v_2a_3 - 2x_0 w_1a_3v_4 - 2x_0 w_1d_3w_3</math>  <math>+2x_0 w_2d_2w_3 - 2x_0 w_2v_2a_3 - 2x_1 w_2v_2d_3v_4 - 2x_1 w_2a_3v_4w_3 + 2x_1 a_1v_2 - 2x_1 a_1v_4</math>  <math>-2x_1 a_2v_2 - 2x_1 a_2v_4 + 2x_1 w_1d_2 + 2x_1 w_1d_3 - 2x_1 w_2d_2 + 2x_1 w_2d_3 + 2x_1 a_1w_1w_2v_2</math>  <math>+2x_1 a_1w_1w_2v_4 - 2x_1 a_2w_1w_2v_2 + 2x_1 a_2w_1w_2v_4 + 2x_1 d_2v_2w_1v_4 + 2x_1 w_1v_2a_3w_3</math>  <math>+2x_1 w_1v_2d_3v_4 - 2x_1 w_1a_3v_4w_3 - 2x_0 a_1w_1w_2v_2w_3</math></p> <p>(2) <math>-2x_2 d_3v_4w_3 + 2x_2 a_3 - 2x_3 w_3a_3 - 2x_3 d_3v_4 + 4y_0 v_4 + 4y_1 w_3v_4 - 4y_2 w_3</math>  <math>-2x_0 v_2a_3w_3 - 2x_0 v_2d_3v_4 - 2x_0 d_2 + 2x_2 a_1w_1v_2v_4w_3 - 2x_2 a_1w_2v_2v_4w_3 - 2x_0 a_1w_2v_4</math>  <math>+2x_2 a_2w_2v_2v_4w_3 - 2x_2 w_1w_2d_2v_2w_3 - 2x_2 w_1w_2d_2v_4w_3 + 2x_2 w_1w_2v_2a_3v_4</math>  <math>+2x_2 w_1w_2v_2d_3w_3 + 2x_2 w_1w_2d_3v_4w_3 + 2x_2 a_1w_1w_3 + 2x_2 a_1w_2w_3 + 2x_2 a_2w_1w_3</math>  <math>+2x_2 a_2w_2w_3 - 2x_2 w_1w_2a_3 - 2x_1 v_2d_3v_4w_3 - 2x_1 d_2w_3 + 2x_1 v_2a_3 + 2x_0 w_1w_2d_2v_2v_4</math>  <math>-2x_0 w_1w_2v_2a_3w_3 - 2x_0 w_1w_2v_2d_3v_4 - 2x_0 w_1w_2a_3v_4w_3 + 2x_0 a_1w_1v_2 - 2x_0 a_1w_1v_4</math>  <math>-2x_0 a_1w_2v_2 - 2x_2 a_2w_1v_2v_4w_3 - 2x_0 a_2w_1v_2 - 2x_0 a_2w_1v_4 + 2x_0 a_2w_2v_2 - 2x_0 a_2w_2v_4</math>  <math>-2x_0 w_1w_2d_2 + 2x_0 w_1w_2d_3 - 2x_0 d_2v_2v_4 - 4y_3 - 2x_1 a_3v_4 - 2x_1 w_3d_3 + 2x_0 a_3v_4w_3</math>  <math>-2x_0 d_3 + 2x_2 d_2v_2w_3 - 2x_2 d_2v_4w_3 + 2x_2 v_2a_3v_4 + 2x_2 v_2d_3w_3 - 2x_3 w_1w_2v_2a_3v_4w_3</math>  <math>+2x_3 w_1a_1v_2v_4 - 2x_3 a_1w_2v_2v_4 - 2x_3 a_2w_1v_2v_4 + 2x_3 a_2w_2v_2v_4 - 2x_3 w_1w_2d_2v_2</math>  <math>-2x_3 w_1w_2d_2v_4 + 2x_3 w_1w_2v_2d_3 + 4y_3 w_1w_2 - 4y_3 v_4v_2 + 2x_1 w_1w_2d_2v_2v_4w_3</math>  <math>-2x_1 w_1w_2v_2d_3v_4w_3 + 2x_1 a_1w_1v_2w_3 - 2x_1 a_1w_1v_4w_3 - 2x_1 a_1w_2v_2w_3 - 2x_1 a_1w_2v_4w_3</math>  <math>-2x_1 a_2w_1v_2w_3 - 2x_1 a_2w_1v_4w_3 + 2x_1 a_2w_2v_2w_3 - 2x_1 a_2w_2v_4w_3 - 2x_1 w_1w_2d_2w_3</math>  <math>+2x_1 w_1w_2v_2a_3 + 2x_1 w_1w_2a_3v_4 + 2x_1 w_1w_2d_3w_3 - 2x_1 d_2v_2v_4w_3 + 2x_3 w_1w_2a_3w_3</math>  <math>+2x_3 w_1w_2d_3v_4 - 2x_3 v_2a_3v_4w_3 + 2x_3 a_1w_1 + 2x_3 a_1w_2 + 2x_3 a_2w_1 + 2x_3 a_2w_2 + 2x_3 d_2v_2</math>  <math>-2x_3 d_2v_4 + 2x_3 v_2d_3 - 4y_0 w_1w_2v_2 - 4y_0 w_1w_2v_4 - 4y_0 v_2 - 4y_1 w_1w_2v_2w_3 - 4y_1 w_3v_2</math>  <math>-4y_1 w_1w_2v_4w_3 - 4y_2 w_1w_2v_2v_4w_3 + 4y_2 w_1w_2w_3 - 4y_2 w_3v_4v_2 - 4y_3 w_1w_2v_2v_4</math></p>
-------------	---

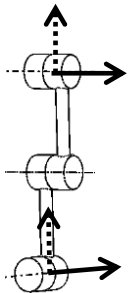
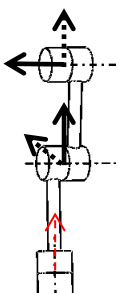
$$\begin{aligned}
(3) \quad & -2x_3 a_2 v_2 w_3 - 2x_3 a_2 v_4 w_3 + 2x_3 w_1 d_2 w_3 - 2x_3 w_1 v_2 a_3 + 2x_3 w_1 a_3 v_4 + 2x_3 w_1 d_3 w_3 \\
& - 2x_3 w_2 d_2 w_3 + 2x_0 a_1 w_1 w_2 v_2 v_4 w_3 - 2x_0 a_2 w_1 w_2 v_2 v_4 w_3 - 2x_0 a_1 w_1 w_2 w_3 + 2x_0 a_1 v_2 v_4 w_3 \\
& - 2x_0 a_2 w_1 w_2 w_3 - 2x_0 a_2 v_2 v_4 w_3 - 2x_0 w_1 d_2 v_2 w_3 + 2x_0 w_1 d_2 v_4 w_3 - 2x_0 w_1 v_2 a_3 v_4 \\
& - 2x_0 w_1 v_2 d_3 w_3 + 2x_0 w_1 d_3 v_4 w_3 - 2x_0 w_2 d_2 v_2 w_3 - 2x_0 w_2 d_2 v_4 w_3 + 2x_0 w_2 v_2 a_3 v_4 \\
& + 2x_0 w_2 v_2 d_3 w_3 + 2x_0 w_2 d_3 v_4 w_3 + 2x_0 a_1 w_3 + 2x_0 a_2 w_3 - 2x_0 w_1 a_3 - 2x_0 w_2 a_3 \\
& - 2x_1 a_1 w_1 w_2 v_2 v_4 + 2x_1 a_2 w_1 w_2 v_2 v_4 - 2x_1 w_1 v_2 a_3 v_4 w_3 + 2x_1 w_2 v_2 a_3 v_4 w_3 + 2x_1 a_1 w_1 w_2 \\
& - 2x_1 a_1 v_2 v_4 + 2x_1 a_2 w_1 w_2 + 2x_1 a_2 v_2 v_4 + 2x_1 w_1 d_2 v_2 - 2x_1 w_1 d_2 v_4 + 2x_1 w_1 v_2 d_3 \\
& - 2x_1 w_1 a_3 w_3 - 2x_1 w_1 d_3 v_4 + 2x_1 w_2 d_2 v_2 + 2x_1 w_2 d_2 v_4 + 2x_3 w_2 v_2 a_3 + 2x_3 w_2 a_3 v_4 \\
& + 2x_3 w_2 d_3 w_3 + 4y_0 w_3 v_4 v_2 w_1 - 4y_0 w_3 v_4 v_2 w_2 + 4y_0 w_3 w_1 + 4y_0 w_3 w_2 - 4y_1 v_4 v_2 w_1 \\
& + 4y_1 v_4 v_2 w_2 - 4y_1 w_1 - 4y_1 w_2 - 4y_2 w_1 v_2 + 4y_2 v_4 w_1 + 4y_2 w_2 v_2 + 4y_2 v_4 w_2 \\
& + 4y_3 w_3 v_2 w_1 - 4y_3 w_3 v_4 w_1 - 4y_3 w_3 v_2 w_2 - 4y_3 w_3 v_4 w_2 - 2x_1 w_2 v_2 d_3 - 2x_1 w_2 a_3 w_3 \\
& - 2x_1 w_2 d_3 v_4 - 2x_1 a_1 - 2x_1 a_2 - 2x_2 a_1 w_1 w_2 v_2 - 2x_2 a_1 w_1 w_2 v_4 + 2x_2 a_2 w_1 w_2 v_2 \\
& - 2x_2 a_2 w_1 w_2 v_4 - 2x_2 d_2 v_2 w_1 v_4 - 2x_2 w_1 v_2 a_3 w_3 - 2x_2 w_1 v_2 d_3 v_4 + 2x_2 w_1 a_3 v_4 w_3 \\
& - 2x_2 d_2 v_2 w_2 v_4 + 2x_2 w_2 v_2 a_3 w_3 + 2x_2 w_2 v_2 d_3 v_4 + 2x_2 w_2 a_3 v_4 w_3 - 2x_2 a_1 v_2 + 2x_2 a_1 v_4 \\
& + 2x_2 a_2 v_2 + 2x_2 a_2 v_4 - 2x_2 w_1 d_2 - 2x_2 w_1 d_3 + 2x_2 w_2 d_2 - 2x_2 w_2 d_3 + 2x_3 a_1 w_1 w_2 v_2 w_3 \\
& + 2x_3 a_1 w_1 w_2 v_4 w_3 - 2x_3 a_2 w_1 w_2 v_2 w_3 + 2x_3 a_2 w_1 w_2 v_4 w_3 + 2x_3 w_1 d_2 v_2 v_4 w_3 \\
& + 2x_3 w_1 v_2 d_3 v_4 w_3 + 2x_3 w_2 d_2 v_2 v_4 w_3 - 2x_3 w_2 v_2 d_3 v_4 w_3 + 2x_3 a_1 v_2 w_3 - 2x_3 a_1 v_4 w_3
\end{aligned}$$

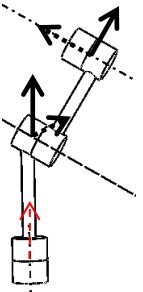
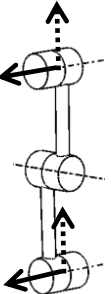
$$\begin{aligned}
(4) \quad & 2x_3 a_3 v_4 w_3 - 2x_3 d_3 + 4y_1 w_3 + 4y_2 w_3 v_4 + 4y_3 v_4 + 2x_1 d_3 v_4 w_3 - 2x_2 a_3 v_4 \\
& - 2x_1 a_3 - 2x_2 w_3 d_3 + 4y_0 + 2x_0 w_3 a_3 + 2x_0 d_3 v_4 + 4y_0 w_1 w_2 v_2 v_4 - 4y_0 w_1 w_2 \\
& + 4y_0 v_4 v_2 + 4y_1 w_1 w_2 v_2 v_4 w_3 - 4y_1 w_1 w_2 w_3 + 4y_1 w_3 v_4 v_2 - 4y_2 w_1 w_2 v_2 w_3 \\
& - 4y_2 w_1 w_2 v_4 w_3 - 4y_2 w_3 v_2 - 4y_3 w_1 w_2 v_2 - 4y_3 w_1 w_2 v_4 - 4y_3 v_2 - 2x_1 a_1 w_1 v_2 v_4 w_3 \\
& + 2x_1 a_1 w_1 v_2 v_4 w_3 + 2x_1 a_2 w_1 v_2 v_4 w_3 - 2x_1 a_2 w_2 v_2 v_4 w_3 + 2x_1 w_1 w_2 d_2 v_2 w_3 - 2x_3 d_2 \\
& + 2x_1 w_1 w_2 d_2 v_4 w_3 - 2x_1 w_1 w_2 v_2 a_3 v_4 - 2x_1 w_1 w_2 v_2 d_3 w_3 - 2x_1 w_1 w_2 d_3 v_4 w_3 - 2x_1 a_1 w_1 w_3 \\
& - 2x_1 a_1 w_2 w_3 - 2x_1 a_2 w_1 w_3 - 2x_1 a_2 w_2 w_3 + 2x_1 w_1 w_2 a_3 - 2x_1 d_2 v_2 w_3 + 2x_1 d_2 v_4 w_3 \\
& - 2x_1 v_2 a_3 v_4 - 2x_1 v_2 d_3 w_3 + 2x_2 w_1 w_2 d_2 v_2 v_4 w_3 - 2x_2 w_1 w_2 v_2 d_3 v_4 w_3 + 2x_2 a_1 w_1 v_2 w_3 \\
& - 2x_2 a_1 w_1 v_4 w_3 - 2x_2 a_1 w_2 v_2 w_3 - 2x_2 a_1 w_2 v_4 w_3 - 2x_2 a_2 w_1 v_2 w_3 - 2x_2 a_2 w_1 v_4 w_3 \\
& + 2x_2 a_2 w_2 v_2 w_3 - 2x_2 a_2 w_2 v_4 w_3 - 2x_2 w_1 w_2 d_2 w_3 + 2x_2 w_1 w_2 v_2 a_3 + 2x_2 w_1 w_2 a_3 v_4 \\
& + 2x_2 w_1 w_2 d_3 w_3 - 2x_2 d_2 v_2 v_4 w_3 - 2x_2 v_2 d_3 v_4 w_3 - 2x_2 d_2 w_3 + 2x_2 v_2 a_3 - 2x_0 w_1 a_1 v_2 v_4 \\
& + 2x_0 w_1 w_2 v_2 a_3 v_4 w_3 + 2x_0 a_1 w_2 v_2 v_4 + 2x_0 a_2 w_1 v_2 v_4 - 2x_0 a_2 w_2 v_2 v_4 + 2x_0 w_1 w_2 d_2 v_2 \\
& + 2x_0 w_1 w_2 d_2 v_4 - 2x_0 w_1 w_2 v_2 d_3 - 2x_0 w_1 w_2 a_3 w_3 - 2x_0 w_1 w_2 d_3 v_4 + 2x_0 v_2 a_3 v_4 w_3 \\
& - 2x_0 a_1 w_1 - 2x_0 a_1 w_2 - 2x_0 a_2 w_1 - 2x_0 a_2 w_2 - 2x_0 d_2 v_2 + 2x_0 d_2 v_4 + 2x_3 w_1 w_2 d_2 v_2 v_4 \\
& - 2x_0 v_2 d_3 - 2x_3 w_1 w_2 v_2 a_3 w_3 - 2x_3 w_1 w_2 v_2 d_3 v_4 - 2x_3 w_1 w_2 a_3 v_4 w_3 + 2x_3 a_1 w_1 v_2 \\
& - 2x_3 a_1 w_1 v_4 - 2x_3 a_1 w_2 v_2 - 2x_3 a_1 w_2 v_4 - 2x_3 a_2 w_1 v_2 - 2x_3 a_2 w_1 v_4 + 2x_3 a_2 w_2 v_2 \\
& - 2x_3 a_2 w_2 v_4 - 2x_3 w_1 w_2 d_2 + 2x_3 w_1 w_2 d_3 - 2x_3 d_2 v_2 v_4 - 2x_3 v_2 a_3 w_3 - 2x_3 v_2 d_3 v_4
\end{aligned}$$

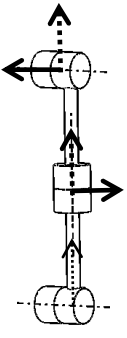
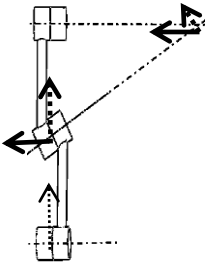


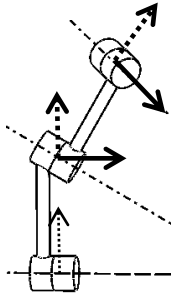
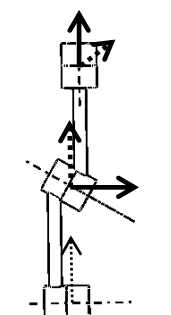
Table A.I.2 Constraint equations for 3J serial kinematic chains using the implicitization algorithm (  $w_i = \tan(\alpha_i / 2)$  , Study parameter:  $[x_0, x_1, x_2, x_3, y_0, y_1, y_2, y_3]$  )

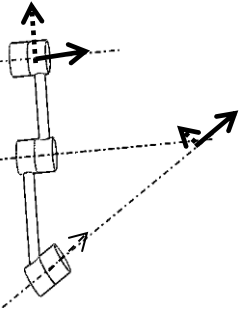
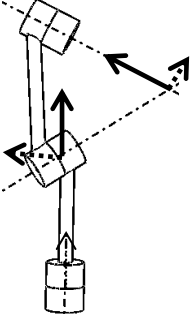
Note: solid arrow represents  $z$  axis, and dotted arrow represents  $x$  axis.

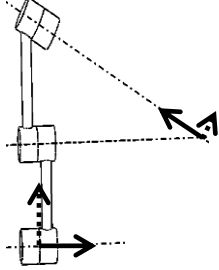
<p>1 RRR a) The axes of the first two R joints are perpendicular but do not intersect. The axes of the last two R joints are parallel.</p>  <p><math>\alpha_1 = \pi/2, d_1 = 0,</math> <math>\alpha_2 = 0, d_2 = 0.</math></p>	$x_0^2 - x_1^2 - x_2^2 + x_3^2$ $x_0 y_1 + x_1 y_0 + x_2 y_3 + x_3 y_2,$ $-x_0 y_2 + x_1 y_3 - x_2 y_0 + x_3 y_1,$ $x_0 y_3 - x_1 y_2 + x_2 y_1 - x_3 y_0,$ $y_2^2 + y_1^2 + a_1 x_1 y_1 + a_1 x_2 y_2 + \frac{1}{4} (a_1^2 - a_2^2) (x_1^2 + x_2^2)$ $y_3^2 + y_0^2 + a_1 x_1 y_1 + a_1 x_2 y_2 + \frac{1}{4} (a_1^2 - a_2^2) (x_1^2 + x_2^2)$ $-a_1 x_3 y_2 - a_1 x_1 y_0 + y_2 y_3 - y_0 y_1 + \frac{1}{4} (a_1^2 - a_2^2) (x_0 x_1 - x_2 x_3)$ $-a_1 x_3 y_1 + a_1 x_2 y_0 + y_0 y_2 + y_1 y_3 - \frac{1}{4} (a_1^2 - a_2^2) (x_0 x_2 + x_1 x_3)$
<p>RRR b) The axes of the first two R joints are perpendicular and intersect. The axes of the last two R joints are parallel.</p>  <p><math>\alpha_1 = \pi/2, d_1 = 0,</math> <math>a_1 = 0,</math> <math>\alpha_2 = 0, d_2 = 0.</math></p>	$x_0^2 - x_1^2 - x_2^2 + x_3^2,$ $x_0 y_1 + x_1 y_0 + x_2 y_3 + x_3 y_2,$ $-x_0 y_2 + x_1 y_3 - x_2 y_0 + x_3 y_1,$ $x_0 y_3 - x_1 y_2 + x_2 y_1 - x_3 y_0,$ $y_1^2 + y_2^2 - \frac{1}{4} a_2^2 (x_1^2 + x_2^2)$ $y_0^2 + y_3^2 - \frac{1}{4} a_2^2 (x_1^2 + x_2^2)$ $y_2 y_3 - y_0 y_1 - \frac{1}{4} a_2^2 (x_0 x_1 - x_2 x_3)$ $y_1 y_3 + y_0 y_2 + \frac{1}{4} a_2^2 (x_1 x_3 + x_0 x_2)$

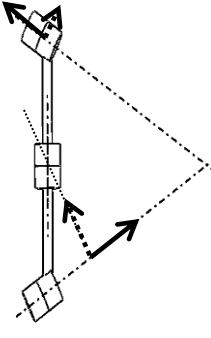
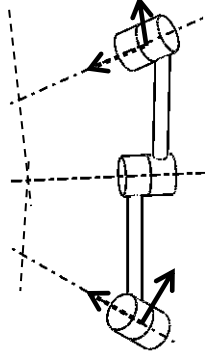
<p>RRR c) The axes of the first two R joints intersect. The axes of the last two R joints are parallel.</p>  <p><math>d_1=0, a_1=0,</math> <math>\alpha_2=0, d_2=0.</math></p>	$-wI^2 x0^2 - wI^2 x3^2 + xI^2 + x2^2,$ $x0 y3 - x1 y2 + x2 y1 - x3 y0,$ $wI^2 x0 y1 + wI^2 x3 y2 + x1 y0 + x2 y3,$ $-wI^2 x0 y2 + wI^2 x3 y1 + x1 y3 - x2 y0,$ $yI^2 + y2^2 - \frac{1}{4} a_2^2 (x0^2 + x3^2)$ $y0^2 + y3^2 - \frac{1}{4} wI^2 a_2^2 (x0^2 + x3^2)$ $y2 y3 - y0 y1 - \frac{1}{4} a_2^2 (x0 x1 - x2 x3)$ $y1 y3 + y0 y2 + \frac{1}{4} a_2^2 (x1 x3 + x0 x2)$
<p>2 RRR a) The axes of the first and third R joints are parallel. The axes of the first two R joints are perpendicular but do not intersect.</p>  <p><math>\alpha_1=\pi/2, d_1=0,</math> <math>\alpha_2=-\pi/2, d_2=0.</math></p>	$x1 y1 + x2 y2,$ $x0 y0 + x3 y3,$ $y0 y2 - \frac{1}{4} x1 x3 a_1^2 + \frac{1}{4} x1 x3 a_2^2,$ $y0 y1 + \frac{1}{4} x2 x3 a_1^2 - \frac{1}{4} x2 x3 a_2^2,$ $\frac{1}{4} x0 x1 a_1^2 - \frac{1}{4} x0 x1 a_2^2 + y2 y3,$ $y1 y3 - \frac{1}{4} x0 x2 a_1^2 + \frac{1}{4} x0 x2 a_2^2,$ $yI^2 + y2^2 - \frac{1}{4} (a_1 + a_2)^2 (x3^2 + x0^2),$ $y3^2 + y0^2 - \frac{1}{4} (a_1 - a_2)^2 (x2^2 + xI^2),$ $(a_1 + a_2) (x0 y3 + x3 y0) + (a_1 - a_2) (x1 y2 - x2 y1),$
<p>RRR b) The axes of the first and third R joints are parallel. The axes of the first two R joints are</p>	$-x1 y2 + x2 y1,$ $x0 y3 - x3 y0,$ $y0 y2 + \frac{1}{4} d_2^2 x0 x2,$ $-\frac{1}{4} d_2^2 x3^2 + y2^2 + yI^2 - \frac{1}{4} d_2^2 x0^2,$

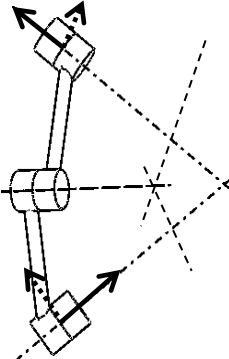
	<p>perpendicular and intersect.</p>  <p><math>\alpha_1=\pi/2, d_1=0,</math> <math>\alpha_2=-\pi/2, a_2=0.</math></p>	$y_0 y_1 + \frac{1}{4} d_2^2 x_0 x_1,$ $\frac{1}{4} d_2^2 x_2 x_3 + y_2 y_3,$ $y_0^2 + y_3^2 - \frac{1}{4} d_2^2 x_2^2 - \frac{1}{4} d_2^2 x_1^2,$ $y_1 y_3 + \frac{1}{4} d_2^2 x_1 x_3$
	<p>RRR c) The axes of the first and third R joints are parallel, the axes of the first two R joints intersect, and the axes of the last two R joints intersect.</p>  <p><math>a_1=0, d_1=0,</math> <math>a_2=0.</math></p>	$(w_2^2 + 1) (w_1^2 + 1) (d_2^2 x_0 x_1 + 4 y_0 y_1) + 2 d_2 (w_1^2 w_2^2 - 1) (x_3 y_1 - x_1 y_3) + 2 d_2 (w_1^2 - w_2^2) (x_2 y_0 - x_0 y_2)$ $(w_2^2 + 1) (w_1^2 + 1) (2 x_3 y_0 - 2 x_0 y_3) + d_2 (w_1^2 w_2^2 - 1) (x_0^2 + x_1^2 + x_2^2 + x_3^2)$ $(w_1^2 w_2^2 - 1) (d_2^2 x_0 x_2 + 4 y_0 y_2) + (w_1^2 - w_2^2) (d_2^2 x_1 x_3 + 4 y_1 y_3) + 2 d_2 (w_2^2 - 1) (w_1^2 - 1) (x_3 y_2 - x_2 y_3)$ $(w_1^2 w_2^2 - 1) (d_2^2 x_1^2 + d_2^2 x_2^2 - 4 y_0^2 - 4 y_3^2) + 2 d_2 (w_2^2 - 1) (w_1^2 - 1) (x_0 y_3 - x_3 y_0)$ $(w_2^2 + 1)^2 (d_2^2 x_0 x_2 + 4 y_0 y_2) + 2 d_2 (w_1^2 - w_2^2) (x_0 y_1 - x_1 y_0) - 2 d_2 (w_1^2 w_2^2 - 1) (x_2 y_3 + x_3 y_2)$ $(w_1^2 - w_2^2) (d_2^2 x_0 x_1 + 4 y_0 y_1) + 2 d_2 (w_2^2 - 1) (w_1^2 - 1) (x_0 y_2 - x_2 y_0) - (w_1^2 w_2^2 - 1) (d_2^2 x_2 x_3 + 4 y_2 y_3)$ $4 d_2 (w_1^2 + w_2^2) (x_3 y_0 - x_0 y_3) + (w_1^2 w_2^2 - 1) (d_2^2 x_1^2 + d_2^2 x_2^2 + 4 y_1^2 + 4 y_2^2)$ $(w_1^2 - w_2^2) (x_3 y_0 - x_0 y_3) + (w_1^2 w_2^2 - 1) (x_1 y_2 - x_2 y_1)$
3	<p>RRR a) The axes of the first two R joints intersect, the axes of the last two R joints are not in the</p>	$a_2 (w_1^2 - w_2^2) (x_0 y_2 - x_3 y_1) + w_2 (w_1^2 + 1) (a_2^2 x_1 x_3 + 4 y_0 y_2)$ $+ a_2 (w_1^2 w_2^2 - 1) (x_1 y_3 - x_2 y_0)$ $- \frac{1}{4} a_2^2 (x_3^2 + x_0^2) + y_2^2 + y_1^2$ $\frac{1}{4} a_2^2 (x_2 x_3 - x_0 x_1) + y_2 y_3 - y_0 y_1$

<p>same plane.</p>  <p><math>a_1=0, d_1=0,</math> <math>d_2=0.</math></p>	$-\frac{1}{4} a_2^2 (x_2^2 + x_1^2) + y_0^2 + y_3^2$ $a_2 (w_1^2 - w_2^2) (x_0^2 + x_1^2 + x_2^2 + x_3^2) - 4 w_2 (w_1^2 + 1) (x_1 y_1 + x_2 y_2)$ $a_2 (w_1^2 - w_2^2) (x_0^2 + x_3^2) + a_2 (w_1^2 w_2^2 - 1) (x_1^2 + x_2^2) + 4 w_2 (w_1^2 + 1) (x_0 y_0 + x_3 y_3)$ $-a_2 (w_1^2 - w_2^2) (x_0 y_1 + x_3 y_2) + a_2 (w_1^2 w_2^2 - 1) (x_1 y_0 + x_2 y_3) + w_2 (w_1^2 + 1) (a_2^2 x_2 x_3 - 4 y_0 y_1)$ $a_2 (w_1^2 - w_2^2) (x_0 y_2 - x_3 y_1) - w_2 (w_1^2 + 1) (a_2^2 x_0 x_2 + 4 y_1 y_3) + a_2 (w_1^2 w_2^2 - 1) (x_1 y_3 - x_2 y_0)$
<p>RRR b) The axes of the first two R joints intersect. The axes of the last two R joints intersect.</p>  <p><math>a_1=0, d_1=0,</math> <math>a_2=0.</math></p>	$(w_2^2 + 1) (w_1^2 + 1) (d_2^2 x_0 x_1 + 4 y_0 y_1) + 2 d_2 (w_1^2 w_2^2 - 1) (x_3 y_1 - x_1 y_3) + 2 d_2 (w_1^2 - w_2^2) (x_2 y_0 - x_0 y_2)$ $(w_2^2 + 1) (w_1^2 + 1) (2 x_3 y_0 - 2 x_0 y_3) + d_2 (w_1^2 w_2^2 - 1) (x_0^2 + x_1^2 + x_2^2 + x_3^2)$ $(w_1^2 w_2^2 - 1) (d_2^2 x_0 x_2 + 4 y_0 y_2) + (w_1^2 - w_2^2) (d_2^2 x_1 x_3 + 4 y_1 y_3) + 2 d_2 (w_2^2 - 1) (w_1^2 - 1) (x_3 y_2 - x_2 y_3)$ $(w_1^2 w_2^2 - 1) (d_2^2 x_1^2 + d_2^2 x_2^2 - 4 y_0^2 - 4 y_3^2) + 2 d_2 (w_2^2 - 1) (w_1^2 - 1) (x_0 y_3 - x_3 y_0)$ $2 d_2 (w_1^2 w_2^2 - 1) (x_3 y_2 - x_2 y_3) + (w_2^2 + 1) (w_1^2 + 1) (d_2^2 x_0 x_2 + 4 y_0 y_2) + 2 d_2 (w_1^2 - w_2^2) (x_0 y_1 - x_1 y_0)$ $2 d_2 (w_2^2 - 1) (w_1^2 - 1) (x_0 y_2 - x_2 y_0) + 2 d_2 (w_1^2 - w_2^2) (d_2^2 x_0 x_1 + 4 y_0 y_1) - (w_1^2 w_2^2 - 1) (d_2^2 x_2 x_3 + 4 y_2 y_3)$ $4 d_2 (w_1^2 + w_2^2) (x_3 y_0 - x_0 y_3) + (w_1^2 w_2^2 - 1) (d_2^2 x_1^2 + d_2^2 x_2^2 + 4 y_1^2 + 4 y_2^2)$ $(w_1^2 - w_2^2) (x_3 y_0 - x_0 y_3) + (w_1^2 w_2^2 - 1) (x_1 y_2 - x_2 y_1)$

<p> <math>\dot{R}\dot{R}\dot{R}</math> c) The axes of the first two R joints intersect. The axes of the last two R joints are parallel. </p>  <p> <math>a_1=0,</math>  <math>a_2=0, d_2=0.</math> </p>	$-wI^2 x0^2 - wI^2 x3^2 + xI^2 + x2^2,$ $-xI y2 - x3 y0 + x2 yI + x0 y3 - \frac{1}{2} d_1 (wI^2 - 1)(x0^2 + x3^2)$ $yI^2 + y2^2 + d_1 (xI y2 - x2 yI) + \frac{1}{4} (wI^2 d_1^2 - a_2^2)(x0^2 + x3^2)$ $y0^2 + y3^2 + d_1 (xI y2 - x2 yI) + \left(-\frac{1}{4} wI^2 a_2^2 - \frac{1}{4} d_1^2 + \frac{1}{2} wI^2 d_1^2\right)(x0^2 + x3^2)$ $xI y0 + x2 y3 + wI^2 (x3 y2 + x0 yI) + \frac{1}{2} d_1 (wI^2 - 1)(xI x3 - x0 x2)$ $xI y3 - x2 y0 + wI^2 (x3 yI - x0 y2) - \frac{1}{2} d_1 (wI^2 - 1)(x0 xI + x2 x3)$ $d_1 x2 y0 - y0 yI + y2 y3 - \frac{1}{2} d_1 (wI^2 - 1)x3 yI + \frac{1}{4} (wI^2 d_1^2 - a_2^2) x0 xI + \left(\frac{1}{4} wI^2 d_1^2 + \frac{1}{4} a_2^2 - \frac{1}{2} d_1^2\right) x2 x3 + \frac{1}{2} d_1 (wI^2 + 1) x0 y2$ $d_1 xI y0 + yI y3 + y0 y2 + \frac{1}{2} d_1 (wI^2 - 1)x3 y2 - \frac{1}{4} (wI^2 d_1^2 - a_2^2) x0 x2 + \left(\frac{1}{4} wI^2 d_1^2 + \frac{1}{4} a_2^2 - \frac{1}{2} d_1^2\right) xI x3 + \frac{1}{2} d_1 (wI^2 + 1) x0 yI$
<p> 4 <math>\dot{R}\dot{R}\dot{R}</math> a) The axes of the first two R joints intersect. The axes of the last two R joints intersect. </p>  <p> <math>a_1=0, d_1=0,</math>  <math>a_2=0.</math> </p>	$(w2^2 + 1) (wI^2 + 1)(d_2^2 x0 xI + 4 y0 yI) + 2 d_2 (wI^2 w2^2 - 1)(x3 yI - xI y3) + 2 d_2 (wI^2 - w2^2)(x2 y0 - x0 y2)$ $(w2^2 + 1) (wI^2 + 1)(2 x3 y0 - 2 x0 y3) + d_2 (wI^2 w2^2 - 1) (x0^2 + xI^2 + x2^2 + x3^2)$ $(wI^2 w2^2 - 1) (d_2^2 x0 x2 + 4 y0 y2) + (wI^2 - w2^2) (d_2^2 xI x3 + 4 yI y3) + 2 d_2 (w2^2 - 1) (wI^2 - 1)(x3 y2 - x2 y3)$ $(wI^2 w2^2 - 1) (d_2^2 xI^2 + d_2^2 x2^2 - 4 y0^2 - 4 y3^2) + 2 d_2 (w2^2 - 1) (wI^2 - 1)(x0 y3 - x3 y0)$ $2 d_2 (wI^2 w2^2 - 1) (x3 y2 - x2 y3) + (w2^2 + 1) (wI^2 + 1) (d_2^2 x0 x2 + 4 y0 y2) + 2 d_2 (wI^2 - w2^2)(x0 yI - xI y0)$ $2 d_2 (w2^2 - 1) (wI^2 - 1)(x0 y2 - x2 y0) + 2 d_2 (wI^2 - w2^2) (d_2^2 x0 xI + 4 y0 yI) - (wI^2 w2^2 - 1) (d_2^2 x2 x3 + 4 y2 y3)$

		$4 d_2 (w l^2 + w^2) (x_3 y_0 - x_0 y_3) + (w l^2 w^2 - 1) (d_2^2 x l^2 + d_2^2 x^2 + 4 y l^2 + 4 y^2)$ $(w l^2 - w^2) (x_3 y_0 - x_0 y_3) + (w l^2 w^2 - 1) (x l y_2 - x_2 y l)$
	<p>RRR b) The axes of the first two R joints are parallel. The axes of the last two R joints intersect.</p>  <p><math>a_1=0, d_1=0,</math> <math>a_2=0.</math></p>	$-w^2 x_0^2 - w^2 x_3^2 + x l^2 + x^2$ $\frac{1}{4} (w^2 d_2^2 - a_1^2) (x_0^2 + x_3^2) + d_2 (x l y_2 - x_2 y l) + y l^2 + y^2$ $-d_2 x_2 y_0 - \frac{1}{4} (w^2 d_2^2 - a_1^2) x_0 x l + y_2 y_3 - \frac{1}{2} d_2 (w^2 - 1) x_0 y_2 + y_0 y l + \left( \frac{1}{4} d_2^2 w^2 + \frac{1}{4} a_1^2 + \frac{1}{2} d_2^2 \right) x_2 x_3$ $- \frac{1}{2} d_2 (w^2 + 1) x_3 y l$ $y_0^2 + y_3^2 - d_2 (x l y_2 - x_2 y l) + \left( -\frac{1}{4} d_2^2 - \frac{1}{4} w^2 a_1^2 - \frac{1}{2} d_2^2 w^2 \right) (x_0^2 + x_3^2)$ $w^2 (x_3 y_2 - x_0 y l) + \frac{1}{2} d_2 (w^2 + 1) (x l x_3 + x_0 x_2) - x l y_0 + x_2 y_3$ $-d_2 x l y_0 + \frac{1}{2} d_2 (w^2 + 1) x_3 y_2 + y l y_3 + \left( \frac{1}{4} d_2^2 w^2 + \frac{1}{4} a_1^2 + \frac{1}{2} d_2^2 \right) x l x_3 + \frac{1}{4} (w^2 d_2^2 - a_1^2) x_0 x_2 - y_0 y_2$ $- \frac{1}{2} d_2 (w^2 - 1) x_0 y l$ $\frac{1}{2} d_2 (w^2 + 1) (x_0 x l - x_2 x_3) + w^2 (x_0 y_2 + x_3 y l) + x l y_3 + x_2 y_0$ $\frac{1}{2} d_2 (w^2 + 1) (x_0^2 + x_3^2) - x_3 y_0 - x_2 y l + x_0 y_3 + x l y_2$
5	<p>RRR The axes of the first and third R joints intersect at some configurations.</p>	$(w^2 + 1) (w l^2 + 1) (d_2^2 x_0 x l + 4 y_0 y l) + 2 d_2 (w l^2 w^2 - 1) (x_3 y l - x l y_3) + 2 d_2 (w l^2 - w^2) (x_2 y_0 - x_0 y_2)$ $(w^2 + 1) (w l^2 + 1) (2 x_3 y_0 - 2 x_0 y_3) + d_2 (w l^2 w^2 - 1) (x_0^2 + x l^2 + x^2 + x_3^2)$ $(w l^2 - w^2) (x_3 y_0 - x_0 y_3) + (w l^2 w^2 - 1) (x l y_2 - x_2 y l)$ $(w l^2 w^2 - 1) (d_2^2 x_0 x_2 + 4 y_0 y_2) + (w l^2 - w^2) (d_2^2 x l x_3 + 4 y l y_3) + 2 d_2 (w^2 - 1) (w l^2 - 1) (x_3 y_2 - x_2 y_3)$ $(w l^2 w^2 - 1) (d_2^2 x l^2 + d_2^2 x^2 - 4 y_0^2 - 4 y_3^2) + 2 d_2 (w^2 - 1) (w l^2 - 1) (x_0 y_3 - x_3 y_0)$

 <p> <math>a_1=0, d_1=0,</math>  <math>a_2=0.</math> </p>	$2 d_2 (w l^2 w^2 - 1) (x_3 y_2 - x_2 y_3) + (w^2 + 1) (w l^2 + 1) (d_2^2 x_0 x_2 + 4 y_0 y_2) + 2 d_2 (w l^2 - w^2) (x_0 y_1 - x_1 y_0)$ $2 d_2 (w^2 - 1) (w l^2 - 1) (x_0 y_2 - x_2 y_0) + 2 d_2 (w l^2 - w^2) (d_2^2 x_0 x_1 + 4 y_0 y_1) - (w l^2 w^2 - 1) (d_2^2 x_2 x_3 + 4 y_2 y_3)$ $4 d_2 (w l^2 + w^2) (x_3 y_0 - x_0 y_3) + (w l^2 w^2 - 1) (d_2^2 x l^2 + d_2^2 x^2 + 4 y l^2 + 4 y^2)$
<p>6 a) The axes of the first and third R joints are symmetric about the axis of the second R.</p>  <p> <math>a_2=a_1,</math>  <math>d_2=-d_1.</math> </p>	$x l^2 d_1 + x^2 d_1 + 2 x_1 y_2 - 2 x_2 y_1$ $2 w l^4 d_1^3 (x_0^2 + x_3^2) + 2 a_1 d_1 w l (w l - 1) (w l + 1) (w l^2 + 1)^2 (x_1 y_1 + x_2 y_2) + (w l^4 a_1 + 2 w l^2 d_1 - a_1) (w l^4 a_1 - 2 w l^2 d_1 - a_1) (x_1 y_2 - x_2 y_1) - 2 d_1 w l^2 (w l^2 + 1)^2 (y l^2 + y^2)$ $d_1 w l^2 (w l^6 a_1^2 + 3 w l^4 a_1^2 + 3 w l^2 a_1^2 + 2 w l^2 d_1^2 + a_1^2) x_0 x_2 - 2 d_1^2 w l^4 (w l^2 + 1) (x_0 y_1 + a_1 w l x_2 x_3) - 2 a_1 d_1 w l (w l^2 + 1)^2 (w l^2 x_0 y_2 - x_1 y_3) - 2 d_1^3 x_1 x_3 w l^4 + 2 d_1 w l^2 (w l^4 - 1) (a_1 w l x_2 y_0 - y_0 y_2) + (w l^8 a_1^2 + 2 w l^6 a_1^2 + 4 w l^4 d_1^2 - 2 w l^2 a_1^2 - a_1^2) x_2 y_3 + 2 d_1^2 w l^4 (w l^2 - 1) x_3 y_2 - 2 d_1 w l^2 (w l^2 + 1)^2 y_1 y_3 - 2 a_1 w l (w l^2 + 1)^3 y_2 y_3$ $a_1 d_1 w l^2 (w l^2 + 1) (w l^6 a_1^2 + w l^4 a_1^2 + 4 w l^4 d_1^2 - w l^2 a_1^2 - 2 w l^2 d_1^2 - a_1^2) x_0 x_2 - 2 a_1 d_1^2 w l^4 (w l^4 - 1) (x_0 y_1 + x_3 y_2) - 2 d_1 w l (w l^6 a_1^2 + w l^4 a_1^2 + 2 w l^4 d_1^2 - w l^2 a_1^2 - a_1^2) (w l^2 x_0 y_2 + x_1 y_3) + 2 a_1 d_1^3 w l^4 (w l^2 + 1) x_1 x_3 - 4 w l^5 d_1^3 x_2 y_0 + a_1 (w l^4 - 1) (w l^6 a_1^2 + w l^4 a_1^2 + 4 w l^4 d_1^2 - w l^2 a_1^2 - a_1^2) x_2 y_3 - 4 w l^7 d_1^3 x_3 y_1 + 4 d_1^2 w l^5 (w l^2 + 1) y_0 y_1 + 2 a_1 d_1 w l^2 (w l^4 - 1) (w l^2 + 1) (y_0 y_2 - y_1 y_3) - 2 w l (w l^2 + 1) (w l^6 a_1^2 + w l^4 a_1^2 + 2 w l^4 d_1^2 - w l^2 a_1^2 - a_1^2) y_2 y_3$

	$d_1 w l^2 (w l^4 a_1^2 + 2 w l^2 a_1^2 + 2 w l^2 d_1^2 + a_1^2) x_0 x_2 + (w l^6 a_1^2 + w l^4 a_1^2 + 2 w l^4 d_1^2 - w l^2 a_1^2 - a_1^2) x_2 y_3 - 2 w l^4 d_1^2 (x_0 y_1 + d_1 x_1 x_2 - x_1 y_0 + x_3 y_2) - 2 d_1 w l (w l^2 + 1) (a_1 x_1 y_3 + a_1 w l^2 x_0 y_2 - w l y_0 y_2 + w l y_1 y_3) d_1 w l - 2 a_1 w l (w l^2 + 1)^2 y_2 y_3$ $d_1 w l^2 (w l^6 a_1^2 + w l^4 a_1^2 - w l^2 a_1^2 - 2 w l^2 d_1^2 - a_1^2) x_0 x_2 + (w l^4 a_1 + 2 w l^2 d_1 - a_1) (w l^4 a_1 - 2 w l^2 d_1 - a_1) x_2 y_3 + 2 d_1^2 w l^4 (w l^2 + 1) (x_0 y_1 - x_1) + 2 d_1 w l^2 (w l^4 - 1) y_0 y_2 (1 + a_1 w l) - 2 a_1 w l (w l^2 - 1) (w l^2 + 1)^2 (y_2 y_3 + d_1 x_1 y_3) + 2 d_1^3 x_1 x_3 w l^4 - 2 d_1^2 w l^4 (w l^2 - 1) x_3 y_2 + 2 d_1 w l^2 (w l^2 + 1)^2 y_1 y_3$ $2 a_1 d_1 w l (w l^2 + 1) (x_1 y_1 + x_2 y_2) + a_1^2 (w l^2 + 1)^2 (x_1 y_2 - x_2 y_1) + 2 d_1 (y_0^2 + y_3^2) - 2 w l^2 d_1 (y l^2 + y_2^2)$ $2 a_1 d_1 w l^3 (w l^2 + 1) (x_1 y_1 + x_2 y_2) + (w l^6 a_1^2 + w l^4 a_1^2 - w l^2 a_1^2 - 2 w l^2 d_1^2 - a_1^2) (x_1 y_2 - x_2 y_1) + 2 w l^2 d_1^2 (x_3 y_0 - x_0 y_3) - 2 d_1 w l^2 (w l^2 + 1) (y l^2 + y_2^2)$
<p>b) The axes of the first and third R joints are symmetric about the plane through the axis of the second R.</p>  <p><math>a_2 = a_1,</math> <math>d_2 = -d_1.</math></p>	$x_0^2 d_1 + x_3^2 d_1 + 2 x_0 y_3 - 2 x_3 y_0$ $(w l^4 a_1^2 + 2 w l^2 a_1^2 + w l^2 d_1^2 + a_1^2) (x_0 y_3 - x_3 y_0) - a_1 d_1 w l (w l^2 + 1) (x_1 y_1 + x_2 y_2) + d_1 (w l^2 + 1) (y l^2 + y_2^2) + w l^2 d_1^2 (x_1 y_2 - x_2 y_1)$ $- 2 w l^3 d_1 (d_1 x_0 x_2 - d_1 x_1 x_3 - 2 x_3 y_2) + a_1 (w l^2 - 1) (w l^2 + 1) ((w l^2 + 1) x_0 y_2 + (w l^2 - 1) x_3 y_1) - 2 d_1 w l^3 (w l^2 + 1) x_1 y_0 - w l (w l^4 - 1) (x_3 + 2 y_1 y_3) + 2 d_1 w l^3 (w l^2 - 1) x_2 y_3 + w l (w l^2 + 1)^2 (a_1 d_1 w l x_0 x_1 - 2 y_0 y_2)$ $(w l^4 a_1^2 + 2 w l^2 a_1^2 + w l^2 d_1^2 + a_1^2) (d_1 w l^2 x_0 x_1 + (w l^2 - 1) x_0 y_2) + d_1 w l^2 (w l^2 + 1) (2 y_0 y_1 + a_1 d_1 w l x_1 x_3 - 2 a_1 w l x_1 y_0 + d_1 x_3 y_1) + a_1 w l (w l^2 + 1)^2 (d_1 x_3 y_2 - 2 y_0 y_2) + w l^4 d_1^3 x_2 x_3 - 2 w l^4 d_1^2 x_2 y_0$ $a_1 d_1 w l^2 (w l^2 + 1) (x_0 x_1 - x_2 x_3) + a_1 (w l^4 - 1) (x_0 y_2 + x_3 y_1) + 2 w l^3 d_1 (x_2 y_3 - x_1 y_0) + 2 w l d_1 (x_3 y_2 - x_0 y_1) - 2 w l (w l^2 + 1) (y_0 y_2 + y_1 y_3)$



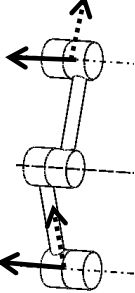
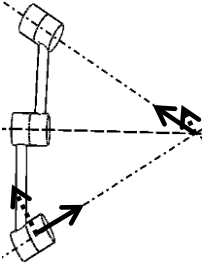
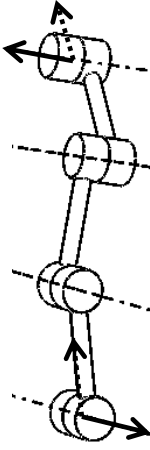
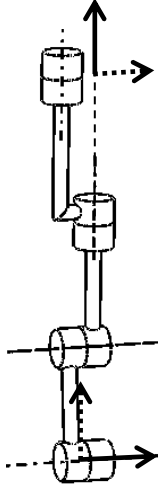
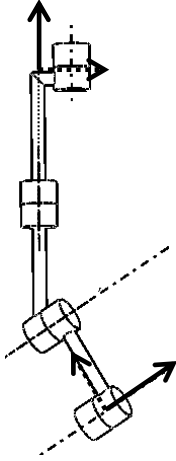
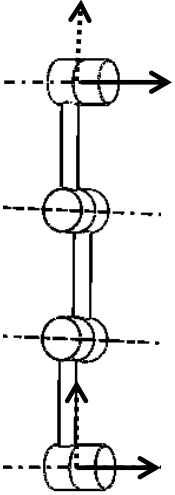
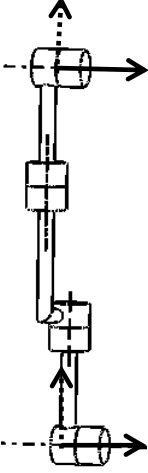
		$2 w l^2 \left( w l^4 a_1^2 + 2 w l^2 a_1^2 + w l^2 d_1^2 + a_1^2 \right) (x_0 y_3 - x_3 y_0) - w l^4 d_1^3 (x_1^2 + x_2^2) - 2 a_1 d_1 w l (w l^2 + 1)^2 (x_1 y_1 + x_2 y_2) + d_1 (w l^2 + 1)^2 (y_1^2 + y_2^2)$ $a_1^2 (w l^2 + 1)^2 (x_0 y_3 - x_3 y_0) - 2 a_1 d_1 w l (w l^2 + 1) (x_1 y_1 + x_2 y_2) + 2 d_1 (-y_0^2 w l^2 + y_1^2 + y_2^2 - y_3^2 w l^2)$ $- w l (w l^2 + 1) (d_1 x_0 y_2 - a_1 d_1 w l x_1 x_3 + 2 y_2 y_3) - 2 x_1 y_3 w l^3 d_1 - d_1^2 w l^3 (x_2 x_3 + x_0 x_1) + d_1 w l (w l^2 - 1) x_3 y_1 + a_1 (w l^4 - 1) x_3 y_2$
7	<p>The axes of the three R joints are parallel.</p>  <p><math>\alpha_1 = \alpha_2 = 0,</math> <math>d_1 = d_2 = 0.</math></p>	$x_1 = 0, \quad x_2 = 0, \quad y_0 = 0, \quad y_3 = 0.$
8	<p>The axes of the three R joints intersect at one point.</p>  <p><math>a_1 = a_2 = 0,</math> <math>d_2 = 0.</math></p>	$y_0 = 0, \quad y_1 = 0, \quad y_2 = 0, \quad y_3 = 0.$

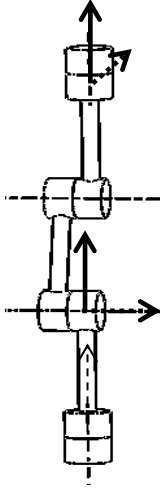
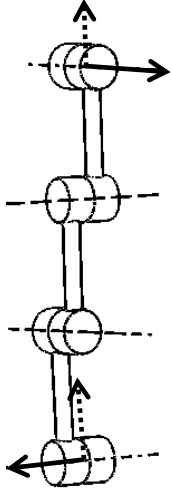
Table A.I.3 Constraint equations for 4J serial kinematic chains using the implicitization algorithm (  $w_i = \tan(\alpha_i / 2)$  , Study parameter:  $[x_0, x_1, x_2, x_3, y_0, y_1, y_2, y_3]$  )

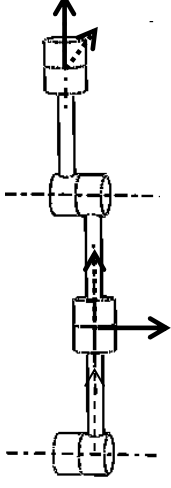
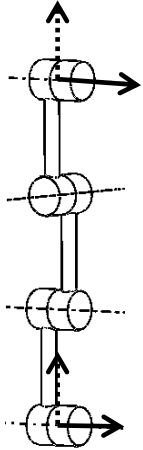
1	<p>RRRR a) The axes of the first two R joints are parallel, the axes of the last two R joints are parallel, the axes of the second and third R joints are perpendicular but not in the same plane.</p>  <p><math>\alpha_1=0, d_1=0,</math>  <math>\alpha_2=\pi/2, d_2=0,</math>  <math>\alpha_3=0, d_3=0.</math></p>	$x_0^2 - x_1^2 - x_2^2 + x_3^2$ $m(x_1^2 + x_2^2)^2 + 8(a_1^2 - a_3^2)(x_2 x_3 y_0 y_1 + x_0 x_1 y_2 y_3 - x_0 x_2 y_1 y_3 - x_1 x_3 y_0 y_2) - n(x_1 y_1 + x_2 y_2)(x_1^2 + x_2^2) + 16 a_2(x_1 y_1 + x_2 y_2)(y_0^2 + y_1^2 + y_2^2 + y_3^2) + 16(y_0^2 + y_3^2)(y_2^2 + y_1^2) + 4 a_2^2 x_3^2 (y_0^2 + y_3^2) + 4 a_2^2 x_2^2 (y_3^2 + y_1^2) + 4 a_2^2 x_1^2 (y_2^2 + y_3^2) + p(x_2 y_2 + x_1 y_1)^2 + 8 a_2^2(x_2 x_3 y_2 y_3 - x_1 x_2 y_1 y_2 + x_1 x_3 y_1 y_3)$ $m = ((a_1 + a_2)^2 - a_3^2)((a_1 - a_2)^2 - a_3^2) :$ $n = 8 a_2(a_1^2 - a_2^2 + a_3^2) :$ $p = (-8 a_1^2 + 24 a_2^2 - 8 a_3^2) :$
	<p>RRRR b) The axes of the first two R joints are parallel, the axes of the last two R joints are parallel, and the axes of the second and third R joints are perpendicular and intersect.</p> <p><math>\alpha_1=0, d_1=0,</math>  <math>\alpha_2=\pi/2, a_2=0, d_2=0,</math>  <math>\alpha_3=0, d_3=0.</math></p>	$y_1^2 + y_2^2 + d_3(x_2 y_1 - x_1 y_2) - \frac{1}{4}(a_1^2 - d_3^2)(x_1^2 + x_2^2)$ $y_0^2 + y_3^2 + d_3(x_2 y_1 - x_1 y_2) - \frac{1}{4}(a_1^2 - d_3^2)(x_1^2 + x_2^2)$ $y_1 y_3 - y_0 y_2 + d_3(x_0 y_1 + x_1 y_0) + \frac{1}{4}(a_1^2 - d_3^2)(x_1 x_3 - x_0 x_2)$ $y_2 y_3 + y_0 y_1 + d_3(x_0 y_2 + x_2 y_0) + \frac{1}{4}(a_1^2 - d_3^2)(x_0 x_1 + x_2 x_3)$ $-x_0 y_1 - x_1 y_0 + x_2 y_3 + x_3 y_2$ $x_0 y_2 + x_1 y_3 + x_2 y_0 + x_3 y_1$ $x_0 y_3 + x_1 y_2 - x_2 y_1 - x_3 y_0$ $x_0^2 - x_1^2 - x_2^2 + x_3^2$

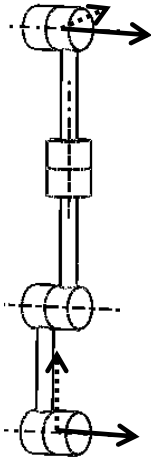
	
<p> <math>\dot{R}\dot{R}\dot{R}\dot{R}</math> c) The axes of the first two R joints are parallel, the axes of the last two R joints are parallel, and the axes of the second and third R joints intersect.         </p>  <p> <math>\alpha_1=0, d_1=0,</math>  <math>a_2=0,</math>  <math>\alpha_3=0, a_3=0.</math> </p>	$-w^2 x_0^2 - w^2 x_3^2 + x_1^2 + x_2^2,$ $y_2^2 + y_1^2 + (d_2 - d_3)(x_1 y_2 - x_2 y_1) + \frac{1}{4} (w^2 (d_2 - d_3)^2 - a_1^2)(x_0^2 + x_3^2)$ $y_0^2 + y_3^2 + (d_2 + d_3)(x_2 y_1 - x_1 y_2) + \left(-\frac{1}{4} w^2 a_1^2 - \frac{1}{2} d_2 d_3 - \frac{1}{4} d_2^2 - \frac{1}{4} d_3^2 - \frac{1}{2} w^2 d_2^2 + \frac{1}{2} w^2 d_3^2\right)(x_0^2 + x_3^2)$ $-x_1 y_0 + x_2 y_3 - w^2 (x_0 y_1 - x_3 y_2) + \left(-\frac{1}{2} w^2 d_3 + \frac{1}{2} d_3 + \frac{1}{2} d_2 + \frac{1}{2} w^2 d_2\right)(x_1 x_3 + x_0 x_2)$ $x_2 y_0 + x_1 y_3 + w^2 (x_0 y_2 + x_3 y_1) + \left(-\frac{1}{2} w^2 d_3 + \frac{1}{2} d_3 + \frac{1}{2} d_2 + \frac{1}{2} w^2 d_2\right)(x_0 x_1 - x_2 x_3)$ $x_1 y_2 - x_3 y_0 - x_2 y_1 + x_0 y_3 + \left(-\frac{1}{2} w^2 d_3 + \frac{1}{2} d_3 + \frac{1}{2} d_2 + \frac{1}{2} w^2 d_2\right)(x_3^2 + x_0^2)$ $y_0 y_1 + y_2 y_3 + (-d_2 + d_3) x_2 y_0 + \left(-\frac{1}{2} w^2 d_2 - \frac{1}{2} d_3 + \frac{1}{2} w^2 d_3 - \frac{1}{2} d_2\right) x_3 y_1 - \frac{1}{4} (w^2 (d_2 - d_3)^2 - a_1^2) x_0 x_1$ $+ \left(\frac{1}{2} w^2 d_3 - \frac{1}{2} w^2 d_2 + \frac{1}{2} d_2 + \frac{1}{2} d_3\right) x_0 y_2 + \left(\frac{1}{4} w^2 d_3^2 - \frac{1}{2} w^2 d_2 d_3 + \frac{1}{4} a_1^2 + \frac{1}{2} d_2^2 - \frac{1}{2} d_3^2 + \frac{1}{4} w^2 d_2^2\right) x_2 x_3$

		$y1 y3 - y0 y2 + (-d_2 + d_3) x1 y0 + \frac{1}{4} (w2^2 (d_2 - d_3)^2 - a_1^2) x0 x2$ $+ \left( \frac{1}{2} w2^2 d_3 - \frac{1}{2} w2^2 d_2 + \frac{1}{2} d_2 + \frac{1}{2} d_3 \right) y1 x0 + \left( -\frac{1}{2} w2^2 d_3 + \frac{1}{2} d_3 + \frac{1}{2} d_2 + \frac{1}{2} w2^2 d_2 \right) y2 x3 + \left( \frac{1}{4} w2^2 d_3^2 - \frac{1}{2} w2^2 d_2 d_3 + \frac{1}{4} a_1^2 + \frac{1}{2} d_2^2 - \frac{1}{2} d_3^2 + \frac{1}{4} w2^2 d_2^2 \right) x1 x3$
2	<p>RRR a) The axes of the first and fourth R joints are parallel, the axes of the second and third R joints are parallel, the axes of the first and second R joints are perpendicular but not in the same plane.</p>  <p><math>\alpha_1 = \pi/2, d_1 = 0,</math>  <math>\alpha_2 = 0, d_2 = 0,</math>  <math>\alpha_3 = -\pi/2, d_3 = 0.</math></p>	$x1 y1 + x2 y2,$ $x0 y0 + x3 y3,$ $m^2 x0^4 + 2 n x0^2 x1^2 + 2 n x0^2 x2^2 + 2 m^2 x0^2 x3^2 + p x0^2 y1^2$ $+ p x0^2 y2^2 + 8 m x0^2 y3^2 + e x0 x1 y2 y3 - e x0 x2 y1 y3$ $+ q^2 x1^4 + 2 q^2 x1^2 x2^2 + 2 n x1^2 x3^2 + p x1^2 y0^2 + 8 q x1^2 y2^2$ $+ p x1^2 y3^2 - e x1 x3 y0 y2 + q^2 x2^4 + 2 n x2^2 x3^2 + p x2^2 y0^2$ $+ 8 q x2^2 y1^2 + 16 q x2^2 y2^2 + p x2^2 y3^2 + e x2 x3 y0 y1$ $+ m^2 x3^4 + 8 m x3^2 y0^2 + p x3^2 y1^2 + p x3^2 y2^2 + 16 m x3^2 y3^2$ $+ 16 y0^4 + 32 y0^2 y1^2 + 32 y0^2 y2^2 + 32 y0^2 y3^2 + 16 y1^4$ $+ 32 y1^2 y2^2 + 32 y1^2 y3^2 + 16 y2^4 + 32 y2^2 y3^2 + 16 y3^4$ $m := (a_1 + a_2 + a_3) (a_1 - a_2 + a_3) :$ $n := (a_1 + a_2 + a_3) (a_1 + a_2 - a_3) (a_1 - a_2 - a_3) (a_1 - a_2 + a_3) :$ $p := -8 a_1^2 - 16 a_1 a_3 - 8 a_2^2 - 8 a_3^2 :$ $q := (a_1 - a_2 - a_3) (a_1 + a_2 - a_3)$ $e := 32(a_1 - a_3) (a_1 + a_3)$

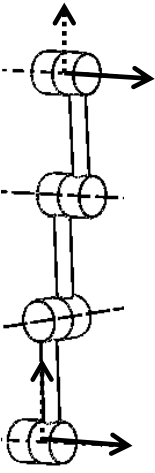
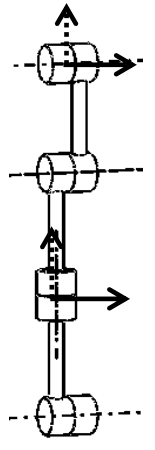
<p>RRR b) The axes of the first and fourth R joints are parallel, the axes of the second and third R joints are parallel, the axes of the first and second R joints are perpendicular and intersect.</p>  <p> <math>\alpha_1 = \pi/2, a_1=0, d_1=0,</math>  <math>\alpha_2=0,</math>  <math>\alpha_3 = -\pi/2, a_3=0.</math> </p>	$y\theta^2 + y2^2 + y3^2 + yI^2 + \left(-\frac{1}{2} d_2 d_3 - \frac{1}{4} d_3^2 - \frac{1}{4} d_2^2 - \frac{1}{4} a_2^2\right)(x\theta^2 + xI^2 + x2^2 + x3^2)$ $-mn^2(xI^2 + x2^2)^2 + 16 m y\theta^2(y\theta^2 + yI^2 + y2^2 + y3^2) - 4 n^2(xI^2 yI^2 + x2^2 y2^2) + 4 m n(xI^2 y3^2 - xI^2 y2^2 + x2^2 y3^2 - x3^2 y3^2 - x3^2 y\theta^2 + x2^2 yI^2) - 8 mn(xI x3 yI y3 + x2 x3 y2 y3) - 8 n p xI x2 yI y2 :$ $m = (d_2 + d_3)^2$ $n = (a_2^2 + d_2^2 + 2 d_2 d_3 + d_3^2)$ $p = (a_2^2 + 2 d_2^2 + 4 d_2 d_3 + 2 d_3^2)$
<p>RRR c) The axes of the first and fourth R joints are parallel, the axes of the second and third R joints are parallel, the axes of the first and second R joints are perpendicular and intersect.</p> <p> <math>\alpha_1 = \pi/2, a_1=0, d_1=0,</math>  <math>\alpha_2=0, d_2=0,</math>  <math>\alpha_3 = \pi/2, a_3=0.</math> </p>	$y\theta^2 + y2^2 + y3^2 + yI^2 + \left(-\frac{1}{4} d_3^2 - \frac{1}{4} a_2^2\right)(x\theta^2 + xI^2 + x2^2 + x3^2)$ $- n(xI^2 + x2^2) - 4 p xI^2(yI^2 - y2^2) + 16 d_3^2 y\theta^2(y\theta^2 + yI^2 + y2^2 + y3^2) + 4 p xI^2(y2^2 + y3^2) + 4 p x2^2(yI^2 + y3^2) - 4 p x3^2(y\theta^2 + y3^2) - 8 p x2 x3 y2 y3 - 8(a_2^2 + 2 d_3^2) m xI x2 yI y2 - 8 p xI x3 yI y3$ $m = (a_2^2 + d_3^2); n = d_3^2(a_2^2 + d_3^2)^2; p = d_3^2(a_2^2 + d_3^2);$

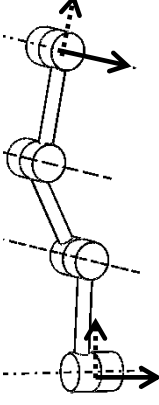
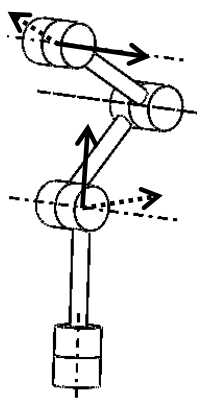
		
3	<p> <math>\dot{R}\ddot{R}\ddot{R}\ddot{R}</math> a) The axes of the first and third R joints are parallel, the axes of the second and fourth R joints are parallel, the axes of the first and second R joints are perpendicular but not in the same plane.         </p>  <p> <math>\alpha_1 = \pi/2, a_1=0, d_1=0,</math>  <math>\alpha_2 = -\pi/2, d_2=0,</math>  <math>\alpha_3 = \pi/2, d_3=0.</math> </p>	$\frac{1}{4} (x_0^2 - x_1^2 - x_2^2 + x_3^2) (a_1^2 - a_2^2 + a_3^2) + y_0^2 - y_1^2 - y_2^2 + y_3^2$ $m(x_1^2 + x_2^2)^2 + 16 a_2(x_1 y_1 + x_2 y_2) (y_0^2 + y_1^2 + y_2^2 + y_3^2) - n x_3 y_0(x_1 y_2 - x_2 y_1) + (8 x_0 x_1 a_1^2 - 8 x_0 x_1 a_3^2 + 8 x_2 x_3 a_2^2) y_3 y_2 + (-8 x_0 x_2 a_1^2 + 8 x_0 x_2 a_3^2 + 8 x_1 x_3 a_2^2) y_3 y_1 - p x_1 x_2 y_2 y_1 + 16 (y_0^2 + y_3^2)(y_2^2 + y_1^2) + 4 a_2^2 x_3^2 y_0^2 + (-8 x_1^2 a_1^2 + 24 x_1^2 a_2^2 - 8 x_1^2 a_3^2 + 4 x_2^2 a_2^2) y_1^2 + (4 x_1^2 a_2^2 - 8 x_2^2 a_1^2 + 24 x_2^2 a_2^2 - 8 x_2^2 a_3^2) y_2^2 + 4 a_2^2 (x_1^2 + x_2^2 + x_3^2) y_3^2 - q(x_1^2 + x_2^2)(x_1 y_1 + x_2 y_2)$ $m = (a_1 + a_2 + a_3) (a_1 + a_2 - a_3) (a_1 - a_2 - a_3) (a_1 - a_2 + a_3);$ $n = 8 (a_1 - a_3) (a_1 + a_3);$ $p = 8 (2 a_1^2 - 5 a_2^2 + 2 a_3^2);$ $q = 8 a_2 (a_1^2 - a_2^2 + a_3^2)$
	<p> <math>\dot{R}\ddot{R}\ddot{R}\ddot{R}</math> b) The axes of the first and third R joints are parallel, the axes of the second and         </p>	$-\frac{1}{4} (x_0^2 + x_1^2 + x_2^2 + x_3^2) (a_2^2 + a_3^2) + y_1^2 + y_0^2 + y_3^2 + y_2^2$

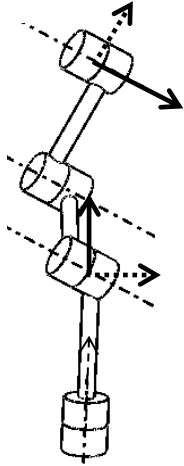
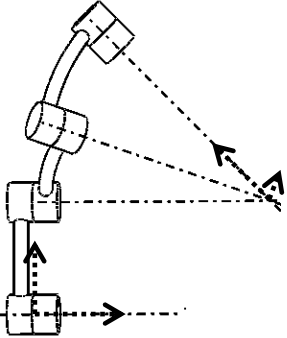
<p>fourth R are parallel, the axes of the first and second R joints are perpendicular and intersect.</p>  <p> <math>\alpha_1 = \pi/2, a_1=0, d_1=0,</math>  <math>\alpha_2 = -\pi/2, a_2=0,</math>  <math>\alpha_3 = \pi/2, a_3=0.</math> </p>	$  \begin{aligned}  & (x_1^2 + x_2^2)^2 m^2 n^2 - 8 mn (x_0 x_1 d_2^2 + x_0 x_1 d_3^2 - x_2 x_3 d_2^2 + x_2 x_3 d_3^2) y_3 y_2 + 8 mn (x_0 x_2 d_2^2 + x_0 x_2 d_3^2 + x_1 x_3 d_2^2 - x_1 x_3 d_3^2) y_3 y_1 + 8 n (3 d_2^4 + 2 d_2^2 d_3^2 + 3 d_3^4) x_1 x_2 y_1 y_2 \\  & + 8 mn^2 x_1 x_3 y_0 y_2 - 8 mn^2 x_2 x_3 y_0 y_1 - 32 mn y_0^2 y_1^2 + (-32 d_2^4 - 32 d_3^4) y_0^2 y_2^2 - 16 m^2 y_0^2 y_3^2 - 16 n^2 y_1^2 y_3^2 \\  & - 16 n^2 y_2^2 y_3^2 - 16 m^2 y_0^4 + 4 n (2 x_1^2 d_2^4 + 4 x_1^2 d_2^2 d_3^2 + 2 x_1^2 d_3^4 - x_2^2 d_2^4 + 2 x_2^2 d_2^2 d_3^2 - x_2^2 d_3^4) y_1^2 + 4 m^2 n x_3^2 y_0^2 \\  & - 4 m^2 n^2 (x_1^2 + x_2^2 - x_3^2) y_3^2 - 4 n (x_1^2 d_2^4 - 2 x_1^2 d_2^2 d_3^2 + x_1^2 d_3^4 - 2 x_2^2 d_2^4 - 4 x_2^2 d_2^2 d_3^2 - 2 x_2^2 d_3^4) y_2^2 : \\  & m = (d_2 - d_3) (d_2 + d_3); n = (d_2^2 + d_3^2)  \end{aligned}  $
<p>4. <math>\hat{R}\hat{R}\hat{R}\hat{R}</math> a) The axes of the first, second and fourth R joints are parallel, the axes of the second and third R joints are perpendicular but not in the same plane with other axes.</p>  <p> <math>\alpha_1 = 0, d_1=0,</math>  <math>\alpha_2 = \pi/2, d_2=0,</math>  <math>\alpha_3 = -\pi/2, d_3=0.</math> </p>	<p>With the conditions: <math>a_1=1, a_2=1, a_3=1.</math></p> $  \begin{aligned}  & y_3^2 - \frac{1}{4} x_2^2 - \frac{1}{4} x_1^2 + y_0^2, \\  & -3 x_0^2 x_1 y_3 - 5 x_0 x_1 x_2 y_1 - 5 x_0 x_2^2 y_2 - 3 x_0 x_2 x_3 y_3 \\  & + 8 x_0 y_2 y_3^2 + 2 x_1 x_2 x_3 y_2 - 3 x_1 x_3^2 y_3 - 4 x_1 y_1^2 y_3 \\  & + 4 x_1 y_2^2 y_3 - 2 x_2^2 x_3 y_1 + 3 x_2 x_3^2 y_0 - 4 x_2 y_0 y_1^2 \\  & - 4 x_2 y_0 y_2^2 - 8 x_2 y_1 y_2 y_3 - 8 x_3 y_0 y_2 y_3  \end{aligned}  $

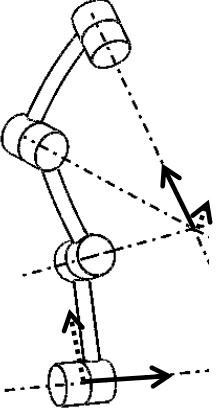
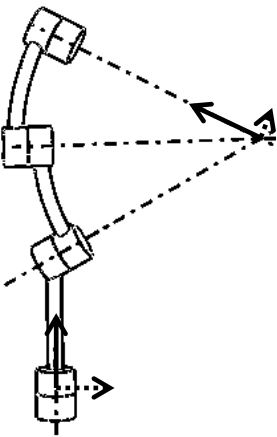
<p>RRRR b) The axes of the first, second and fourth R joints are parallel in some configuration, the axes of the second and third R joints are perpendicular and intersect with the second and fourth R axes.</p>  <p> <math>\alpha_1 = 0, d_1 = 0,</math>  <math>\alpha_2 = \pi/2, a_2 = 0,</math>  <math>\alpha_3 = -\pi/2, a_3 = 0.</math> </p>	$x_0 y_3 + x_1 y_2 - x_2 y_1 - x_3 y_0 + \frac{1}{2} d_2 (x_0^2 + x_1^2 + x_2^2 + x_3^2)$ $- m x_0 y_3 (x_1^2 + x_2^2 - x_3^2) + n (x_1^2 x_2 y_1 - x_1 x_2^2 y_2)$ $- m (x_3^3 y_0 - x_2^3 y_1 + x_1^3 y_2) - 8 d_2^4 x_0 x_2 y_1 y_3 + 8$ $d_2^4 x_0 x_1 y_2 y_3 + 8 d_2^3 y_0 (y_0^2 - y_1^2 - y_2^2 + y_3^2) x_3 + (4 y_0 y_1$ $a_1^4 - 8 y_0 y_1 a_1^2 d_3^2 + 4 y_0 y_1 d_2^4 + 4 y_0 y_1 d_3^4 + 4 y_2 y_3 a_1^4$ $- 8 y_2 y_3 a_1^2 d_3^2 - 12 y_2 y_3 d_2^4 + 4 y_2 y_3 d_3^4) x_3 x_2 + (-4 y_0 y_2 a_1^4$ $+ 8 y_0 y_2 a_1^2 d_3^2 - 4 y_0 y_2 d_2^4 - 4 y_0 y_2 d_3^4 + 4 y_1 y_3 a_1^4 - 8 y_1 y_3$ $a_1^2 d_3^2 - 12 y_1 y_3 d_2^4 + 4 y_1 y_3 d_3^4) x_3 x_1 + 8 d_2^3 y_3 (y_1^2 + y_2^2) x_0$ $+ 16 d_2^2 (y_1^2 + y_2^2) (y_0^2 + y_3^2) + 8 d_2^3 (y_0^2 y_2 + y_0 y_1 y_3$ $- y_1^2 y_2 - y_2^3 + 2 y_2 y_3^2) x_1 - 8 d_2^3 (y_0^2 y_1 - y_0 y_2 y_3 - y_1^3$ $- y_1 y_2^2 + 2 y_1 y_3^2) x_2 + 4 (y_0^2 + y_3^2) (a_1^4 - 2 a_1^2 d_3^2 - 2 d_2^4$ $+ d_3^4) x_3^2 - 4 d_2^2 (2 y_1^2 a_1^2 + 3 y_1^2 d_2^2 - 2 y_1^2 d_3^2 + 2 y_2^2 a_1^2$ $+ 2 y_2^2 d_2^2 + 2 y_2^2 d_3^2 - y_3^2 d_2^2) x_2^2 - 4 d_2^2 (2 y_1^2 a_1^2 + 2 y_1^2 d_2^2$ $+ 2 y_1^2 d_3^2 + 2 y_2^2 a_1^2 + 3 y_2^2 d_2^2 - 2 y_2^2 d_3^2 - y_3^2 d_2^2) x_1^2 + 8$ $d_2^2 (d_2^2 - 4 d_3^2) x_1 x_2 y_1 y_2 + m x_0 x_3 (x_2 y_2 + x_1 y_1) - p (x_1^2$ $+ x_2^2)$ $m = 2 d_2 (a_1^2 + d_2^2 - d_3^2) (a_1^2 - d_2^2 - d_3^2);$ $n = 2 d_2 (a_1^2 + 3 d_2^2 - d_3^2) (a_1^2 + d_2^2 - d_3^2);$ $p = 2 d_2^2 (a_1^2 + d_2^2 - d_3^2)^2;$
<p>5 RRRR a) The axes of the first, third and fourth R joints are parallel, the axes of the second and third R joints are perpendicular but not in the same plane.</p> <p> <math>\alpha_1 = \pi/2, d_1 = 0,</math>  <math>\alpha_2 = -\pi/2, d_2 = 0,</math>  <math>\alpha_3 = 0, d_3 = 0.</math> </p>	<p>With the conditions: <math>a_1 = 1, a_2 = 3, a_3 = 4.</math></p> $x_1^2 y_1^2 + 9 x_1^2 y_2^2 - 16 x_1 x_2 y_1 y_2 + 9 x_2^2 y_1^2 + x_2^2 y_2^2 - y_0^2 y_1^2$ $- y_0^2 y_2^2 - y_1^2 y_3^2 - y_2^2 y_3^2$ $- x_1^2 y_1^2 y_3^2 - 9 x_1^2 y_2^2 y_3^2 + 16 x_1 x_2 y_1 y_2 y_3^2 - 9 x_2^2 y_1^2 y_3^2$ $- x_2^2 y_2^2 y_3^2 + y_0^2 y_1^2 y_3^2 + y_0^2 y_2^2 y_3^2 + y_1^2 y_3^4 + y_2^2 y_3^4$



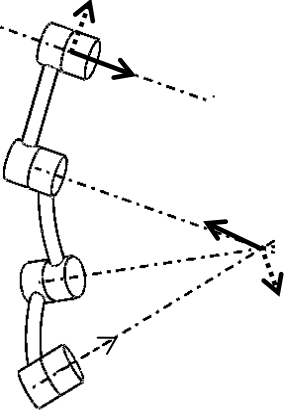
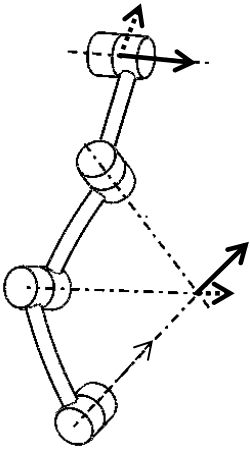
	
<p> <math>\dot{R}\dot{R}\dot{R}\dot{R}</math> b) The axes of the first, third and fourth R joints are parallel, the axes of the second R joints are perpendicular and intersect with the first and third R axes.         </p>  <p> <math>\alpha_1 = \pi/2, a_1=0, d_1=0,</math>  <math>\alpha_2 = -\pi/2, a_2=0,</math>  <math>\alpha_3=0, d_3=0.</math> </p>	$x_0 y_3 - x_1 y_2 + x_2 y_1 - x_3 y_0,$ $m(x_1^2 + x_2^2)(x_0^2 + x_3^2) + (-8x_1^2 a_3^2 + 8x_1^2 d_2^2 - 8x_2^2 a_3^2 - 8x_2^2 d_2^2)y_2^2 + (-8x_1^2 a_3^2 - 8x_1^2 d_2^2 - 8x_2^2 a_3^2 + 8x_2^2 d_2^2)y_1^2 - 32d_2^2 x_1 x_2 y_1 y_2 + 16(y_0^2 + y_3^2)(y_2^2 + y_1^2)$ $m = (a_3 - d_2)^2 (a_3 + d_2)^2;$

<p>6 RRRR a) The axes of the last three R joints are parallel, the axes of the first R is perpendicular but not in the same plane with other axes.</p>  <p><math>\alpha_1 = \pi/2, d_1=0,</math>  <math>\alpha_2 = 0, d_2=0,</math>  <math>\alpha_3=0.</math></p>	$x_0^2 - x_1^2 - x_2^2 + x_3^2,$ $-d_3^2 x_1^2 - d_3^2 x_2^2 + 2 d_3 x_1 y_2 - 2 d_3 x_2 y_1 + y_0^2 - y_1^2 - y_2^2 + y_3^2$ $d_3 x_0 x_2 - d_3 x_1 x_3 + x_0 y_1 + x_1 y_0 + x_2 y_3 + x_3 y_2,$ $d_3 x_0 x_1 + d_3 x_2 x_3 - x_0 y_2 + x_1 y_3 - x_2 y_0 + x_3 y_1,$ $d_3 x_1^2 + d_3 x_2^2 + x_0 y_3 - x_1 y_2 + x_2 y_1 - x_3 y_0,$
<p>RRRR b) The axes of the last three R joints are parallel, the axes of the first R is perpendicular and intersect with the second axis.</p> <p><math>\alpha_1 = \pi/2, a_1=0, d_1=0,</math>  <math>\alpha_2 = 0, d_2=0,</math>  <math>\alpha_3=0, d_3=0.</math></p> 	$x_0^2 - x_1^2 - x_2^2 + x_3^2,$ $y_0^2 - y_1^2 - y_2^2 + y_3^2,$ $x_0 y_1 + x_1 y_0 + x_2 y_3 + x_3 y_2,$ $-x_0 y_2 + x_1 y_3 - x_2 y_0 + x_3 y_1,$ $x_0 y_3 - x_1 y_2 + x_2 y_1 - x_3 y_0,$ <p>Without the condition: <math>d_3=0.</math></p> $x_0^2 - x_1^2 - x_2^2 + x_3^2$ $-d_3^2 x_1^2 - d_3^2 x_2^2 + 2 d_3 x_1 y_2 - 2 d_3 x_2 y_1 + y_0^2 - y_1^2 - y_2^2 + y_3^2$ $d_3 x_0 x_2 - d_3 x_1 x_3 + x_0 y_1 + x_1 y_0 + x_2 y_3 + x_3 y_2$ $d_3 x_0 x_1 + d_3 x_2 x_3 - x_0 y_2 + x_1 y_3 - x_2 y_0 + x_3 y_1$ $d_3 x_1^2 + d_3 x_2^2 + x_0 y_3 - x_1 y_2 + x_2 y_1 - x_3 y_0$
<p>RRRRc) The axes of the</p>	$-w_1^2 x_0^2 - w_1^2 x_3^2 + x_1^2 + x_2^2,$

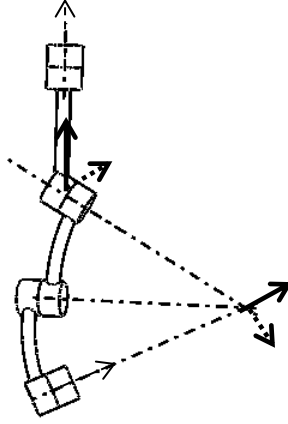
<p>last three R joints are parallel, and the axis of the first R joint intersects with the second axis.</p>  <p> <math>a_1=0, d_1=0,</math>  <math>\alpha_2=0, d_2=0,</math>  <math>\alpha_3=0, d_3=0.</math> </p>	$-w l^2 y l^2 - w l^2 y 2^2 + y 0^2 + y 3^2,$ $w l^2 x 0 y l + w l^2 x 3 y 2 + x l y 0 + x 2 y 3,$ $-w l^2 x 0 y 2 + w l^2 x 3 y l + x l y 3 - x 2 y 0,$ $x 0 y 3 - x l y 2 + x 2 y l - x 3 y 0,$
<p>7 RRRR a) The axes of the first two R joints are parallel, and the axes of the last three R joints intersect.</p>  <p> <math>a_1=0, d_1=0,</math>  <math>a_2=0,</math>  <math>a_3=0, d_3=0.</math> </p>	$y 2^2 + y l^2 + d_2 (x l y 2 - x 2 y l) + \frac{1}{4} d_2^2 (x l^2 + x 2^2) - \frac{1}{4} a_1^2 (x 0^2 + x 3^2)$ $y 0^2 + y 3^2 + d_2 (x 2 y l - x l y 2) - \frac{1}{4} d_2^2 (x 0^2 + x 3^2) - \frac{1}{4} (a_1^2 + 2 d_2^2) (x l^2 + x 2^2)$ $y 2 y 3 + y 0 y l + \frac{1}{2} d_2 (x 0 y 2 - x 2 y 0 - x 3 y l + x l y 3) + \frac{1}{4} (a_1^2 + d_2^2) (x 0 x l + x 2 x 3)$ $y l y 3 - y 0 y 2 + \frac{1}{2} d_2 (x 3 y 2 - x l y 0 - x 2 y 3 + x 0 y l) + \frac{1}{4} (a_1^2 + d_2^2) (x l x 3 - x 0 x 2)$ $x l y 2 - x 2 y l + x 0 y 3 - x 3 y 0 + \frac{1}{2} d_2 (x 0^2 + x l^2 + x 2^2 + x 3^2)$

<p>RRR<math>\dot{R}</math> b) The axes of the first two R joints are perpendicular but not in the same plane, the axes of the last three R joints intersect.</p>  <p><math>\alpha_1=\pi/2, d_1=0,</math>  <math>a_2=0,</math>  <math>a_3=0, d_3=0.</math></p>	$x_0 y_3 + x_1 y_2 - x_2 y_1 - x_3 y_0,$ $y_1^2 + y_2^2 - \frac{1}{4} (a_1^2 + d_2^2) (x_0^2 + x_3^2)$ $y_0^2 + y_3^2 - \frac{1}{4} (a_1^2 + d_2^2) (x_1^2 + x_2^2)$ $y_0 y_1 + y_2 y_3 + \frac{1}{4} (a_1^2 + d_2^2) (x_0 x_1 + x_2 x_3)$ $y_1 y_3 - y_0 y_2 + \frac{1}{4} (a_1^2 + d_2^2) (x_1 x_3 + x_0 x_2)$
<p>RRR<math>\dot{R}</math> c) The axes of the first two intersect, and the axes of the last three R joints intersect.</p>  <p><math>a_1=0,</math>  <math>a_2=0,</math>  <math>a_3=0, d_3=0.</math></p>	$w l^4 x_1^2 d_1^2 - 2 w l^4 x_1^2 d_1 d_2 + w l^4 x_1^2 d_2^2 + w l^4 x_2^2 d_1^2$ $- 2 w l^4 x_2^2 d_1 d_2 + w l^4 x_2^2 d_2^2 + 4 w l^4 x_1 y_2 d_1$ $- 4 w l^4 x_1 y_2 d_2 - 4 w l^4 x_2 y_1 d_1 + 4 w l^4 x_2 y_1 d_2 + 4 w l^4 y_1^2$ $+ 4 w l^4 y_2^2 - 4 w l^2 d_2^2 x_0^2 + 2 w l^2 x_1^2 d_1^2 - 2 w l^2 x_1^2 d_2^2$ $+ 2 w l^2 x_2^2 d_1^2 - 2 w l^2 x_2^2 d_2^2 - 4 w l^2 d_2^2 x_3^2 + 8 w l^2 x_1 y_2 d_1$ $- 8 w l^2 x_2 y_1 d_1 + 8 w l^2 y_1^2 + 8 w l^2 y_2^2 + x_1^2 d_1^2 + 2 x_1^2 d_1 d_2$ $+ x_1^2 d_2^2 + x_2^2 d_1^2 + 2 x_2^2 d_1 d_2 + x_2^2 d_2^2 + 4 x_1 y_2 d_1$ $+ 4 x_1 y_2 d_2 - 4 x_2 y_1 d_1 - 4 x_2 y_1 d_2 + 4 y_1^2 + 4 y_2^2$ $w l^2 x_0 x_1 d_1^2 - 2 w l^2 x_0 x_1 d_1 d_2 + w l^2 x_0 x_1 d_2^2 + w l^2 x_2 x_3 d_1^2$ $- 2 w l^2 x_2 x_3 d_1 d_2 + w l^2 x_2 x_3 d_2^2 + 2 w l^2 x_0 y_2 d_1$ $- 2 w l^2 x_0 y_2 d_2 + 2 w l^2 x_1 y_3 d_1 - 2 w l^2 x_1 y_3 d_2$ $- 2 w l^2 x_2 y_0 d_1 + 2 w l^2 x_2 y_0 d_2 - 2 w l^2 x_3 y_1 d_1$ $+ 2 w l^2 x_3 y_1 d_2 + 4 w l^2 y_0 y_1 + 4 w l^2 y_2 y_3 + x_0 x_1 d_1^2$ $+ 2 x_0 x_1 d_1 d_2 + x_0 x_1 d_2^2 + x_2 x_3 d_1^2 + 2 x_2 x_3 d_1 d_2 + x_2 x_3 d_2^2$ $+ 2 x_0 y_2 d_1 + 2 x_0 y_2 d_2 + 2 x_1 y_3 d_1 + 2 x_1 y_3 d_2 - 2 x_2 y_0 d_1$ $- 2 x_2 y_0 d_2 - 2 x_3 y_1 d_1 - 2 x_3 y_1 d_2 + 4 y_0 y_1 + 4 y_2 y_3$

	$ \begin{aligned} & w l^4 x \theta^2 d_1^2 - 2 w l^4 x \theta^2 d_1 d_2 + w l^4 x \theta^2 d_2^2 + 2 w l^4 x l^2 d_1^2 \\ & - 4 w l^4 x l^2 d_1 d_2 + 2 w l^4 x l^2 d_2^2 + 2 w l^4 x 2^2 d_1^2 \\ & - 4 w l^4 x 2^2 d_1 d_2 + 2 w l^4 x 2^2 d_2^2 + w l^4 x 3^2 d_1^2 - 2 w l^4 x 3^2 d_1 d_2 \\ & + w l^4 x 3^2 d_2^2 + 4 w l^4 x l y 2 d_1 - 4 w l^4 x l y 2 d_2 - 4 w l^4 x 2 y l d_1 \\ & + 4 w l^4 x 2 y l d_2 - 4 w l^4 y \theta^2 - 4 w l^4 y 3^2 + 2 w l^2 x \theta^2 d_1^2 \\ & - 2 w l^2 d_2^2 x \theta^2 + 4 w l^2 x l^2 d_1^2 + 4 w l^2 x 2^2 d_1^2 + 2 w l^2 x 3^2 d_1^2 \\ & - 2 w l^2 d_2^2 x 3^2 + 8 w l^2 x l y 2 d_1 - 8 w l^2 x 2 y l d_1 - 8 w l^2 y \theta^2 \\ & - 8 w l^2 y 3^2 + x \theta^2 d_1^2 + 2 x \theta^2 d_1 d_2 + x \theta^2 d_2^2 + 2 x l^2 d_1^2 \\ & + 4 x l^2 d_1 d_2 + 2 x l^2 d_2^2 + 2 x 2^2 d_1^2 + 4 x 2^2 d_1 d_2 + 2 x 2^2 d_2^2 \\ & + x 3^2 d_1^2 + 2 x 3^2 d_1 d_2 + x 3^2 d_2^2 + 4 x l y 2 d_1 + 4 x l y 2 d_2 \\ & - 4 x 2 y l d_1 - 4 x 2 y l d_2 - 4 y \theta^2 - 4 y 3^2 \end{aligned} $ $ \begin{aligned} & w l^2 x \theta x 2 d_1^2 - 2 w l^2 x \theta x 2 d_1 d_2 + w l^2 x \theta x 2 d_2^2 - w l^2 x l x 3 d_1^2 \\ & + 2 w l^2 x l x 3 d_1 d_2 - w l^2 x l x 3 d_2^2 - 2 w l^2 x \theta y l d_1 \\ & + 2 w l^2 x \theta y l d_2 + 2 w l^2 x l y \theta d_1 - 2 w l^2 x l y \theta d_2 \\ & + 2 w l^2 x 2 y 3 d_1 - 2 w l^2 x 2 y 3 d_2 - 2 w l^2 x 3 y 2 d_1 \\ & + 2 w l^2 x 3 y 2 d_2 + 4 w l^2 y \theta y 2 - 4 w l^2 y l y 3 + x \theta x 2 d_1^2 \\ & + 2 x \theta x 2 d_1 d_2 + x \theta x 2 d_2^2 - x l x 3 d_1^2 - 2 x l x 3 d_1 d_2 - x l x 3 d_2^2 \\ & - 2 x \theta y l d_1 - 2 x \theta y l d_2 + 2 x l y \theta d_1 + 2 x l y \theta d_2 + 2 x 2 y 3 d_1 \\ & + 2 x 2 y 3 d_2 - 2 x 3 y 2 d_1 - 2 x 3 y 2 d_2 + 4 y \theta y 2 - 4 y l y 3 \end{aligned} $ $ \begin{aligned} & w l^2 x \theta^2 d_1 - w l^2 x \theta^2 d_2 + w l^2 x l^2 d_1 - w l^2 x l^2 d_2 + w l^2 x 2^2 d_1 \\ & - w l^2 x 2^2 d_2 + w l^2 x 3^2 d_1 - w l^2 x 3^2 d_2 + 2 w l^2 x \theta y 3 \\ & + 2 w l^2 x l y 2 - 2 w l^2 x 2 y l - 2 w l^2 x 3 y \theta + x \theta^2 d_1 + x \theta^2 d_2 \\ & + x l^2 d_1 + x l^2 d_2 + x 2^2 d_1 + x 2^2 d_2 + x 3^2 d_1 + x 3^2 d_2 + 2 x \theta y 3 \\ & + 2 x l y 2 - 2 x 2 y l - 2 x 3 y \theta \end{aligned} $
--	---

<p>8 <math>\dot{R}\dot{R}\dot{R}R</math> a) The axes of the first three R joints intersect, and the axes of the last two are parallel.</p>  <p> <math>\alpha_1=0, d_1=0,</math>  <math>a_2=0, d_2=0,</math>  <math>\alpha_3=0.</math> </p>	$y2^2 + y1^2 - d_3 (x1 y2 - x2 y1) + \frac{1}{4} d_3^2 (x1^2 + x2^2) - \frac{1}{4} a_3^2 (x0^2 + x3^2)$ $y0^2 + y3^2 - d_3 (x2 y1 - x1 y2) - \frac{1}{4} d_3^2 (x0^2 + x3^2) - \frac{1}{4} (a_3^2 + 2 d_3^2) (x1^2 + x2^2)$ $-x1 y2 + x2 y1 + x0 y3 - x3 y0 + \frac{1}{2} d_3 (x0^2 + x1^2 + x2^2 + x3^2)$ $y1 y3 + y0 y2 + \frac{1}{2} d_3 (-x3 y2 - x1 y0 + x2 y3 + x0 y1) + \frac{1}{4} (a_3^2 + d_3^2) (x1 x3 + x0 x2)$ $y2 y3 - y0 y1 + \frac{1}{2} d_3 (x0 y2 - x2 y0 + x3 y1 - x1 y3) - \frac{1}{4} (a_3^2 + d_3^2) (x0 x1 - x2 x3)$
<p><math>\dot{R}\dot{R}\dot{R}R</math> b) The axes of the first three R joints intersect, the axes of the last two R joints are perpendicular but do not intersect.</p>  <p> <math>\alpha_1=0, d_1=0,</math>  <math>a_2=0, a_2=0,</math>  <math>\alpha_3=\pi/2, d_3=0.</math> </p>	$x0 y3 - x1 y2 + x2 y1 - x3 y0$ $y1^2 + y2^2 - \frac{1}{4} (a_3^2 + d_3^2) (x0^2 + x3^2)$ $y0^2 + y3^2 - \frac{1}{4} (a_3^2 + d_3^2) (x1^2 + x2^2)$ $-y0 y1 + y2 y3 - \frac{1}{4} (a_3^2 + d_3^2) (x0 x1 - x2 x3)$ $y1 y3 + y0 y2 + \frac{1}{4} (a_3^2 + d_3^2) (x1 x3 + x0 x2)$

$\dot{R}\dot{R}\dot{R}R$  c) The axes of the first three R joints intersect, and the axes of the last two R intersect.



$$\begin{aligned} a_1 &= 0, d_1 = 0, \\ a_2 &= 0, a_2 = 0, \\ a_3 &= 0. \end{aligned}$$

$$\begin{aligned} &w_3^4 x l^2 d_3^2 + w_3^4 x^2 d_3^2 + 4 w_3^4 x l y_2 d_3 - 4 w_3^4 x^2 y l d_3 \\ &+ 4 w_3^4 y l^2 + 4 w_3^4 y^2 - 4 w_3^2 d_3^2 x^2 - 2 w_3^2 x l^2 d_3^2 \\ &- 2 w_3^2 x^2 d_3^2 - 4 w_3^2 d_3^2 x^2 + 8 w_3^2 y l^2 + 8 w_3^2 y^2 + d_3^2 x l^2 \\ &+ d_3^2 x^2 - 4 d_3 x l y_2 + 4 d_3 x^2 y l + 4 y l^2 + 4 y^2 \end{aligned}$$

$$\begin{aligned} &w_3^2 x_0 x l d_3^2 - w_3^2 x_2 x_3 d_3^2 + 2 w_3^2 x_0 y_2 d_3 - 2 w_3^2 x l y_3 d_3 \\ &- 2 w_3^2 x_2 y_0 d_3 + 2 w_3^2 x_3 y l d_3 + 4 w_3^2 y_0 y l - 4 w_3^2 y_2 y_3 \\ &+ d_3^2 x_0 x l - d_3^2 x_2 x_3 - 2 d_3 x_0 y_2 + 2 d_3 x l y_3 + 2 d_3 x_2 y_0 \\ &- 2 d_3 x_3 y l + 4 y_0 y l - 4 y_2 y_3 \end{aligned}$$

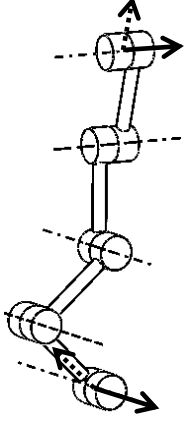
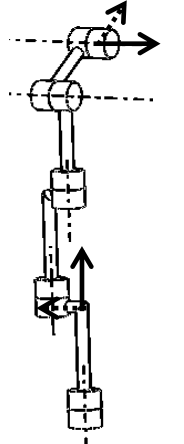
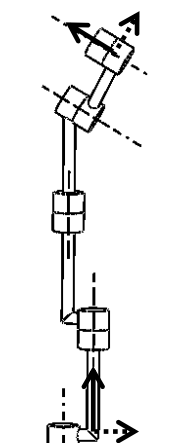
$$\begin{aligned} &w_3^4 x_0^2 d_3^2 + 2 w_3^4 x l^2 d_3^2 + 2 w_3^4 x^2 d_3^2 + w_3^4 x^2 d_3^2 \\ &+ 4 w_3^4 x l y_2 d_3 - 4 w_3^4 x^2 y l d_3 - 4 w_3^4 y_0^2 - 4 w_3^4 y_3^2 \\ &- 2 w_3^2 d_3^2 x_0^2 - 2 w_3^2 d_3^2 x^2 - 8 w_3^2 y_0^2 - 8 w_3^2 y_3^2 + d_3^2 x_0^2 \\ &+ 2 d_3^2 x l^2 + 2 d_3^2 x^2 + d_3^2 x^2 - 4 d_3 x l y_2 + 4 d_3 x^2 y l - 4 y_0^2 \\ &- 4 y_3^2 \end{aligned}$$

$$\begin{aligned} &w_3^2 x_0 x_2 d_3^2 + w_3^2 x l x_3 d_3^2 - 2 w_3^2 x_0 y l d_3 + 2 w_3^2 x l y_0 d_3 \\ &- 2 w_3^2 x_2 y_3 d_3 + 2 w_3^2 x_3 y_2 d_3 + 4 w_3^2 y_0 y_2 + 4 w_3^2 y l y_3 \\ &+ d_3^2 x_0 x_2 + d_3^2 x l x_3 + 2 d_3 x_0 y l - 2 d_3 x l y_0 + 2 d_3 x_2 y_3 \\ &- 2 d_3 x_3 y_2 + 4 y_0 y_2 + 4 y l y_3 \end{aligned}$$

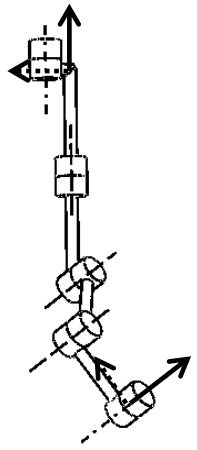
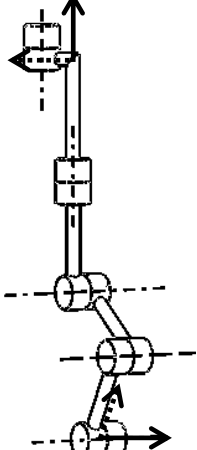
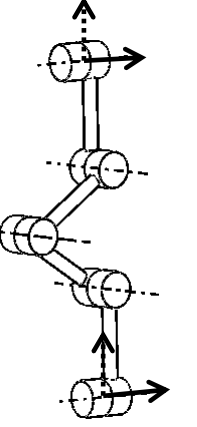
$$\begin{aligned} &w_3^2 x_0^2 d_3 + w_3^2 x l^2 d_3 + w_3^2 x^2 d_3 + w_3^2 x^2 d_3 - 2 w_3^2 x_0 y_3 \\ &+ 2 w_3^2 x l y_2 - 2 w_3^2 x^2 y l + 2 w_3^2 x_3 y_0 - d_3 x_0^2 - d_3 x l^2 \\ &- d_3 x^2 - d_3 x^2 - 2 x_0 y_3 + 2 x l y_2 - 2 x^2 y l + 2 x_3 y_0 \end{aligned}$$

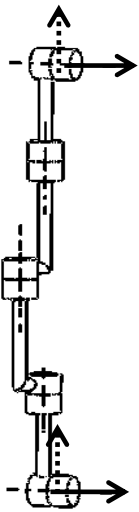
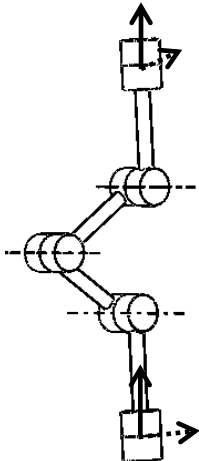
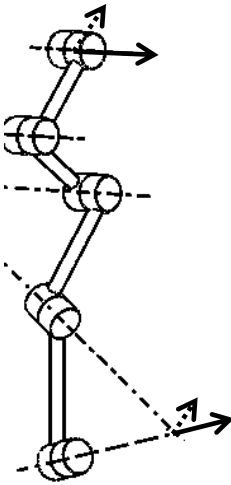
Table A.I.4 Constraint equations for 5J serial chains using the implicitization algorithm

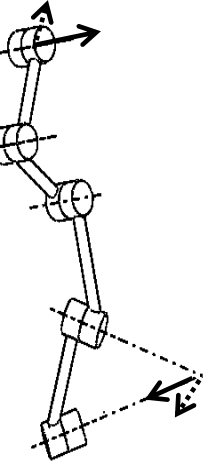
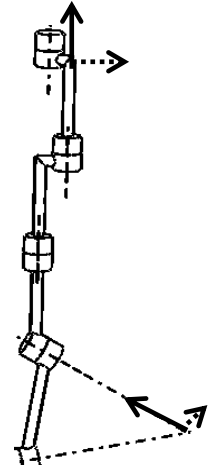
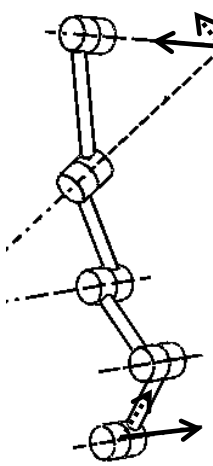
( $w_i = \tan(\alpha_i / 2)$ , Study parameter:  $[x_0, x_1, x_2, x_3, y_0, y_1, y_2, y_3]$ )

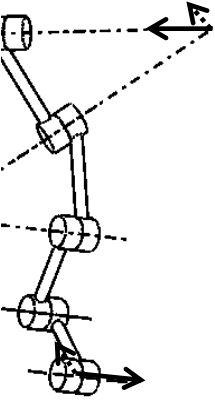
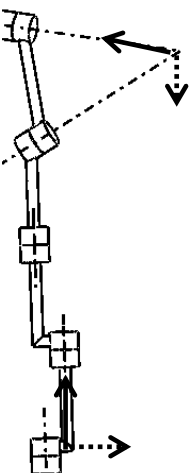
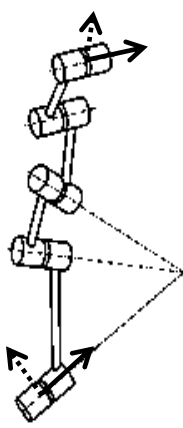
1	<p>1 <math>\dot{R}\dot{R}\ddot{R}\ddot{R}\ddot{R}</math> a)</p> 	<p>The axes of the first three R joints are parallel, and the axes of the last two R joints are parallel. The axes of the third and fourth R joints are perpendicular but not in the same plane.</p> $\alpha_1=0, d_1=0, \quad \alpha_2=0, d_2=0,$ $\alpha_3=\pi/2, d_3=0, \quad \alpha_4=0, d_4=0.$ $x_0^2 - x_1^2 - x_2^2 + x_3^2$
	<p><math>\dot{R}\dot{R}\ddot{R}\ddot{R}\ddot{R}</math> b)</p> 	<p>The axes of the first three R joints are parallel, and the axes of the last two R joints are parallel. The axes of the third and fourth R joints are perpendicular and intersect.</p> $\alpha_1=0, d_1=0, \quad \alpha_2=0,$ $\alpha_3=\pi/2, d_3=0, \quad \alpha_4=0, d_4=0.$ $x_0^2 - x_1^2 - x_2^2 + x_3^2$
	<p><math>\ddot{R}\ddot{R}\ddot{R}\dot{R}\dot{R}</math> c)</p> 	<p>The axes of the first three R joints are parallel, and the axes of the last two R joints are parallel. The axes of the third and fourth R joints intersect.</p> $\alpha_1=0, d_1=0, \quad \alpha_2=0,$ $d_3=0, \quad \alpha_4=0, d_4=0.$ $-w_3^2 x_0^2 - w_3^2 x_3^2 + x_1^2 + x_2^2$

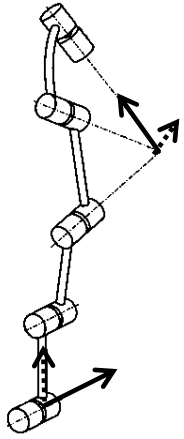
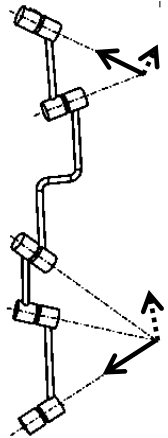
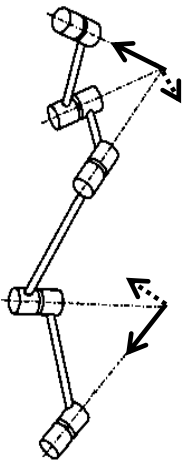


	<p>RRRRR d)</p> 	<p>The axes of the first three R joints are parallel, and the axes of the last two R joints are parallel. The axes of the third and fourth R joints intersect.</p> $\alpha_1=0, d_1=0, \quad \alpha_2=0, d_2=0,$ $a_3=0, \quad a_4=0.$ <hr/> $-w3^2 x0^2 - w3^2 x3^2 + x1^2 + x2^2$
	<p>RRRRR e)</p> 	<p>The axes of the first three R joints are parallel, and the axes of the last two R joints are parallel. The axes of the third and fourth R joints are perpendicular and intersect.</p> $\alpha_1=0, d_1=0, \quad \alpha_2=0, d_2=0,$ $\alpha_3=\pi/2, a_3=0, \quad a_4=0.$ <hr/> $x0^2 - x1^2 - x2^2 + x3^2$
2	<p>RRRRR a)</p> 	<p>The axes of the three successive R in the middle are parallel, and the axes of other two R joints are parallel. The axes of two group R joints are perpendicular but not in the same plane.</p> $\alpha_1=\pi/2, d_1=0, \quad \alpha_2=0, d_2=0,$ $\alpha_3=\pi/2, d_3=0, \quad \alpha_4=0, d_4=0.$ <hr/> $x1 y1 + x2 y2$ $x0 y0 + x3 y3$

	<p>ŘŘŘŘŘ b)</p> 	<p>The axes of the three successive R in the middle are parallel, and the axes of other two R joints are parallel. The axes of two group R joints are perpendicular and intersect.</p> $\alpha_1 = \pi/2, a_1=0, d_1=0, \quad \alpha_2=0,$ $\alpha_3=\pi/2, \quad \alpha_4=0, a_4=0.$ $(d_2^2 + 2 d_2 d_3 + 2 d_2 d_4 + d_3^2 + 2 d_3 d_4 + d_4^2)(x\theta^2 + x3^2) + (x1^2 + x2^2) - 4 (x1 y1 + x2 y2)^2$
	<p>ŘŘŘŘŘ c)</p> 	<p>The axes of the three successive R in the middle are parallel, and the axes of other two R joints are parallel. The axes of two group R joints are perpendicular and intersect.</p> $\alpha_1 = \pi/2, a_1=0, \quad \alpha_2=0, d_2=0,$ $\alpha_3=0, d_3=0, \quad \alpha_4 = \pi/2, a_4=0.$ $d_4^2(x\theta^2 + x3^2)(x1^2 + x2^2) - 4 (x1 y1 + x2 y2)^2$
3	<p>ŘŘŘŘŘ a)</p> 	<p>The axes of the first two R joints intersect, and the axes of the last three R joints are parallel. The axes of the second and third R joints intersect.</p> $a_1=0, \quad a_2=0,$ $a_3=0, d_3=0, \quad a_4=0, a_4=0.$ $(2 w2^2 + 2)(x\theta y3 + x2 y1 - x1 y2 - x3 y\theta) + (w2^2 d_1 - w2^2 d_2 + d_1 + d_2)(x\theta^2 + x3^2) + (-w2^2 d_1 - w2^2 d_2 - d_1 + d_2)(x1^2 + x2^2)$

	<p>RRRRR b)</p> 	<p>The axes of the first two R joints intersect, and the axes of the last three R joints are parallel. The axes of the second and third R are not in the same plane.</p> <p><math>a_1=0,</math>  <math>\alpha_3=0, d_3=0, \quad \alpha_4=0, a_4=0.</math></p> $(2w^2 + 2)(x_0y_3 + x_2y_1 - x_1y_2 - x_3y_0) + (w^2d_1 - w^2d_2 + d_1 + d_2)(x_0^2 + x_3^2) + (-w^2d_1 - w^2d_2 - d_1 + d_2)(x_1^2 + x_2^2)$
	<p>RRRRR c)</p> 	<p>The axes of the first two R joints intersect, and the axes of the last three R joints are parallel. The axes of the second and third R joints intersect.</p> <p><math>a_1=0, \quad a_2=0,</math>  <math>\alpha_3=0, \quad \alpha_4=0.</math></p> $(2w^2 + 2)(x_0y_3 + x_2y_1 - x_1y_2 - x_3y_0) + (w^2d_1 - w^2d_2 + w^2d_3 + w^2d_4 + d_1 + d_2 + d_3 + d_4)(x_0^2 + x_3^2) + (-w^2d_1 - w^2d_2 + w^2d_3 + w^2d_4 - d_1 + d_2 + d_3 + d_4)(x_1^2 + x_2^2)$
4	<p>RRRRR a)</p> 	<p>The axes of the first three R joints are parallel, and the axes of the last two R joints intersect. The axes of the third and fourth R joints intersect.</p> <p><math>a_1=0, d_1=0, \quad a_2=0, d_2=0,</math>  <math>a_3=0, \quad a_4=0.</math></p> $(2w^3 + 2)(x_0y_3 + x_1y_2 - x_2y_1 - x_3y_0) + (w^3d_3 - w^3d_4 + d_3 + d_4)(x_0^2 + x_1^2 + x_2^2 + x_3^2)$

<p>RRRRR b)</p> 	<p>The axes of the first three R joints are parallel, and the axes of the last two R joints intersect. The axes of the third and fourth R are not in the same plane.</p> $a_1=0, d_1=0, \quad a_2=0, d_2=0, \\ a_4=0.$ $(2w^3 + 2)(x_0y_3 + x_1y_2 - x_2y_1 - x_3y_0) + (w^3d_3 - w^3d_4 + d_3 + d_4)(x_0^2 + x_1^2 + x_2^2 + x_3^2)$
<p>RRRRR c)</p> 	<p>The axes of the first three R joints are parallel, and the axes of the last two R joints intersect. The axes of the third and fourth R joints intersect.</p> $\alpha_1=0, a_1=0, \quad a_2=0, \\ a_3=0, \quad a_4=0.$ $(2w^3 + 2)(x_0y_3 + x_1y_2 - x_2y_1 - x_3y_0) + (w^3d_1 + w^3d_2 + w^3d_3 - w^3d_4 + d_1 + d_2 + d_3 + d_4)(x_0^2 + x_1^2 + x_2^2 + x_3^2)$
<p>5 RRRRR</p> 	<p>The axes of the first three R joints intersect, and the axes of the last two R joints are parallel. The axes of the second and third R joints intersect.</p> $a_1=0, \quad a_2=0, d_2=0, \\ a_3=0, \quad d_4=0.$ $(2w^3 + 2)(x_0y_3 + x_2y_1 - x_1y_2 - x_3y_0) + (w^3d_1 - w^3d_3 + d_1 + d_3)(x_0^2 + x_3^2) + (-w^3d_1 - w^3d_3 - d_1 + d_3)(x_1^2 + x_2^2)$

6	$\ddot{R}\ddot{R}\ddot{R}\ddot{R}$ 	<p>The axes of the first two R joints are parallel, and the axes of the last three R joints intersect. The axes of the second and third R joints intersect.</p> $\alpha_1=0, d_1=0, \quad a_2=0,$ $a_3=0, \quad a_4=0, d_4=0.$ $(2w^2 + 2)(x_0y_3 + x_1y_2 - x_2y_1 - x_3y_0) + (w^2d_2 - w^2d_3 + d_2 + d_3)(x_0^2 + x_1^2 + x_2^2 + x_3^2)$
7	$(\ddot{R}\ddot{R}\ddot{R})_s\ddot{R}\ddot{R}$ 	<p>The axes of the first three R joints intersect, and the axes of the last two R joints intersect. The axes of the second and third R are not in the same plane.</p> $a_1=0, \quad a_2=0, d_2=0,$ $a_4=0.$ $y_0^2 + y_1^2 + y_2^2 + y_3^2 + \left(-\frac{1}{4}d_3^2 - \frac{1}{4}d_4^2 - \frac{1}{4}\sqrt{3}d_3d_4 + \frac{1}{4}d_1^2 - \frac{1}{4}a_3^2\right)(x_0^2 + x_1^2 + x_2^2 + x_3^2) - d_1(x_2y_1 - x_3y_0 + x_0y_3 + x_1y_2)$
8	$\ddot{R}\ddot{R}(\ddot{R}\ddot{R})_s$ 	<p>The axes of the first two R joints intersect, and the axes of the last three R joints intersect. The axes of the second and third R are not in the same plane.</p> $a_1=0,$ $a_3=0, \quad a_4=0, d_4=0.$ $y_0^2 + y_1^2 + y_2^2 + y_3^2 + \left(-\frac{1}{4}d_2^2 - \frac{1}{4}\sqrt{3}d_2d_3 - \frac{1}{4}a_2^2 + \frac{1}{4}d_1^2 - \frac{1}{4}d_3^2\right)(x_0^2 + x_1^2 + x_2^2 + x_3^2) - d_1(x_2y_1 + x_3y_0 - x_0y_3 - x_1y_2)$

## Appendix II – Expressions of $S_1$ , $S_2$ and $S_3$ in the Algebraic Approach in Chapter 5

$S_1$ :

$$\begin{aligned}
& 5.14340728 \cdot 10^8 - 4.974625224 \cdot 10^{20} v v^3 + 3.729581608 \cdot 10^{21} v^2 v^3 - \\
& 1.492387569 \cdot 10^{21} v^3 v^3 + 5.965621960 \cdot 10^{30} v^4 v^3 + 3.716176112 \cdot 10^{11} v^6 v^3 + \\
& 4.858452837 \cdot 10^{11} v^4 v^3 - 1.492387569 \cdot 10^{21} v^5 v^3 + 3.729581608 \cdot 10^{21} v^6 v^3 - \\
& 4.286183942 \cdot 10^{11} v^5 v^3 + 3.716176112 \cdot 10^{11} v^2 v^3 - \\
& 4.974625224 \cdot 10^{20} v^7 v^3 + 1.176152683 \cdot 10^{11} v v^3 - \\
& 4.286183942 \cdot 10^{11} v^3 v^3 + 5.14340728 \cdot 10^8 v^8 + 1.193124390 \cdot 10^{31} v^2 - 1.492387568 \cdot 10^{21} v^3 - \\
& 2.982810976 \cdot 10^{30} v^3 + 9.856286305 \cdot 10^9 v^4 - \\
& 1.492387568 \cdot 10^{21} v^5 + 2.386248781 \cdot 10^{31} v^4 + 1.193124390 \cdot 10^{31} v^6 - 4.974625226 \cdot 10^{20} v - \\
& 4.974625226 \cdot 10^{20} v^7 + 9.856286305 \cdot 10^9 v^8 v^3 - 2.982810976 \cdot 10^{30} v^8 v^3 + 1.176152683 \cdot 10^{11} v^7 v^3
\end{aligned}$$

(A.II.1)

$S_2$ :

$$\begin{aligned}
& -2.729093868 \cdot 10^{23} v^3 v^3 - 8.219725596 \cdot 10^{22} v^4 v^3 - 9.415309985 \cdot 10^{22} v^5 v^3 - \\
& 1.563227815 \cdot 10^{24} v^6 v^3 + 1.296609173 \cdot 10^{23} v^2 v^3 - 7.332677035 \cdot 10^{23} v^4 v^3 - \\
& 3.317711885 \cdot 10^{23} v^5 v^3 - 6.304446700 \cdot 10^{22} v^4 v^3 - \\
& 9.350993671 \cdot 10^{23} v^5 v^3 + 4.705010277 \cdot 10^{23} v^4 v^3 + 1.029431363 \cdot 10^{24} v^6 v^3 - \\
& 3.013000688 \cdot 10^{22} v^2 v^3 - 7.746981730 \cdot 10^{23} v^5 v^3 - 9.407343642 \cdot 10^{19} v^6 v^3 - \\
& 2.245548577 \cdot 10^{23} v^{16} v^3 + 1.601045900 \cdot 10^{10} v^{17} v^3 + 1.671978220 \cdot 10^{21} v^{18} v^3 + \\
& 6.949085491 \cdot 10^{22} v^{16} v^3 - 2.015199031 \cdot 10^{23} v^2 v^3 - 4.179048701 \cdot 10^{22} v^3 v^3 - \\
& 7.426364984 \cdot 10^{21} v v^3 - 3.778545211 \cdot 10^{22} v^2 v^3 - 1.291751125 \cdot 10^{23} v^3 v^3 - 2.130135835 \cdot 10^{22} v v^3 - \\
& 1.114703942 \cdot 10^{21} v^{17} v^3 + 3.021460303 \cdot 10^{22} v^6 v^3 + 9.497362709 \cdot 10^{22} v^7 v^3 - \\
& 2.906182293 \cdot 10^{23} v^8 v^3 + 3.631406041 \cdot 10^{20} v^{17} v^3 + 1.391713069 \cdot 10^{22} v^{16} v^3 - \\
& 4.509679151 \cdot 10^{10} v^{14} v^3 + 6.610588067 \cdot 10^{20} v^{14} v^3 + 1.430990542 \cdot 10^{22} v^{16} v^3 + \\
& 3.237636303 \cdot 10^{21} v^{17} v^3 + 1.20464970 \cdot 10^{20} v^{16} v^3 + 1.267069468 \cdot 10^{22} v^{16} + 2.874684456 \cdot 10^{22} v^{17} + \\
& 2.116091480 \cdot 10^{20} v^{18} + 2.131332064 \cdot 10^{23} v^{15} - \\
& 5.012490592 \cdot 10^{19} v^3 + 2.739223748 \cdot 10^9 v^{10} + 3.395418194 \cdot 10^{21} v^{18} v^3 + \\
& 1.537105723 \cdot 10^{20} v^{18} v^3 + 2.353935684 \cdot 10^{20} v^{18} v^3 + 7.202206012 \cdot 10^{21} v^{18} v^3 + \\
& 3.231842146 \cdot 10^{23} v^{12} v^3 - 9.061650742 \cdot 10^{23} v^{11} v^3 - \\
& 8.451154603 \cdot 10^{22} v^8 v^3 + 3.492850997 \cdot 10^{23} v^7 v^3 - 1.236446233 \cdot 10^{23} v^6 v^3 - \\
& 3.666548230 \cdot 10^{22} v^5 v^3 + 3.396942214 \cdot 10^{22} v^{11} v^3 - 2.657235535 \cdot 10^{23} v^7 v^3 - \\
& 2.401407925 \cdot 10^{23} v^6 v^3 + 4.855801959 \cdot 10^{21} v^{15} v^3 + 1.035323096 \cdot 10^{22} v^{15} v^3 + \\
& 3.682717202 \cdot 10^{21} v^{15} v^3 + 1.318474402 \cdot 10^{20} v^{17} v^3 - 2.584017612 \cdot 10^{23} v^3 v^3 - \\
& 3.717136071 \cdot 10^{22} v v^3 + 1.020247595 \cdot 10^{22} v^{15} v^3 + 1.872910691 \cdot 10^{22} v^{15} v^3 - \\
& 9.209535196 \cdot 10^{22} v^{15} v^3 + 8.956395465 \cdot 10^{21} v^{18} v^3 - 3.121087654 \cdot 10^{22} v^{18} v^3 -
\end{aligned}$$

$$\begin{aligned}
& 4.202215811 \cdot 10^{22} v^{17} v^3 - 2.631478265 \cdot 10^{10} v^{16} v^3 - \\
& 3.271580401 \cdot 10^{20} v^{16} v^3 + 3.065049286 \cdot 10^{21} v^{17} v^3 - \\
& 1.036711486 \cdot 10^{22} v^{17} v^3 + 1.793494749 \cdot 10^{21} v^{17} v^3 + 3.224010277 \cdot 10^{20} v^{17} v^3 + \\
& 1.077218029 \cdot 10^{22} v^{15} v^3 + 3.050778033 \cdot 10^{23} v^{15} v^3 + 1.537442313 \cdot 10^{21} v^{10} v^3 + \\
& 8.342942074 \cdot 10^{11} v^{10} v^3 - \\
& 4.228619986 \cdot 10^{20} v^{11} v^3 + 5.235276346 \cdot 10^{10} v^3 v^3 + 1.660389881 \cdot 10^{21} v^3 - \\
& 2.732015855 \cdot 10^{21} v^3 - 1.000695269 \cdot 10^{19} v^3 - 3.670260035 \cdot 10^{18} v^3 - \\
& 1.269214034 \cdot 10^{20} v^3 v^3 + 1.720991949 \cdot 10^{10} v^2 v^3 - \\
& 2.523167259 \cdot 10^{20} v^2 v^3 + 1.406795912 \cdot 10^{10} v v^3 + 1.376178294 \cdot 10^{19} v v^3 + \\
& 5.815925426 \cdot 10^{20} v^{15} v^3 + 1.484944730 \cdot 10^{10} v^{15} v^3 + 4.587540209 \cdot 10^{22} v^{16} v^3 - \\
& 5.677910937 \cdot 10^{11} v^{11} v^3 - 2.618407384 \cdot 10^{19} v^{12} v^3 + 2.625934822 \cdot 10^{11} v^{12} v^3 - \\
& 2.558026327 \cdot 10^{22} v^{10} + 1.230036118 \cdot 10^{24} v^{11} - \\
& 3.775149946 \cdot 10^{23} v^{13} v^3 + 1.811095632 \cdot 10^{23} v^{14} v^3 + 3.188603172 \cdot 10^{22} v^8 v^3 + \\
& 9.598538192 \cdot 10^{22} v^9 v^3 - 2.027997927 \cdot 10^{23} v^{10} v^3 - 1.323983355 \cdot 10^{23} v^{11} v^3 + \\
& 8.011669620 \cdot 10^{23} v^{12} v^3 - 1.737196388 \cdot 10^{22} v^{13} v^3 - 7.450739151 \cdot 10^{23} v^{14} v^3 - \\
& 3.116986665 \cdot 10^{22} v^9 v^3 - 1.320916071 \cdot 10^{23} v^{10} v^3 + 2.471985259 \cdot 10^{23} v^{11} v^3 + \\
& 3.864849903 \cdot 10^{22} v^{12} v^3 - 9.931611718 \cdot 10^{23} v^{13} v^3 + 2.314864589 \cdot 10^{23} v^{14} v^3 + \\
& 8.233479779 \cdot 10^{21} v^{10} v^3 + 6.824949120 \cdot 10^{23} v^{13} + 5.757483610 \cdot 10^{22} v^{11} v^3 - \\
& 6.491079126 \cdot 10^{22} v^{12} v^3 - \\
& 4.123656256 \cdot 10^{22} v^{13} v^3 + 2.769185526 \cdot 10^{23} v^{14} v^3 + 6.372648990 \cdot 10^{21} v^{11} v^3 - \\
& 5.968259264 \cdot 10^{22} v^{12} v^3 + 5.518883577 \cdot 10^{22} v^{16} v^3 - 3.618179662 \cdot 10^{21} v^{16} v^3 - \\
& 1.427931754 \cdot 10^{22} - 2.388161499 \cdot 10^{23} v^9 v^3 - 1.564266114 \cdot 10^{23} v^{11} v^3 - \\
& 1.529349097 \cdot 10^{24} v^{12} v^3 + 4.301113314 \cdot 10^{22} v^{13} v^3 - \\
& 5.229005887 \cdot 10^{22} v^7 v^3 + 7.345207896 \cdot 10^{20} v^{13} v^3 - 1.838966820 \cdot 10^{11} v^{13} v^3 - \\
& 2.076061212 \cdot 10^{21} v^7 v^3 - \\
& 3.491945140 \cdot 10^{11} v^7 v^3 + 1.988330841 \cdot 10^{21} v^8 v^3 + 9.682708067 \cdot 10^{11} v^8 v^3 - \\
& 2.005703663 \cdot 10^{21} v^9 v^3 - 6.815067148 \cdot 10^{11} v^9 v^3 - \\
& 2.320794093 \cdot 10^{20} v^4 v^3 + 1.372774005 \cdot 10^{11} v^4 v^3 - \\
& 9.186784216 \cdot 10^{20} v^5 v^3 + 1.954373409 \cdot 10^{21} v^{18} v^3 - 4.647338417 \cdot 10^{19} v^{18} v^3 + \\
& 4.200143081 \cdot 10^9 v^{18} v^3 - 1.445841816 \cdot 10^{10} v^5 v^3 + 7.751910156 \cdot 10^{20} v^6 v^3 + \\
& 5.339586520 \cdot 10^{11} v^6 v^3 - 4.326692914 \cdot 10^{22} v^6 v^3 - 1.308829187 \cdot 10^{24} v^7 v^3 - \\
& 3.496097199 \cdot 10^{22} v v^3 - 4.635391610 \cdot 10^{23} v^7 v^3 - 1.847512211 \cdot 10^{24} v^7 v^3 - \\
& 1.007659192 \cdot 10^{23} v^7 v^3 + 1.357352103 \cdot 10^{24} v^{10} v^3 + 4.357658036 \cdot 10^{23} v^{10} v^3 + \\
& 3.204970204 \cdot 10^{23} v^{10} v^3 - 3.711618302 \cdot 10^{23} v^9 v^3 - 1.365739731 \cdot 10^{24} v^9 v^3 + \\
& 1.378160493 \cdot 10^{23} v^8 v^3 - 3.435459472 \cdot 10^{22} v^9 v^3 - 2.199156271 \cdot 10^{24} v^8 v^3 - \\
& 2.169615058 \cdot 10^{24} v^{10} v^3 + 2.226642309 \cdot 10^{23} v^8 v^3 + 1.460796538 \cdot 10^{24} v^8 v^3 - \\
& 1.224281821 \cdot 10^{22} v^3 v^3 - 2.315631047 \cdot 10^{24} v^9 v^3 - 4.972961027 \cdot 10^{22} v^4 v^3 + \\
& 1.966909840 \cdot 10^{23} v^5 v^3 - 8.124695859 \cdot 10^{22} v^6 v^3 + 1.281356065 \cdot 10^{22} v^4 v^3 +
\end{aligned}$$

$$\begin{aligned}
& 5.485095452 \cdot 10^{22} v^5 v^3 - 1.673713969 \cdot 10^{23} v^8 v^3 + 3.790788291 \cdot 10^{23} v^9 v^3 - \\
& 1.836026617 \cdot 10^{22} v^{10} v^3 - 1.895375315 \cdot 10^{24} v^{11} v^3 + 4.214891222 \cdot 10^{23} v^{12} v^3 + \\
& 8.648707732 \cdot 10^{22} v^{13} v^3 + 3.757043911 \cdot 10^{22} v^{14} v^3 - 1.300881573 \cdot 10^{22} v^{12} v^3 + \\
& 1.988105525 \cdot 10^{22} v^{13} v^3 + 9.245415773 \cdot 10^{21} v^{14} v^3 + 1.963834250 \cdot 10^{22} v^{13} v^3 - \\
& 1.346751537 \cdot 10^{22} v^{14} v^3 - 1.222933114 \cdot 10^{22} v^{14} v^3 - \\
& 1.176247323 \cdot 10^{22} v v^3 + 9.076241636 \cdot 10^{21} v v^3 - \\
& 5.478560916 \cdot 10^{20} v^2 v^3 + 2.126281914 \cdot 10^{21} v v^3 - 2.898900491 \cdot 10^{22} v^2 v^3 - \\
& 7.032280984 \cdot 10^{22} v^3 v^3 + 9.252874582 \cdot 10^{22} v^{12} + 6.017375655 \cdot 10^{22} v^{14} - \\
& 1.554240437 \cdot 10^{21} v v^3 - 8.455618050 \cdot 10^{21} v^2 v^3 + 6.338157158 \cdot 10^{22} v^3 v^3 - \\
& 3.034474190 \cdot 10^{22} v^4 v^3 + 2.085568621 \cdot 10^{21} v^2 v^3 + 1.693489424 \cdot 10^{22} v^3 v^3 - \\
& 1.153376251 \cdot 10^{23} v^4 v^3 - 1.818484557 \cdot 10^{23} v^5 v^3 - 6.235435335 \cdot 10^{21} v^3 - \\
& 2.431963915 \cdot 10^{22} v^3 + 9.013201546 \cdot 10^{22} v^3 - 4.615163407 \cdot 10^{21} v^3 - \\
& 9.708252461 \cdot 10^{22} v^2 - 2.712284396 \cdot 10^{23} v^4 - 3.880677938 \cdot 10^{23} v^6 + \\
& 1.669498494 \cdot 10^{22} v^3 + 3.937576605 \cdot 10^{23} v^5 + 8.420093360 \cdot 10^{21} v + \\
& 9.402581825 \cdot 10^{23} v^7 - 2.700368993 \cdot 10^{23} v^8 + 1.360140012 \cdot 10^{24} v^9
\end{aligned}$$

(A.II.2)

$S_3$ :

$$\begin{aligned}
& 3.990045362 \cdot 10^{33} v^5 v^3 - 1.906546148 \cdot 10^{31} v^4 v^3 + 2.296394278 \cdot 10^{32} v^3 v^3 + \\
& 1.951298274 \cdot 10^{33} v^3 v^3 - 5.812123865 \cdot 10^{31} v^5 v^3 - \\
& 4.827086746 \cdot 10^{32} v^4 v^3 + 5.280010610 \cdot 10^{32} v^3 v^3 - 6.016597735 \cdot 10^{32} v^5 v^3 - \\
& 3.342554298 \cdot 10^{32} v^7 v^3 + 7.542872295 \cdot 10^{31} v v^3 + 8.760836205 \cdot 10^{31} v^6 v^3 + \\
& 2.640005305 \cdot 10^{33} v^7 v^3 - 2.861873158 \cdot 10^{33} v^7 v^3 + 1.598539782 \cdot 10^{33} v^7 v^3 - \\
& 2.535198074 \cdot 10^{33} v^8 v^3 + 1.230826426 \cdot 10^{33} v^{10} v^3 + 3.314434734 \cdot 10^{33} v^{10} v^3 - \\
& 8.760836205 \cdot 10^{31} v^{10} v^3 - 1.976845023 \cdot 10^{33} v^{10} v^3 - \\
& 2.861873158 \cdot 10^{33} v^9 v^3 + 2.640005305 \cdot 10^{33} v^9 v^3 - \\
& 1.598539782 \cdot 10^{33} v^9 v^3 + 3.342554298 \cdot 10^{32} v^9 v^3 + 4.712020506 \cdot 10^{33} v^8 v^3 - \\
& 2.155613374 \cdot 10^{31} v^3 + 5.614836355 \cdot 10^{21} v^5 - 8.847937850 \cdot 10^{31} v^4 - \\
& 2.211984462 \cdot 10^{32} v^6 + 7.594963935 \cdot 10^{21} v^3 - 3.228957702 \cdot 10^{31} v^3 v^3 - \\
& 1.656517424 \cdot 10^{33} v^4 v^3 + 3.512336893 \cdot 10^{33} v^5 v^3 + 6.889182835 \cdot 10^{32} v^5 v^3 - \\
& 1.906546146 \cdot 10^{31} v^6 v^3 + 6.016597735 \cdot 10^{32} v^{11} v^3 + 1.951298274 \cdot 10^{33} v^7 v^3 - \\
& 5.188109825 \cdot 10^{33} v^6 v^3 - 8.791617325 \cdot 10^{31} v^3 - \\
& 1.474656308 \cdot 10^{31} v^2 + 8.760836210 \cdot 10^{31} v^4 v^3 + 3.314434734 \cdot 10^{33} v^6 v^3 + \\
& 2.877371606 \cdot 10^{33} v^5 v^3 + 9.744448600 \cdot 10^{32} v^4 v^3 - 2.237625055 \cdot 10^{32} v^2 v^3 - \\
& 1.230826426 \cdot 10^{33} v^4 v^3 + 1.584003182 \cdot 10^{33} v^5 v^3 - 9.114523580 \cdot 10^{32} v^4 v^3 - \\
& 1.976845023 \cdot 10^{33} v^6 v^3 - 1.717123895 \cdot 10^{33} v^5 v^3 - \\
& 1.230826426 \cdot 10^{33} v^6 v^3 + 3.197079563 \cdot 10^{32} v v^3 - \\
& 5.274970395 \cdot 10^{32} v^2 v^3 + 1.598539782 \cdot 10^{33} v^3 v^3 + 3.754644091 \cdot 10^{31} v^2 v^3 - \\
& 6.685108595 \cdot 10^{31} v v^3 - 3.342554298 \cdot 10^{32} v^3 v^3 - 8.176780455 \cdot 10^{31} v v^3 -
\end{aligned}$$



$$\begin{aligned}
& 5.723746320 \cdot 10^{32} v^3 v^3 - 4.671694796 \cdot 10^{31} v^2 v^3 - \\
& 6.273732740 \cdot 10^{31} v^3 + 3.990045362 \cdot 10^{33} v^{11} v^3 + 1.906546146 \cdot 10^{31} v^{10} v^3 - \\
& 6.453840515 \cdot 10^{31} v^2 v^3 - 1.360973320 \cdot 10^{33} v^4 v^3 + 1.330015120 \cdot 10^{33} v^3 v^3 - \\
& 8.170912070 \cdot 10^{30} v^2 v^3 + 3.280563254 \cdot 10^{31} v v^3 - 1.360973320 \cdot 10^{33} v^6 v^3 - \\
& 3.597172912 \cdot 10^{20} - 9.114523580 \cdot 10^{32} v^{12} v^3 - 1.598539782 \cdot 10^{33} v^{13} v^3 - \\
& 4.671694796 \cdot 10^{31} v^{14} v^3 + 1.148197140 \cdot 10^{33} v^9 v^3 - 8.847937850 \cdot 10^{31} v^{12} + \\
& 6.257740155 \cdot 10^{30} v^3 - 2.684426957 \cdot 10^{31} v^2 v^3 - 6.457915405 \cdot 10^{30} v v^3 - \\
& 5.832742800 \cdot 10^{32} v^2 v^3 - \\
& 9.374186485 \cdot 10^{10} v^6 v^3 + 3.709352560 \cdot 10^{20} v^6 v^3 + 5.229555090 \cdot 10^{30} v^6 v^3 + \\
& 2.347307064 \cdot 10^{31} v^6 v^3 - 3.617136838 \cdot 10^{10} v^5 v^3 - \\
& 8.905757360 \cdot 10^{19} v^5 v^3 + 2.090922903 \cdot 10^{22} v^5 v^3 - \\
& 9.142675110 \cdot 10^{31} v^5 v^3 + 2.554614344 \cdot 10^{10} v^4 v^3 + 2.967482048 \cdot 10^{20} v^4 v^3 + \\
& 1.034347964 \cdot 10^{30} v^4 v^3 + 2.347307065 \cdot 10^{31} v^4 v^3 + 1.361436500 \cdot 10^{10} v^3 v^3 - \\
& 4.947643038 \cdot 10^{19} v^3 v^3 - 1.244643334 \cdot 10^{11} v^9 v^3 + 4.947642948 \cdot 10^{19} v^9 v^3 + \\
& 3.875811498 \cdot 10^{22} v^9 v^3 + 5.079263950 \cdot 10^{31} v^9 v^3 + 3.280563254 \cdot 10^{31} v^{15} v^3 + \\
& 6.685108595 \cdot 10^{31} v^{15} v^3 - 8.176780455 \cdot 10^{31} v^{15} v^3 - 3.197079563 \cdot 10^{32} v^{15} v^3 + \\
& 7.542872295 \cdot 10^{31} v^{15} v^3 + 2.287889851 \cdot 10^{10} v^{14} v^3 - 7.418705120 \cdot 10^{19} v^{14} v^3 - \\
& 4.570575250 \cdot 10^{29} v^{14} v^3 - 1.005988742 \cdot 10^{31} v^{14} v^3 + 6.23978001 \cdot 10^8 v^3 - \\
& 5.333963550 \cdot 10^9 v^3 - 1.888346556 \cdot 10^{29} v^3 + 1.676647904 \cdot 10^{30} v^3 + \\
& 2.311427381 \cdot 10^{21} v^{15} + 5.405983040 \cdot 10^{21} v^3 v^3 - 5.079263950 \cdot 10^{31} v^3 v^3 - \\
& 3.597172912 \cdot 10^{20} v^{16} - 2.211984462 \cdot 10^{32} v^{10} - 2.949312616 \cdot 10^{32} v^8 - 4.950318962 \cdot 10^{21} v^9 - \\
& 9.721238000 \cdot 10^{31} v^3 + 7.477259030 \cdot 10^{31} v^3 - \\
& 1.361818680 \cdot 10^{30} v^3 + 4.773912180 \cdot 10^{30} v^3 + 5.614836355 \cdot 10^{21} v^{11} + \\
& 7.594963935 \cdot 10^{21} v^{13} + 2.287889851 \cdot 10^{10} v^2 v^3 + 7.418705120 \cdot 10^{19} v^2 v^3 - \\
& 4.570575250 \cdot 10^{29} v^2 v^3 + 1.005988742 \cdot 10^{31} v^2 v^3 + 7.445942390 \cdot 10^9 v v^3 - \\
& 9.895286260 \cdot 10^{18} v v^3 + 4.371918688 \cdot 10^{20} v v^3 - 1.015852790 \cdot 10^{31} v v^3 - \\
& 1.951298274 \cdot 10^{33} v^9 v^3 - \\
& 2.877371606 \cdot 10^{33} v^{11} v^3 + 9.744448600 \cdot 10^{32} v^{12} v^3 + 3.342554298 \cdot 10^{32} v^{13} v^3 + \\
& 1.148197140 \cdot 10^{33} v^7 v^3 + 6.650075605 \cdot 10^{33} v^9 v^3 + 1.360973320 \cdot 10^{33} v^{10} v^3 + \\
& 1.584003182 \cdot 10^{33} v^{11} v^3 + 1.230826426 \cdot 10^{33} v^{12} v^3 - 5.723746320 \cdot 10^{32} v^{13} v^3 - \\
& 3.754644091 \cdot 10^{31} v^{14} v^3 - 1.720420200 \cdot 10^{33} v^8 v^3 + 3.228957702 \cdot 10^{31} v^9 v^3 - \\
& 5.188109825 \cdot 10^{33} v^{10} v^3 - 3.512336893 \cdot 10^{33} v^{11} v^3 - 1.951298274 \cdot 10^{33} v^{13} v^3 - \\
& 1.656517424 \cdot 10^{33} v^{12} v^3 + 5.812123865 \cdot 10^{31} v^{11} v^3 - 1.273606457 \cdot 10^{33} v^{10} v^3 + \\
& 5.274970395 \cdot 10^{32} v^{14} v^3 + 5.280010610 \cdot 10^{32} v^{13} v^3 + 1.360973320 \cdot 10^{33} v^{12} v^3 - \\
& 1.940661756 \cdot 10^{11} v^8 v^3 - 1.474656308 \cdot 10^{31} v^{14} - 8.760836210 \cdot 10^{31} v^{12} v^3 - \\
& 1.273606457 \cdot 10^{33} v^6 v^3 - 3.228957702 \cdot 10^{31} v^7 v^3 - 7.266418520 \cdot 10^{33} v^8 v^3 - \\
& 1.717123895 \cdot 10^{33} v^{11} v^3 + 6.650075605 \cdot 10^{33} v^7 v^3 + 1.900021600 \cdot 10^{32} v v^3 + \\
& 3.902596548 \cdot 10^{32} v v^3 - 6.453840515 \cdot 10^{31} v^{14} v^3 + 8.170912070 \cdot 10^{30} v^{14} v^3 +
\end{aligned}$$

$$\begin{aligned}
& 2.296394278 \cdot 10^{32} v^{13} v^3{}^8 + 2.311427381 \cdot 10^{21} v - 4.950318962 \cdot 10^{21} v^7 - \\
& 2.684426957 \cdot 10^{31} v^{14} v^3{}^6 + 3.228957702 \cdot 10^{31} v^{13} v^3{}^7 - 4.827086746 \cdot 10^{32} v^{12} v^3{}^8 + \\
& 5.832742800 \cdot 10^{32} v^{14} v^3{}^5 + 1.330015120 \cdot 10^{33} v^{13} v^3{}^6 + 1.906546148 \cdot 10^{31} v^{12} v^3{}^7 + \\
& 6.889182835 \cdot 10^{32} v^{11} v^3{}^8 - 2.237625055 \cdot 10^{32} v^{14} v^3{}^4 + 7.853968510 \cdot 10^{30} v^8 v^3{}^{10} - \\
& 1.244643334 \cdot 10^{11} v^7 v^3{}^{12} - 4.947642948 \cdot 10^{19} v^7 v^3{}^{11} + 3.875811498 \cdot 10^{22} v^7 v^3{}^{10} - \\
& 5.079263950 \cdot 10^{31} v^7 v^3{}^9 + 1.361436500 \cdot 10^{10} v^{13} v^3{}^{12} + 4.947643038 \cdot 10^{19} v^{13} v^3{}^{11} + \\
& 5.405983040 \cdot 10^{21} v^{13} v^3{}^{10} + 5.079263950 \cdot 10^{31} v^{13} v^3{}^9 + 2.554614344 \cdot 10^{10} v^{12} v^3{}^{12} - \\
& 2.967482048 \cdot 10^{20} v^{12} v^3{}^{11} + 1.034347964 \cdot 10^{30} v^{12} v^3{}^{10} - 2.347307065 \cdot 10^{31} v^{12} v^3{}^9 - \\
& 3.617136838 \cdot 10^{10} v^{11} v^3{}^{12} + 8.905757360 \cdot 10^{19} v^{11} v^3{}^{11} + 2.090922903 \cdot 10^{22} v^{11} v^3{}^{10} + \\
& 9.142675110 \cdot 10^{31} v^{11} v^3{}^9 - 9.374186485 \cdot 10^{10} v^{10} v^3{}^{12} - \\
& 3.709352560 \cdot 10^{20} v^{10} v^3{}^{11} + 5.229555090 \cdot 10^{30} v^{10} v^3{}^{10} - \\
& 2.347307064 \cdot 10^{31} v^{10} v^3{}^9 + 6.23978001 \cdot 10^8 v^{16} v^3{}^{12} + 5.333963550 \cdot 10^9 v^{16} v^3{}^{11} - \\
& 1.888346556 \cdot 10^{29} v^{16} v^3{}^{10} - 1.676647904 \cdot 10^{30} v^{16} v^3{}^9 + 9.721238000 \cdot 10^{31} v^{16} v^3{}^5 + \\
& 7.477259030 \cdot 10^{31} v^{16} v^3{}^6 + 1.361818680 \cdot 10^{30} v^{16} v^3{}^7 + 4.773912180 \cdot 10^{30} v^{16} v^3{}^8 - \\
& 6.257740155 \cdot 10^{30} v^{16} v^3 - 6.273732740 \cdot 10^{31} v^{16} v^3{}^2 + 8.791617325 \cdot 10^{31} v^{16} v^3{}^3 - \\
& 2.155613374 \cdot 10^{31} v^{16} v^3{}^4 + 7.445942390 \cdot 10^9 v^{15} v^3{}^{12} + 9.895286260 \cdot 10^{18} v^{15} v^3{}^{11} + \\
& 4.371918688 \cdot 10^{20} v^{15} v^3{}^{10} + 1.015852790 \cdot 10^{31} v^{15} v^3{}^9 - \\
& 3.902596548 \cdot 10^{32} v^{15} v^3{}^5 + 1.900021600 \cdot 10^{32} v^{15} v^3{}^6 + 6.457915405 \cdot 10^{30} v^{15} v^3{}^7
\end{aligned}$$

(A.II.3)

## Appendix III – Kinematic Analysis of Multi-Loop Multi-Mode Reconfigurable Mechanisms

This appendix mainly deals with the kinematic analysis of MLMMRMs based on work proposed in the text of this thesis. Constraint equations of serial chains with transformations in the base and moving frame (platform) are firstly unified and the kinematic analysis of a 3-RRRR MMRM is then carried out.

### A.III.1 Unifying the Constraint Equations of Serial Chains with Transformations in the Base and Moving Frames

The constraint equations obtained in Chapter 3 and Appendix I only refer to simple kinematic chains. Thus the transformations in the base and moving frame need to be unified into the constraint equations in the kinematic analysis of a parallel mechanism. Generally, the base frame is fixed at the centre of a base or at the start of a leg and the moving frame is fixed in the centre of a platform or at the end of a leg. In this appendix, the parameters from the base to the start of a leg and from the end of a leg to the moving frame are first defined.

#### A.III.1.1 Transformation in the Base

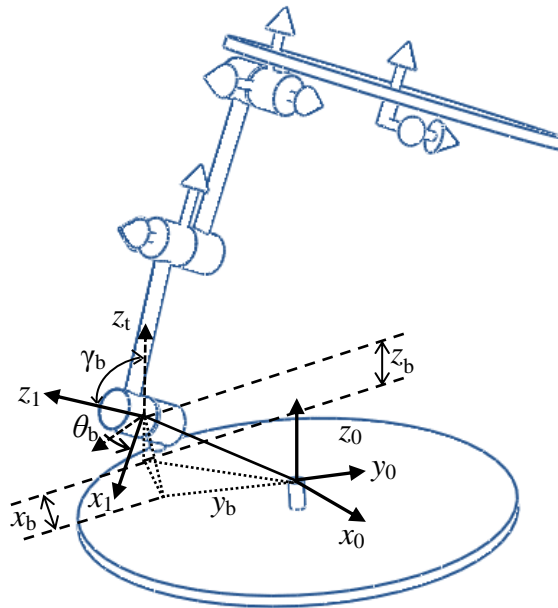


Figure A.III.1 Parameters from the base to the start of a leg

As shown in Fig. A.III.1, the origin of the base frame  $\sum_0$  is at the centre of the base with axis  $z_0$  is perpendicular with the base plane and axis  $x_0$  is parallel with the base plane. The origin of the frame  $\sum_1$  is at the centre of the first R joint with axis  $z_1$  is coincident with the axis of the first R joint and the axis  $x_1$  placed such that the plane formed by axes  $z_1$  and  $x_1$  is parallel to axis  $z_0$ .

Here, the transformation from  $\sum_0$  to  $\sum_1$  can be obtained by translating  $[x_b, y_b, z_b]$  in the frame  $\sum_0$ , then rotating  $\theta_b$  about axis  $z_1$  (as shown in Fig. A.III.1, a transition axis) and rotating  $\gamma_b$  about axis  $y_1$ , which can be represented by

$$B = B_1 \cdot B_2 \cdot B_3 \quad (\text{A.III.1})$$

where

$$B_1 = \begin{bmatrix} 1 & 0 & 0 & 0 \\ x_b & 1 & 0 & 1 \\ y_b & 0 & 1 & 0 \\ z_b & 0 & 0 & 1 \end{bmatrix} \quad (\text{A.III.2})$$

$$B_2 = \begin{bmatrix} 1 & 0 & 0 & 0 \\ 0 & \cos(\theta_b) & -\sin(\theta_b) & 0 \\ 0 & \sin(\theta_b) & \cos(\theta_b) & 0 \\ 0 & 0 & 0 & 1 \end{bmatrix} \quad (\text{A.III.3})$$

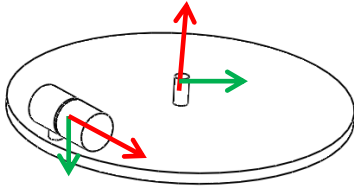
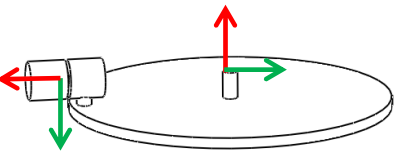
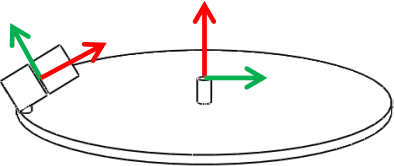
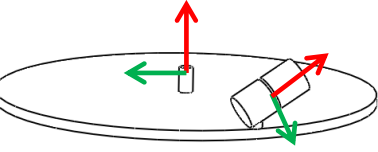
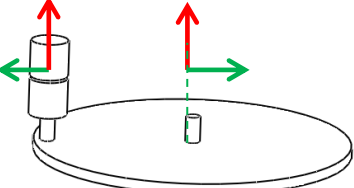
$$B_3 = \begin{bmatrix} 1 & 0 & 0 & 0 \\ 0 & \cos(\gamma_b) & 0 & \sin(\gamma_b) \\ 0 & 0 & 0 & 0 \\ 0 & -\sin(\gamma_b) & 0 & \cos(\gamma_b) \end{bmatrix} \quad (\text{A.III.4})$$

The transformation from the base to the start of a leg can be obtained by multiplying the three matrixes together:

$$B = \begin{bmatrix} 1 & 0 & 0 & 0 \\ x_b & \cos(\theta_b)\cos(\gamma_b) & -\sin(\theta_b) & \cos(\theta_b)\sin(\gamma_b) \\ y_b & \sin(\theta_b)\cos(\gamma_b) & \cos(\theta_b) & \sin(\theta_b)\sin(\gamma_b) \\ z_b & -\sin(\gamma_b) & 0 & \cos(\gamma_b) \end{bmatrix} \quad (\text{A.III.5})$$

Generally, there are some common arrangements for the connection of the base and the legs; some cases along with simple transformations are listed in Table A.III.1.

Table A.III.1 Some usual arrangements between a base and a leg

<p>(1)</p>  <p><math>z_b = 0, \gamma_b = \pi/2.</math></p>	$B = \begin{bmatrix} 1 & 0 & 0 & 0 \\ x_b & 0 & -\sin(\theta_b) & \cos(\theta_b) \\ y_b & 0 & \cos(\theta_b) & \sin(\theta_b) \\ 0 & -1 & 0 & 0 \end{bmatrix}$
<p>(2)</p>  <p><math>z_b = 0, \gamma_b = \pi/2.</math></p>	$B = \begin{bmatrix} 1 & 0 & 0 & 0 \\ x_b & 0 & -\sin(\theta_b) & \cos(\theta_b) \\ y_b & 0 & \cos(\theta_b) & \sin(\theta_b) \\ 0 & -1 & 0 & 0 \end{bmatrix}$
<p>(3)</p>  <p><math>z_b = 0.</math></p>	$B = \begin{bmatrix} 1 & 0 & 0 & 0 \\ x_b & \cos(\theta_b)\cos(\gamma_b) & -\sin(\theta_b) & \cos(\theta_b)\sin(\gamma_b) \\ y_b & \sin(\theta_b)\cos(\gamma_b) & \cos(\theta_b) & \sin(\theta_b)\sin(\gamma_b) \\ 0 & -\sin(\gamma_b) & 0 & \cos(\gamma_b) \end{bmatrix}$
<p>(4)</p>  <p><math>z_b = 0.</math></p>	$B = \begin{bmatrix} 1 & 0 & 0 & 0 \\ x_b & \cos(\theta_b)\cos(\gamma_b) & -\sin(\theta_b) & \cos(\theta_b)\sin(\gamma_b) \\ y_b & \sin(\theta_b)\cos(\gamma_b) & \cos(\theta_b) & \sin(\theta_b)\sin(\gamma_b) \\ 0 & -\sin(\gamma_b) & 0 & \cos(\gamma_b) \end{bmatrix}$
<p>(5)</p>  <p><math>z_b = 0, \gamma_b = 0.</math></p>	$B = \begin{bmatrix} 1 & 0 & 0 & 0 \\ x_b & \cos(\theta_b) & -\sin(\theta_b) & 0 \\ y_b & \sin(\theta_b) & \cos(\theta_b) & 0 \\ 0 & 0 & 0 & 0 \end{bmatrix}$

### A.III.1.2 Transformation in the Platform

The origin of the platform frame  $\Sigma_m$  is at the centre of the platform, axis  $z_m$  is perpendicular with the platform plane and axis  $x_m$  is parallel with the platform plane.

The origin of the frame  $\Sigma_i$  is at the centre of the last  $R$  joint of a leg, axis  $z_i$  is coincident with the axis of the  $R_i$  joint and axis  $x_i$  is parallel with the platform plane (Fig. A.III.2).

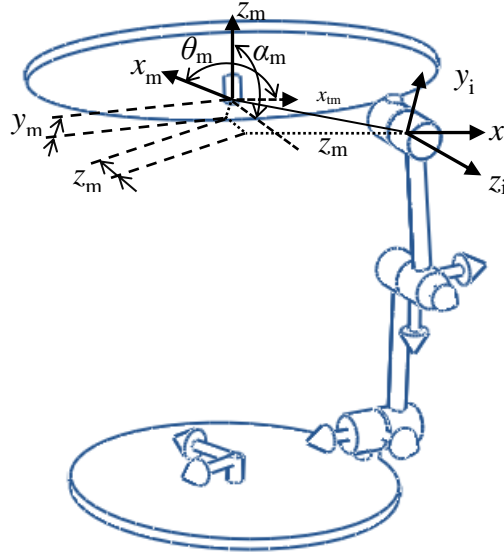


Figure A.III.2 Parameters from the end of a leg to the platform

The transformation can be continued in the frame  $\Sigma_i$  by first translating  $[x_m, y_m, z_m]$ , then rotating  $\alpha_m$  about  $x_i$  and rotating  $\theta_m$  about  $z_m$  which can be expressed as:

$$M = M_1 \cdot M_2 \cdot M_3 \quad (\text{A.III.6})$$

where

$$M_1 = \begin{bmatrix} 1 & 0 & 0 & 0 \\ x_m & 1 & 0 & 1 \\ y_m & 0 & 1 & 0 \\ z_m & 0 & 0 & 1 \end{bmatrix} \quad (\text{A.III.7})$$

$$M_2 = \begin{bmatrix} 1 & 0 & 0 & 0 \\ 0 & 1 & 0 & 1 \\ 0 & 0 & \cos(\alpha_m) & -\sin(\alpha_m) \\ 0 & 0 & \sin(\alpha_m) & \cos(\alpha_m) \end{bmatrix} \quad (\text{A.III.8})$$

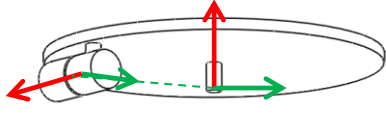
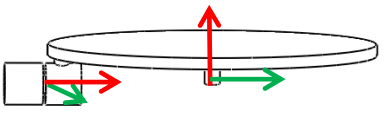
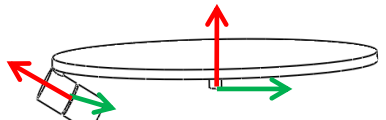
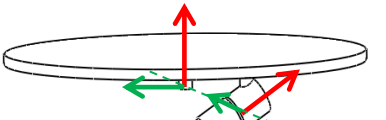
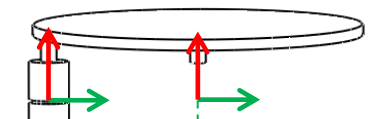
$$M_3 = \begin{bmatrix} 1 & 0 & 0 & 0 \\ 0 & \cos(\theta_m) & -\sin(\theta_m) & 0 \\ 0 & \sin(\theta_m) & \cos(\theta_m) & 0 \\ 0 & 0 & 0 & 1 \end{bmatrix} \quad (\text{A.III.9})$$

then multiplying the above three matrixes together gives:

$$M = \begin{bmatrix} 1 & 0 & 0 & 0 \\ x_m & \cos(\theta_m) & -\sin(\theta_m) & 0 \\ y_m & \cos(\alpha_m)\sin(\theta_m) & \cos(\alpha_m)\cos(\theta_m) & -\sin(\alpha_m) \\ z_m & \sin(\alpha_m)\sin(\theta_m) & \sin(\alpha_m)\cos(\theta_m) & \cos(\alpha_m) \end{bmatrix} \quad (\text{A.III.10})$$

Some common cases of the connection between a leg and platform along with their transformations are shown in Table A.III.2.

Table A.III.2 Some common arrangements between a leg and a platform

<p>(1)</p>  <p><math>\alpha_m = \pi/2, z_m = 0.</math></p>	$M = \begin{bmatrix} 1 & 0 & 0 & 0 \\ x_m & \cos(\theta_m) & -\sin(\theta_m) & 0 \\ y_m & 0 & 0 & -1 \\ 0 & \sin(\theta_m) & \cos(\theta_m) & 0 \end{bmatrix}$
<p>(2)</p>  <p><math>\alpha_m = \pi/2, z_m = 0.</math></p>	$M = \begin{bmatrix} 1 & 0 & 0 & 0 \\ x_m & \cos(\theta_m) & -\sin(\theta_m) & 0 \\ y_m & 0 & 0 & -1 \\ 0 & \sin(\theta_m) & \cos(\theta_m) & 0 \end{bmatrix}$
<p>(3)</p>  <p><math>z_m = 0.</math></p>	$M = \begin{bmatrix} 1 & 0 & 0 & 0 \\ x_m & \cos(\theta_m) & -\sin(\theta_m) & 0 \\ y_m & \cos(\alpha_m)\sin(\theta_m) & \cos(\alpha_m)\cos(\theta_m) & -\sin(\alpha_m) \\ 0 & \sin(\alpha_m)\sin(\theta_m) & \sin(\alpha_m)\cos(\theta_m) & \cos(\alpha_m) \end{bmatrix}$
<p>(4)</p>  <p><math>z_m = 0.</math></p>	$M = \begin{bmatrix} 1 & 0 & 0 & 0 \\ x_m & \cos(\theta_m) & -\sin(\theta_m) & 0 \\ y_m & \cos(\alpha_m)\sin(\theta_m) & \cos(\alpha_m)\cos(\theta_m) & -\sin(\alpha_m) \\ 0 & \sin(\alpha_m)\sin(\theta_m) & \sin(\alpha_m)\cos(\theta_m) & \cos(\alpha_m) \end{bmatrix}$
<p>(5)</p>  <p><math>\alpha_m = 0, z_m = 0.</math></p>	$M = \begin{bmatrix} 1 & 0 & 0 & 0 \\ x_m & \cos(\theta_m) & -\sin(\theta_m) & 0 \\ y_m & \sin(\theta_m) & \cos(\theta_m) & 0 \\ 0 & 0 & 0 & 1 \end{bmatrix}$

### ***A.III.1.3 Obtaining Complete Constraint Equations for a Parallel Mechanism by Unifying Transformations in the Base and Platform***

Once the transformations in the base and platform are obtained, the associated study parameters can be calculated according to Eqs. (2.31) and (2.32) leading to the construction of the projective transformation matrixes in the kinematic mapping space. Then the projective transformation matrixes can be applied to a serial chain (leg) by

$$X_i = (T_b \cdot T_m)^{-1} \cdot X \quad (\text{A.III.11})$$

where  $X$  is study parameters in the constraint equations for a serial chain,  $X_i$  is study parameters in the constraint equations of a parallel mechanism. The next step is to replace  $X$  using  $X_i$  so that the constraint equations for a parallel mechanism, “Eq. (p)”, can be obtained

$$\text{Eq. (p)} = \text{Eq. (s)}(X \rightarrow X_i) \quad (\text{A.III.12})$$

where “Eq. (s)” represent the constraint equations for a serial chain.

### ***A.III.1.4 An Example of Obtaining Complete Constraint Equations for a Leg of a Parallel Mechanism***

In the following, an example to obtain the constraint equations for a 3R-leg parallel mechanism is demonstrated. A 3R chain in Table 3.3 1-(a) is arranged as one leg for a parallel mechanism, as shown in the Fig. A.III.3. The parameters for the leg are listed below:

$$\begin{aligned} x_b=0, y_b=1, z_b=0, \theta_b=0, \gamma_b=-\pi/3, \\ x_m=0, y_m=0, z_m=1, \alpha_m=\pi/2, \theta_m=\pi/6, \\ a_1=1, a_2=1, \end{aligned} \quad (\text{A.III.13})$$



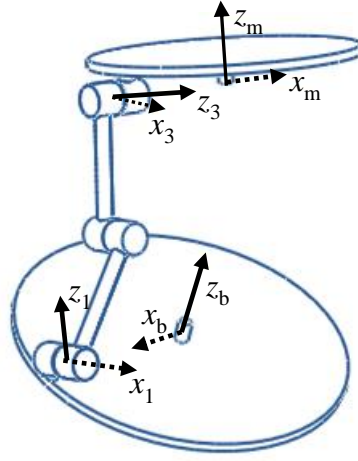


Figure A.III.3 Parallel mechanism with 3R-leg

There are nine equations for this 3R chain, and three equations (Eqs. (3.2), (3.3) and (3.9)) are selected according to the previous analysis in Chapter 3. Meanwhile, their transformations in the base and platform can be obtained according to Tables A.III.1-(4) and A.III.2-(2):

$$B = \begin{bmatrix} 1 & 0 & 0 & 0 \\ 0 & 1/2 & 0 & -\sqrt{3}/2 \\ 1 & 0 & 1 & 0 \\ 0 & \sqrt{3}/2 & 0 & 1/2 \end{bmatrix} \quad (\text{A.III.14 a})$$

$$M = \begin{bmatrix} 1 & 0 & 0 & 0 \\ 0 & \sqrt{3}/2 & -1/2 & 0 \\ 0 & 0 & 0 & -1 \\ 1 & 1/2 & \sqrt{3}/2 & 0 \end{bmatrix} \quad (\text{A.III.14 b})$$

Calculating the study parameters  $[b_0, b_1, b_2, b_3, b_4, b_5, b_6, b_7]$  in the base from  $B$ , and  $[m_0, m_1, m_2, m_3, m_4, m_5, m_6, m_7]$  in the platform from  $M$ , we can obtain  $T_b$  and  $T_m$  according to Eqs. (2.34) and (2.35):

$$T_b = \begin{bmatrix} 3 & 0 & \sqrt{3} & 0 & 0 & 0 & 0 & 0 \\ 0 & 3 & 0 & -\sqrt{3} & 0 & 0 & 0 & 0 \\ -\sqrt{3} & 0 & 3 & 0 & 0 & 0 & 0 & 0 \\ 0 & \sqrt{3} & 0 & 3 & 0 & 0 & 0 & 0 \\ -\sqrt{3}/2 & 0 & \frac{3}{2} & 0 & 3 & 0 & \sqrt{3} & 0 \\ 0 & -\sqrt{3}/2 & 0 & -\frac{3}{2} & 0 & 3 & 0 & -\sqrt{3} \\ -3/2 & 0 & -\sqrt{3}/2 & 0 & -\sqrt{3} & 0 & 3 & 0 \\ 0 & 3/2 & 0 & -\sqrt{3}/2 & 0 & \sqrt{3} & 0 & 3 \end{bmatrix} \quad (\text{A.III.15})$$

$$T_m = \begin{bmatrix} \frac{\sqrt{3}}{2}+1 & -\frac{\sqrt{3}}{2}-1 & \frac{1}{2} & -\frac{1}{2} & 0 & 0 & 0 & 0 \\ \frac{\sqrt{3}}{2}+1 & \frac{\sqrt{3}}{2}+1 & \frac{1}{2} & \frac{1}{2} & 0 & 0 & 0 & 0 \\ -\frac{1}{2} & -\frac{1}{2} & \frac{\sqrt{3}}{2}+1 & \frac{\sqrt{3}}{2}+1 & 0 & 0 & 0 & 0 \\ \frac{1}{2} & -\frac{1}{2} & -\frac{\sqrt{3}}{2}-1 & \frac{\sqrt{3}}{2}+1 & 0 & 0 & 0 & 0 \\ \frac{1}{4} & \frac{1}{4} & \frac{\sqrt{3}}{4}+\frac{1}{2} & \frac{\sqrt{3}}{4}+\frac{1}{2} & \frac{\sqrt{3}}{2}+1 & -\frac{\sqrt{3}}{2}-1 & \frac{1}{2} & -\frac{1}{2} \\ -\frac{1}{4} & \frac{1}{4} & -\frac{\sqrt{3}}{4}-\frac{1}{2} & \frac{\sqrt{3}}{4}+\frac{1}{2} & \frac{\sqrt{3}}{2}+1 & \frac{\sqrt{3}}{2}+1 & \frac{1}{2} & \frac{1}{2} \\ -\frac{\sqrt{3}}{4}-\frac{1}{2} & \frac{\sqrt{3}}{4}+\frac{1}{2} & \frac{1}{4} & -\frac{1}{4} & -\frac{1}{2} & -\frac{1}{2} & \frac{\sqrt{3}}{2}+1 & \frac{\sqrt{3}}{2}+1 \\ -\frac{\sqrt{3}}{4}-\frac{1}{2} & -\frac{\sqrt{3}}{4}-\frac{1}{2} & \frac{1}{4} & \frac{1}{4} & \frac{1}{2} & -\frac{1}{2} & -\frac{\sqrt{3}}{2}-1 & \frac{\sqrt{3}}{2}+1 \end{bmatrix}$$

(A.III.16)

Therefore, obtaining the new study parameters  $X_i$  according to Eq. (A.III.11) and substituting them to the corresponding parameters  $X$  in the Eqs. (3.2), (3.3) and (3.9), three constraint equations for the parallel mechanism are obtained which can be used for the followed kinematic analysis of the mechanism. The three equations are detailed below

$$\begin{aligned} & -9.900834470x_0^2 + 19.80166888x_0x_1 - 39.60333788x_0y_1 - 11.43249886x_0x_2 \\ & + 34.29749668x_0x_3 + 22.86499772x_0y_3 - 9.900834470x_1^2 - 34.29749668x_1x_2 \\ & + 11.43249886x_1x_3 + 39.60333788x_1y_0 + 22.86499772x_1y_2 + 9.900834470x_2^2 \\ & + 19.80166888x_2x_3 - 22.86499772x_2y_1 - 39.60333788x_2y_3 + 9.900834470x_3^2 \\ & - 22.86499772x_3y_0 + 39.60333788x_3y_2 \end{aligned}$$

(A.III.17)

$$\begin{aligned} & -34.29749666x_1x_2 + 11.43249887x_1x_3 + 34.29749668x_1y_0 + 11.43249887x_1y_1 \\ & + 19.80166888x_1y_2 + 19.80166895x_1y_3 + 9.900834478x_2^2 + 19.80166889x_2x_3 \\ & - 19.80166895x_2y_0 + 19.80166888x_2y_1 - 11.43249887x_2y_2 + 34.29749668x_2y_3 \\ & + 9.900834465x_3^2 - 19.80166888x_3y_0 + 19.80166895x_3y_1 + 34.29749668x_3y_2 \\ & - 11.43249887x_3y_3 - 9.900834478x_0^2 + 19.80166889x_0x_1 - 11.43249888x_0x_2 \\ & + 34.29749666x_0x_3 + 11.43249887x_0y_0 + 34.29749668x_0y_1 - 19.80166895x_0y_2 \\ & - 19.80166888x_0y_3 - 9.900834465x_1^2 \end{aligned}$$

(A.III.18)

$$\begin{aligned}
& 21.33333332x_1x_2 + 9.900834462x_1x_3 - 18.68041272x_1y_0 + 27.04958283x_1y_1 \\
& + 18.68041275x_1y_2 - 18.68041274x_1y_3 + 18.47520862x_2^2 + 17.14874833x_2x_3 \\
& - 27.04958278x_2y_0 - 4.184584969x_2y_1 + 18.68041275x_2y_2 - 58.28375060x_2y_3 \\
& - 1.326460288x_3^2 - 18.68041275x_3y_0 - 12.55375506x_3y_1 + 4.184585055x_3y_2 \\
& + 18.68041274x_3y_3 + 12.96416330y_0^2 + 19.80166888y_0y_1 - 11.43249887y_0y_2 \\
& + 34.29749668y_0y_3 + 12.96416330y_1^2 - 34.29749668y_1y_2 + 11.43249887y_1y_3 \\
& + 32.76583225y_2^2 + 19.80166888y_2y_3 + 32.76583225y_3^2 + 24.19145807x_0^2 \\
& + 17.14874833x_0x_1 - 9.900834468x_0x_2 + 1.531664446x_0x_3 + 27.04958282x_0y_0 \\
& - 35.41875283x_0y_1 + 58.28375061x_0y_2 + 4.184584969x_0y_3 + 4.389789141x_1^2
\end{aligned}$$

(A.III.19)

### A.III.2 Kinematic Analysis of a 3-RRRR MMRM

In Chapters 5 and 6, two single-loop multi-mode reconfigurable mechanisms (SLMMRMs) have been designed and analysed using the explicitation approach based on the kinematic mapping method and it proved that the method is quite effective for the kinematic analysis of SLMMRMs. In [120], the implicitization approach was used to complete the forward kinematic problem for a multi-loop parallel mechanism. With similar motivation in this appendix, the aim is to analyse a Multi-Mode Multi-Loop Reconfigurable Mechanism (MLMMRM) using the implicitization approach.

#### A.III.2.1 Description of the MLMMRM

A 3-RRRR mechanism presented in [133] was regarded as a 3-DOF parallel mechanism which is in fact a MLMMRM with one DOF, as demonstrated in Fig. A.III.4. Its three legs are exactly the same as the leg of the 7R SLMMRM proposed in Chapter 5 and the three R joints in the base and platform are line symmetrical. The relationships of its parameters are as follows:

$$R_{i1} // R_{i3} // R_{i4} \perp R_{i2} \quad (\text{A.III.20})$$

$$a_{11}=a_{21}=a_{31}, a_{12}=a_{22}=a_{32}, a_{11}=a_{21}=a_{31} \quad (\text{A.III.21})$$

$$a_{i1}+a_{i2}=a_{i3} \quad (\text{A.III.22})$$

The parameters for the legs are listed in Table A.III.3. The parameters from the centre of the base to the starts of the three legs are listed in Table A.III.4. The parameters from the ends of the legs to the centre of the platform are listed in Table A.III.5.

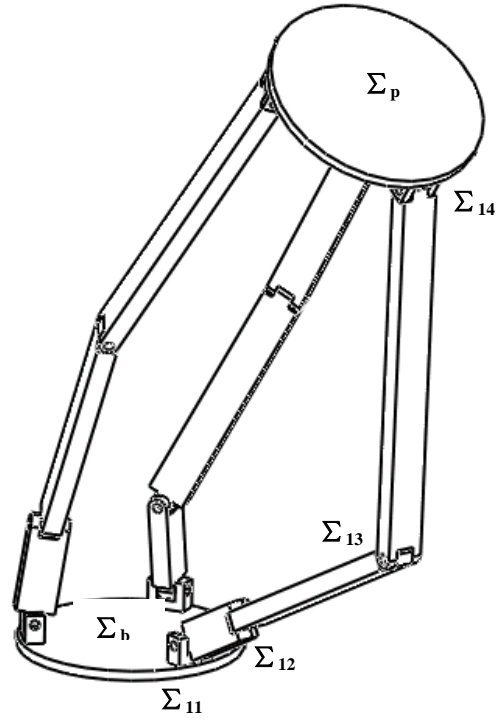


Figure A.III.4 Structure of 3-RRRR MMRM

Table A.III.3 Parameters for the legs of the 3-RRRR MMRM

$i$	$a_{i1}$	$a_{i2}$	$a_{i3}$	$d_{i1}$	$d_{i2}$	$d_{i3}$	$\alpha_{i1}(\text{deg})$	$\alpha_{i2}(\text{deg})$	$\alpha_{i3}(\text{deg})$
1	1.00	1.00	1.00	0.00	0.00	0.00	90.00	90.00	90.00
2	3.00	3.00	3.00	0.00	0.00	0.00	-90.00	-90.00	-90.00
3	4.00	4.00	4.00	0.00	0.00	0.00	0.00	0.00	0.00

Table A.III.4 Parameters from the centre of the base to the starts of the legs

$i$	$x_{bi}$	$y_{bi}$	$z_{bi}$	$\theta_{bi}(\text{deg})$	$\gamma_{bi}(\text{deg})$
1	0.00	1.00	0.00	0.00	90.00
2	0.50	0.87	0.00	120.00	90.00
3	0.50	-0.87	0.00	-150.00	90.00

Table A.III.5 Parameters from the ends of the legs to the centre of the platform

$i$	$x_{mi}$	$y_{mi}$	$z_{mi}$	$\alpha_{mi}(\text{deg})$	$\theta_{mi}(\text{deg})$
1	1.00	0.00	0.00	-90.00	-90.00
2	1.00	0.00	0.00	-90.00	150.00
3	1.00	0.00	0.00	-90.00	30.00

### *A.III.2.2 Motion Patterns of the 3-RRRR MMRM*

Several operation modes can be identified by the CAD models as shown in Fig. A.III.5. Figure A.III.5(a) shows a translational operation mode which is the same as that of the 7R SLMMRM (Fig. 5.1(b)). Figure A.III.5(b) shows 1-DOF planar operation mode similar to the operation mode I of the 7R SLMMRM. Figures A.III.5(c) shows another 1-DOF planar operation mode similar to the operation mode II of the 7R SLMMRM.

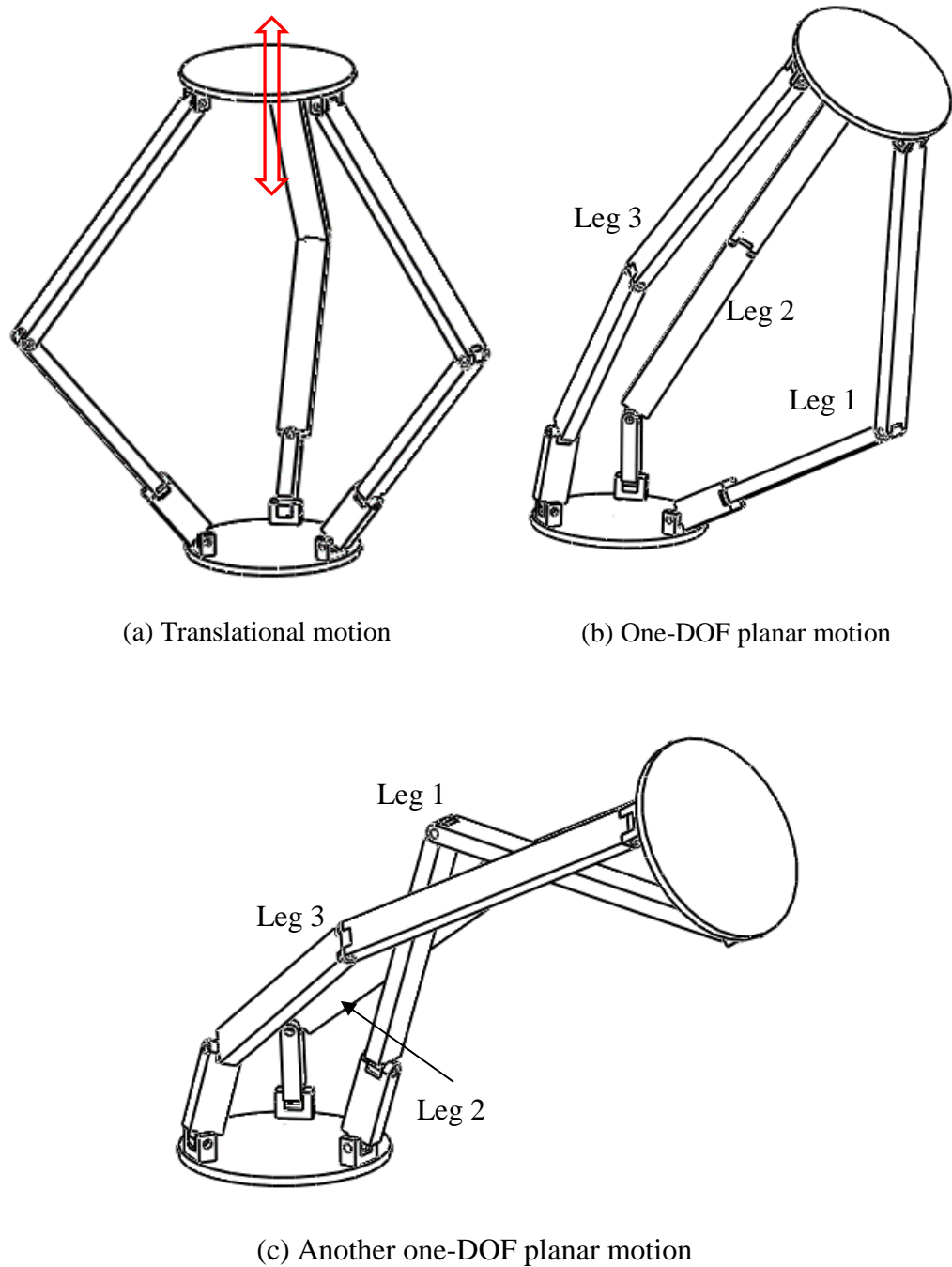


Figure A.III.5 Some operation modes of the 3-RRRR MMRM

### A.III.2.3 Kinematic Analysis of the 3-RRRR MMRM

In this section, constraint equations for the 3-RRRR MMRM are derived. The constraint equations for the leg have been obtained using the implicitization approach in Table A.I.3 5-a):

$$x_1^2 y_1^2 + 9x_1^2 y_2^2 - 16x_1 x_2 y_1 y_2 + 9x_2^2 y_1^2 + x_2^2 y_2^2 - y_0^2 y_1^2 - y_0^2 y_2^2 - y_1^2 y_3^2 - y_2^2 y_3^2 = 0 \quad (\text{A.III.23})$$

$$\begin{aligned} & -12x_0 x_1 y_2 y_3 + 12x_0 x_2 y_1 y_3 - 4x_1^2 y_1^2 - 8x_1 x_2 y_1 y_2 + 12x_1 x_3 y_0 y_2 \\ & - 4x_2^2 y_2^2 - 12x_2 x_3 y_0 y_1 + y_0^2 y_1^2 + y_0^2 y_2^2 + y_1^2 y_3^2 + y_2^2 y_3^2 = 0 \end{aligned} \quad (\text{A.III.24})$$

Adding the transformation in the base and in the platform separately into legs 1, 2 and 3, then six constraint equations are obtained with two equations for each leg. Take leg 1 for an example, the transformations in the base frame  $B_1$  and moving frame  $M_1$  are

$$B_1 = \begin{bmatrix} 1 & 0 & 0 & 0 \\ 0 & 0 & 0 & 1 \\ 1 & 0 & 1 & 0 \\ 0 & -1 & 0 & 0 \end{bmatrix}, \quad M_1 = \begin{bmatrix} 1 & 0 & 0 & 0 \\ 1 & 0 & 1 & 0 \\ 0 & 0 & 0 & 1 \\ 0 & 1 & 0 & 0 \end{bmatrix} \quad (\text{A.III.25})$$

The transformations matrixes  $T_{b1}$  and  $T_{m1}$  in the kinematic mapping space can be derived after calculating the Study parameters, leading to execution of the transformations to the Eqs. (A.III.23) and (A.III.24) and then constraint equations for the 3-RRRR MMRM are obtained:

$$\begin{aligned} & 8.0x_0^2 x_2 y_0 + 36.0x_0^2 x_3^2 - 4.0x_0^2 y_0^2 - 4.0x_0^2 y_1^2 - 64.0x_0 x_2 x_3 y_3 + 16.0x_0 x_2 y_0 y_2 \\ & + 72.0x_0 x_3^2 y_2 - 8.0x_0 y_0^2 y_2 - 8.0x_0 y_1^2 y_2 + 32.0x_2^2 y_3^2 - 64.0x_2 x_3 y_2 y_3 + 8.0x_2 y_0 y_2^2 \\ & + 8.0x_2 y_0 y_3^2 + 36.0x_3^2 y_2^2 + 4.0x_3^2 y_3^2 - 4.0y_0^2 y_2^2 - 4.0y_0^2 y_3^2 - 4.0y_1^2 y_2^2 - 4.0y_1^2 y_3^2 \\ & = 0 \end{aligned} \quad (\text{A.III.26})$$

$$\begin{aligned} & 4.0y_0^2 y_2^2 + 4.0y_0^2 y_3^2 + 4.0y_1^2 y_2^2 + 4.0y_1^2 y_3^2 - 16.0x_3^2 y_3^2 - 32.0x_2 x_3 y_2 y_3 \\ & - 8.0x_2 y_0 y_2^2 - 8.0x_2 y_0 y_3^2 - 12.0x_2^2 y_2^2 + 4.0x_2^2 y_3^2 + 48.0x_1 x_2 y_0 y_3 - 48.0x_1 x_3 y_0 y_2 \\ & - 48.0x_1 x_2^2 y_3 + 48.0x_1 x_2 x_3 y_2 + 8.0x_0 y_1^2 y_2 - 32.0x_0 x_2 x_3 y_3 - 16.0x_0 x_2 y_0 y_2 \\ & - 48.0x_0 x_2 y_1 y_3 + 48.0x_0 x_3 y_1 y_2 + 8.0x_0 y_0^2 y_2 + 48.0x_0 x_1 x_2 x_3 - 48.0x_0 x_1 x_3 y_0 \\ & - 24.0x_0 x_2^2 y_2 - 12.0x_0^2 x_2^2 - 8.0x_0^2 x_2 y_0 + 48.0x_0^2 x_3 y_1 + 4.0x_0^2 y_0^2 + 4.0x_0^2 y_1^2 \\ & = 0 \end{aligned} \quad (\text{A.III.27})$$

The equations for legs 2 and 3 are too long to show in the text. In brief, a total of eight constraint equations for the mechanism can be obtained including the six

equations for the three legs, the equation Eq. (A.III.28) and the equation of the Study quadric, i.e., Eq. (2.33).

$$\Delta = x_0^2 + x_1^2 + x_2^2 + x_3^2 = 1 \quad (\text{A.III.28})$$

Although the set of constraint equations are obtained for the forward kinematic analysis of the 3-RRRR MMRM, it will be quite difficult to use “resultant method” to obtain a univariate expression due to their high degrees of polynomials. In the process of dealing with the constraint equations of forward kinematic problem of a 5-RPUR parallel mechanisms (3T2R) as reported in [120], the authors tried to use a numerical algebraic geometry algorithm through *Bertini* (a software to solve polynomials using homotopy continuation approach) where 1680 infinite real and complex solutions have been obtained of which 208 are real solutions. However, the numbers are not the upper bound for the solutions. In order to obtain the upper bound for the solutions a univariate expression for the forward kinematic analysis of the 3-RRRR MMRM needs to be developed which will be an extremely difficult and complicated task. According to Bezour’s theorem [130,131] the set of solutions of these constraint equations will have an upper bound of solutions

$$4^6 \times 2 \times 2 = 16384 \quad (\text{A.III.29})$$

where there are six equations of degree 4, and two equations of degree 2.

Therefore, this appendix terminates without giving the complete solutions of the forward kinematic analysis of the 3-RRRR MMRM due to the above issue.

### A.III.3 Summary

In this appendix the constraint equations of serial chains with transformations in the base and moving frame have been unified, which is used to obtain constraint equations for parallel mechanisms. A 3-RRRR MMRM proposed before turns out to have several operation modes using CAD models. The forward kinematic analysis for the 3-RRRR MMRM is attempted to undertake and its constraint equations have been obtained. However, solving the constraint equations to obtain the complete solutions is extremely difficult task and is left for the future work.

## References

- [1] <http://www.adept.com/products/robots/scara/cobra-s600/general> (Accessed on 01 April 2015)
- [2] J.P. Merlet, “*Parallel Robots*”, Springer, Netherlands (2006)
- [3] X. Kong, C.M. Gosselin, “*Type Synthesis Parallel Manipulator*”, Springer, Berlin (2007)
- [4] <http://www.parallemic.org/> (Accessed on 23 November 2011)
- [5] <http://www.abb.com/product/seitp327/cf1b0a0847a71711c12573f40037d5cf.aspx>  
(Accessed on 01 April 2015)
- [6] X. Kong, C.M. Gosselin, “Type Synthesis of 3-DOF Translational Parallel Manipulator Based on Screw Theory”, *Journal of Mechanical Design*, 126, 83-92 (2004)
- [7] X. Kong, C.M. Gosselin, “Type Synthesis of 3-DOF Spherical Parallel Manipulator Based on Screw Theory”, *Journal of Mechanical Design*, 129, 101-108 (2004)
- [8] [Http://en.wikipedia.org/wiki/Flight\\_simulator](http://en.wikipedia.org/wiki/Flight_simulator) (Accessed on 01 April 2015)
- [9] K.L. Hunt, “*Kinematic Geometry of mechanism*”, Cambridge University Press, Cambridge (1978)
- [10] G. Yang, I. Chen, K.M. Lim, Y.S. Huat, “Design and Kinematic Analysis of Modular Reconfigurable Parallel Robots”, *1999 IEEE Conference on Robotics and Automation*, Detroit, MI, US, 4, 2501-2506 (1999)
- [11] G. Yang, W. Chen, Y. Chen, Y.S. Huat, Chen, G. “*Design and Kinematic Analysis of Modular Reconfigurable Parallel Robot*”, Springer, 10, 83-89 (2001)
- [12] M. Yim, P. White, M. Park, J. Sastra, “*Encyclopedia of Complexity and System Science*”, Springer, New York (2009)
- [13] S. Murata, E. Yoshida, A. Kamimura, H. Kurokawa, K. Tomita, S. Kokaji, “M-TRAN: Self-Reconfigurable Modular Robotic System”, *IEEE/ASME Transactions on Mechatronics*, 7, 431-441 (2002)
- [14] L. Zhang, J. Dai, “An Overview of the Development on Reconfiguration of Metamorphic Mechanisms”, *ASME/IFTOMM International Conference on Reconfigurable Mechanisms and Robots*, London, UK, 8-12 (2009)
- [15] J. Dai, J. Rees Jones, “Mobility in Metamorphic Mechanisms of Foldable/Erectable Kinds”, *Journal of Mechanical Design*, 121(3), 375-382 (1998)
- [16] J.J. Parise, L.L. Howell, S.P. Magleby, “Ortho-Planar Mechanisms”, *Proceedings of the 2000 ASME Design Engineering Technical Conferences*, DETC2000/MECH-14193 (2000)



- [17] C. Liu, T. Yang, "Essence and Characteristics of Metamorphic Mechanisms and Their Metamorphic Ways", *Proc. 11th World Congress in Mechanism and Machine Science*, Tianjin, China, 1285-1288 (2004)
- [18] D.W. Carroll, S.P. Magleby, L.H. Howell, R.H. Todd, C.P. Lusk, "Simplified Manufacturing through a Metamorphic Process for Compliant Ortho-Planar Mechanisms", *2005 ASME International Mechanical Engineering Congress and Exposition*, November, Orlando, USA (2005)
- [19] D. Wang, and J. Dai, "Theoretical Foundation of Metamorphic Mechanism and its Synthesis", *Chinese Journal of Mechanical Engineering*, 43(8), 32-42 (2007)
- [20] J. Dai, J. Rees Jones, "Matrix Representation of Topological Changes in Metamorphic Mechanisms", *Journal of Mechanical Design*, 127, 837-840 (2005)
- [21] L. Zhang, D. Wang, and J.S. Dai, "Biological Modeling and Evolution Based Synthesis of Metamorphic Mechanisms", *Journal of Mechanical Design*, 130(7), 072303-1-11 (2008)
- [22] D. Wang, and J. Dai, "Geometric Analysis and Synthesis of the Metamorphic Robotic Hand", *Journal of Mechanical Design*, 129(11), 1191-1197 (2007)
- [23] L. Zhang, J. Dai, "Metamorphic Techniques and Geometric Reconfiguration Principles", *Proc. ASME/IFTOMM International Conference on Reconfigurable Mechanisms and Robots*, June 2009, London, UK (2009)
- [24] C. Kuo, J. Dai, "Reconfiguration Principles and Strategies for Reconfigurable Mechanisms", *Proc. ASME/IFTOMM International Conference on Reconfigurable Mechanisms and Robots*, June 2009, London, (2009)
- [25] N. Liu, "*Configuration Synthesis of Mechanisms with Variable Chains*", Ph.D. Dissertation, National Cheng Kung University, Taiwan (2001)
- [26] H. Yan, N. Liu, "Finite-State-Machine Representations for Mechanisms and Chains with Variable Topologies", *Proceedings of the 26th ASME Mechanisms Conference*, Baltimore, Maryland 10-13, DETC2000/MECH-14054, (2000)
- [27] C. Kuo, "*Structural Characteristics of Mechanisms with Variable Topologies Taking into Account the Configuration Singularity*", Master thesis, National Cheng Kung University, Tainan, Taiwan (2004)
- [28] H. Yan, C. Kuo, "Topological Representations and Characteristics of Variable Kinematic Joints", *Journal of Mechanical Design*, 128(2), 384-391 (2006)
- [29] H. Yan, C. Kuo, "Representations and Identifications of Structural and Motion State Characteristics of Mechanisms with Variable Topologies", *Transactions of the Canadian Society for Mechanical Engineering*, 30 (1), 19-40 (2006)

- [30] H. Yan, C. Kuo, "On the Mobility and Configuration Singularity of Mechanisms with Variable Topologies", *Journal of Mechanical Design*, 129 (6), 617-624 (2007).
- [31] H. Yan, C. Kuo, "Configuration Synthesis of Mechanisms with Variable Topologies", *Mechanism and Machine Theory*, 44, 896-911 (2009)
- [32] K. Wohlhart, Kinematotropic Linkages, "Recent Advances in Robot Kinematics", (J. Lenarčič and V. Parenti-Castelli, Eds.), Netherlands: Kluwer Academic Publishers, 359-368 (1996)
- [33] C. Galletti and P. Fanghella, "Single-Loop Kinematotropic Mechanisms", *Mechanism and Machine Theory*, 36, 743-761 (2001).
- [34] P. Fanghella, C. Galletti, and E. Giannotti, "Parallel Robots that Change Their Group of Motion," *Advances in Robot Kinematics: Mechanisms and Motion*, (J. Lenarcic and M. Roth, Eds.), Springer, 49-56 (2006).
- [35] E. Giannotti, C. Galletti, "Synthesis of Single-Loop Kinematotropic Mechanisms", *XIX Congress AIMETA*, Ancona, 14-17 September, 2009.
- [36] C. Galletti, P. Fanghella, "Kinematotropic Properties and Pair Connectivities in Single-Loop Spatial Mechanisms", *Proc. 10th World Congress on the Theory of Machines and Mechanisms*, Oulu, Finland, 20-24 (1999)
- [37] C. Galletti, E. Giannotti, Multiloop Kinematotropic Mechanisms, *Proc. ASME Design Engineering Technical Conference*, Montreal, Canada, 455-460 (2002)
- [38] N. Wang, Y. Fang, D. Zhang, "A Spatial Single Loop Kinematotropic Mechanism Used for Biped/Wheeled Switchable Robots", *The International Journal of Mechanics and Materials in Design*, DOI 10.1007/s10999-014-9274-x, springer, Netherland (2014)
- [39] C. Lee, J.M. Herve, "Discontinuous Mobility of Four-Link Mechanisms with Revolute, Prismatic, and Cylindric Pairs through the Group Algebraic Structure of Displacement Set", *Proc. VIII International Conference on the Theory of Machines and Mechanisms*, Liberec, Czech, 377-382 (2000)
- [40] C. Lee, J.M. Herve, "Discontinuous Mobility of One Family of Spatial 6R Mechanisms through the Group Algebraic Structure of Displacement Set", *Proc. ASME Design Engineering Technical Conferences*, Montreal, Canada, DETC2002/MECH-34273, (2002)
- [41] C. Lee, J.M. Herve, "Synthesis of Two Kinds of Discontinuously Movable Spatial 7R Mechanisms through the Group Algebraic Structure of Displacement Set", *Proc. 11th IFToMM Word Congress*, Tianjin, China, 197-201(2004)

- [42] C. Lee, J.M. Herve, “Discontinuously Movable Seven-Link Mechanisms via Group-Algebraic Approach”, *Journal of Mechanical Engineering Science, Proceedings of the Institution of Mechanical Engineers*, 219 (C 6), 577-587 (2005)
- [43] C. Lee, J.M. Herve, “Discontinuously Movable 8R Mechanisms with an Infinity of Bifurcations”, *Proc. 12th IFToMM Word Congress*, Besancon, France (2007)
- [44] D. Zlatanov, I.A. Bonev, C.M. Gosselin, “Constraint Singularity as C-Space Singularities”, *Advances in Robot Kinematics-Theory and Application* (J. Lenarčič and F. Thomas eds.), Kluwer Academic Publishers, 183-192 (2002)
- [45] D. Zlatanov, I.A. Bonev, C.M. Gosselin, “Constraint Singularity as C-Space Singularities”, *Proc. 8th International Symposium on Advances in Robot Kinematics* (ARK 2002), Caldes de Malavella, Spain (2002)
- [46] L.W. Tsai, R.E. Stamper, “A Parallel Manipulator with Only Translational Degrees of Freedom”, *Proc. 1996 ASME Design Engineering Technical Conferences*, Irvine, CA, USA (1996)
- [47] R. Di Gregorio, V. Parenti-Castelli, “A Translational 3-DOF Parallel Manipulator”, *Advances in Robot Kinematics-Theory and Application*, (J. Lenarčič and M.L.Husty, eds.), Kluwer Academic Publishers, 49-58 (1998)
- [48] M. Karouia, J.M. Herve, “A Three-DOF Tripod for Generating Spherical Rotation”, *Advances in Robot Kinematics* (J. Lenarčič and M.L.Husty, eds.), Kluwer Academic Publishers, 395-402 (2000)
- [49] Y. Chen, Z. You, “Two-Fold Symmetrical 6R Foldable Frames and Their Bifurcations”, *International Journal of Solids and Structures*, 46(25-26), 4504-4514 (2009)
- [50] Y. Chen, W. Chai, “Bifurcation of a Special Line and Plane Symmetric Bricard Linkage”, *Mechanism and Machine Theory*, 46, 515-533 (2011)
- [51] C. Song, Y. Chen, “A 6R Linkage Reconfigurable between the Line-symmetric Bricard Linkage and the Bennett Linkage”, *Mechanism and Machine Theory*, 70, 278-292 (2013)
- [52] Q. Li, J.M. Hervé, “Parallel Mechanisms with Bifurcation of Schoenflies Motion”, *IEEE Transactions on Robotics*, 25 (1), 158-164 (2009)
- [53] G. Gogu, “Maximally Regular T2R1-Type Parallel Manipulators with Bifurcated Spatial Motion”, *Journal of Mechanisms and Robotics*, 3 (2011)
- [54] P. Fanghella, C. Galleti, E. Gianotti, “Parallel Robots that Change Their Group of Motion”, *Advances in Robot Kinematics* (J. Lenarčič, B. Roth (Eds.)), Springer, Netherlands, 49–56 (2006)

- [55] X. Kong, C. Huang, 2009, "Type Synthesis of Single-DOF Single-loop Mechanisms with Two Operation Modes", *Proc. ASME/IFTOMM International Conference on Reconfigurable Mechanisms and Robots*, London, UK (2009)
- [56] X. Kong, C.M. Gosselin, P.L. Richard, "Type Synthesis of Parallel Manipulator with Multiple Operation Modes", *Journal of Mechanical Design*, 129, 595-601 (2007)
- [57] X. Kong, "Type Synthesis of 3-DOF Parallel Manipulators with Both a Planar Operation Mode and a Spatial Translational Operation Mode", *Journal of Mechanisms and Robotics*, 5(4), 041005 (2013)
- [58] X. Kong, "Type Synthesis of Variable Degrees-of-Freedom Parallel Manipulators with Both Planar and 3T1R Operation Modes", *Proc. ASME 2012 International Design Engineering Technical Conferences and Computers and Information in Engineering Conference*, DETC2012-70621, 497-504 (2012)
- [59] K.H. Hunt, "*Kinematic Geometry of Mechanisms*", Oxford University Press, Oxford (1979)
- [60] J.M. McCarthy, G. S. Soh, "*Geometric Design of Linkages*", 2nd Edition, Springer (2010)
- [61] E. Delassus, Les Chaînes "Fermées et Déformables à Quatre Membres", *Bull. Sci. Math.* 46, 283–304 (1922)
- [62] R.L. Norton, "*Design of Machinery: An Introduction to the Synthesis and Analysis of Mechanisms and Machines*", 3<sup>rd</sup> Edition, McGraw Hill. (2003)
- [63] W.Z. Guo, R. Du, "Mobility of Single-Loop N-Bar Linkage with Active/Passive Prismatic Joints", *Journal of Mechanical Design*, 128(6), 1261-1271 (2005)
- [64] <http://synthetica.eng.uci.edu/mechanicaldesign101/McCarthyNotes-3.pdf> (Accessed on 09/04/2015)
- [65] G. T. Bennett, "A New Mechanism", *Engineering*, 76, 777-778 (1903)
- [66] G. T. Bennett, "The Skew Isogram Mechanism", *Proc. London Mathematics Society*, 2nd series, 13, 151-173 (1914)
- [67] C. Huang, H. T. Tu, "Linear Property of the Screw Surface of the Spatial RPRP Linkage", *Journal of Mechanical Design*, 128(3), 581-586 (2005)
- [68] H. Tipparthi, P. Larochelle, "Orientation Order Analysis of Spherical Four-Bar Mechanisms", *Journal of Mechanisms and Robotics* 3(4), 044501 (2011)
- [69] F. E. Myard, "Contribution à la Géométrie des Systèmes Articulés", *Bulletin de la Société Mathématique de France*, Vol. 59, pp. 183-210 (1931)
- [70] F. E. Myard, "Sur les chaînes fermées à quatre couples rotatifs nonconcurrents, déformables au premier degré de liberté", *Isogramme torique, Comptes Rendus Hebdomadaires des Séances de l'Académie de Science*, Paris, 192, 1194-1196 (1931)

- [71] Y. Chen, Z. You, “An Extended Myard Linkage and its Derived 6R Linkage”, *Journal of Mechanical Design*, 130(5) (2008)
- [72] M. Goldberg, “New Five-Bar and Six-Bar Linkages in Three Dimensions”, *Transactions of the ASME*, 65, 649-661 (1943)
- [73] C. Song, Y. Chen, “A Spatial 6R Linkage Derived from Subtractive Goldberg 5R Linkages”, *Mechanism and Machine Theory*, 46(8), 1097-1106 (2011)
- [74] C. Mavroidis, B. Roth, “Analysis and Synthesis of Overconstrained Mechanism”, *Proc. 1994 ASME Design Technical Conference*, Minneapolis, MI, 115-133 (1994)
- [75] P. T. Sarrus, “*Note sur la Transformation des Mouvements Rectilignes Alternatifs, en Mouvements Circulaires*”, et reciproquement, Académie des Sciences, 36, 1036-1038 (1853)
- [76] [http://en.wikipedia.org/wiki/Sarrus\\_linkage](http://en.wikipedia.org/wiki/Sarrus_linkage) (Accessed on 13/04/2015)
- [77] R. Bricard, “*Leçons de Cinématique, Tome II Cinématique Appliquée*”, Gauthier Villars, Paris, 7-12 (1927)
- [78] K. J. Waldron, “Hybrid Overconstrained Linkages”, *Journal of Mechanisms*, 3, 73-78 (1968)
- [79] K. Wohlhart, “Merging Two General Goldberg 5R Linkages to Obtain a New 6R Space Mechanism”, *Mechanism and Machine Theory*, 26(2), 659-668 (1991)
- [80] K. Wohlhart, “On Isomeric Overconstrained Space Mechanisms”, *Proc. 8th World Congress IFToMM*, Prague, Czechoslovakia, 26-31, 153-158 (1991)
- [81] J. E. Baker, “On Generating a Class of Foldable Six-Bar Spatial Linkages”, *Journal of Mechanical Design*, 128, 374-383 (2006)
- [82] Y. Chen, “*Design of Structural Mechanism*”, Ph.D. thesis, University of Oxford (2003)
- [83] C. Song, Y. Chen, “A Family of Mixed Double-Goldberg 6R Linkages”, *Proc. R. Soc. A*, 468, 871-890 (2012)
- [84] J. E. Baker, “An Analysis of Bricard Linkages”, *Mechanism and Machine Theory*, 15, 267-286 (1980)
- [85] J. E. Baker, “Screw Replacements in Isomeric Variants of Bricard's Line Symmetric Six-Bar”, *Proceedings of the Institution of Mechanical Engineers Part C: Journal of Mechanical Engineering Science*, 223, 2391-2398 (2009)
- [86] P. G. Altmann, Communications to Grodzinski, P. and M'Ewen, E, “Link Mechanisms in Modern Kinematics”, *Proceedings of the Institution of Mechanical Engineers Part C: Journal of Mechanical Engineering Science*, 168(37), 889-896 (1954)
- [87] Y. Chen, Z. You, “Spatial 6R Linkages Based on the Combination of Two Goldberg 5R Linkages”, *Mechanism and Machine Theory*, 42, 1484-1498 (2007)

- [88] E. J. Baker, "A Comparative Survey of the Bennett-Based, 6-Revolute Kinematic Loops", *Mechanism and Machine Theory*, 28, 83-96 (1993)
- [89] E. J. Baker, "Displacement-Closure Equations of the Unspecialised Double Hooke's-Joint Linkage", *Mechanism and Machine Theory*, 37, 1127-1144 (2002)
- [90] G. T. Bennett, "*The Parallel Motion of Sarrus and Some Allied Mechanisms*", *Philosophy Magazine*, 6th series, 9, 803-810 (1905)
- [91] J. Phillips, "*Freedom of Machinery*", Volume II, Cambridge University Press, Cambridge (1990)
- [92] K. Wohlhart, "A New 6R Space Mechanism", *Proc. the 7th World Congress on the Theory of Machines and Mechanisms*, Seville, Spain, 1, 193-198 (1987)
- [93] P. Dietmaier, "A New 6R Space Mechanism", *Proc. 9th World Congress IFToMM*, Milano, 1, 52-56 (1995)
- [93] J. E. Baker, "Using the Single Reciprocal Screw to Confirm Mobility of a Six-Revolute Linkage", *Proceedings of the Institution of Mechanical Engineers Part C: Journal of Mechanical Engineering Science*, 224, 2247-2255 (2010)
- [95] C. Mavroidis, B. Roth, "Structural Parameters which Reduce the Number of Manipulator Configurations", *Journal of Mechanical Design*, 116(1), 3-10 (1994)
- [96] X. Kong, "Type Synthesis of Single-Loop Overconstrained 6R Mechanisms for Circular Translation", *Journal of Mechanisms and Robotics*, 6(4), 041016 (2014)
- [97] L.M. Surhone, M.T. Timpelton, M.T. Tennoe, S.F. Henssonow, S.F. Marseken, "*Tangent Half-angle Formula: Trigonometry, Trigonometric Functions, Rational Function, Polynomial, Antiderivative, Unit Circle*", VDM Publishing (2013)
- [98] P.K. Jain, "*Analytical Geometry of Three Dimensions*", New Age International (2005)
- [99] B. Jacob, "*Linear Algebra*", W.H. Freeman and Company, New York (1990)
- [100] L. E. Mansfield, "*Linear Algebra with Geometric Applications*", Marcel Dekker, New York (1976)
- [101] L.W. Johnson, R.D. Riess, J.T. Arnold, "*Introduction to Linear Algebra*", Addison-Wesley Publishing Company, Inc, America (1989)
- [102] R.S. Hartenberg, J. Denavit, "*Kinematic Synthesis of Linkages*", McGraw-Hill, New York (1964)
- [103] J. Denavit, R.S. Hartenberg, "A Kinematic Notation for Lower-Pair Mechanisms Based on Matrices", *ASME Journal of Applied Mechanics*, 23, 215-221 (1955)
- [104] P. Richard, "*Robot Manipulators: Mathematics, Programming, and Control: the Computer Control of Robot Manipulators*", Cambridge, MA: MIT Press (1981)

- [105] L. Harvey, "A Note on Denavit-Hartenberg Notation in Robotics", *Proc. ASME 2005 International Design Engineering Technical Conferences & Computers and Information in Engineering Conference*, Long Beach, California USA, 921-926 (2005)
- [106] S. Qiao, Q. Liao, S. Wei, H. Su, "Inverse Kinematic Analysis of the General 6R Serial Manipulators Base on Double Quaternions", *Mechanism and Machine Theory*, 45, 193-199 (2010)
- [107] L.W. Tsai, A. P. Morgan, "Solving the Kinematics of the Most General Six- and Five-Degree-of-Freedom Manipulators by Continuation Methods", *Journal of Mechanical Design*, 107(2), 189-200 (1985)
- [108] M. Raghavan, B. Roth, "Kinematic Analysis of the 6R Manipulator of General Geometry", *Proc. The fifth international symposium on Robotics research*, MA, USA, 263-269 (1990)
- [109] C. Mavroidis, F.B. Ouezdou, P. Bidaud, "Inverse Kinematics of Six-Degree of Freedom "General" and "Special" Manipulators Using Symbolic Computation", *Robotica*, 12, 421-430 (1994)
- [110] C. Huang, R. Tseng, X. Kong, "Design and Kinematic Analysis of a Multiple-Mode 5R2P Closed-Loop Linkage", *New Trends in Mechanism Science: Analysis and Design*. Springer, Netherlands, 5, 3-10 (2010)
- [111] C. Huang, X. Kong, "Position Analysis of a Bennett-Based Multiple-Mode 7R Linkage", *Proc. ASME 2009 International Design Engineering Technical Conferences & Computers and Information in Engineering Conference*, USA (2009)
- [112] H. Lee, C. Liang, "Displacement analysis of the general spatial 7-link 7R mechanism", *Mechanism and Machine Theory*, 23(3), 219-216 (1988)
- [113] L.W. Tsai, "*Robot Analysis: The Mechanics of Serial and Parallel Manipulators*", John Wiley & Sons, New York (1999)
- [114] X. Wang, M. Hao, Y. Cheng, "On the Use of Different Evaluation for Forward Kinematics of Parallel Manipulators", *Applied Mathematics and Computation*, 25, 760-769 (2008)
- [115] I.A. Bonev, D.Zlatanov, C.M. Gosselin, "Singularity Analysis of 3-DOF Planar Parallel Mechanisms via Screw Theory", *Journal of Mechanical Design*, 125, 573-581 (2003)
- [116] M.L. Husty, M. Pfurner, H.P. Schrockner, "A New and Effective Algorithm for the Inverse Kinematics of a General Serial 6R Manipulator", *Mechanism and Machine Theory*, 42, 66-81 (2007)

- [117] M.L. Husty, M. Pfurner, H.P. Schrockner, K. Brunnthaler, “Algebraic Method in Mechanism Analysis and Synthesis”, *Robotica*, 25, 661-675 (2007)
- [118] M. Pfurner, “*Analysis of Spatial Serial Manipulators Using Kinematic Mapping*”, PhD Thesis, University of Innsbruck, Austria (2006)
- [119] D.R. Walter, M.L. Husty, “On Implicitization of Kinematic Constraint Equations”, *Machine Design & Research*, 26, 218-226 (2010)
- [120] M.T. Masouleh, “*Kinematic Analysis of Five-DoF (3T2R) Parallel Mechanisms with Identical Limb Structures*”, PhD thesis, University Laval, Quebec, Canada (2010)
- [121] M.T. Masouleh, C. Gosselin, M.L. Husty, D.R. Walter, “Forward Kinematic Problem of 5-PRUR Parallel Mechanisms with Identical Limb Structure”, *Mechanism and Machine Theory*, 46, 945-959 (2011)
- [122] M.T. Masouleh, M.L. Husty, C. Gosselin, “Forward Kinematic Problem of 5-PRUR Parallel Mechanisms Using Study Parameters”, *Advances in Robot Kinematics* (J. Lenarčič and M. M. Stanisic, Eds.) Springer, 211-221 (2010)
- [123] D.R. Walter, M.L. Husty, M. Pfurner, “A Complete Kinematic Analysis of the SNU 3-UPU Parallel Manipulator”, *Contemporary Mathematics, American Mathematical Society*, 496, 331-346 (2009)
- [124] M.L. Husty, A. Karger, H. Sachs, “*Steinhilper, Kinematik and Robotik*”, Springer-Verlag, Berlin, Heidelberg, New York (1997)
- [125] E. Study, “*Geometrie der dynamen. Die zusammensetzung von kräften und verwandte gegenstände der geometrie bearb*”, Leipzig, B.G. Teubner (1903)
- [126] X. Kong, M. Pfurner, “Type Synthesis and Reconfiguration Analysis of a Class of Variable-DOF Single-Loop Mechanisms”, *Mechanism and Machine Theory*, 85, 116-128 (2015)
- [127] M. Pfurner, X. Kong, C. Huang, “Complete Kinematic Analysis of Single-Loop Multiple-Mode 7-Link Mechanisms Based on Bennett and Overconstrained RPRP Mechanisms”, *Mechanism and Machine Theory*, 73, 117-129 (2014)
- [128] C. Huang, X. Kong, T. Ou, “Position Analysis of a Bennett-Based Multiple-Mode 7R Linkage”, *Proceedings of ASME 2009 International Design Engineering Technical Conferences & Computers and Information in Engineering Conference*, DETC2009-87241 (2009)
- [129] K. Wohlhart, “Multifunctional 7R Linkages”, *Proceedings of the International Symposium on Mechanisms and Machine Theory*, AzCIFTtoMM, Izmir, Turkey, 85-91 (2010)
- [130] R. Walker, “*Algebraic Curves*”, Vol.2, Springer (1950)



- [131] J.P. Merlet, “Algebraic-Geometry Tools for the Study of the Kinematics of the Parallel Manipulators”, *Computational Kinematics*, Kluwer Academic Publishers, 183-194 (1993)
- [132] K. Kong, “Reconfiguration analysis of a 3-DOF parallel mechanism using Euler parameter quaternions and algebraic geometry method”, *Mechanism and Machine Theory*, 74:188-201 (2014)
- [133] I.E. Moghaddam, M. Bahrami, “A Numerical Algorithm for Solving Displacement Kinematics of Parallel Manipulators”, 31st Annual Conference of IEEE, Industrial Electronics Society, 1864-1869 (2005)
- [134] E. Emmanouil, G. Wei, K. Zhang, J. Dai, “The Kinematics of KCL Five Fingered Metamorphic Hand”, King’s College London (2012)
- [135] <https://www.youtube.com/watch?v=hEC8l8vqLXg> (Accessed on 22 September 2015)
- [136] K. Six, A. Kecskeméthy, “Steering Properties of a Combined Wheeled and Legged Striding Excavator”, *Proceedings of the Tenth World Congress on the Theory of Machines and Mechanisms*, IFToMM, oulu, Finland, 135-140 (1999)